Acta Universitatis Tamperensis 2338

HENRIK HAMMARÉN

Intramolecular Regulation of Janus Kinases

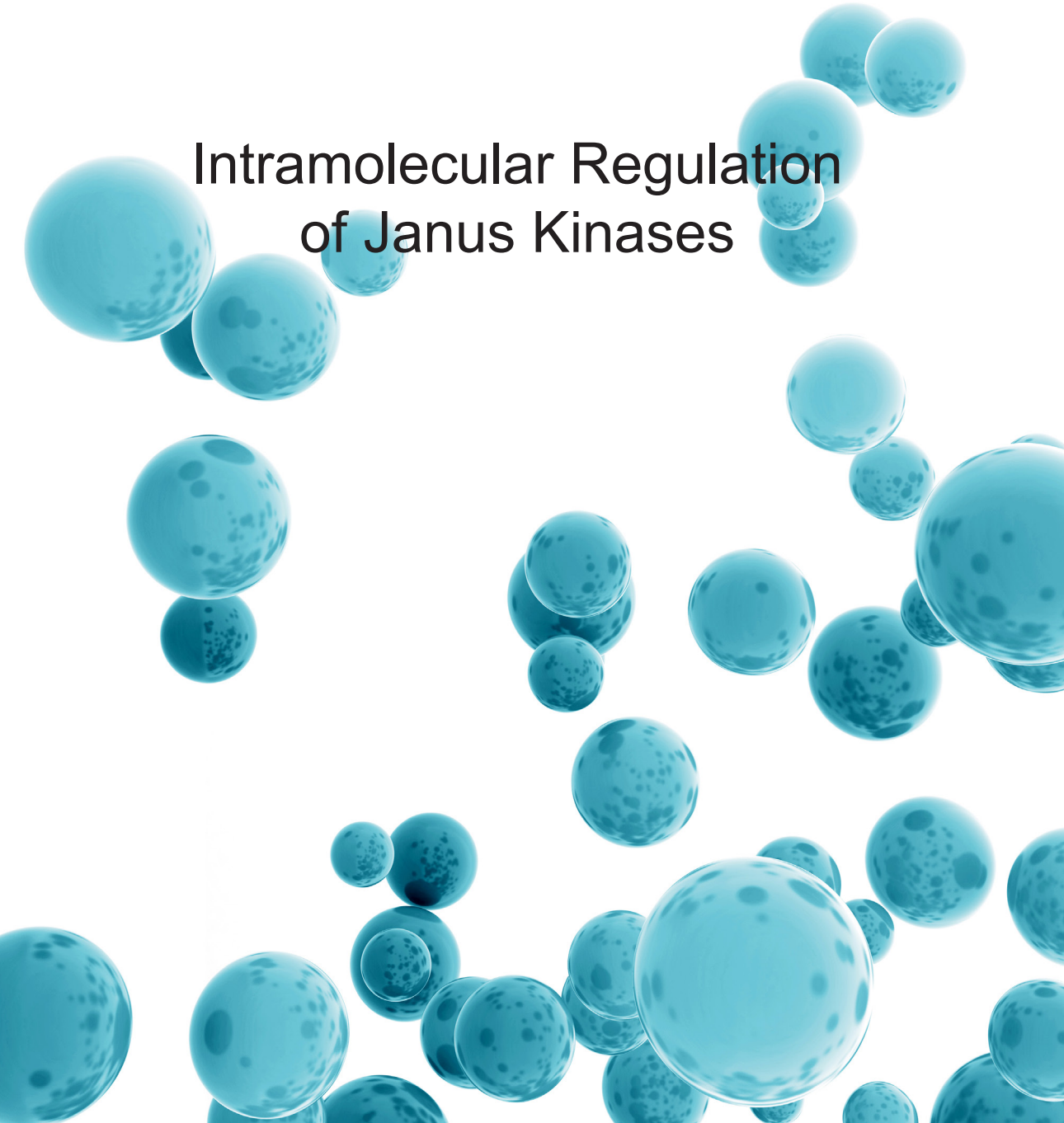

HENRIK HAMMARÉN

Intramolecular Regulation of Janus Kinases

■

ACADEMIC DISSERTATION
To be presented, with the permission of
the Faculty Council of the Faculty of Medicine and Life Sciences
of the University of Tampere,
for public discussion in the Jarmo Visakorpi auditorium
of the Arvo building, Arvo Ylpön katu 34, Tampere,
on 15 December 2017, at 12 o'clock.

UNIVERSITY OF TAMPERE

HENRIK HAMMARÉN

Intramolecular Regulation of Janus Kinases

Acta Universitatis Tamperensis 2338
Tampere University Press
Tampere 2017

ACADEMIC DISSERTATION
University of Tampere, Faculty of Medicine and Life Sciences
Finland

Supervised by
Professor Olli Silvennoinen
University of Tampere
Finland

Reviewed by
Adjunct professor Michael Courtney
University of Turku
Finland
Adjunct professor Outi Kilpivaara
University of Helsinki
Finland

Cover design by
Mikko Reinikka

Acta Universitatis Tamperensis 2338
ISBN 978-952-03-0607-6 (print)
ISSN-L 1455-1616
ISSN 1455-1616

Acta Electronica Universitatis Tamperensis 1843
ISBN 978-952-03-0608-3 (pdf)
ISSN 1456-954X
http://tampub.uta.fi

Suomen Yliopistopaino Oy – Juvenes Print
Tampere 2017

Contents

List of Original Communications

This thesis is based on the following original communications, which are referred to hereafter by their roman numerals (I-IV).

I. MIN, X., UNGUREANU, D., MAXWELL, S., **HAMMARÉN, H.M.**, THIBAULT, S., HILLERT, E., AYRES, M., GREENFIELD, B., EKSTEROWICZ, J., GABEL, C., WALKER, N., SILVENNOINEN, O. and WANG, Z., 2015. Structural and Functional Characterization of the JH2 Pseudokinase Domain of JAK family Tyrosine Kinase 2 (TYK2). *Journal of Biological Chemistry*, 290(45), pp. 27261-27270.

II. **HAMMARÉN, H.M.**, UNGUREANU, D., GRISOUARD, J., SKODA, R.C., HUBBARD, S.R. and SILVENNOINEN, O., 2015. ATP binding to the pseudokinase domain of JAK2 is critical for pathogenic activation. *Proceedings of the National Academy of Sciences of the United States of Americ*a, 112(15), pp. 4642-4647.

III. SHAN, Y., GNANASAMBANDAN, K., UNGUREANU, D., KIM, E.T., **HAMMARÉN, H.**, YAMASHITA, K., SILVENNOINEN, O., SHAW, D.E. and HUBBARD, S.R., 2014. Molecular basis for pseudokinase-dependent autoinhibition of JAK2 tyrosine kinase. *Nature Structural & Molecular Biology*, 21, pp. 579-584.

IV. **HAMMARÉN, H.M.**, PEUSSA, H., HUBBARD, S.R., AND SILVENNOINEN O., Inhibitory mutations reveal distinct JAK activation mechanisms for different pathogenic mutations and ligand-mediated activation. *Manuscript.*

List of Abbreviations

aa	amino acid
ADP	adenosine-5'-diphosphate
ALL	acute lymphoblastic leukaemia
AMKL	acute megakaryoblastic leukaemia
APS	adapter protein with PH (pleckstrin homology) and SH2 domains
ATP	adenosine-5'-triphosphate
ATPγS	adenosine 5'-[γ-thio]triphosphate
B-ALL	B cell acute lymphoblastic leukaemia
BSA	bovine serum albumin
BSF-3	B cell-stimulating factor-3
CALR	calreticulin
CD45	cluster of differentiation 45, a.k.a. PTPRC, protein tyrosine phosphatase, receptor type C
CDK	cyclin-dependent kinase
cDNA	complementary DNA
CIS	cytokine inducible SH2-containing protein. Member of the SOCS family
CLC	cardiotrophin-like cytokine
CLCF1, CLC	cardiotrophin-like cytokine factor 1
CLF	cytokine-like factor
CNTF	ciliary neutotrophic factor
CNTFR	ciliary neutotrophic factor receptor
coIP	coimmunoprecipitation
CRLF	cytokine receptor-like factor
CSF3R	granulocyte colony-stimulating factor receptor
CT-1	cardiotrophin 1
DMEM	Dulbecco's modified Eagle medium
DSF	differential scanning fluorometry
EBI3	Epstein-Barr virus induced 3
ECD	extracellular domain
EGFR	epidermal growth factor receptor
ePK	eukaryotic protein kinase
EPO	erythropoietin

EPOR	erythropoietin receptor
ET	essential thrombocythaemia
FAK	focal adhesion kinase
FBS	foetal bovine serum
FERM	4.1-band, ezrin, radexin, moiesin
FGFR	fibroblast growth factor receptor
FRET	Förster resonance energy transfer
GCN2	general control non-derepressible 2
GCSFR	granulocyte-macrophage colony stimulating factor receptor
GOF	gain-of-function
gp140	glycoprotein 140, a.k.a. common β chain
HA	hemagglutinin tag (aa sequence: YPYDVPDYA)
HER3/ERBB3	human epidermal growth factor receptor 3
Hop	hopscotch (*Drosophila* JAK homologue)
IFN	interferon
IL	interleukin
IMF	idiopathic myelofibrosis
IP	immunoprecipitation
JAK	Janus kinase
JH	Janus homology domain
KSR	kinase suppressor of Ras
LEPR	leptin receptor
LNK	lymphocyte-specific adaptor protein
LOF	loss-of-function
MANT	2'/3'-(N-methyl-anthraniloyl)
MPL / TPOR	myeloproliferative leukaemia protein / thrombopoietin receptor
MS	mass spectrometry
MW	molecular weight
NNT-1	novel neurotrophin-1
NP	neuropoietin
OBR	receptor of the mouse *obesity* (ob) gene's product (leptin). See LEPR
OSM	oncostatin M
PDB	Protein data bank, found at www.rcsb.org
PDK	3-phosphoinositide-dependent kinase
PHK	phosphorylase kinase
PI3K	phosphoinositide 3-kinase / Phosphatidylinositol-4,5-bisphosphate 3-kinase
PIAS	protein inhibitor of activated STATs

pJAK	JAK phosphorylated on its JH1 activation loop tyrosines (e.g., Y1007/Y1008 in JAK2)
PKA	cAMP-dependent protein kinase A
PSK	protein serine/threonine kinase
pSTAT	STAT tyrosine phosphorylated near its C-terminus to enable dimerisation and function as transcription factor (e.g., Y701 in STAT1)
PTK	protein tyrosine kinase
PTP	protein tyrosine phosphatase
PTP1B	protein tyrosine phosphatase 1 B
PTPN	protein tyrosine phosphatase non-receptor type
PV	polycythaemia vera
pY	phosphotyrosine
RA	rheumatoid arthritis
RTK	receptor tyrosine kinase
SAXS	small-angle X-ray scattering
SCID	severe combined immune deficiency
sCNTFR	soluble ciliary neutotrophic factor receptor
SH2	Src homology 2
SH2B	SH2 domain containing protein B
SH2B3	SH2B adaptor protein 3
SHP1	SH2 domain-containing phosphatase 1, a.k.a. PTPN6
SHP2	SH2 domain-containing phosphatase 2, a.k.a. PTPN11
SOCS	suppressor of cytokine signalling
STAT	signal transducer and activator of transcription
SYK	spleen tyrosine kinase
T-ALL	T cell acute lymphoblastic leukaemia
TBS	Tris-buffered saline
TCCR	T cell cytokine receptor
TCPTP	T cell protein tyrosine phosphatase, a.k.a. PTPN2
TSA	thermal stability assay
TSLP	thymic stromal lymphopoietin
TYK2	non-receptor protein-tyrosine kinase 2
WNK	with no Lys (K)
ZAP70	70 kDa zeta-chain associated protein
β_c	common β chain, a.k.a. gp140
γ_c	common γ chain, a.k.a. IL-2R subunit γ

Abstract

Janus kinases (JAKs) are non-receptor tyrosine kinases that mediate signalling of around sixty different cytokines governing various biological processes from the regulation of the immune system, to control of haematopoiesis, metabolism, and development. JAKs are multidomain proteins, in which the tyrosine kinase domain (JH1) is preceded by a pseudokinase domain (JH2). JH2 has critical regulatory functions and is a hotspot for many known oncogenic driver mutations. These mutations, which cause ligand-independent JAK activation, underlie various diseases—most notably haematopoietic malignancies caused by somatic JAK2 JH2 mutations. In the work presented here, we analysed the functions of JH2 and its mutations in the regulation of JAK activity. We found that all JAK JH2s have functional nucleotide-binding sites accessible to ATP and small molecule inhibitors. Most importantly, we found that disruption of ATP binding to JAK2 JH2 suppresses ligand-independent activation, thus identifying the JAK2 JH2 ATP-binding site as a potential drug target for the development of mutation-specific inhibitors. These inhibitors would be a distinct improvement over inhibitors of JAK2 currently used to treat MPNs, as current inhibitors do not distinguish between mutated and wild-type JAK2, and are unable to eradicate the disease. We also present a collaboration effort leading to a simulation-based model for JH2-mediated inhibition of JH1, thereby providing rationale for most known clinical JAK2 mutations. Moreover, we refine our understanding of ligand-mediated and ligand-independent activation of JAKs by presenting a systematic analysis of JAK2 mutations capable of inhibiting ligand-independent hyperactivation. We further identify a novel interface in JAK2 JH2, which is needed for heteromeric JAK2 activation in interferon-γ signalling.

Tiivistelmä

Janus-kinaasit (JAKit) ovat ei-reseptorisia tyrosiinikinaaseja, jotka välittävät yli 60 sytokiinin viestejä soluissa. Nämä viestit säätelevät lukuisia biologisia tapahtumia, kuten immuunijärjestelmän toimintaa, hematopoieesia, aineenvaihduntaa sekä kehitystä. JAKit ovat monidomeenisia proteeineja, joissa viestivää, aktiivista tyrosiinikinaasidomeenia (JH1) edeltää nk. pseudokinaasidomeeni (JH2). JH2 on ensisijaisen tärkeä JAK-aktiivisuuden säätelyssä. Domeenista onkin löydetty lukuisia kliinisesti merkittäviä mutaatioita, kuten autosomaalisia JAK2-mutaatioita, jotka aiheuttavat ligandiriippumatonta JAK-aktivaatiota ja siten johtavat hematopoieettisiin maligniteetteihin. Tässä työssä esitellyissä tutkimuksissa selvitettiin JH2:n sekä sen mutaatioiden toimintaa JAK-säätelyssä. Tutkimuksissa havaittiin, että kaikissa JAK JH2:ssa on toiminnallinen nukleotidinsitomistasku, joka kykenee sitomaan ATP:ta ja pienmolekyylisiä inhibiittoreita. Tärkeimpänä löydöksenä havaittiin, että ATP:n sitoutumisen estäminen JAK2 JH2:n ATP-sitomistaskuun alentaa ligandiriippumatonta JAK2-aktivaatiota. Nämä havainnot osoittavat, että JAK2 JH2 on mahdollinen lääkekohde kohdennettujen JAK-inhibiittoreiden kehittämiselle. Tällaiset inhibiittorit, jotka estäisivät kohdennetusti mutatoituneen (muttei villityyppisen) JAKin toimintaa, olisivat merkittävä parannus verrattuna nykyisiin JAK-estäjiin, jotka eivät kykene erottelemaan villityyppisen ja mutatoituneen JAKin välillä, eivätkä siten pysty parantamaan tautia. Tutkimuksissa kehitettiin yhteistyöprojektina myös molekyylimalli JH2:n toiminnasta JH1:n aktiivisuuden säätelijänä. JH2–JH1-malli selittää useimpien tunnettujen kliinisten JAK2-mutaatioiden toiminnan molekyylitasolla. Lisäksi suoritettiin systemaattinen analyysi JAK2-mutaatioista, jotka voivat estää tautia aiheuttavan JAK2-hyperaktivaation. Tämä analyysi tarkentaa ymmärrystämme JAKien toiminnasta sytokiinivälitteisessä sekä sytokiineista riippumattomassa JAK-aktivaatiossa ja samalla tunnistaa aiemmin tuntemattoman JAK2 JH2 -rajapinnan, joka on välttämätön interferoni-γ-signaloinnille.

1 Prelude

The accrual of knowledge and the progression of understanding in the natural sciences do not follow a linear path, nor do they occur at a constant rate. Rather, advances in a certain field seem to happen in fits, with bursts of new data being produced and published often in rapid succession, followed by seemingly quieter periods. So too, has the understanding of the molecular structure and regulation of Janus kinases (JAKs) seemed to have undergone a quantum leap in the past half-dozen years or so. Upon beginning of the work leading up to this thesis, only the crystal structure of the JAK tyrosine kinase domains had been solved (Boggon et al. 2005, Lucet et al. 2006, Williams et al. 2009, Chrencik et al. 2010). In contrast, now (in 2017) all individual JAK domains have had their structures solved, and we even have molecular understanding of many of the functions of the different JAK domains.

This thesis is my attempt to describe this progress and the part our findings had in it. This thesis is structured as follows: The Review of the Literature aims to summarize the lay of the land relevant to this work as it stood at the onset of my foray into JAKs (in 2012). More recent results from other laboratories not directly impacting the rationale of the work presented here, are mentioned in the Review as well where appropriate. The Aims of the Study (p 49), Materials and Methods (pp 50–58), and the Summary of the Results (pp 59–72) will cover some of our contribution. The Discussion will analyse our results, as well as presenting and discussing other important findings and advancements published by others during this thesis work (p 73 onwards). At the end, some implications and future perspectives of this work will be proposed.

2 Review of the Literature

2.1 Protein kinases and cytokine signalling

Multi-cellular organisms rely heavily on cellular signalling to control the many functions and interactions of cells. Much of this signalling is mediated by soluble, proteinaceous signalling molecules, called cytokines (Liongue, Sertori & Ward 2016). The functions and roles of cytokines have been thoroughly studied especially in the differentiation of myeloid and lymphoid cell types and the regulation of the immune system (Oppenheim 2001, Schwartz et al. 2016).

Cytokines exert their biological functions by binding to specific cytokine receptors on the surfaces of cells and causing a chain of biomolecular events that results in propagation of the signal through the cytoplasm to effector proteins. These effector proteins can take the form of metabolic enzymes, leading to changes in the cells metabolism, components of the cells cytoskeleton, causing the cell to change its shape or motility, and/or transcription factors, leading to changes in the collection of gene products being expressed (Alberts et al. 2013). This chain of events, called signal transduction, is mediated by various kinds of second messengers and relay proteins, one important class of which are protein kinases.

2.1.1 The eukaryotic protein kinase family

The first signs of regulation by protein phosphorylation were discovered in the 1950s in metabolic enzymes (Fischer, Krebs 1955, Krebs, Fischer 1956), and since, protein phosphorylation has been found to regulate practically all aspects of cellular biology (Krebs 1994), with an estimated 30% of all human proteins being phosphorylated at any given time (Cohen 2002). The enzyme family responsible for this phosphorylation are the eukaryotic protein kinases (ePK), which catalyse the transfer of the γ-phosphate of ATP to substrate proteins. The protein family was first systematically described by Hanks and colleagues

(Hanks, Quinn & Hunter 1988), at a time when ~100 protein kinases were known. Later, upon completion of the human genome project, Manning and colleagues compiled the first complete catalogue of protein kinases (the so-called 'kinome') based on similarity of particular sequence motifs (Manning et al. 2002). They identified a total of 518 protein kinases (478 ePKs, the rest being 'atypical kinases'), although the exact number is still being adjusted as the classification of protein kinases is refined[1].

2.1.1.1 The PKL/ePK Fold

EPKs consist of 388 protein serine/threonine and 90 protein tyrosine kinases (PSK and PTK, respectively), named based on the phosphoryl-receiving residue of the substrate protein (Endicott, Noble & Johnson 2012). All ePKs belong to the superfamily of protein kinase-like (PKL) proteins, which also includes many non-ePK kinases, like the phosphatidylinositol-4,5-bisphosphate 3-kinase (PI3K) (Kannan et al. 2007).[2] All PKL proteins share a conserved structural fold and catalytic mechanism, despite tremendous sequence variation (Scheeff, Bourne 2005, Kannan et al. 2007). This structural fold, which constitutes the most abundant catalytic domain in eukaryotic genomes, is characterised by a purely α-helical C lobe and an N-terminal lobe comprised of mostly β-sheets and one α-helix (αC), with the catalytically active, nucleotide-binding site wedged between the lobes (Figure 1). Comprehensive sequence analysis of PKL member proteins has identified 10 extremely conserved characteristic single residues scattered throughout the domain, which seem to be defining features of all PKLs (Figure 1) (Kannan et al. 2007). Six of these residues are involved in ATP or substrate binding (G52, K72, E91, D166, N171, D184; numbering for the archetypal protein kinase cAMP-dependent protein kinase A, PKA, which will be used throughout this review, unless noted otherwise), some of which were already known to be crucial for catalysis from early work (Gibbs, Zoller 1991, Knighton et al. 1991, Grant et al. 1998). In fact, in ePKs, these residues fall into the classical protein kinase sequence motifs identified by Hanks et al. (Hanks,

[1] Tony Hunter, *personal communication* at Kinases and Pseudokinases: Spines, Scaffolds and Molecular Switches, 5.-8.12.2015, in San Diego, California, USA.

[2] Notably, histidine kinases, i.e. protein kinases that phosphorylate histdine residues and play an important role especially in prokaryote cellular signalling (Kannan et al. 2007), are evolutionarily and structurally distinct from PKLs based on the kinase classification of Manning et al. See http://kinase.com/wiki/index.php/Standard_Kinase_Classification_Scheme (accessed 20.10.17).

Quinn & Hunter 1988). Namely, the glycine-rich loop (consensus sequence ψGδ**G**XφGXV[3], including **G**52), the VAI**K**Xψ motif (including the β4 lysine, **K**72), and the αC glutamate (**E**91) in the N lobe, as well as the extended HRD motif (ψψHR**D**ψKXδ**N**ψψψ including **D**166 and **N**171) and the DFG motif (**D**FGψ, including **D**184), in the C lobe (Hanks, Quinn & Hunter 1988, Kannan et al. 2007, Zeqiraj, van Aalten 2010). The function of the remaining four is still not fully understood, but three (H158, H164, D220) probably play a part in positioning the catalytically important DFG motif (Kannan et al. 2007, Taylor, Kornev 2011).

It should be noted that, although the nucleotide-binding pocket is highly conserved in the ePK fold, the architecture of the pocket is not conserved throughout other nucleotide-binding protein families (Zheng, Goncearenco & Berezovsky 2015), despite them sharing similar structural features due to them binding chemically highly similar (or indeed identical) ligands (Gherardini et al. 2010).

Comparative analysis of multiple ePK crystal structures revealed two hydrophobic structures that run through most ePK domains, linking the N and C lobes (Kornev et al. 2006, Kornev, Taylor & Ten Eyck 2008). These structures were termed the regulatory (R) and the catalytic (C) spine (Kornev, Taylor & Ten Eyck 2008, Taylor, Kornev 2011). In the spine model, formation of the R spine via inward movement of L95 (in αC) and F185 (in DFG; the so-called 'DFG-in' position (Möbitz 2015)) is representative of an active, catalytically competent protein kinase conformation (Taylor, Kornev 2011). This conformation, often also called the 'closed conformation', is characterised overall by an inward-turned αC, which lines the boundary of the N and C lobes, with the αC N-terminus close to the activation loop (shown in Figure 1) (Taylor, Kornev 2011). The C spine is completed through binding of the purine ring of ATP in its binding pocket and is thus also indicative of a catalytically active, nucleotide-bound state (Figure 1).

2.1.1.2 Nucleotide binding to protein kinases and mode of catalysis

Protein kinases bind their substrate ATP between the N and C lobes using most of the critically conserved residues described above. Briefly, the purine ring of

[3] Symbols for consensus amino acids are: ψ – hydrophobic, φ – large hydrophobic (F, Y, or W), δ – hydrophilic, X – any amino acid

ATP is positioned between hydrophobic residues from the N and C lobe (part of the C spine, see Figure 1: PKA), with the phosphate groups pointing towards αC, and the adenine base making specific hydrogen bonds to the peptide backbone of the hinge region (Endicott, Noble & Johnson 2012). The phosphates are positioned between the tip of the Gly-rich loop (also called the 'phosphate-binding loop' or 'P-loop') and a basic residue from the C lobe's side (K168 in PKA; usually an arginine in tyrosine kinases) (Taylor et al. 2004). The α and β phosphates bind to K72, which also links to E91 in αC (Figure 1). The canonical binding mode involves two cations (usually Mg^{2+}) bound between the three ATP phosphate groups. The resulting ATP–cation complex is coordinated by N171 and D184 from the DFG motif, so that the γ phosphate is correctly positioned relative to D166, which functions as the catalytic base in the phosphotransfer reaction (Valiev et al. 2003, Iyer et al. 2005).

2.1.1.3 Regulation of protein kinase activity

The mechanisms how protein kinases shuttle from inactive states/conformations to the active ('closed') catalytically competent state described above, vary widely from protein to protein (Endicott, Noble & Johnson 2012, Bayliss, Haq & Yeoh 2015). Some general features do apply, however. For most known protein kinases, the features of the active conformation are very similar. Namely (1) an ordered C helix in the 'in' position with K72–E91 intact, (2) a DFG-in orientation completing the R spine, (3) a functional peptide substrate-binding pocket, usually formed by ordering of the activation loop, and lastly (4) expelling of any potential inhibitory structural components from the active site as often found in tyrosine kinases (Taylor, Kornev 2011, Endicott, Noble & Johnson 2012, Bayliss, Haq & Yeoh 2015, Möbitz 2015). Which of these factors is primarily in use as a "switch" is determined by the individual kinase in question.

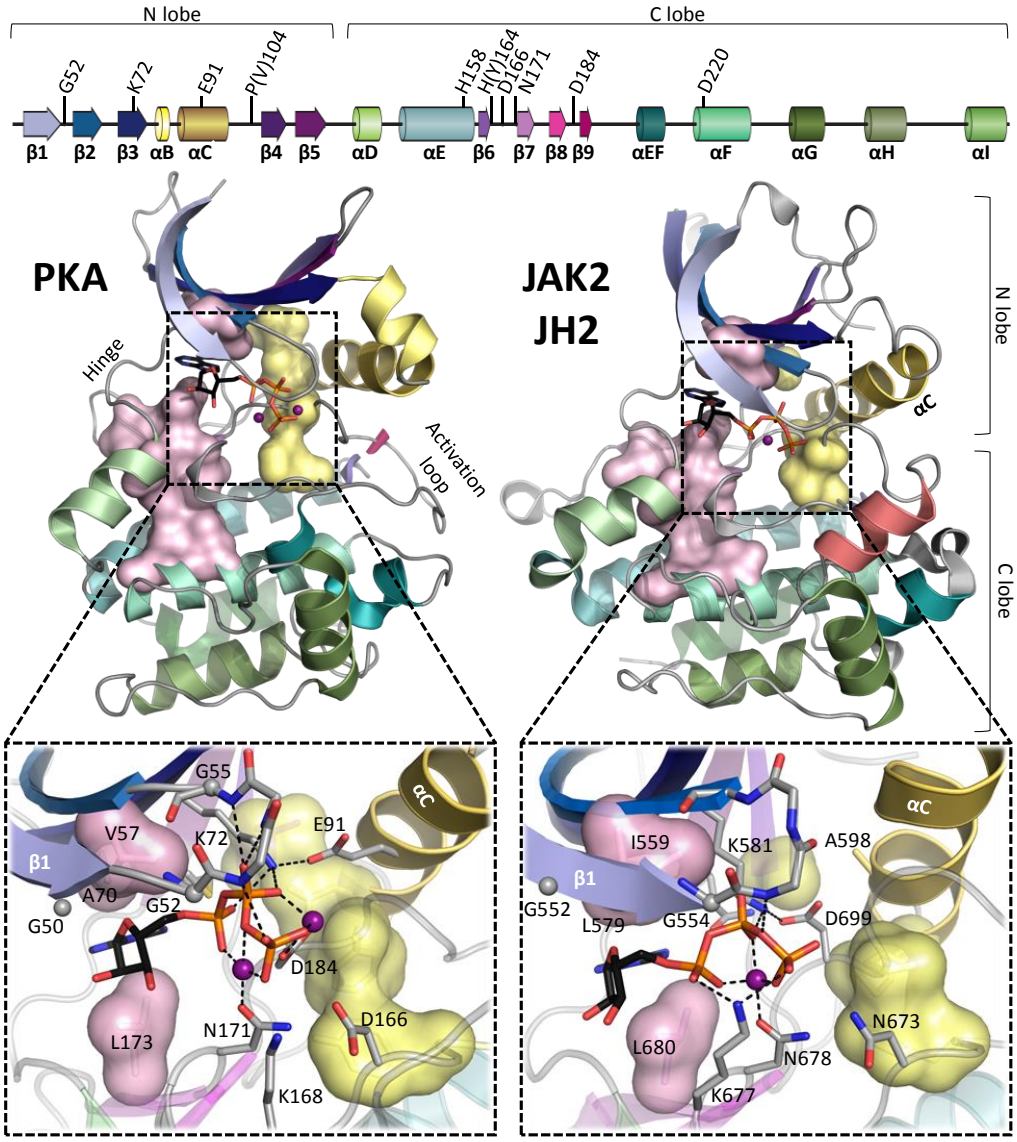

Figure 1: The eukaryotic protein kinase structure and its mode of nucleotide binding. Top: The secondary structure of the archetypal protein kinase PKA. The 10 characteristic residues conserved in all PKLs (Kannan et al. 2007) are shown above with the corresponding PKA residue in parenthesis, in case of deviation from the consensus sequence. Middle: The crystal structures of PKA (PDB: 4WB5) and JAK2 JH2 (PDB: 4FVQ). The colouring of the secondary structure elements is the same throughout the figure. Note that αB is missing from JAK2 JH2. The additional helix (αAL) in the JAK2 JH2 activation loop is shown in salmon red. Bottom: Close-ups of the ATP-binding sites of PKA and JAK2 JH2. PKA exhibits a canonical nucleotide-binding mode. Bound ATP and amino acids critical for nucleotide binding are shown as stick models. The colouring of the stick model atoms are: carbon – grey/black, oxygen – red, nitrogen – blue, phosphorus – orange. The cation cofactors (Mg^{2+}) are shown as purple spheres. Main chain atoms are shown as a cartoon model for clarity, except for the glycine-rich loop. Critical ATP-binding site interactions are shown as black dotted lines. The C and R spines are shown as volume-filling

models in pink and yellow, respectively. Note that only the top-most C spine residue from the C lobe is shown in the close-up. The structure figures, as all other structure figures in this thesis, were made using PyMOL[4].

Some protein kinase domains are constitutively active on their own (e.g., 3-phosphoinositide-dependent kinase-1, PDK1, and phosphorylase kinase, PHK) and need primarily inhibition of activity (by restriction of conformation) or restriction of access to substrates for regulation. A prime example, in which regulation is primarily exerted via intramolecular inhibition is the proto-oncogene tyrosine-protein kinase Src. In Src, SH2 and SH3 domains bind to the hinge side of the kinase domain, thus forcing the C helix in an inactive conformation (Bradshaw 2010). Upon relaxation of this inhibition (by binding of the SH2 and SH3 domains to other recognition sites) the kinase domain relaxes to the active conformation. Other protein kinases are by themselves inactive (e.g., cyclin-dependent kinase 2, CDK2) and need binding or phosphorylation by other proteins or domains in order to adopt the active conformation (Endicott, Noble & Johnson 2012).

Out of activating phosphorylation events, phosphorylation of the activation loop (leading to ordering of the loop and subsequently to strengthening potentially all aspects 1 through 4 mentioned above) is probably the most frequently observed means of regulation (Endicott, Noble & Johnson 2012). Notable exceptions, which do not require activation loop phosphorylation include EGFR, CDK5, and PHK (Endicott, Noble & Johnson 2012).

2.1.2 Pseudokinases

Mapping of the kinome also identified some outlier proteins, which clearly had sufficiently high sequence similarity to be expected to adopt the protein kinase fold, but which were lacking some or all of the residues known to be critical for catalytic activity (Manning et al. 2002). These proteins, which constituted ~10% of the kinome, were collectively dubbed 'pseudokinases'. Some of the identified pseudokinases were already then known to possess catalytic activity through non-canonical ways: the most prominent example being WNK1 (With-No-Lysine(K) 1), which was known to substitute for its lack of K72 with another lysine structurally close by (Xu et al. 2000, Min et al. 2004). Nevertheless, most of them

[4] The PyMOL Molecular Graphics System, Version 1.3 Schrödinger, LLC

were presumed catalytically inactive and, in most cases, their biological function remained a mystery.

Since then, the study of pseudokinases has expanded significantly (Boudeau et al. 2006, Zeqiraj, van Aalten 2010, Reiterer, Eyers & Farhan 2014, Hammarén, Virtanen & Silvennoinen 2015). Out of the 50 originally identified human pseudokinases (Manning et al. 2002), 14 have published crystal structures by 2017[5], along with multiple other interesting pseudokinases from other kingdoms of life, including plants, fungi, protists, and bacteria (Hammarén, Virtanen & Silvennoinen 2015). Upon closer inspection, a few pseudokinases have shown to possess some catalytic activity, most notably HER3 (Shi et al. 2010), CASK (Mukherjee et al. 2008), KSR (Brennan et al. 2011), and JAK2 JH2 (see below), explaining some of their biological function. Still, these seem to be exceptions, and most pseudokinases' functions do not rely on catalysis of phosphotransfer, but rather on functions as (allosteric) regulators, binding competitors, and/or signal integrators (Zeqiraj, van Aalten 2010, Reiterer, Eyers & Farhan 2014, Kung, Jura 2016).

Interestingly, many pseudokinases have retained the ability to bind nucleotides in their (in)active site, even if the ability for catalysis has been lost (Murphy et al. 2014). The biological function of this nucleotide binding is only known for a few cases, however (Hammarén, Virtanen & Silvennoinen 2015).

2.2 Janus kinases and JAK–STAT signalling

2.2.1 A brief history of JAK–STAT

Janus kinases (JAKs) are a group of non-receptor protein tyrosine kinases, which mediate signalling of type I and type II cytokines (Table 1) (Ihle et al. 1995, Schwartz et al. 2016, Villarino, Kanno & O'Shea 2017). JAKs reside in the cytoplasm and are most probably constitutively bound to their cognate receptors (Huang, Constantinescu & Lodish 2001, Giese et al. 2003, Haan et al. 2006). There are four JAKs in mammals, birds, and fish: JAK1, JAK2, JAK3, and

[5] Last checked on PDB on 13.8.2017

TYK2, with JAK1, JAK2, and TYK2 ubiquitously expressed in all cell types, but JAK3 expression restricted mainly to haematopoietic cell types (Yamaoka et al. 2004).

JAK1 and JAK2 were initially identified as protein kinases using PCR with partially-degenerate PTK-specific oligonucleotide probes from cDNA libraries (Wilks et al. 1989, Wilks et al. 1991). Informally the genes were named JAKs for 'Just another kinase', even though the acronym was eventually published to refer to the two-faced ancient Roman god Janus due to the peculiar domain structure of JAKs, which includes two sequential PTK-like domains (Figure 3) (Wilks et al. 1991, Wilks 2008). TYK2 (non-receptor tyrosine kinase 2) was identified simultaneously to JAK1 and 2, albeit with different methodology (Firmbach-Kraft et al. 1990), and JAK3 only some time later (Kawamura et al. 1994, Takahashi, Shirasawa 1994, Witthuhn et al. 1994).

Critically, many of the signalling functions of JAKs were deciphered using mutant cell lines irresponsive to various cytokines (Bonjardim 1998, Stark, Darnell 2012). Analysis of a cell line irresponsive to interferon (IFN) α/β, for example, showed that TYK2 was required for signalling of these cytokines (Velazquez et al. 1992), while another cell line, irresponsive to IFN-γ in addition to IFN-α/β, was found to be lacking JAK1, thus identifying the importance of JAK1 for both of these cytokine classes (Müller et al. 1993, Kohlhuber et al. 1997). Using similar methodology, IFN-γ was found to signal also through JAK2 (Watling et al. 1993, Kohlhuber et al. 1997), and interleukin (IL) 3 and erythropoietin (EPO) solely through JAK2 (Silvennoinen et al. 1993, Witthuhn et al. 1993) (see also Table 1). The signalling cascade was completed by identification of the STAT family of transcription factors as substrates for JAKs (Shuai et al. 1992, Darnell Jr, Kerr & Stark 1994, Wakao, Gouilleux & Groner 1994, Stark, Darnell 2012) (Figure 2). Since then, over 50 cytokines have been found to signal through the JAK–STAT pathway via 4 JAKs and 6 STATs (Table 1), and much has been learned about the regulation of JAK–STAT signalling, as well as the functions of the individual proteins involved.

2.2.2 The JAK–STAT signal transduction pathway

Signalling through the JAK–STAT pathway is initiated by binding of a cytokine to the extracellular domain(s) of its receptor chain(s). This induces dimerisation/oligomerisation of the receptor chains or a conformational change

in the receptor (the details are still poorly understood, see also Discussion 6.3.5) (Ihle et al. 1995), which activates JAKs and causes trans-autophosphorylation of the activation loop of the JAK tyrosine kinase domains (Feng et al. 1997) leading to an increase in catalytic activity (Chatti, Farrar & Duhé 2004). Activated JAKs next phosphorylate the receptor chains on specific tyrosine residues, which serve as docking sites for further JAK substrates, the primary one of which are STATs (Darnell 1997). STATs bind the phosphorylated receptor via their SH2 domains, and are subsequently themselves phosphorylated by JAKs on a specific tyrosine in the C-terminal tail near their SH2 domain (Darnell 1997). This phosphorylation allows STATs to dimerise via their SH2 domains, move into the nucleus and directly bind to DNA, where they act as transcription factors[6] (Darnell 1997, Becker, Groner & Müller 1998, Chen et al. 1998).

Activation of various JAK signalling pathways has been found to cause concomitant activation of (and cross-talk with) other pathways like the MAPK and PI3K pathways, and STATs can also be activated by the action of other tyrosine kinases (Quintás-Cardama et al. 2011, Vainchenker, Constantinescu 2013). Furthermore, non-canonical, phosphorylation-independent (JAK–)STAT signalling has also been described (Majoros et al. 2017, Stark, Cheon & Wang 2017). In this signalling mode, unphosphorylated STATs can regulate gene expression given the correct interaction partner proteins. For example, unphosphorylated STAT1 dimers form and act as transcription factors when bound by IRF9 upon IFN-γ stimulation (Majoros et al. 2017). The remainder of this thesis, however, will focus on canonical, phosphorylation-dependent JAK–STAT signalling.

[6] The effects of JAK–STAT signalling on transcription and epigenetics have been extensively studied (Villarino, Kanno & O'Shea 2017), but will not be discussed further here.

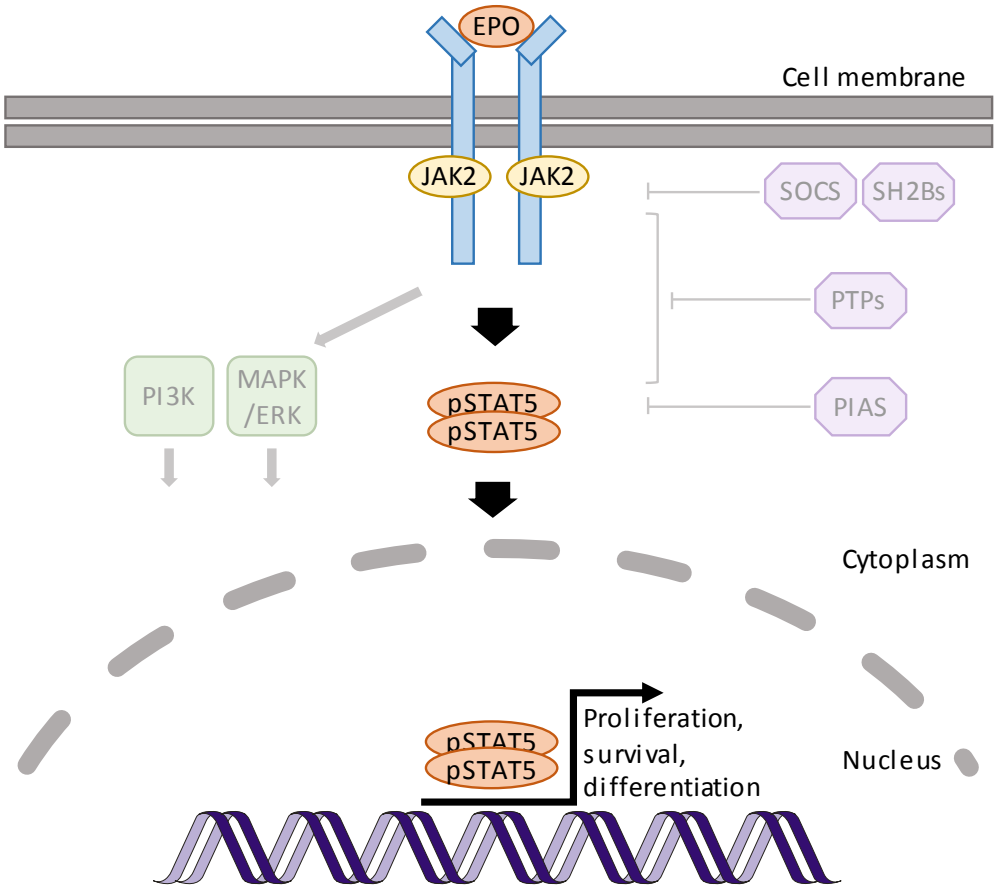

Figure 2: Signalling through the JAK–STAT pathway. The erythropoietin (EPO) signalling pathway is shown as an example of the canonical JAK–STAT pathway. Additional signalling components not part of the archetypal JAK–STAT core are shown faded. Figure is based on following reviews: (Oh, Gotlib 2010, Quintás-Cardama et al. 2011, Vainchenker, Constantinescu 2013).

2.2.2.1 Cytokines and cytokine receptors that signal through JAK–STAT

Type I and type II cytokine receptors (also called haematopoietic and IFN cytokine receptors, respectively (Spangler et al. 2015)) are characterised by conserved features in their extracellular ligand binding domains, which all include so-called cytokine-binding homology regions/domains (CHR/CHD) composed of two fibronectin type III domains (Liongue, Ward 2007). The CHRs of both type I and II receptors include four characteristic cysteines forming two intrachain disulphide bridges (Ihle et al. 1995, Liongue, Ward 2007). Additionally, type I cytokine receptors (but not type II receptors) have a conserved extracellular WSXWS sequence motif near their single transmembrane helix

(Gadina et al. 2001, Liongue, Ward 2007). The cytoplasmic parts of type I and II receptors are highly variable, but most include two somewhat conserved, membrane-proximal JAK-binding regions: a proline-rich region termed box1 and a mostly hydrophobic region called box2 (Murakami et al. 1991). The intracellular parts lack any recognisable protein domain features, and are thought to be mostly unstructured (Bugge et al. 2016, Ferrao, Lupardus 2017).

Type I and II receptors signal in different configurations to activate different JAK pairs, which in turn activate various STATs downstream (Table 1). Evolutionarily the most ancient configuration is probably exemplified by the simplicity of the homotypic receptors of the single chain family (see Table 1), where two identical chains make up the receptor, which signals through a single JAK (JAK2 in mammals) and STAT (STAT5) (Liongue, Sertori & Ward 2016). Concomitantly, out of the mammalian JAKs and STATs, JAK2 and STAT5 are most closely related to the single *Drosophila melanogaster* homologues, Hopscotch (Hop) and STAT92E (Nicola, Hilton 1998, Zeidler, Bausek 2013). Most mammalian type I and II cytokines signal through a combination of receptor chains, which form dimers (e.g., IL-4R), trimers (e.g., IL-2R), tetramers (e.g., G-CSFR), hexamers (e.g., IL-6R) or even dodecamers (GM-CSFR) (Wang et al. 2009). In these configurations, a non-specific "common", JAK-binding, subunit is often coupled to a ligand-specific, high-affinity subunit for signalling (Ihle et al. 1995, Baker, Rane & Reddy 2007). For type I receptors, the shared receptor chains are gp130 (binding at least JAK1 and TYK2), the common β chain (β_c/gp140, binding JAK2), and the common γ chain (γ_c, binding JAK3) (Wang et al. 2009, Wallweber et al. 2014, Ferrao, Lupardus 2017).

The JAK–STAT-utilising cytokines themselves have a characteristic four-helix bundle architecture, in which the topology (up-up-down-down) is constant, but the lengths of the helices vary (Nicola, Hilton 1998, Wang et al. 2009). While both short- (helices of 8–10 residues in length, e.g., IL-2 and IL-3) and long-chain (10–20 residues per helix, e.g., EPO and IL-6) four-helix bundle cytokines signal through type I and II cytokine receptors, some short-chain cytokines activate receptor tyrosine kinases (RTKs) instead (Nicola, Hilton 1998, Wang et al. 2009). Furthermore, some of the four-helix cytokines form dimers of two four-helix bundles to produce the active, signalling form (e.g. IL-5 and IFN-γ) (Wang et al. 2009).

Table 1: JAK–STAT signalling pathways. See opposite page for details.

		Cytokine	Receptor chain(s)			JAKs	STATs	References
TYPE II CYTOKINE RECEPTORS	IFN family	IFN-I (typeI)*	IFNAR1	IFNAR2		**JAK1**, TYK2	**STAT1, STAT2**, STAT3, STAT4 (STAT5, STAT6)	I, II
		IFN-γ (typeII)	IFNGR1	IFNGR2		**JAK1, JAK2**	**STAT1**	I, II, X
		IL-28a, IL-28b, IL-29‡	IL-28R / IFNLR1	IL-10Rβ		**JAK1**, TYK2	**STAT1, STAT2,** STAT3, STAT5	I, VIII, XII, XIII
		IL-10	IL-10Rα	IL-10Rβ		**JAK1, TYK2**	**STAT3**, STAT1	I, II, XII
		IL-19	IL-20Rα	IL-20Rβ		JAK1, JAK2	**STAT3,** STAT1	I, X, XII
		IL-20, IL-24 / mda7	IL-20Rα or IL-22R	IL-20Rβ		JAK1, JAK2	**STAT3,** STAT1	I, X, XI, XII
		IL-22 / IL-TIF†	IL-22R	IL-10Rβ		JAK1, TYK2	**STAT3,** STAT1, (STAT5)	I, X
		IL-26 / AK155	IL-20Rα	IL-10Rβ		JAK1, TYK2	**STAT3,** STAT1	I, XI, XII
TYPE I CYTOKINE RECEPTORS	gp130 family	IL-6	IL-6Rα	gp130		**JAK1,** JAK2, TYK2	**STAT3,** STAT1	I, II, IX
		IL-11	IL-11Rα	gp130		**JAK1,** JAK2, TYK2	**STAT3,** STAT1	I, II, IX
		LIF	LIFRβ	gp130		**JAK1,** JAK2, TYK2	**STAT3,** STAT1	I, II, VI, IX
		CNTF	CNTFRα	LIFRβ	gp130	JAK1, (JAK2, TYK2)	**STAT3,** (STAT1)	I, II, IX, XIV
		CLCF1§, NP	CNTFRα	LIFRβ	gp130	JAK1, (JAK2)	**STAT3,** STAT1	I, IX, XIV
		CT-1	CNTFRα	LIFRβ	gp130	JAK1, (JAK2, TYK2)	**STAT3**	I, II, IX
		OSM	OSMRβ or LIFRβ	gp130		JAK1, (JAK2, TYK2)	**STAT3,** STAT1	I, II, VI, IX
		IL-31	IL-31Rα / GLMR	OSMRβ		JAK1, (JAK2)	STAT3, STAT5, STAT1	I, V
		G-CSF	GCSFR / CSF3R			JAK1, (JAK2)	**STAT3**	I, II, IX
		Leptin	LEPR / OBR			JAK2	**STAT3**	I
		IL-12 (p35+p40)	IL-12Rβ2	IL-12Rβ1		**TYK2,** JAK2	**STAT4**	I, II, XV
		IL-23 (p19+p40)	IL-23R	IL-12Rβ1		**TYK2,** JAK2	**STAT3, STAT4,** STAT1	I, XV
		IL-27 (p28+EBI3)‖	IL-27Rα¶	gp130		JAK1, JAK2, TYK2	**STAT1, STAT3**, STAT4, (STAT5)	I, IX, XV
		IL-35 (p35+EBI3)#	IL-12Rβ2	gp130		JAK1, JAK2	STAT1, STAT4	I, XV
	γ_c family	IL-2	IL-2Rα	IL-2Rβ	γ_c	**JAK1, JAK3**, (JAK2)	**STAT5,** (STAT3)	I, II, IX, XVI
		IL-4	IL-4Rα	γ_c		**JAK1, JAK3**	**STAT6**	I, II, IX, XVI
		IL-7	IL-7Rα	γ_c		**JAK1, JAK3**	**STAT5,** (STAT3)	I, II, IX, XVI
		IL-9	IL-9Rα	γ_c		JAK1, JAK3	**STAT5,** STAT3	I, II, IX, XVI
		IL-15	IL-15Rα	IL-2Rβ	γ_c	**JAK1, JAK3**	**STAT5,** (STAT3)	I, IX, XVI
		IL-21	IL-21R	γ_c		JAK1, JAK3	**STAT3,** STAT5, (STAT1)	I, IX, XVI
		TSLP	IL-7Rα	TSLPR / CRLF2		JAK1, JAK2	STAT1, STAT3, STAT4, STAT5, STAT6	I, XVI, XVII
		IL-13	IL-4Rα	IL-13R		JAK1, JAK2, TYK2	**STAT6,** (STAT3)	I, II, XVI
	IL-3 / β_c	IL-3	IL-3Rα	β_c (gp140)		JAK2, (JAK1)	**STAT5**, STAT3	I, II, IX, XVIII
		IL-5	IL-5Rα	β_c (gp140)		JAK2	**STAT5**, STAT1, STAT3	I, II, IX
		GM-CSF	GM-CSF-Rα	β_c (gp140)		JAK2	**STAT5**	I, II, IX
	Single chain	EPO	EPOR			**JAK2**	**STAT5**	I, II, IX
		GH	GHR			**JAK2**	**STAT5,** (STAT3)	I, II, IX
		PRL	PRLR			**JAK2**	**STAT5**	I, IX
		TPO	TPOR / MPL			**JAK2**	**STAT5**	I, II, IX

*Table 1 legend: Type I and II cytokines, their receptor chain configurations, as well as the corresponding JAKs and STATs are shown. JAKs and STATs critical for signalling identified with the highest confidence are shown in **bold**, associated JAKs and STATs for which the data is weaker are shown in parentheses. Cytokines that signal through the same receptor-JAK–STAT configuration are separated by commas. See List of Abbreviations for explanations of abbreviations. Synonyms are separated by a slash. In case of three or more often-used synonyms (or for additional explanations), see the following notes:*

**In humans this family consists of 12 IFN-αs, IFN-ω and Limitin (a.k.a. IFN-ζ).*
†IL-22 also has a soluble receptor IL-22BP, which probably works as an agonist in vivo (Renauld 2003, Rutz, Wang & Ouyang 2014).
‡Interleukins 28 and 29 are also called Type III IFNs, or IFN-λs, as follows: IL-29/IFN-λ1, IL-28a/IFN-λ2, and IL-28b/IFN-λ3.
§a.k.a. CLC, CLF, NNT-1, BSF-3; CLCF1 is secreted either with sCNTFR or CRLF1.
||IL-27 p28 subunit is also called IL-30, which might signal through IL-6Rα (Aparicio-Siegmund, Garbers 2015).
¶a.k.a. WSX-1, TCCR.
#IL-35 has also been reported to signal through IL-12Rβ2 or gp130 homodimers (Vignali, Kuchroo 2012).

Data on this table was compiled from the following references:

I: (Schindler, Plumlee 2008)
II: (Baker, Rane & Reddy 2007)
III: (Spangler et al. 2015)
IV: (Liongue, Ward 2007)
V: (Zhang et al. 2008)
VI: (Dey et al. 2013)
VII: (Ihle et al. 1995)
VIII: (Quintás-Cardama et al. 2011)
IX: (Wang et al. 2009)
X: (Renauld 2003)
XI: (Rutz, Wang & Ouyang 2014)
XII: (Commins, Steinke & Borish 2008)
XIII: (Kotenko 2011)
XIV: (Sims 2015)
XV: (Vignali, Kuchroo 2012)
XVI: (Kovanen, Leonard 2004)
XVII: (Zhong et al. 2014)
XVIII: (Rodig et al. 1998)

In addition to these cytokines and their receptors, JAKs have been reported to be (co)activated upon stimulation of a wide range of cytokines, including some growth factors, which primarily signal through RTKs. JAKs have also been implicated to act in the nucleus to directly phosphorylate various transcription factors and histones (Zouein, Duhé & Booz 2011). These data may represent aspects of cross talk between various signalling pathways (most of which are not critically dependent on JAKs) or specialised functions in certain disease states or stages of development, and are not discussed further in this review.

2.3 Regulation of JAK–STAT signalling

Activity of the JAK–STAT pathway is tightly regulated on both intra- and intermolecular levels to ensure suppression of signalling in the absence of cytokine stimulation, and to allow rapid, transient activation of signalling upon stimulation. In the absence of stimulation, arguably the most important level of

regulation inhibiting protein tyrosine kinase activity (referred to as 'kinase activity' hereafter in the context of JAKs) is mediated through intramolecular regulation of JAKs by the pseudokinase domain (JH2) (discussed in detail in 2.5 below).

In terms of phosphorylation, JAK2, for instance, is phosphorylated in the basal state (i.e. in the absence of a stimulating cytokine signal) on a single inhibitory residue only (S523), which seems to be needed for keeping JAK2 in an autoinhibited state (Ishida-Takahashi et al. 2006, Ungureanu et al. 2011). Upon stimulation, JAK2 is activated by (*trans*-)autophosphorylation on the tyrosine kinase domain's activation loop (Y1007/Y1008), as well as multiple other residues (Y637, Y868, Y966, Y972), which are needed for full activation of kinase activity (Table 2) (Robertson et al. 2009). Subsequently, termination of signalling is thought to be initiated by phosphorylation of multiple inhibitory residues all along the protein. These may cause dissociation of JAK2 from its receptors (Y119 (Funakoshi-Tago et al. 2006)) or directly inhibit catalytic activity (e.g., Y570 (Robertson et al. 2009, Ungureanu et al. 2011)). In most cases, the phosphorylation of these sites has been reported to be dependent on JAK2 kinase activity or activation loop phosphorylation of the tyrosine kinase domain (see also Table 2). The exact sequence of phosphorylation events during receptor-mediated activation is yet to be fully elucidated, nor is it clear, whether or how these phosphorylation events vary in different cytokine receptor contexts.

After stimulation, signalling is also terminated by multiple other means including (de)phosphorylation, production of inhibitory proteins, and the lowering of available signalling complexes through internalisation and lysosomal as well as ubiquitination-mediated proteasomal degradation of receptors (Vainchenker, Constantinescu 2013, Babon et al. 2014). Dephosphorylation of both JAK and receptor tyrosines is induced by multiple protein tyrosine phosphatases, especially SHP1 and 2, PTP1B, TCPTP, and CD45 (Argetsinger et al. 2004, Babon et al. 2014). Other inhibitory proteins that participate in the termination of JAK–STAT signalling include the family of suppressors of cytokine signalling (SOCS1–7 and CIS), whose transcription is induced by activated STATs, thus forming a negative feedback loop (Vainchenker, Constantinescu 2013). The mechanism of action of SOCS proteins has been revealed for SOCS3, which was shown to bind to both JAK and the associated cytokine receptor, and to inhibit activity of the

tyrosine kinase domain by directly interacting with its activation loop, as well as initiating ubiquitination of JAKs (Babon et al. 2012, Kershaw et al. 2013).

Other regulatory proteins acting on JAKs are members of the SH2B family of proteins (including SH2B, APS, and SH2B3 a.k.a. LNK), which have been reported to solely bind to phosphorylated Y813 on JAK2, and have differing effects: while SH2B and APS are able to activate JAK2-mediated signalling, LNK is a well-defined inhibitor of JAK2 (reviewed in (Babon et al. 2014)). JAK–STAT signalling is also regulated at the level of STATs, by protein inhibitor of activated STATs (PIAS) proteins, which inhibit signalling by inducing SUMOylation of STATs (Vainchenker, Constantinescu 2013, Rabellino, Andreani & Scaglioni 2017).

2.4 JAK mutations and JAK-mediated diseases

In general, JAKs govern key signalling steps in development and growth, but are especially important in the regulation of haematopoiesis and the immune system. Owing to their differences in cellular signalling pathways (see Table 1), different JAKs are implicated in different diseases—be it as parts of signalling pathways associated with the pathogenesis of a disease, or as drivers of disease due to specific JAK mutations. Examples of the former are especially found in immunological diseases, like rheumatoid arthritis (RA) and other autoimmune disorders, where JAK inhibitors are currently being tested and successfully applied (Norman 2014, Yamaoka 2016, Winthrop 2017). Lately, JAKs have also been found to be potentially interesting targets and prognostic markers in the treatment of various cancers (Zhang et al. 2016, Pencik et al. 2016).

Examples of diseases caused or driven by JAK mutations are most commonly found in immunodeficiencies, leukaemia as well as other haematological malignancies, and are discussed in more detail below.

Table 2: Known regulatory phosphorylation sites on JAK2. See opposite page for details.

Structure		Residue	Basal activity	Phosphorylated upon	Phosphorylated by	Effect of phosphorylation / mutation of site	References
FERM	Y	119	-	Stimulation (EPO)	Probably JH1*	Phosphorylation likely to mimic Y119E, which induces dissociation from EPOR, GHR, PRLR, but not IFNGR2.	(Funakoshi-Tago et al. 2006)
	Y	201	+§	?	Autophos. (in vitro)	Y201F inhibits Ang II-mediated JAK2-signalling. §	(Godeny et al. 2007, Robertson et al. 2009)
	Y	206	NE	?	?	Y206F has no appreciable effect on EPO signalling.	(Godeny et al. 2007, Robertson et al. 2009)
	Y	221	+	Stimulation (GH, IL-3)	Autophos. (in vitro and in cells)	Y221F decreases basal pJAK2.	(Argetsinger et al. 2004, Feener et al. 2004)
	Y	317	-	Stimulation (EPO)	Probably mostly JH1*	Y317F causes ligand-independent pJAK2.	(Robertson et al. 2009)
	Y	372	-	?	?	Y372F decreases basal and stimulated (IFN-γ, EGF) pJAK2, pSTAT1 and JAK2-STAT1 interaction.	(Robertson et al. 2009, Sayyah et al. 2011)
	Y	373	+	?	?	Y373F decreases basal pJAK2.	(Sayyah et al. 2011)
Link	S	523	-	Constitutive	JH2 (in vitro)	S523A slightly increases basal pJAK2.	(Ishida-Takahashi et al. 2006, Mazurkiewicz-Munoz et al. 2006, Ungureanu et al. 2011)
JH2	Y	570	-	Stimulation (GH, EPO, IL-3)	Autophos. (in vitro), JH2 (in vitro)	Y570F increases basal pJAK2, pSTAT3 and prolongs EPO-induced activity.	(Argetsinger et al. 2004, Feener et al. 2004)
	Y	637	+	Stimulation (EPO)	Probably mostly JH1*	Y637F lessens and shortens JAK2 activation upon EPO stimulation and partially inhibits V617F.	(Robertson et al. 2009)
Link	Y	813	+	Stimulation (GH)	Autophos. (in vitro)	Y813F reduces SH2-Bβ induced pJAK2 and pSTAT5. pY813 putative binding site for activator protein SH2-Bβ.	(Kurzer et al. 2004)
JH1	Y	868	+	Stimulation (GH)	JH1 (in vitro)	Y868F decreases basal and GH-induced pJAK2, pSTAT3/5.	(Argetsinger et al. 2010)
	Y	913	-	Upon and after stimulation (EPO)	Probably JH1*	Y913F increases EPO-induced pJAK2/pSTAT5. Y913E removes EPO-induced JAK2 activation.	(Funakoshi-Tago et al. 2008b)
	Y	966	+	Stimulation (GH)	JH1 (in vitro)	Y966F decreases basal and GH-induced pJAK2, pSTAT3/5	(Argetsinger et al. 2010)
	Y	972	+	Stimulation (GH)	JH1 (in vitro)	Y972F decreases basal and GH-induced pJAK2, pSTAT3/5	(Argetsinger et al. 2010)
	Y	1007	+	Stimulation	JH1	Y1007F removes basal and cytokine-induced JAK2 activation and downstream signalling	(Feng et al. 1997, Chatti, Farrar & Duhé 2004)
	Y	1008	NE	Stimulation	JH1	Y1008F has little effect on JAK2 activation.	(Feng et al. 1997)

Table 2 legend: Regulatory phosphorylation sites, their effect on basal JAK2 activity (measured as pJAK2 (pY1007/Y1008) or a downstream measure like STAT phosphorylation (pSTAT) or transcriptional reporter activity), the probable phosphorylating kinase, and assumed effects of phosphorylation (mostly based on mutagenesis experiments) are shown. The cytokines, which have been experimentally tested for inducing specific phosphorylation, are shown in parenthesis. Sites for which no functional follow-up data has been published, have been omitted for clarity (Matsuda et al. 2004, Rikova et al. 2007). NE – no effect. Autophos. – autophosphorylation by full-length JAK2. ? – no data available.

**Dependent on JAK2 Y1007/Y1008 phosphorylation and/or JH1 kinase activity.*

[§]Y201F has no effect on EPO-induced pJAK2, but inhibits Ang II-mediated pJAK2, pSTAT1/3. Phosphorylation probably enables binding of SHP-2 and subsequent binding to AT1 receptor. Y201F has also been shown to inhibit activation by JAK2 V617F (Yan, Hutchison & Mohi 2012).

2.4.1 JAK loss-of-function mutations

Currently, there are no known diseases caused by JAK1 or JAK2 loss-of-function (LOF) mutations (Hirahara et al. 2016). This is probably best explained by the essential roles of JAK1 and JAK2 in many crucial signalling pathways (Table 1), which is also highlighted by experimental loss-of-function models. JAK2 knock-outs are embryonic lethal due to a lack of definitive erythropoiesis (Neubauer et al. 1998), and while JAK1 knock-out mice are viable, they die soon after birth due to neurological defects (in addition to having immunological problems) (Rodig et al. 1998). Some somatic JAK1 LOFs have been reported (Hayashi et al. 2006), but the biological relevance of these is not well established.

For JAK3, multiple known clinical LOF mutations are associated with (and the cause of) severe combined immunodeficiency (SCID) characterised by lymphopenia due to a lack of signalling by γ_c cytokines (Table 1) (O'Shea et al. 2004). Patient homozygous for TYK2 LOF mutations, on the other hand, exhibit primary immunodeficiencies due to deficient signalling of multiple cytokines (IL-12, IFN-α/β, and IL-23 among others) and higher susceptibility to viral, bacterial (including mycobacterial), and fungal infections (Minegishi et al. 2006, Casanova, Holland & Notarangelo 2012, Kreins et al. 2015).

2.4.2 JAK gain-of-function mutations

The first gain-of-function (GOF) point mutations in JAKs were identified in the *Drosophila melanogaster* JAK homologue, Hop. The first allele identified was termed Hopscotch$^{Tumorous\text{-}lethal}$ (Hop$^{Tum\text{-}l}$), since it caused a dominant, leukaemia-like melanotic tumour (Corwin, Hanratty 1976, Hanratty, Ryerse 1981). The mutation was identified to be caused by a GOF mutation in the FERM-domain (Hop G341E) (Luo, Hanratty & Dearolf 1995). Interestingly, another mutation (Hop^{T42}) causing a similar disease phenotype was also identified, but in JH2 (Hop E695K) (Luo et al. 1997). This second finding in particular turned out to be highly prescient, as JH2 was soon found out to be a veritable hot spot for clinically highly-relevant JAK GOF mutations (Vainchenker, Constantinescu 2013).

2.4.2.1 JAK2 GOF mutations and myeloproliferative neoplasms

Despite the earlier findings of rare oncogenic JAK2 fusion proteins as drivers for human leukaemia (e.g., constitutively active, dimeric TEL-JAK2 fusions (Lacronique et al. 1997)), the clinical significance of JAK mutations as causes for diseases virtually exploded with the finding of a single somatic JAK2 mutation underlying ∼50% of all myeloproliferative neoplasms (MPNs) (Vainchenker, Constantinescu 2013). The mutation in question, JAK2 V617F caused by a single G-to-T transition (changing GTC to TTC), was identified practically simultaneously by four different teams in 2005 (Baxter et al. 2005, James et al. 2005, Kralovics et al. 2005, Levine et al. 2005). It was found to underlie over 95% of polycythaemia vera (PV) and around 50% to 60% of essential thrombocythaemia (ET) and primary myelofibrosis (PMF) cases (Baxter et al. 2005, Skoda, Duek & Grisouard 2015).

MPNs are a group of diseases characterised by the overproliferation of myeloid cells, where the overproliferating cell type determines the MPN in question—e.g. overproliferation of erythroid cells leading to erythrocytosis and PV. In practice, MPNs seem to be caused by acquired, activating somatic mutations (JAK2 V617F being the most common) in haematopoietic stem cells, which lead to growth factor-independent growth and expansion of the mutated clone (Skoda, Duek & Grisouard 2015). Work on mouse models of MPNs has shown

that the disease can be initiated by a single haematopoietic stem cell carrying JAK2 V617F, which then gradually overpopulates its niche and outcompetes wild-type cells (Lundberg et al. 2014). Homozygosity for JAK2 V617F seems to also be selected for, as a distinct loss of heterozygosity (i.e. enrichment of JAK2 V617F alleles) has been observed in human MPNs (James et al. 2005, Kralovics et al. 2005).

Other genes that are frequently mutated and act as drivers in MPNs are the JAK2-associated receptors thrombopoietin receptor (TPOR/MPL) and granulocyte colony-stimulating factor 3 receptor (GCFSR/CSF3R) (see also Table 1), as well as the multifunctional endoplasmic reticulum protein calreticulin (CALR) (Skoda, Duek & Grisouard 2015). All of these eventually lead to increased signalling through JAK2, as has lately also been shown for CALR mutations. All MPN-associated CALR mutations are frame-shifts, which result in the formation of a highly positively charged protein sequence at the C-terminus of mutated CALR (Elf et al. 2016). This seems to enable mutated CALR to directly interact with TPOR, potentially while still in the endoplasmic reticulum, leading to activation of the receptor and associated JAK2 (Elf et al. 2016, Araki, Komatsu 2017).

After JAK2 V617F, many other similar mutations in JAK2 and other JAKs have been identified and found to be causative of not only MPNs, but also B and T-cell leukaemia (JAK1, JAK2, and JAK3 mutations (Flex et al. 2008, Mullighan et al. 2009, Zhang et al. 2012, Bellanger et al. 2014, Springuel et al. 2014, Losdyck et al. 2015)), acute megakaryoblastic leukaemia (AMKL, JAK2 and JAK3 mutations (Hama et al. 2012, Koo et al. 2012, Bellanger et al. 2014)), as well as solid cancers (JAK1 and JAK3 mutations (Jeong et al. 2008)) among others.

In addition to JAK mutations identified in patients, multiple experimental mutagenesis screens have been performed to discover mutations affecting JAK activity (Yeh et al. 2000, Zhao et al. 2009, Gordon et al. 2010). Most of these mutations cluster strongly into the SH2-JH2 linker and JH2 (See Table 3 for known JAK2 mutations) (Gnanasambandan, Sayeski 2011). Due to its relatively high frequency of occurrence, JAK2 V617F is by far the most studied of these mutations, and often serves as the archetypal hyperactivating JAK mutation. Analysis in cell culture models has shown that, while JAK2 carrying the V617F mutation is able to activate in a ligand-independent fashion (and consequently

phosphorylate/activate downstream STATs), it does still require the presence of JAK2-associated, homotypic receptors to transform cells (e.g., EPOR, TPOR, GCSFR) (Lu et al. 2005, Lu, Huang & Lodish 2008). This finding was initially postulated to explain, why only myeloid lineage cells seemed to be affected by JAK2 V617F, as lymphoid cells do not express homotypic receptors (Lu, Huang & Lodish 2008). Later work has shown, however, that this requirement is not absolute, as ligand-independent activation of JAK2 by the mutation V617F is firstly dependent on JAK2 V617F expression levels (Haan et al. 2009), and secondly that JAK2 V617F can also utilise lymphoid receptors like IL-27Rα, IL-3Rα, and β_c (at least in cell culture models) (Pradhan et al. 2010).

The different MPN driver mutations, including the different JAK2 mutations, have somewhat different biological activity and disease profiles. For example, CALR mutations primarily lead to thrombocytosis and associated ET and PMF (Cazzola, Kralovics 2014), which is readily understood from their probable mode of action in activating TPOR, as described above (Elf et al. 2016). With JAK2, exon 12 mutations mostly lead to erythrocytosis (and thus PV), whereas V617F and exon 16 mutations (see Table 3) can also lead to associated granulocytosis, thrombocytosis, and leukaemia (Scott et al. 2007, Skoda, Duek & Grisouard 2015). This differential pattern of activating mutations leading to diseases is also true for some recently identified germline JAK2 mutations, which seem to preferentially cause thrombocytosis (Skoda, Duek & Grisouard 2015).

Furthermore, different mutations have been reported to have differing levels of enzymatic kinase activity, which, however, do not directly translate into transformation potential in cell culture models (Zou, Yan & Mohi 2011). Out of JAK2 V617F, K539L and T875N, immunoprecipitated T875N shows the highest kinase activity *in vitro*, but V617F has the highest transforming potential (Zou, Yan & Mohi 2011). These differences have been suggested to be due to differing affinities for the interaction of mutated JAK2 and different receptors (Zou, Yan & Mohi 2011), or differing signalling patterns on different receptors (Yao et al. 2017). However, overall the differences in activation mechanisms of the different mutations have not been well understood (see also 2.5.3 below).

Table 3: Clinical and noteworthy experimental mutations in JAK2. Clinical mutations were expanded from similar compilations in (Gnanasambandan, Sayeski 2011, Lupardus et al. 2014). Clin – clinical, found in patient samples; Exp – experimental mutations; Basal JAK activity – measured as pJAK2, pSTAT, or transcriptional activity in reporter assay: +/- increase/decrease in basal activity, respectively; NE – no appreciable effect.

#	Start residue	End residue	JAK structure	Mutation	Clinical/Experimental	Basal JAK activity	Effect	Disease?	Reference
Exon structure									
3	1	75							
			FERM	E 61 K	Clin			Putative Primary Erythrocytosis	(Camps et al. 2016)
4	77	116	FERM	T 108 A	Clin	NE	Slightly EPO hypersensitive	Found as germline mutation in V617F-positive PV patient	(Lanikova et al. 2016)
			FERM	Y 114 A	Exp	-	Probably disrupts receptor recruitment of JAK2. Suppresses V617F.		(Wernig et al. 2008, Andraos et al. 2012)
5	118	156	FERM	Y 119 E	Exp	-	Induces dissociation from receptor by mimicking Y119 phosphorylation		(Funakoshi-Tago et al. 2006)
			FERM	Y 119 F	Exp	+	Removes putative negative phosphorylation site		(Funakoshi-Tago et al. 2006)
			FERM	E 177 V	Clin			Putative Primary Erythrocytosis	(Camps et al. 2016)
6	157	204	FERM	Y 201 F	Exp	-	Reduces JAK2 activation in Ang II signalling. Suppresses V617F.		(Godeny et al. 2007, Yan, Hutchison & Mohi 2012)
7	206	312	FERM	G 276 A	Clin			Putative Primary Erythrocytosis	(Camps et al. 2016)
			FERM	Y 317 F	Exp	+	Removes putative negative phosphorylation site		(Robertson et al. 2009)
8	313	352	FERM	R 340 Q	Clin			PV	(Aranaz et al. 2010, Lupardus et al. 2014)
			FERM	Y 372 F	Exp	-	Removes putative positive phosphorylation site		(Sayyah et al. 2011)
			FERM	Y 373 F	Exp	(-)	Removes putative positive phosphorylation site		(Sayyah et al. 2011)
9	353	404	Link	L 393 V	Clin	NE	Might be weakly EPO hypersensitive	Found as germline mutation in V617F-positive PV patient	(Lanikova et al. 2016)
10	406	442	SH2	R 426 K	Exp	NE	Suppresses V617F; stimulatable with cytokine (EPO and IL-3)		(Gorantla et al. 2010)
11	443	504							

			Linker	T	514	M	Clin			MPNs	(Ma et al. 2009)
				N	531	I	Exp	(+)			(Zhao et al. 2009)
				N	533	I/Y	Clin			PV (together with K539L)	(Gnanasambandan, Sayeski 2011)
				M	535	I	Clin	+		AMKL	(Zhao et al. 2009, Lupardus et al. 2014)
			JH2	H	538	L	Exp	+			(Zhao et al. 2009)
12	506	547		K	539	L	Clin	+		PV	(Scott et al. 2007)
				I	540	T	Clin			PV	(Lupardus et al. 2014)
					538-547		Clin		Various deletions and insertions	MPNs	(Lupardus et al. 2014, Delic et al. 2016)
				D	544	G	Clin			PV	(Lupardus et al. 2014)
				L	545	S	Clin			PV	(Lupardus et al. 2014)
				F	547	L	Clin			PV	(Lupardus et al. 2014)
				F	556	L	Clin			MPNs	(Gnanasambandan, Sayeski 2011)
				R	564	Q	Clin	+		Hereditary ET	(Etheridge et al. 2014)
				V	567	A	Clin			MPNs	(Gnanasambandan, Sayeski 2011)
				Y	570	F	Exp	+	Removes negative phosphorylation site		(Feener et al. 2004)
				G	571	S	Clin	NE		Asymptomatic / Erythrocytosis	(Bahar, Barton & Kini 2016, Milosevic Feenstra et al. 2016)
13	548	592		L	579	F	Clin	-		MPNs (most likely passenger*)	(Ma et al. 2009, Gnanasambandan, Sayeski 2011)
				K	581	A	Exp	+	Disrupts ATP-binding site of JH2, loss of S523 and Y570 phosphorylation		(Ungureanu et al. 2011)
				H	587	N	Clin			MPNs	(Gnanasambandan, Sayeski 2011)
				R	588	A	Exp	(+)			(Wan et al. 2013)
				S	591	L	Clin			MPNs	(Gnanasambandan, Sayeski 2011)
				E	592	A	Exp	(+)			(Wan et al. 2013)
				F	595	A	Exp	NE	Suppresses V617F; stimulatable with EPO		(Dusa et al. 2010)
				H	606	Q	Clin			MPNs	(Gnanasambandan, Sayeski 2011)
				K	607	N	Clin	+		AML	(Gnanasambandan, Sayeski 2011)
				H	608	Y	Clin			MPNs	(Gnanasambandan, Sayeski 2011)
14	593	621		L	611	S	Clin	+		ALL	(Gnanasambandan, Sayeski 2011)
				Y	613	E	Exp	+	Increases JH1 activity, when EPOR is present		(Funakoshi-Tago et al. 2008a)
				V	617	F	Clin	+		MPNs	(Baxter et al. 2005, James et al. 2005, Kralovics et al. 2005, Levine et al. 2005)
				V	617	I	Clin	+		MPNs	(Gnanasambandan, Sayeski 2011)

*Probably a passenger mutation, as L579F does not appreciably increase basal JAK2 activation (see Results of Article II)

			JH2	C	618	R	Clin	+		MPNs	(Wu et al. 2012)
				D	620	E	Clin			MPS	(Schnittger et al. 2006)
				N	622	I	Exp	+		Erythrocytosis in mice	(Zhao et al. 2009)
				L	624	P	Clin			MPNs	(Gnanasambandan, Sayeski 2011)
				E	627	E	Clin			MPS (passenger?)	(Schnittger et al. 2006)
				K	630	G	Exp	NE	Designed to add flexibility to the JH2 hinge		(Zhao et al. 2009)
15	623	664		F	631	G	Exp	(+)	Designed to add flexibility to the JH2 hinge		(Zhao et al. 2009)
				Y	637	F	Exp	(-)	Removal of putative positive phosphorylation site. Slight suppression of V617F and cytokine stimulation		(Robertson et al. 2009)
				I	645	V	Clin			MPNs	(Gnanasambandan, Sayeski 2011)
				E	665	K	Exp	+	Corresponds to Hop^{T42} mutant		(Luo et al. 1997)
				I	682	F	Clin	+		ALL	(Mullighan et al. 2009)
16	665	710		R	683	G[†]	Clin	+		ALL	(Bercovich et al. 2008, Mullighan et al. 2009)
				F	694	L/S	Exp	+			(Zhao et al. 2009)
				V	706	A	Exp	(+)			(Wan et al. 2013)
				L	707	A	Exp	(+)			(Wan et al. 2013)
				F	739	R	Exp	(+)	Disrupts JH2 C lobe, mimics JH2 deletion		(Ungureanu et al. 2011)
17	712	761		S	755	R	Clin			Hereditary thrombocythaemia (together with R938Q *in cis*)	
18	762	811		Y	766	E	Exp	-	Probably disrupts JH2 C lobe		(Funakoshi-Tago et al. 2008a)
19	813	857	Linker	Y	813	D	Clin			IMF	(Lupardus et al. 2014)
				E	846	D	Clin	(+)	Increases JH1 activity, when EPOR is present, EPO hypersensitivity	Germ-line mutation found in erythrocytosis and megakaryocytic atypia	(Kapralova et al. 2016)
			JH1	R	867	Q	Clin	+		ALL, hereditary thrombocythaemia	(Suryani et al. 2014, Marty et al. 2014)
				D	873	N	Clin	+		ALL	(Mullighan et al. 2009)
20	858	920		T	875	N	Clin	+		AMKL	(Mercher et al. 2006)
				L	884	P	Exp	+	FERM-independent hyperactivation of JH1	Homologous to JAK3 L857P found in ALL	(Losdyck et al. 2015)
				I	901	A	Exp	-			(Wan et al. 2013)
21	922	962		Y	931	C	Exp	+	Confers resistance to ATP competitive inhibitors (e.g. CMP6)		(Hornakova et al. 2011)
				P	933	R	Clin	+		ALL	(Mullighan et al. 2009)

[†] also S/K/T as well as multiple insertion and deletion mutations (Lupardus et al. 2014)

				R	938	Q	Clin	+		Hereditary thrombocythaemia (together with S755R *in cis*)	
22	963	1019		R	971	A	Exp	-			(Wan et al. 2013)
				I	973	A	Exp	-			(Wan et al. 2013)
				E	1028	A	Exp	-			(Wan et al. 2013)
23	1021	1059		K	1030	A	Exp	-			(Wan et al. 2013)
				V	1033	A	Exp	-			(Wan et al. 2013)
				F	1061	A	Exp	-			(Haan et al. 2009)
				M	1062	A	Exp	+			(Haan et al. 2009)
24	1060	1097		R	1063	H	Clin	(+)	Increases JH1 activity, when EPOR is present, EPO hypersensitivity	Germ-line mutation found in erythrocytosis and megakaryocytic atypia	(Kapralova et al. 2016)
				M	1064	A	Exp	(-)			(Haan et al. 2009)
				I	1065	A	Exp	-	Catalytically inactive, but able to confer IFN-γ signal		(Haan et al. 2009)
25	1098	1132		N	1108	S	Clin			PV	(Lupardus et al. 2014)

2.5 Structure and function of JAK domains

JAK proteins consist of four domains: an N-terminal FERM (4.1-band, ezrin, radexin, moiesin (Chishti et al. 1998)), an SH2-like (Src homology 2), a pseudokinase domain, and a tyrosine kinase domain (Figure 3) (Yamaoka et al. 2004). Upon first identification of JAKs, only the two kinase-like domains were identified as independent protein domains, while the rest of the sequence was divided into "JAK homology domains" (JH) based on sequence conservation within the family, thus following the naming convention used previously for Src proteins (Wilks 2008). Seven such regions of homology were identified, with the C-terminal tyrosine kinase domain being JH1, and the pseudokinase domain JH2 (Figure 3) (Schindler, Plumlee 2008, Wilks 2008).

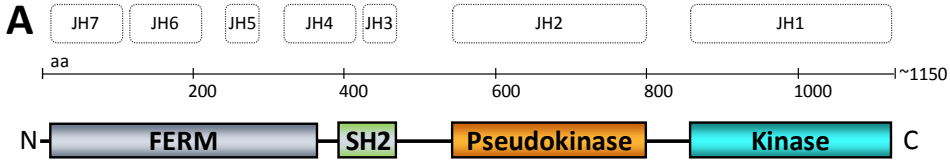

B

	aa FERM		SH2			Pseudokinase			Kinase		End	MW
JAK1	34	420	439	527		575	849		875	1154	1154	**133 kDa**
JAK2	37	380	399	482		537	809		849	1127	1132	**131 kDa**
JAK3	24	356	375	458		513	781		822	1099	1124	**125 kDa**
TYK2	26	431	450	534		581	870		897	1174	1187	**134 kDa**

Figure 3: The domain structure of JAKs. A: The JAK homology domains (JH (Schindler, Plumlee 2008, Wilks 2008)) and their correspondence to structural protein domains. The amino acid (aa) ruler shown depicts residue numbers for human JAK2, but is roughly comparable to other JAKs as well. B: The domain boundaries for the four human JAKs. The number of the first and last residue of each domain are shown, and defined as follows: FERM: starting before F1 β1 (start of TYK2 crystal structure, PDB: 4PO6), ending between F3 αA and α helix in linker L2 (Ferrao et Lupardus 2017); SH2: starting at end of α helix in L2, ending with αB; pseudokinase: starting at conserved phenylalanine before β1 (Bandaranayake et al. 2012) and ending at end of αI; kinase: beginning of β1 to end of αI. Note that the end of JH1 is loosely defined as the lengths of JH1 αI differ somewhat in different JAKs. JAK3 boundaries inferred from sequence homology, where structural data is not available. MW, molecular weight as calculated from the primary sequence.

Evolutionarily, the domain structure of JAKs is preserved throughout bilateria exemplified by the *Drosophila* JAK Hop, while JAK-like proteins with the architecture FERM-SH2-PTK, but lacking the pseudokinase domain, are found in

present-day sponges (Liongue et al. 2012). Individually, the FERM domain resembles most closely the FERM domain in Focal adhesion kinase (FAK), and the SH2 domain is similar to spleen tyrosine kinase (SYK) and ZAP70 (Liongue et al. 2012). Interestingly, JH1 and JH2 are evolutionarily distinct, and JH1 is more closely related to RTKs like EGFR and FGFR than to JH2 (Gu, Wang & Gu 2002). The arrangement of a pseudokinase being present alongside an active protein kinase in the same protein, is only found in a single other human protein besides JAKs, namely General control non-derepressible 2 (GCN2) (Manning et al. 2002), a PSK involved in the control of protein synthesis (Qiu, Garcia-Barrio & Hinnebusch 1998).

2.5.1 FERM-SH2

Early work on JAKs identified the N-terminal parts of JAKs (JH7–JH3, see Figure 3) as necessary for the receptor interaction (Haan et al. 2001), correct processing and cell surface expression of JAK-associated receptors, like EPOR (Huang, Constantinescu & Lodish 2001, Zhao et al. 2009), as well as regulating catalytic activity of JAKs (Zhou et al. 2001, Zhao et al. 2010). The region was identified to consist of a FERM domain (JH7–JH5 and parts of JH4), which is generally found mediating interactions of cytoplasmic proteins to integral, single-pass membrane proteins (Haan et al. 2001). Interestingly, full recruitment to receptors is only achieved, however, with the inclusion of the neighbouring domain (JH4–3) as well (Radtke et al. 2005, Zhao et al. 2009). This neighbouring domain (JH3 and parts of JH4) strongly resembled SH2 domains, but was found not to act like a classical SH2 domain and probably did not function through binding of phosphotyrosine (pY) residues (Radtke et al. 2005).

Many of these early findings were strikingly explained by the recent solving of the crystal structures of the FERM-SH2 portions of first TYK2 (Wallweber et al. 2014), and then JAK1 (Ferrao et al. 2016, Zhang, Wlodawer & Lubkowski 2016) and JAK2 (McNally, Toms & Eck 2016). The structures revealed that the FERM and SH2 domains form a single, structurally tightly linked, continuous module. The JAK FERM domain consists of three FERM subdomains (termed F1, F2, and F3) and are arranged in the typical cloverleaf pattern (Ceccarelli et al. 2006, Ferrao, Lupardus 2017). The domain does, however, differ in details from traditional FERM domains with elongated linker structures, enabling the tight contact with the SH2 domain, and a highly basic patch in F2, which is speculated

to be involved in interactions with negatively charged plasma membrane phospholipids (Ferrao, Lupardus 2017). The JAK SH2 domain resembles canonical SH2 domains, except for two loops, which normally form the pY peptide-binding groove of SH2 domains (Ferrao, Lupardus 2017).

The first JAK FERM-SH2 structure was obtained by fusing TYK2 FERM-SH2 to box2 from IFNAR1 with a flexible linker in order to overcome previous problems caused by poor expression and solubility of JAK fragments and low affinity of the receptor–JAK interaction (Wallweber et al. 2014). Interestingly, JAK1 could be crystallised in the presence of a free receptor peptide including box1 and box2 from IFNLR1 (Ferrao et al. 2016), and the JAK2 FERM-SH2 crystal was obtained without any receptor peptide at all (McNally, Toms & Eck 2016). The first-published structures only included either box2 (for TYK2 (Wallweber et al. 2014)) or box1 (for JAK1 (Ferrao et al. 2016)) bound to FERM-SH2, and lead to some speculation as to the possibility of crossover binding of one receptor peptide to two JAK molecules (Ferrao et al. 2016). Zhang and colleagues, however, obtained a structure of JAK1 bound simultaneously to both box1 and box2 of IFNLR1, indicating that each receptor peptide most probably binds a single JAK FERM-SH2 (Zhang, Wlodawer & Lubkowski 2016).

The interaction between JAK FERM-SH2 and the receptor peptide spans the whole FERM-SH2 module (Zhang, Wlodawer & Lubkowski 2016). The proline-rich box1 segment (consensus PxxLxF for JAK1-associated receptors (Ferrao et al. 2016, Ferrao, Lupardus 2017)) interacts mostly with a deep hydrophobic groove on the FERM F2 subdomain (Ferrao, Lupardus 2017). The mostly hydrophobic box2, on the other hand, interacts with the SH2 domain in a manner strikingly resembling the interaction between classical SH2 domains and a pY peptide ligand, with the exception of a somewhat conserved receptor peptide glutamate taking the position of pY in the SH2 binding pocket (Wallweber et al. 2014, Zhang, Wlodawer & Lubkowski 2016). In JAK1 (Zhang, Wlodawer & Lubkowski 2016), this interaction is mediated by the conserved pY-binding arginine of SH2 domains (Waksman et al. 1992). In TYK2, this residue is replaced with a histidine, but the SH2–pY-like binding mode is retained by compensatory interactions between the receptor glutamate and nearby serine and threonine residues (Wallweber et al. 2014).

Analysis of the interaction of JAK1 FERM-SH2 and its cognate receptor peptides showed that box1 is the primary driver of the interaction, but the interaction is further stabilised by box2 (Ferrao et al. 2016). This corroborates earlier mutation experiments, which showed that the SH2 arginine (binding box2) is not required for correct subcellular localisation of JAK1 (Radtke et al. 2005). Despite the current availability of FERM-SH2 structures for three out of four JAKs, pinpointing determinants explaining JAK-specificity of receptor interactions is difficult due to the poor conservation of receptor sequences (Ferrao, Lupardus 2017).

2.5.2 JH2 and JH1

The single-most defining domain for JAKs is probably its pseudokinase domain, JH2, constituting the second face of the two-faced Janus kinase molecule. While still strongly resembling ePKs (and indeed sharing their structural fold, see below), all JAK JH2s are characterised by the same pattern of deviations from canonical ePKs. They all present a partially degraded Gly-rich loop (the third glycine is replaced by a threonine), lack the conserved glutamate in their αC ($E91^{PKA}$, replaced by alanine), have their DFG motif replaced by DPG, and the HRD motif by HGN. Critically, the change in HRD removes the catalytic base ($D166^{PKA}$) needed in the phosphotransfer reaction (see also 2.1.1.2 above), and this caused the initial classification of JH2s as inactive pseudokinases (Manning et al. 2002). The defining lack of a proper HRD motif puts the JH2s into the same group with many other pseudokinases, most notably the EGFR-family pseudokinase HER3 and the pseudokinase-containing membrane guanylate cyclases (Boudeau et al. 2006, Hammarén, Virtanen & Silvennoinen 2015).

2.5.2.1 JH2 is needed for inhibition and activation of JH1

The first clues about the functions of JH2 came from domain deletion experiments with TYK2, which showed that deletion of either JH2 or JH1 results in loss of IFN-α signalling (Velazquez et al. 1995), hinting at a positive regulatory role for JH2 in activating JAKs. The potential for JH2 to activate JAK activity was also seen with the Drosophila JAK which replicated the result of deletion of JH2 causing loss-of-function, but crucially also showed that JH2 could harbour constitutively activating mutations (see also 2.4.2.1) (Luo et al. 1997). After

these early findings, seminal work in the Silvennoinen lab showed that besides removing cytokine stimulatability, deletion of JH2 also increased basal JAK activity and consecutive activation of STATs (Saharinen, Takaluoma & Silvennoinen 2000, Saharinen, Silvennoinen 2002). It was also found that adding JH2 to isolated JH1 significantly decreased the kinase activity of JH1 (Chen et al. 2000, Saharinen, Takaluoma & Silvennoinen 2000). Furthermore, a mutation screen approach in TYK2 identified both activating and inhibiting mutations in TYK2 JH2 (Yeh et al. 2000).

What emerged from these studies was a picture of JH2 as a regulatory domain with two roles: (1) basal inhibition of the kinase activity of JH1, and (2) mediation of the stimulatory signal from the cytokine receptor to JH1 (Saharinen, Silvennoinen 2002). The presumable mode of action of the various mutations found was thus that activating mutations probably acted through inhibition of the first function, while inhibiting mutations through disruption of the second.

2.5.2.2 Analysis of recombinant JH2 and JH1 fragments

A major breakthrough in the study of JH2 was the ability to produce and purify recombinant fragments of the domain (Ungureanu et al. 2011). This enabled controlled biochemical analyses and revealed that recombinant JAK2 JH2 fragments actually have catalytic, dual-specificity kinase activity and autophosphorylate two residues on themselves: S523 *in cis* and Y570 *in trans* (Ungureanu et al. 2011, Bandaranayake et al. 2012). Both of these residues had previously been identified as inhibitory phosphorylation sites in JAK2 (Argetsinger et al. 2004, Feener et al. 2004, Ishida-Takahashi et al. 2006, Mazurkiewicz-Munoz et al. 2006), and neither of the residues are conserved in other JAKs. Mutation of the β3 lysine in JAK2 JH2 (K581A) was also shown to remove S523 and Y570 phosphorylation in isolated, recombinant JAK2 JH2, as well as in the context of full length JAK2 in a cell culture model, suggesting that JAK2 JH2 was the kinase domain responsible for S523 and Y570 phosphorylation also in a biologically relevant context (Ungureanu et al. 2011). Accordingly, JAK2 K581A was also shown to have increased basal activation (Ungureanu et al. 2011).

Analysis of recombinant JAK fragments has shown that isolated JH1 is constitutively active and able to phosphorylate its activation loop in solution

(Sanz et al. 2011, Lupardus et al. 2014) leading to full activation of kinase activity (Chatti, Farrar & Duhé 2004). Although the unphosphorylated activation loop is likely to inhibit activity by inserting into the active site (as seen with other tyrosine kinases) currently, no crystal structures exist of this inactive form (Lucet, Bamert 2013). Kinase activity assays have also shown that addition of JH2 to the construct lower kinase activity significantly (20-fold for JAK2 (Sanz et al. 2011), ~100-fold for TYK2 (Lupardus et al. 2014)), and that some of this inhibition can be relieved by addition of clinical, activating mutations, like JAK2 V617F.

2.5.2.3 Structure and noncanonical ATP-binding mode of JH2

Production and purification of recombinant JH2 also allowed crystallisation trials, and eventually resulted in the solving of the crystal structure of JAK2 JH2 both with and without bound ATP by the Hubbard lab (Bandaranayake et al. 2012). The overall structure showed a canonical ePK fold with an extended β7-β8 loop, but a short activation loop, which does not include phosphorylatable residues and forms an α helix (αAL, see Figure 1) (Bandaranayake et al. 2012). Furthermore, the noncanonical amino acids in its ATP-binding site cause an unusual architecture (Figure 1), seen previously in the pseudokinase domain of HER3 (Jura et al. 2009). Firstly, the lack of the conserved glutamate in αC (A598; $E91^{PKA}$), causes the β3 lysine (K581; $K72^{PKA}$) to make an ionic interaction with the DFG/DPG aspartate (D699; $D184^{PKA}$). Secondly, the R spine is poorly defined with P700 replacing the canonical phenylalanine in the DFG motif, and the second residue from the top out of place/missing (Figure 1).

A structure with ATP bound to JAK2 JH2 revealed a noncanonical binding mode involving only a single divalent cation complexed in between the triphosphate group and the conserved N678 ($N171^{PKA}$), where K677 takes the place of the second cation (Figure 1). Other noncanonical features include an abnormally hydrophilic 'gatekeeper' residue (Knight, Shokat 2007) (Q626; $M120^{PKA}$) contacting the adenine base and D699, as well as a large hydrophobic residue (L579; $A70^{PKA}$) flanking the purine-binding pocket from the N lobe's side. The differences between the apo and ATP-bound structures are small, probably due to an interaction between R715 from the C lobe and T555 from the Gly-rich loop keeping the lobes together even in the absence of a bound ligand (Bandaranayake et al. 2012). The only difference observed was a slight kink in

αC caused by insertion of a water molecule into the structure of the apo protein (Bandaranayake et al. 2012).

Solving of the structure of JAK1 JH2 shortly thereafter, showed a domain very similar to JAK2 JH2, including the unconventional architecture of the ATP-binding site (Toms et al. 2013). JAK1 JH2, did however, show differences in the linking of the activation loop to the N and C lobes, deemed inconsistent with phosphotransfer (Toms et al. 2013). This conclusion was also supported by experiments showing no autophosphorylation or phosphorylation of exogenous substrates with JAK1 JH2 (Toms et al. 2013).

2.5.3 Mechanism of JAK2 hyperactivation — lessons from inhibitory mutations

2.5.3.1 Role of the JH2 C helix — F595A, F594A

Along with the wild-type JAK2 JH2 structure, the structure of JAK2 JH2 V617F was also solved in its ATP-bound form (Bandaranayake et al. 2012). Overall, introduction of V617F in the β4-β5 loop causes only minor changes to the structure of JH2. Notable differences are, however, seen in αC, which is extended by an additional turn on the N-terminal side in JAK2 V617F, thus shortening the β3-αC loop (Bandaranayake et al. 2012). Furthermore, addition of V617F causes changes in the side chain positions of F594, F595 as they adopt T-shaped π-stacking interactions with F617, thus stabilizing αC (Bandaranayake et al. 2012). This phenylalanine stack was previously predicted to form in V617F, and it was shown to be critical for its activation mechanism, as addition of the mutation F595A (and to a lesser extent F594A) abrogates JAK2 hyperactivation (Dusa et al. 2010, Gnanasambandan, Magis & Sayeski 2010). This finding also explained, why JAK2 V617F-analogous mutations do also activate JAK1 (V658F) and TYK2 (V678F), but not JAK3 (Staerk et al. 2005), since F595 is not conserved in JAK3. The importance of a hydrophobic interaction for V617F-hyperactivation also explained the earlier result that cytokine-independent activation can be achieved by mutating V617 to any large hydrophobic amino acid (W, F, M, I, L, in order of lowering activating potential) (Dusa et al. 2008).

Intriguingly, however, the experimental mutation F595A used to inhibit hyperactivation by JAK2 V617F also inhibits activation by other activating JAK2 mutations: namely R683S and T875N (Table 3) (Dusa et al. 2010), neither of which are structurally close to F595 or the putative hydrophobic stack. Molecular dynamics simulations of JAK2 JH2 F595A suggest that αC is markedly destabilised by the addition of F595A, implying that stability of αC is needed for mutational hyperactivation of JAK2 not only by V617F, but also by other activating mutations (Bandaranayake et al. 2012).

2.5.3.2 The SH2-JH2 linker — F537A

Structural analysis of JAK1 JH2 also identified JAK1 F575 (JAK2 F537) as required for JAK1 V658F/JAK2 V617F activation, and replacing this residue with alanine (JAK1 F575A or JAK2 F537A) could remove V658F/V617F-mediated hyperactivation (Toms et al. 2013). This residue lies in the SH2-JH2 linker (exon 12 in JAK2) and is not visible in the slightly shorter JAK2 JH2 structure. In wild-type JAK1 JH2, F575 can stack with F636 (analogous to JAK2 F595) in its 'in' position, but it is displaced outwards by the mutationally-introduced phenylalanine in JAK1 V658F (Toms et al. 2013).

2.5.3.3 The FERM domain — Y201F

Cytokine-independent activation caused by JAK2 V617F has also been inhibited successfully by JAK2 Y201F in the FERM domain (Yan, Hutchison & Mohi 2012). This was speculated to be due to Y201 potentially being a binding site for regulators of JAK2 activity (including SHP2, see Table 2), but the mechanism is yet to be definitively determined. The importance of the FERM domain for V617F-mediated activation was also shown by Zhao et al., who showed that, while V617F increases JAK2 kinase activity (by decreasing $K_{m,\ peptide}$), this increase is removed, upon deletion of the FERM domain (Zhao et al. 2010).

2.5.3.4 The SH2 domain — R426K

The importance of N-terminal JAK regions for the activation of V617F was also demonstrated by Gorantla et al., who mutated the conserved SH2 arginine

(R426K) needed for pY binding in canonical SH2 domains (Gorantla et al. 2010). They found that R426K suppressed V617F, but also that this suppression could be overcome when overexpressing EPOR (Gorantla et al. 2010).

2.5.3.5 Activation of JAK2 by mutation vs activation by cytokine

Intriguingly, analysis of JAK2 F595A (Dusa et al. 2010), Y201F (Yan, Hutchison & Mohi 2012), and R426K (Gorantla et al. 2010) showed that, while activation by V617F is inhibited, cytokine-mediated activation is not. These data hint at the possibility that the mechanism of V617F-activation is distinct from activation by cytokine-activated receptors.

These experimental mutations are thus in stark contrast with mutations that clearly disrupt the structure of JAKs, and thereby inhibit V617F. Examples of this class of V617F-suppressing mutations include a mutation in the FERM domain based on the known SCID-causing LOF JAK3 mutation Y100C, which inhibits interaction with γ_c (Cacalano et al. 1999). The analogous mutation in JAK1 inhibits interaction with gp130 (Haan et al. 2001), and the analogous JAK2 mutation (JAK2 Y114A) has been shown to suppress V617F activity (Wernig et al. 2008, Zhao et al. 2010). This is not surprising, as V617F requires the presence of receptors for activation as previously discussed (2.4.2.1 above) (Lu, Huang & Lodish 2008). Another example of a disrupting V617F-inhibitory mutation is JAK2 F739R, which is located in the F helix of the JH2 C lobe, and is expected to severely disorder the structure of the domain (Bandaranayake et al. 2012). This mutation somewhat suppresses V617F activation, but also causes basal JAK2 activation, as well as suppression of cytokine-stimulation (Bandaranayake et al. 2012), thus practically mimicking the effects of JH2 deletion (Saharinen, Takaluoma & Silvennoinen 2000, Saharinen, Silvennoinen 2002).

Furthermore, activating disease mutations in JH2 (V617F, K539L, or R683S) have been shown to cause reduction in phosphorylation of S523 and Y570, hinting at the possibility that loss of phosphorylation of these residues could be (at least part of) the activation mechanism of activating JH2 mutations (Ungureanu et al. 2011). However, since neither of the residues are conserved in other JAK JH2s (which can still be activated by the analogous mutations), this cannot constitute the whole activation mechanism.

Taken together, these data present a picture of mutational activation of JAKs being distinct from disruption of JH2 and thus simple removal of JH2-mediated inhibition. Additionally, mutational activation probably is distinct from cytokine-mediated JAK activation. What the determinants of these activation mechanisms are, how they differ, and what the specific roles of FERM, SH2, and JH2 are in either of these, has remained unknown.

3 Aims of the Study

Since their discovery almost three decades ago, much has been learned about the biological and signalling functions of JAKs as well as the functions of the individual JAK domains. However, the identification of a functional ATP-binding site in JAK2 JH2 also raises the question of the role of this site for the function of JAKs, as well as the potential of the site for therapeutic intervention. Furthermore, the precise mechanisms of how JAK activity is inhibited when not stimulated, and how it is activated upon cytokine stimulation, has been unknown. Moreover, despite the ever-growing amount of known clinical JAK mutations, how these mutations function in activating JAKs has remained elusive. This lack of mechanistic knowledge about JAK function has been a severely limiting factor in the design and search for novel pharmacological modalities targeting this critically important class of signalling molecules.

The specific aims of the study were

1. To characterise the ATP-binding pockets of JAK JH2s and to evaluate their potential as drug targets.
2. To understand the mechanism of intramolecular JAK inhibition, specifically JH2-mediated inhibition of JH1.
3. To decipher the mechanism(s) of ligand-dependent and -independent JAK activation, and thus provide knowledge for the rational design of novel JAK drugs.

4 Materials and Methods

4.1 Plasmid constructs, cloning, and site-directed mutagenesis (I–IV)

4.1.1 Mammalian expression constructs (I–IV)

The following constructs for mammalian expression were in pCI-neo expression vector (Promega, Madison, WI, USA) using SalI-NotI restriction sites: full-length human JAK1, JAK2, and EPOR. Human STAT5A was in pXM vector (Wakao, Gouilleux & Groner 1994). JAK1, JAK2, and STAT5A were C-terminally tagged with the human influenza hemagglutinin tag (HA; amino acid sequence YPYDVPDYA), and EPOR tagged at the N-terminus after the signal sequence between residues 30 and 31.

Constructs for *in vivo* work in mice (Article II) were done by collaborators under Prof. R. Skoda at University Hospital Basel in Basel, Switzerland. Constructs and experiments for mammalian expression of TYK2 constructs (Article I) were done by D. Ungureanu.

4.1.2 Expression constructs for recombinant protein production in insect cells (I, II, IV)

For recombinant expression of human proteins in insect cells, the Bac-to-Bac system was used (Invitrogen, Thermo Fisher Scientific, Waltham, MA, USA). Constructs (see Table 4) were in pFastBac1 vector (Invitrogen) using SalI-NotI restriction sites, and bacmids were produced in and isolated from DH10Bac cells (Invitrogen) according to manufacturer's instructions. All recombinant protein constructs were C-terminally tagged with a thrombin cleavage site followed by a hexahistidine tag (LVPRGSHHHHHH).

Table 4: Recombinant expression constructs

Protein	Expression Boundaries	Additional mutations	Used in
JAK2 JH2 536	536-812	W659A, W777A, F794H	II
JAK2 JH2 513	513-827		II
TYK2 JH2	556-871		I
JAK1 JH2	553-856		II

4.1.3 Site-directed mutagenesis (I–IV)

Mutations were introduced using QuikChange site-directed mutagenesis (Agilent Technologies, Santa Clara, CA, USA) following manufacturer's instructions, and resulting constructs were analysed and confirmed by Sanger sequencing. See Table 5 for all point mutations used in the study.

Table 5: Experimental mutations used in the study.

JAK	Mutation	Rationale / mode of action	Reference
JAK2	V511R	Designed to disrupt SH2-JH2 linker from FERM-SH2.	(IV)
	S523A	Removes S523 phosphorylation	(Ungureanu et al. 2011), (II)
	F537A	F537 proposed to stack with F595 in wild-type JAK2 JH2. Known to inhibit V617F	(Toms et al. 2013), (IV)
	K539L	Activating. Causes PV.	(Scott et al. 2007), (II, IV)
	G552A + G554A	Designed to remove flexible glycines usually needed for ATP binding.	(II)
	I559F	Designed to sterically inhibit ATP binding. Verified to inhibit ATP binding.	(II)
	L579F	Alone does not have an effect (Article II). Together with L680F should fuse C spine.	(II)
	K581A	Removes conserved β3 lysine.	(Ungureanu et al. 2011), (II, IV)
	Y570F	Removes Y570 phosphorylation	(Ungureanu et al. 2011), (II)
	E592R	Outer face of JH2 αC	(Shan et al. 2014), (IV)
	F595A	Inner face of JH2 αC. Known to inhibit V617F and others.	(Dusa et al. 2010, Gnanasambandan, Magis & Sayeski 2010, Bandaranayake et al. 2012), (IV)
	E596R	Outer face of JH2 αC. Known to inhibit V617F and others.	(Leroy et al. 2016), (IV)
	M601A	R spine residue (RS3). Mutation should disrupt R spine.	(IV)
	V610A	R spine residue (Sh1). Mutation should disrupt R spine.	(IV)
	V617F	Activating. Causes MPNs.	(Baxter et al. 2005, James et al. 2005, Kralovics et al. 2005, Levine et al. 2005), (II, IV)

	W659A	Mutation designed to remove surface hydrophobicity to stabilize recombinant JH2.	(Bandaranayake et al. 2012), (II, IV)
	K677E	Inhibits ATP binding by electrostatic interactions. Verified to inhibit ATP binding.	(II)
	N678A	Removes catalytic loop asparagine coordinating binding of cation needed for ATP binding	(II)
	L680F	Together with L579F should fuse C spine	(IV)
	R683S	Activating. Causes ALL.	(Bercovich et al. 2008, Mullighan et al. 2009), (II, IV)
	D699A	D in DPG. Mutating disrupts K581-D699 salt bridge.	(II)
	P700A	P in DPG (RS2). Mutating should disrupt R spine.	(IV)
	P700F	P in DPG (RS2). Mutating could reinforce R spine.	(IV)
	F739R	αF within C lobe. Mutation disrupts C lobe and mimics JH2 deletion.	(Bandaranayake et al. 2012), (II)
	W777A	Mutation designed to remove surface hydrophobicity to stabilize recombinant JH2.	(Bandaranayake et al. 2012), (II, IV)
	N782K	Outer face of αH in JH2. Designed to disrupt a potential interface based on the EGFR activator/receiver model.	(IV)
	N786K/E	Outer face of αH in JH2. Designed to disrupt a potential interface based on the EGFR activator/receiver model.	(IV)
	F794H	Mutation designed to remove surface hydrophobicity to stabilize recombinant JH2.	(Bandaranayake et al. 2012), (II, IV)
	T875N	Activating. Causes AMKL.	(Mercher et al. 2006), (IV)
	L884P	Activating. Homologous to JAK3 L857P found in ALL.	(Losdyck et al. 2015), (IV)
	E896A + E900A	Outer face of JH1 αC. Designed to disrupt a potential interface based on the EGFR activator/receiver mode.	(IV)
	D976N	D in HRD. Mutation is kinase dead.	(IV)
JAK1	G590A + G592A	Homologous to JAK2(G552A + G554A).	(II)
	E609R	Predicted to interact with JAK1 K888 in the JH2-JH1 autoinhibitory model.	(III)[7]
	L633D/K	Outer face of JH2 αC. Homologous to JAK2 E592.	(IV)
	K622A	Homologous to JAK2(K581A).	(II)
	V658F	Activating. Causes ALL. Homologous to JAK2 V617F	(Mullighan et al. 2009), (II, IV)
	R724E	Predicted to interact with JAK1 E897 in the JH2-JH1 autoinhibitory model.	(III)[7]
	K888E	Predicted to interact with JAK1 E609 in the JH2-JH1 autoinhibitory model.	(III)[7]
	D899A	Removes charge near predicted R724-E897 salt bridge in the JH2-JH1 autoinhibitory model.	(III)[7]
	K911E	Predicted to interact with JAK1 E609 in the JH2-JH1 autoinhibitory model.	(III)[7]

[7] Data withheld from the final published manuscript. See Results section 5.4.2.

4.2 Mammalian cell culture, transfection, and cytokine stimulation (II, III, IV)

JAK2-deficient (γ2A) and JAK1-deficient (U4C) human fibrosarcoma cells (Kohlhuber et al. 1997, Bonjardim 1998) and African green monkey kidney cells (COS7, American Type Culture Collection CRL-1651) were cultured using standard methods in Dulbecco's Modified Eagle's Medium (DMEM; Lonza, Basel, Switzerland) supplemented with 10% foetal bovine serum (FBS; Sigma-Aldrich, St. Louis, MO, USA), 2 mM L-Glutamine (Lonza), and 0.5% Penicillin-Streptomycin (Lonza). Cells were cultured at 37 °C at 5% CO_2 in a humidified incubator, and split upon reaching ~80% confluency using Trypsin-EDTA (Lonza) according to manufacturer's instructions.

For transfection, cells were seeded onto 6-, 12-, or 24-well tissue culture plates and transfected the following day using FuGENE HD (Promega), FuGENE6 (Promega) or Xtreme-GENE9 (Roche, Basel, Switzerland) according to manufacturers' instructions. After 24 h or 48 h, cells were washed with cold PBS and lysed using cold cell lysis buffer (50 mM Tris-Cl pH 7.5, 10% glycerol, 150 mM NaCl, 1 mM EDTA, 1% Triton X-100, 50 mM NaF) supplemented with 2 mM vanadate (Sigma-Aldrich) for inhibition of tyrosine phosphatases as well as protease inhibitors (8.3 µg/ml aprotinin (Sigma-Aldrich), 4.2 µg/ml pepstatin (Roche), and 1 mM phenylmethanesulfonyl fluoride (Sigma-Aldrich)). Lysates were centrifuged and used directly for SDS-PAGE and immunoblotting or stored at -20 °C.

For cytokine stimulation experiments, cells were transfected for 10–24 h and subsequently starved for 12–24 h in serum-free DMEM supplemented with L-Glutamine and antibiotics before stimulation with human EPO (NeoRecormon, Roche), TPO or IFN-γ (Peprotech, Rocky Hill, NJ USA) in starvation medium.

4.2.1 Luciferase reporter signalling assays (III, IV)

For Article III, luciferase reporter assays were performed by our collaborator K. Gnanasambandan under Prof. S. R. Hubbard at New York University School of Medicine, New York, NY, USA. Briefly, an acute phase response element–firefly luciferase STAT3 reporter (APRE-luc) was used together with a *Renilla* luciferase

reporter in COS7 cells and luciferase activity was measured with the Dual-Glo Luciferase assay kit (Promega).

For Article IV, a SPI-Luc STAT5 reporter construct (Sliva et al. 1994) was used together with a constitutively expressing β-gal plasmid. After transfection and stimulation on 96-well plates, cells were washed twice with ice cold PBS and lysed using Reporter Lysis Buffer (Promega). The lysate was split for luciferase detection (with Luciferase Assay Substrate, Promega E4530) and β-galactosidase normalisation (ortho-Nitrophenyl-β-galactoside (ONPG), Sigma-Aldrich). Luminescence and absorbance was detected on an EnVision multiplate reader (Perkin Elmer). Each sample was done in quadruplicate.

4.3 SDS-PAGE and immunoblotting (II, III, IV)

Cell lysates or protein preparations were run on lab-made SDS-PAGE gels using standard methodology, and either stained using the non-specific protein stain Instant Blue (Expedeon, Harston, UK), or transferred onto Protran 0.45 µm nitrocellulose membranes (GE Healthcare, Chicago, IL, USA) and blocked using 4% BSA (Sigma-Aldrich) in TBS-Tween (0.05%). Blots were double-stained using rabbit and mouse primary antibodies and a mix of labelled secondary antibodies (Table 6). Signals were detected on an Odyssey CLx (LI-COR, Lincoln, NE, USA) and analysed using Image Studio software (LI-COR).

4.4 Recombinant protein production and purification (I, II, IV)

Proteins were expressed in *Spodoptera frugiperda* Sf9 cells and affinity-purified as described earlier (Ungureanu et al. 2011). Ni-NTA-affinity-purified protein was used directly for differential scanning fluorometry (DSF) if sufficient purity was obtained (judged by SDS-PAGE), or further purified for other biochemical assays with anion-exchange chromatography as described in (Ungureanu et al. 2011), or gel filtration with a Superdex200 10/300 GL column (GE Healthcare) on an ÄKTA (GE Healthcare) or Shimadzu (Shimadzu Corp., Kyoto, Japan) HPLC system. Protein purity was estimated from SDS-PAGE gels, and proper functionality/folding with DSF and gel filtration.

Table 6: Antibodies used for immunodetection.

Name	Antibody	Manufacturer	Cat. No	Used in
HA	Anti-HA.11 Epitope Tag	Covance	MMS-101P	I, II, III
HA	HA Tag	Aviva Systems Biology	OAEA00009	IV
pJAK2	Phospho-Jak2 (Tyr1007/1008)	Cell Signaling	3771	II
pJAK2	Anti-phospho-JAK2 (Tyr1007/1008)	Millipore	07-606	IV
pSTAT1	Phospho-Stat1 (Tyr701)	Cell Signaling	9171	II
pSTAT1	Phospho-Stat1 (Tyr701) (D4A7)	Cell Signaling	7649	IV
pSTAT5A	Phospho-Stat5 (Tyr694)	Cell Signaling	9351	II, IV
pJAK1	Anti-phospho-JAK1 (Tyr1022/1023)	Millipore	07-849	II, IV
pJAK1	Phospho-Jak1 (Tyr1022/1023)	Cell Signaling	3331	IV
STAT1	Anti-STAT1	BD Biosciences	610116	IV
αRabbit	IRDye® 680LT Goat anti-Rabbit IgG	LI-COR	926-68021	II
αMouse	Goat anti-mouse IgG, DyLight 800	Thermo Scientific	35521	II, IV
αRabbit	Goat anti-rabbit IgG, DyLight 680	Thermo Scientific	35568	IV

4.5 Analysis of recombinant proteins (I, II, IV)

4.5.1 Thermal shift assay (TSA) by differential scanning fluorometry (DSF) (I, II, IV)

Thermal shift assays were carried out using the protein dye Sypro Orange (Molecular Probes, Thermo Fisher Scientific) in a CFX96 real-time PCR cycler (Bio-Rad, Hercules, CA, USA) as described in (Vedadi et al. 2006). Briefly, samples are heated at 1 °C per min from 4 °C to 95 °C and fluorescence read every 1 °C. Fluorescence data was normalised and fitted to a Boltzmann sigmoidal equation using GraphPad Prism (GraphPad Software, San Diego, CA, USA) to obtain melting temperatures.

4.5.2 Fluorometric nucleotide-binding assay with MANT-ATP (I, II)

Binding of ATP labelled with the fluorescent label MANT (Jena Bioscience, Jena, Germany) to JAK JH2s was measured by observing FRET between protein tryptophans and the fluorescent label in a Quantamaster cuvette

spectrofluorometer (Photon Technology International, Edison, NJ, USA) essentially as described in (Niranjan et al. 2013). Dissociation constants (K_d) were calculated from at least triplicate measurements using GraphPad Prism (GraphPad Software) and taking into account ligand depletion, using the following equation, where P is total protein, L is total ligand, PL is the protein–ligand complex, and K_d is the dissociation constant:

$$K_d = \frac{[P_{free}][L_{free}]}{[PL]}$$

Substituting in

$$[L_{free}] = [L] - [PL]$$
$$[P_{free}] = [P] - [PL]$$

and rearranging

$$[PL]^2 - ([P] + [L] + K_d)[PL] + [P][L] = 0$$

yields a quadratic equation for $[PL]$, which when solved using the quadratic formula (and choosing the negative before the square root) gives

$$[PL] = \frac{[P] + [L] + K_d - \sqrt{([P] + [L] + K_d)^2 - 4[P][L]}}{2}$$

and can be used to fit binding data to solve K_d.

4.5.3 ADP production assay (I)

ATP hydrolysis activity was estimated by measuring the production rate of ADP in solutions containing purified JAK2 JH2 or TYK2 JH2 using the ADP-Glo kinase assay (Promega) according to the manufacturer's instructions. Specific ADP hydrolysis activity was calculated by comparison of the produced signal to an ADP/ATP standard curve.

4.5.4 Surface plasmon resonance measurements (I)

Affinities for nucleotide and small-molecule binding to TYK2 JH2 using surface plasmon resonance on a Biacore T-1000 (GE Healthcare) were measured by

collaborators in the Wang group at the Departments of Therapeutic Discovery and Inflammation, Amgen Inc. in South San Francisco, CA, USA.

4.5.5 Protein structure determination with X-ray crystallography and small-angle X-ray scattering (I)

The crystal structure of TYK2 JH2 was solved and small-angle X-ray scattering (SAXS) analyses were performed by collaborators in the Wang group at Amgen Inc. Briefly, the protein construct (TYK2 556-871) was expressed in High Five cells (Invitrogen) with a C-terminal tobacco etch virus cleavage site followed by a hexahistidine tag, purified with immobilised metal anion chromatography, digested with tobacco etch virus, and further purified with anion exchange chromatography and gel filtration, before crystallisation and structure determination as well as SAXS measurements.

4.6 *In vivo* bone marrow transplantation model (II)

The *in vivo* mouse work was conducted as a collaboration by J. Grisouard under Prof. R. Skoda at University Hospital Basel in Basel, Switzerland, using previously published methodology (Tiedt et al. 2008). Briefly, bone marrow cells from donor C57BL/6 mice (Harlan Laboratories, Indianapolis, IN, USA) were transduced *ex vivo* with retroviruses containing the desired human JAK2 construct, and transplanted into lethally irradiated recipient mice. Recipient mice were kept in pathogen-free conditions and blood was collected 12 weeks after transplantation for analysis.

4.7 Molecular dynamics simulations and analysis of trajectories (II, III)

All molecular dynamics simulations were carried out by our collaborators under supervision of Y. Shan and D. E. Shaw at D. E. Shaw Research in New York, NY, USA. The simulations used the CHARMM36 force field for all-atom simulations on Anton, a supercomputer specially designed for molecular dynamics simulations (Shaw et al. 2008). For Article II, the simulation trajectories were

kindly provided by Y. Shan. The trajectories were analysed using the VMD (Visual molecular dynamics) software (Humphrey, Dalke & Schulten 1996). For Article III, analysis of the simulation trajectories was conducted by our collaborators at D. E. Shaw Research.

5 Summary of the Results

5.1 Structural and functional characterisation of recombinant JAK JH2s (I, II)

5.1.1 The crystal structure of TYK2 JH2 (I)

JAK2 JH2 was the first JAK pseudokinase domain to be functionally and structurally characterised (Ungureanu et al. 2011, Bandaranayake et al. 2012). In a collaboration with the Wang group at Amgen Inc., we thus characterised and solved the crystal structure of TYK2 JH2. Two crystal structures were obtained, one bound to ATPγS (resolution 1.9 Å) and one bound to a small-molecule pyrazine compound (resolution 2.15 Å). Both structures showed a mostly canonical ePK fold in a closed conformation with a functional and accessible nucleotide-binding site. The domain did exhibit some peculiar features for ePKs, which resembled features of JAK2 JH2 (Bandaranayake et al. 2012). For example, the binding of ATPγS was non-canonically mediated by only one cation and the canonical β3–αC link (K72–E91^{PKA}) was replaced by an interaction between the β3 lysine and the DPG (DFG) motif aspartate (K642–D759 in TYK2). Furthermore, the activation loop formed a short, non-canonical α-helix stabilised by multiple ionic interactions.

5.1.2 TYK2 JH2 is an inactive pseudokinase (I)

Since the crystal structure showed that TYK2 JH2 had an accessible nucleotide-binding site, we set out to investigate whether the domain had catalytic protein kinase activity. To this end, autophosphorylation *in vitro* kinase assays were performed with γ-^{32}P-labelled ATP followed by autoradiography, as well as with cold ATP followed by mass spectrometry (MS) analysis. Even though some experiments showed weak incorporation of γ-^{32}P into TYK2 JH2 over time, the effect was not consistently reproducible (and thus likely to be caused by trace

amounts of contaminating protein kinases), nor could any autophosphorylation sites be identified with MS. We also measured the domain's ability to hydrolyse ATP in an *in vitro* assay measuring production of ADP and found that TYK2 JH2 hydrolyses ATP at ~50% of the rate of JAK2 JH2, which is known to possess low catalytic activity (Ungureanu et al. 2011). Due to this low rate of hydrolysis and, especially, the lack of known physiological substrates (e.g. the known autophosphorylation sites of JAK2 JH2 are not conserved on TYK2 JH2) TYK2 JH2 was deemed to probably be an inactive pseudokinase.

5.1.3 Characterisation of the nucleotide-binding site of JAK JH2s (I, II)

We characterised the binding of a fluorescently-tagged ATP analogue to all JAK JH2 domains we were able to produce and purify as recombinant protein at the time, namely JAK1, JAK2, and TYK2 JH2s. For comparing binding affinities, we used a FRET-based fluorometric binding assay using ATP labelled with the fluorophore MANT (Niranjan et al. 2013). Measurements in the absence and presence of different cation salts ($MgCl_2$, $MnCl_2$ or $CaCl_2$) showed tightest binding of MANT-ATP to all measured JAK JH2s in the presence of $MgCl_2$ and $MnCl_2$ with a significant loss of affinity in the presence of $CaCl_2$ or without cations at all. We quantified the dissociation constants (K_d) for binding of MANT-ATP to JAK JH2s in the presence of $MgCl_2$, and found that JAK2 JH2 and JAK1 JH2 showed comparable tight binding constants for MANT-ATP, while TYK2 JH2 exhibited lower binding affinity (Figure 4).

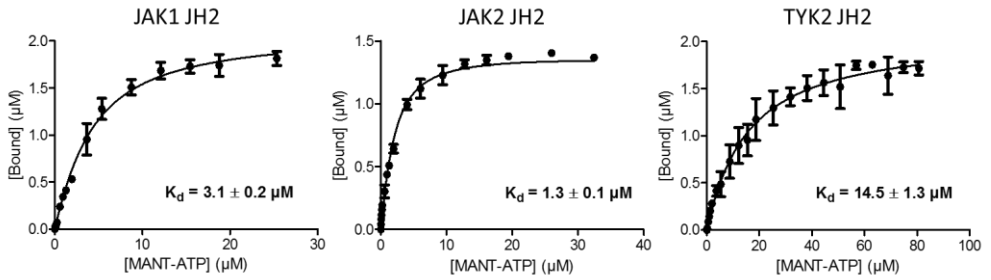

Figure 4: Comparison of MANT-ATP-binding affinity of isolated JAK JH2s. All measurements were done in the presence of $MgCl_2$ at a starting protein concentration of 2 µM for JAK1 and TYK2 JH2 and 1.5 µM for JAK2 JH2. [Bound] corresponds to the concentration of the protein-ligand complex ([PL] in 4.5.2 above). N = 4 for JAK1 JH2 and N = 3 for JAK2 and TYK2 JH2. Curves show fits to the data of binding equations for tight binding taking ligand-depletion into account (see section 4.5.2 above).

While the values obtained for MANT-ATP binding do enable comparison between highly related proteins, as is the case for JAK JH2s, it should be noted, that they do not necessarily correspond to binding affinities of untagged ATP. Kd values for MANT-ATP have been reported to be as much as 3 orders of magnitude lower than for untagged ATP, depending on the assay method and target protein used (see, e.g., (Vertommen et al. 1996) and references therein). Estimation from DSF curves from ATP titration experiments for JAK2 JH2 (Figure 5 A) and TYK2 JH2 (data not shown) suggest affinities for untagged ATP in the 100–200 µM and 400–600 µM ranges, respectively. Even though DSF-derived affinity estimations can occasionally be very comparable to, e.g., isothermal titration calorimetry (ITC) data (Murphy et al. 2014), DSF should in general be deemed semiquantitative at best (Matulis et al. 2005, Garbett, Chaires 2012). For the case of TYK2 JH2, the effects of MANT on the binding of ATP could be estimated by comparing to surface plasmon resonance measurements with untagged ATP (Article I), which yielded a very comparable Kd of 24 µM. Follow-up experiments, like ITC or competition assays with untagged ATP, however, are needed to accurately estimate this difference for the other JAK JH2s, but were not done in this context due to high protein demands.

5.2 Effects of mutational disruption of the JAK JH2 ATP-binding site (I, II)

To assess the functional significance of the nucleotide-binding site of JAK JH2s for JAK activity, we took a rational mutagenesis approach. Previous analyses of JAK2 had shown that disruption of the JAK2 JH2 ATP-binding site by mutation of the β3 lysine (K581 in JAK2) increased basal JAK2 activity (Ungureanu et al. 2011). Similarly, we found that the same mutation in TYK2 (K642A) had a comparable effect (Article I), yet JAK1 showed the opposite, as JAK1 K622A decreased basal activity (Article II).

Although mutation of the conserved β3 lysine ($K72^{PKA}$) is a common method to disrupt a functional kinase ATP-binding site (Iyer et al. 2005, Kannan et al. 2007, Ungureanu et al. 2011), multiple protein kinase examples exist, where mutating the β3 lysine does not remove nucleotide binding (Carrera, Alexandrov & Roberts 1993, Robinson et al. 1996, Cheng, Koland 1998, Iyer et al. 2005). Furthermore, β3 lysine mutations have been reported to be potentially

structurally disrupting (Fukuda et al. 2011). Thus, to circumvent these potential limitations and to properly assess the effects of loss of ATP binding to JH2, we designed multiple ways of inhibiting ATP binding. These include (among others) steric filling of the purine pocket (JAK2 I559F), electrostatic repulsion of ATP phosphates (JAK2 K677E), and disruption of ATP-binding pocket flexibility (JAK2 G552A + G554A) (Article II, Table 5).

We furthermore set out to verify the effects of the mutations in recombinant JAK2 JH2. Out of the seven ATP-binding site mutations tested, three (I559F, K677E, and L579F) yielded recombinant JAK2 JH2 protein, and could be tested for their ability to bind ATP. We were unable to produce useful amounts (judged from protein-stained SDS-PAGE gels) and folded (judged from DSF unfolding curves) proteins for the rest of the tested mutant constructs. Out of the proteins that could be produced, L579F did not suppress binding of ATP, but both I559F and K677E showed no ATP-induced T_m shift in DSF, thus suggesting that binding of ATP was successfully prevented (Figure 5 A).

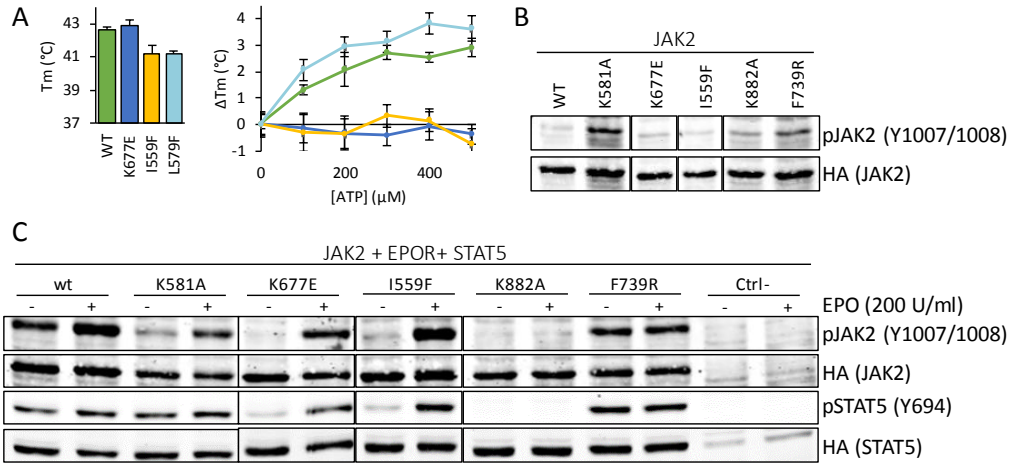

Figure 5: Characterisation of selected JAK2 JH2 ATP-binding site mutants. A: DSF on recombinant JAK2 JH2. Shown are averages and standard deviations from three independent measurements. B: Immunoblot of whole-cell lysate from γ2A cells transiently transfected with only JAK2. C: Immunoblot of whole-cell lysate from γ2A cells transiently transfected with JAK2, EPOR, and STAT5, or nothing (Ctrl-). Signal from kinase-dead JAK2 K882A shows antibody background signal with JAK2, while Ctrl- sample shows antibody background without JAK2. See Table 5 for explanation of the mutations. The blots are cropped for clarity. A minimum of three independent experiments were done for each condition. Quantifications of the immunoblot data can be found in Article II.

To analyse the effects on JAK2 activation, mutated full-length JAK2 constructs were transiently transfected into JAK2-deficient γ2A cells. Interestingly, while

K581A did increase basal JAK2 activation, the other ATP-binding site mutations (including the ATP-blocking I559F and K677E) only showed modest or no increase in basal activation (Figure 5 B). Furthermore, while addition of a homotypic JAK2-associated receptor (EPOR) increased basal (i.e. ligand-independent) activation of wild-type JAK2, no such increase could be seen for the ATP-binding site mutations (Figure 5 C, see also Figure 9 A and Article IV). Upon cytokine stimulation with a high concentration of EPO (Figure 5 C) or IFN-γ (Article II), all tested ATP-binding site mutations exhibited similar activation levels compared to wild type JAK2.

The effects of JAK2 K581A were initially attributed to the loss of pS523 and pY570 (Ungureanu et al. 2011). Due to varying quality of non-commercial pS523 and pY570 antibodies available, we could not thoroughly assess the phosphorylation state of these residues in our ATP-binding site mutants. Preliminary data did suggest, however, that S523 is phosphorylated despite the presence of an ATP-binding site mutation (JAK2 N678A, *unpublished observations*). Whether this means that S523 (and potentially Y570) are phosphorylated *in vivo* by another protein kinase in addition to JAK2 JH2 remains unclear. Our result showing basal activation with the analogous β3 mutation in TYK2 (Article I), for which no autoinhibitory phosphorylation sites are known, also argues for a structural effect caused by the mutation itself, which compromises autoinhibition by JH2.

5.3 Hyperactivation of JAKs requires a functional ATP-binding site in JH2 (II)

We next analysed the function of the JAK2 JH2 ATP-binding site in the context of JAK hyperactivation. Strikingly, we found that adding an ATP-binding site-disrupting mutation to the hyperactivating mutant V617F reverted JAK2 activation back to near-wild-type levels (Figure 6). Interestingly, suppression of V617F activity was only partial in L579F, which did not successfully inhibit binding of ATP to JH2 (Figure 5 A), thus strongly suggesting that the suppressing effect observed is linked to the loss of ATP binding to JH2. Furthermore, the suppression of V617F was seen with all mutations designed to inhibit ATP binding to JH2 (except the unsuccessful L579F mentioned above) irrespective of their mode of inhibition of ATP binding (Figure 6, Table 5).

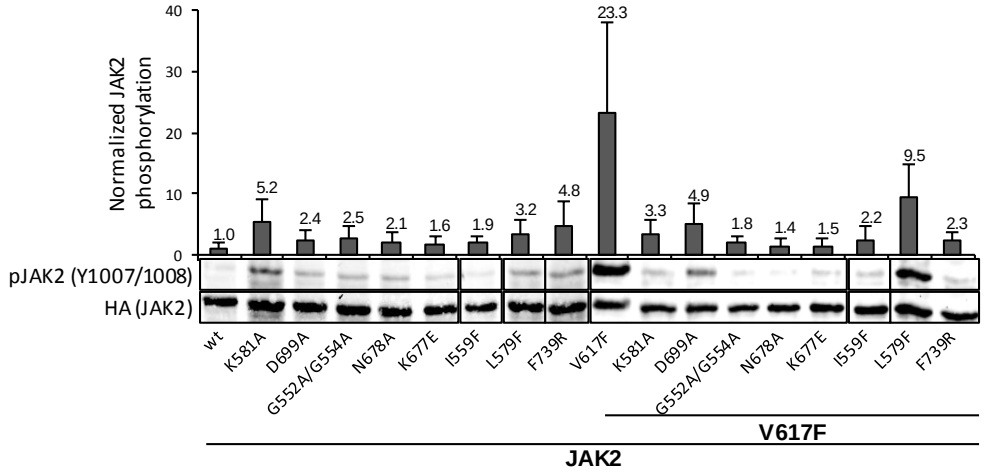

Figure 6: Preventing binding of ATP to JAK2 JH2 prevents hyperactivation. Immunoblot of whole-cell lysate from γ2A cells transiently transfected with full-length JAK2. Quantifications from immunoblots (pJAK2 signal divided by HA(JAK2) signal and normalised to wild-type) of three individual experiments are shown above as a bar graph. Error bars are standard deviation. See Table 5 for explanations of the mutations.

The dependence of JAK hyperactivation on a functional ATP-binding site in JH2 was also seen with JAK1 and the analogous activating JAK1 mutation V658F (Article II).

To assess whether the effect of suppression of JAK2 signalling seen in a cell culture model would translate to amelioration of JAK2 V617F-driven disease *in vivo*, we used a bone-marrow transplantation MPN mouse model in collaboration with Prof. R. Skoda's group at University Hospital Basel (Switzerland). Analysis of mice transplanted with bone marrow cells containing either wild-type JAK2, JAK2 K581A, JAK2 V617F, or JAK2 K581A V617F showed that adding the JH2 ATP-binding site mutation K581A to V617F kept haemoglobin levels at wild-type levels, whereas V617F alone caused erythrocytosis and accompanying abnormally high haemoglobin levels (Article II). This result was later further verified using the JAK2 JH2 ATP-binding site double mutant JAK2 G552A G554A (J. Grisouard, R. Skoda, *unpublished observations*).

5.4 The Inhibitory JH2–JH1 Interaction (III)

5.4.1 Modelling the interaction using a supercomputer

Despite the fact that the autoinhibitory function of JH2 had been known for over a decade (Chen et al. 2000, Saharinen, Takaluoma & Silvennoinen 2000, Yeh et al. 2000, Saharinen, Silvennoinen 2002, Saharinen, Vihinen & Silvennoinen 2003), no satisfactory model for the mechanism of autoinhibition had been suggested, or indeed tested. We set out to decipher the interaction in a collaborative effort with Y. Shan at DE Shaw Research and Prof. S. R. Hubbard at NYU (both in New York, NY, USA), using a computational molecular dynamics approach on the supercomputer Anton (Shaw et al. 2008).

Briefly, a model of JAK2 JH2-JH1 was generated by simulating the individual domains in different arbitrary orientations to one another, and analysing the interface of any resulting JH2-JH1 complex. Out of the 14 different poses generated, one was deemed most likely, as the JH2–JH1 interface included JH2 αC known to probably be important for the regulation of JH1 (Dusa et al. 2010, Bandaranayake et al. 2012). Next, the JH2-JH1 linker was added and the simulation continued, after which the model was completed with the addition of the SH2-JH2 linker, resulting in a JAK2 model encompassing residues 520–1131, which was subjected to an extremely long-scale simulation of ∼40 μs. During this final simulation, a stable JH2–JH1 interaction was established after several microseconds highlighting the need for extremely long-scale simulations in the study of interdomain interactions.

5.4.2 Characterisation and functional validation of the JH2–JH1 inhibitory interaction

The resulting JH2-JH1 conformation (see Figure 7) exhibits multiple interaction regions between the domains. Firstly, the extended β2-β3 loop of JH2, including the known inhibitory phosphorylation site Y570 (Argetsinger et al. 2004, Ungureanu et al. 2011), lies on top of the JH1 N lobe, which contains a basic patch for pY570. Secondly, the JH2 β7-β8 loop contacts the JH1 β2-β3 loop via ionic interactions between R683 and D873.

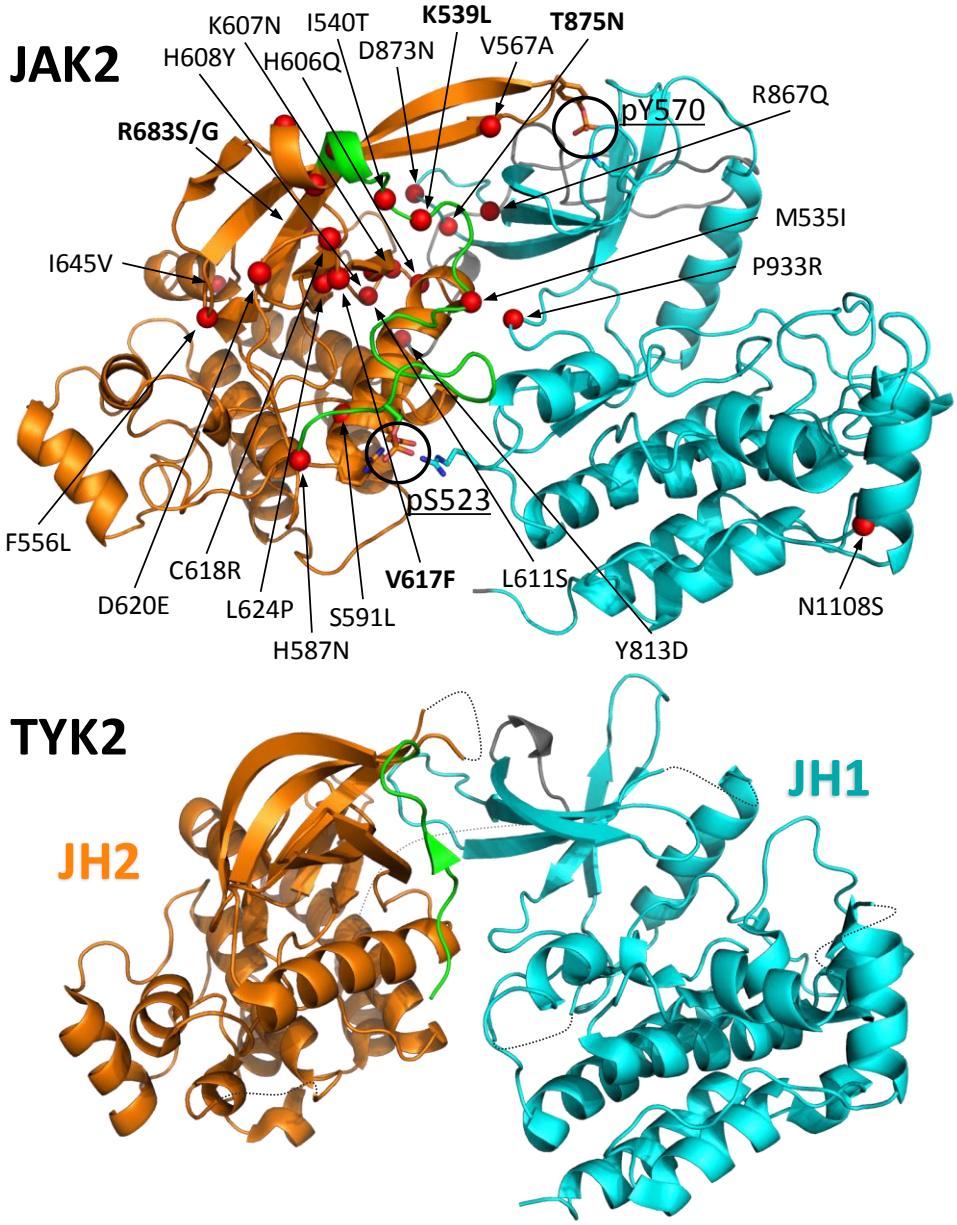

*Figure 7: The inhibitory JAK JH2–JH1 interaction. JH2 is shown in orange, JH1 in cyan, the SH2-JH2 linker in green and the JH2-JH1 linker in dark grey. Known JAK2 clinical disease mutations (see Table 3) are shown as red spheres (positions of α carbon atom) and labelled. The mutations shown in **bold** have been analysed in Articles II and/or IV. Autoinhibitory phosphorylation sites in JAK2 (pS523 and pY570) are circled. The TYK2 JH2-JH1 crystal structure (PDB: 4OLI) is shown underneath in the same orientation. Gaps in the TYK2 crystal structure are linked with dotted lines.*

Interestingly, both R683 and D873 are known sites of clinical disease-causing, gain-of-function mutations (Vainchenker, Constantinescu 2013). Thirdly, the C-terminal end of JH2 αC contacts the JH1 hinge region, and finally, the SH2-JH2 linker lies on top of the interface between the domains.

The SH2-JH2 linker includes the known inhibitory phosphorylation site S523 (Ishida-Takahashi et al. 2006, Ungureanu et al. 2011), which lies between E592, R588, and R947. Strikingly, most of the known activating disease mutants in JH2 and JH1 map to (or near to) the interface (Figure 7), and many of their effects can be readily explained by weakening of the interaction (see Discussion 6.3.3.1).

We functionally verified the interaction by structure-guided mutagenesis in a cell culture model for JAK activation. To this end, charge-reversal mutations and novel ionic interactions were engineered into the JAK2 JH2–JH1 interface: (a) Y570R + K883E, (b) R683E + D873R, (c) Q603E (in murine Jak2) + P933R, and (d) E592R + R947E. With these charge-reversal mutations, mutating one interaction partner is expected to weaken the inhibitory interaction and show increased activation, while mutating both residues should rescue the interaction and lower activity back to near-wild-type levels. For Y570R + K883E, the result was exactly as expected from an inhibitory JH2–JH1 interaction. For (b), activation caused by R683E could only be rescued with the secondary mutation D873N (not D873R), indicating that probably due to the local structural environment, a Glu-Asn interaction is more favourable than Glu-Arg, but still validating the JH2-JH1 model. For (c), Q603E was not activating, but it was able to suppress activation by mutation of its presumed interaction partner, P933R, which is a known disease-mutation (Mullighan et al. 2009) (Table 3). Further for (d), R947E was suppressed by E592R, even though E592R was not activating by itself.

We also introduced similar charge-reversal mutations into JAK1 assuming a similar JH2–JH1 interaction. We thus engineered the following mutations: JAK1 E609R + K888E, E609R + K911E, and R724E + E897K (+ D899A), where D899A was added to remove a secondary negative charge in the JH1 β2-β3 loop containing E897K, and thus enable a one-to-one charge reversal between R724 and E897. Firstly, the mutants R724E (+ D899A) and E897K (+ D899A) were activating as predicted, and this activation could be suppressed by the triple mutant R724E + E897K (+ D899A). Furthermore, the single mutation E609R was also activating as

predicted. Unfortunately, however, the mutations in JH1 of the presumed interaction partners (K888E and K911E) of E609R strongly suppressed basal JAK1 activation thus precluding definitive confirmation of the model for JAK1, and as such, the data was withheld from the final manuscript (Article III).

The computationally generated JH2-JH1 model was further independently verified by simultaneous publication of a TYK2 JH2-JH1 crystal structure by researchers at Genentech (Lupardus et al. 2014) (Figure 7). The overall conformation of the domains is virtually identical even though the JAK-specific details differ (see Discussion for further analysis). Overall, based on the evidence from cell experiments, as well as the agreement with earlier mutagenesis data, we concluded that the identified structure likely represented the JH2–JH1 autoinhibitory interaction.

5.5 Mechanisms of JAK activation and inhibition thereof (II, IV)

To better understand the determinants of JAK activation, we took a systematic approach, and characterised known JAK2 JH2 mutations capable of inhibiting ligand-independent activation caused by clinical JAK2 disease mutations like V617F (hereafter referred to as 'inhibitory mutations') (Table 5). Additionally, we also explored various hypotheses for the function of JH2 in JAK activation and identified new inhibitory mutations in the FERM-SH2 module and in JH1 (Figure 8).

5.5.1 Systematic analysis of inhibitory mutations

In addition to JAK2 JH2 ATP-binding site mutations, we expanded our analysis of ligand-independent JAK2 activation to other known inhibitory mutations, as well as searching for novel ones. To assess the propensity of JAK2 to self-activate (i.e. potential for ligand-independent activation), we co-transfected the homotypic receptor EPOR, which is known to increase basal (i.e. ligand-independent) activation of wild-type JAK2 at high expression levels (Pradhan et al. 2010). Although expression levels of EPOR used were potentially non-physiological due to transient overexpression, the result indicates that inhibitory mutations suppress the potential of otherwise wild-type JAK2 to activate in a ligand-independent manner (Figure 9 A).

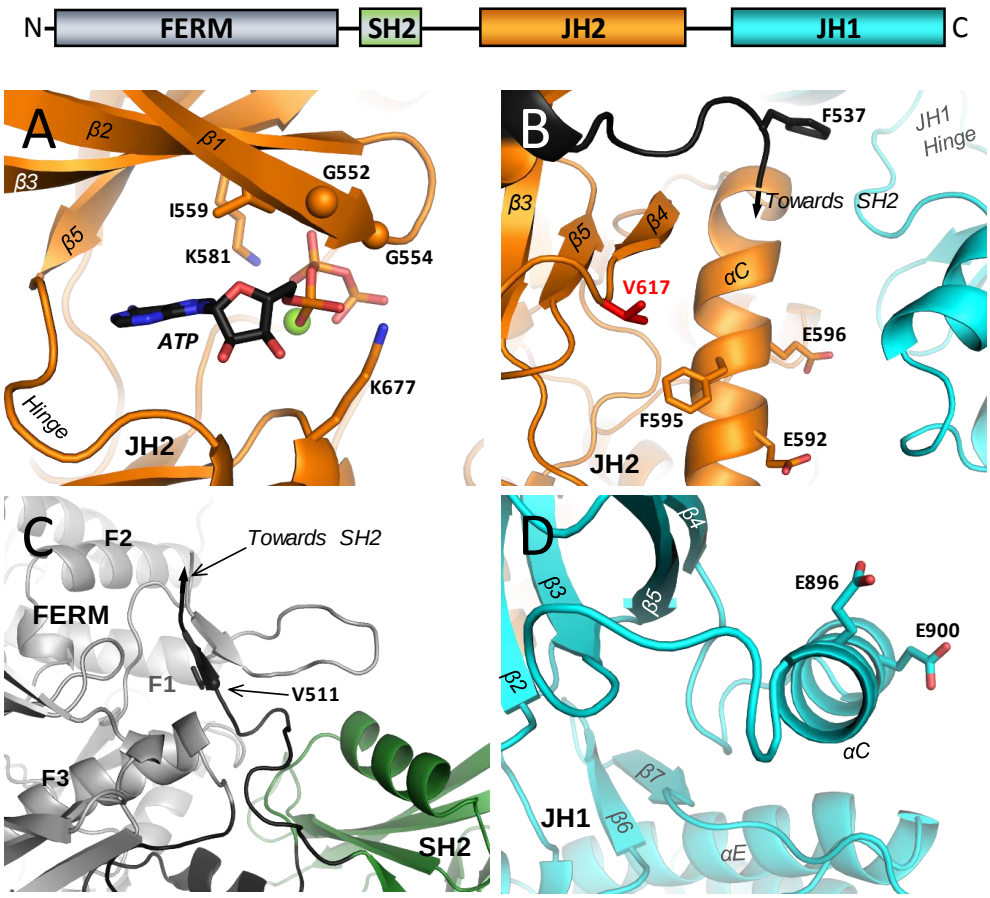

Figure 8: Structural locations of the different known and novel inhibitory JAK2 mutations (see text). A: Close-up of the ATP-binding site of JH2 (PDB: 4FVQ) showing critical residues for ATP binding. The Mg^{2+} ion is shown in light green. B: The region surrounding JH2 αC including the position of V617 (shown in red). Position of JH1 is shown according to the autoinhibitory JH2-JH1 model from Article III. C: Position of V511 in regards to FERM-SH2 (PDB: 4Z32). D: The outer face of JH1 αC (model from Article III). The position of the JH2-JH1 linker has been omitted for clarity. Colouring of the structures is as in the JAK2 domain schematic shown above (domain linkers are shown in black).

Previous studies with inhibitory mutations have indicated that not all activating mutations are inhibited equally (Dusa et al. 2010, Leroy et al. 2016). To systematise these findings, we characterised the inhibition profiles of our panel of inhibitory mutations (Figure 9 B–D). While V617F was inhibited by most mutations (with the exception of E896A+E900A), we found distinctly different profiles for K539L and R683S (see also Discussion 6.3.4.1).

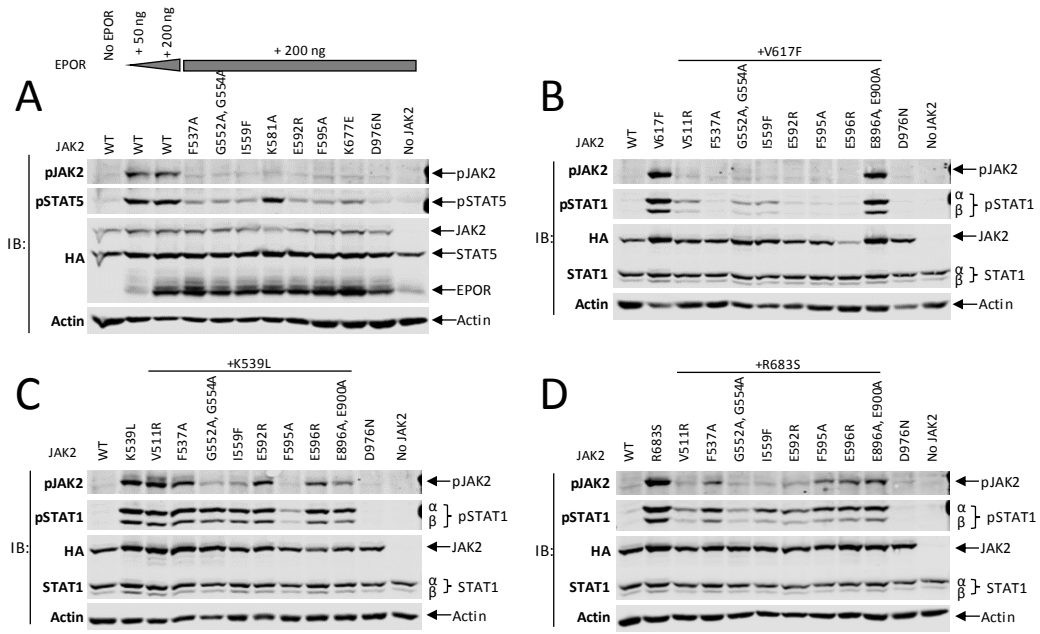

Figure 9: Systematic profiling of inhibitory mutations. Immunoblots of whole-cell lysates from γ2A cells transiently transfected with indicated full-length JAK2 mutants (A-D) and STAT5+EPOR (A).

5.5.2 Testing other hypotheses for the function of JH2 (IV)

Several hypotheses have been put forward to explain the requirements for JH2 in mutational activation of JAKs. Using structure-guided site-directed mutagenesis, we tested some of these hypotheses as well as novel ones (see Table 7). In summary, we found that the protein kinase spine model (see 2.1.1.1 in Review) does not explain the effects of loss of ATP binding, as a triple mutation designed to block ATP binding, but complete the C spine (JAK2 I559F, L579F, L680F; see Figure 1 inset of JAK2 JH2 ATP-binding site), did not restore V617F activity (Article IV). Furthermore, disruption of the R spine by multiple mutations (Table 5) could not inhibit V617F activation, suggesting that inhibitory mutations potentially affecting the R spine (e.g. F595A in αC) probably exert their functions by other means (Article IV).

We also tested an HER3/EGFR-like activator/receiver model (Zhang et al. 2006, Jura et al. 2009) for the activating effect of JH2 on JH1 in full-length JAK2, but did not find evidence for a similar interaction between JH2 and JH1. However, testing of this model did identify the importance of the JH1 αC (Figure 8 D) in the

ligand-independent activation of wild-type JAK2 (Article IV), as well as for activation caused by K539L (Figure 9 D).

We also tested mutations of FERM-SH2 designed to disrupt the putative interaction between FERM-SH2 and JH2, and found that disruption of the SH2-JH2 linker at the N-terminal end (JAK2 V511R, Figure 8 C), resulted in inhibition of multiple activating mutations, namely V617F, R683S (Figure 9 B, D), and T875N (Article IV). Despite trying numerous additional point mutations on different potential interaction surfaces of FERM-SH2 (*unpublished observations*), we could not identify a FERM-SH2–JH2 interface, which would be needed for a detailed molecular model of activation of full-length JAK.

Table 7: Hypotheses tested in Article IV.

Hypothesis	Experiment	Result
Mechanism of ligand-independent activation is the same or similar in wild-type JAK2 as in V617F.	Effect of inhibitory mutations on otherwise wild-type JAK2 in the presence of EPOR.	Hypothesis supported. All inhibitory mutations also inhibit EPOR-induced ligand-independent activation of JAK2.
Mechanism of activation in V617F is the same as in K539L and R683S.	Profile inhibitory mutations against V617F, K539L, and R683S.	Hypothesis rejected (partially). Activating mutations rely differentially on specific regions in JAK2.
Effect of loss of ATP-binding to JH2 in inhibiting V617F can be explained by lack of C spine completion.	Complete C spine mutationally (I559F + L579F + L680F) and test, whether V617F activity is restored.	Hypothesis rejected. V617F activity is not restored by C spine completion.
Completion of JH2 R spine is necessary for V617F activity (via positioning of αC or otherwise).	Disrupt R spine mutationally (M601A, V610A, P700A) and see, whether V617F is inhibited.	Hypothesis rejected. V617F activity is not affected by R spine mutations.
JH2 could act as an HER3/EGFR-like activator for JH1.	Mutate putative activator (N782K, N786K, N786E) and receiver (E896A + E900A) interfaces. Analyze ligand-independent and -dependent activation.	Hypothesis rejected, but JH1 αC important for ligand-independent activation.
Interaction between FERM-SH2 and JH2 is critical for correct positioning of JH2-JH1 for ligand-independent activation.	Disrupt link between FERM-SH2 and JH2 mutationally (V511R) and analyze ligand-independent activation.	Hypothesis supported. V511R inhibits EPOR-induced activation as well as activation by mutation (V617F, R683S, T875N).

5.5.3 Identification of a JH2 interface critical for heteromeric JAK2 signalling

To assess the effects of inhibitory mutations on the activity of otherwise wild-type JAK2, we analysed responses to homomeric (EPO) and heteromeric (IFN-γ) cytokines. We found slightly impaired responses to EPO with αC (E592R, F595A) and JH2-SH2 linker (F537A) mutations (Figure 10 A). Strikingly, we found that those same mutations severely inhibited signalling in response to IFN-γ (Figure 10 B). In contrast, inhibitory mutations in the JH2 ATP-binding site (I559F, K677E), SH2 (V511R) or JH1 αC (E896A+E900A) did not show significant effects on cytokine stimulatability (Figure 10, Article IV).

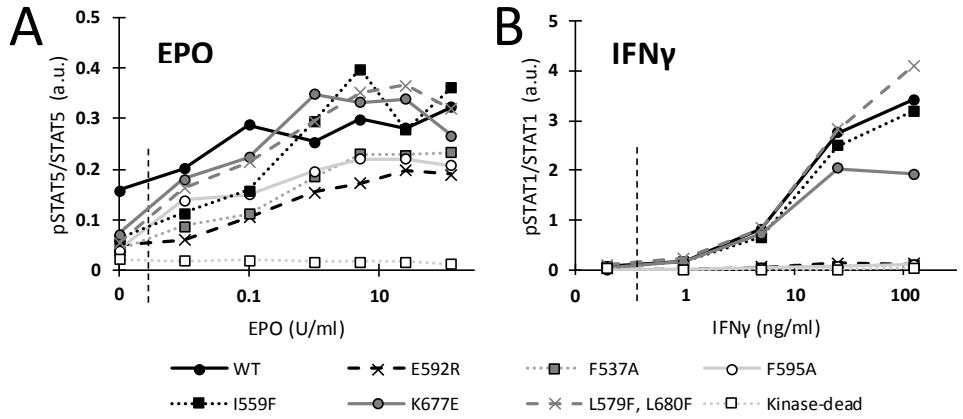

Figure 10: Inhibitory mutations in JH2 αC and the C-terminus of the SH2-JH2 linker differentially affect responses to homomeric (EPO, panel A) and heteromeric (IFN-γ, panel B) JAK2 signalling. Shown are quantifications from immunoblots of whole-cell lysates from γ2A cells transiently transfected with full-length JAK2, STAT5, and EPOR (A) or full-length JAK2 only (B). Cells were stimulated before lysis for 30 min with differing amounts of cytokine. pSTAT5 (A) and pSTAT1 (B) signals are shown normalised to total STAT5 or STAT1 levels, respectively; a.u. arbitrary units. Note that the difference in initial activation between wild-type and the inhibitory mutations in panel A reflects the lowering of basal activation described in Figure 9 A.

6 Discussion

JAKs are of key, and rapidly growing, clinical and pharmacological interest, as exemplified by two new JAK inhibitors ('Jakinibs') approved in Europe within the last year (mid-2016 to mid-2017) alone, raising the number of European medicines agency (EMA)-approved Jakinibs to four[8]. Currently, the main clinical targets for JAK inhibition are in MPNs, especially myelofibrosis (O'Sullivan, Harrison 2017) as well as RA (Yamaoka 2016). JAK inhibition is, however, also being actively tested for numerous other indications—primarily autoimmune and inflammatory diseases (Banerjee et al. 2017) including dermatological disorders (Damsky, King 2017). Preclinically, JAK inhibitors have shown promising results also against diabetes (Trivedi et al. 2017) and various cancers (Gao et al. 2016).

Despite this high clinical importance and interest, much of the molecular detail of JAK function and regulation has remained elusive. JAK activity is regulated on multiple levels, but the intramolecular regulation of JAK activity is likely the primary means of regulation. Most of the extrinsic mechanisms of JAK regulation by, e.g., phosphatases or regulator proteins, are fine-tuning the cytokine-response, as evidenced by the fact, that none of them can inhibit mutationally hyperactivated JAK (or indeed mutationally hyperactivated JAK-associated receptors) (Vainchenker, Constantinescu 2013). How this intramolecular regulation comes about in inhibition and activation of JAKs, however, has been mostly unclear.

Starting from the major advances made in the understanding of the molecular structure of JAKs, the findings presented in this thesis are put into the context of other recent discoveries in the field below. Additionally, the current limitations and boundaries of our understanding as well as outstanding questions are delineated.

[8] http://www.ema.europa.eu/ema/ . Currently (as of July 2017) approved Jakinibs are Ruxolitinib, Tofacitinib, Baricitinib, and Oclacitinib (veterinary medicine). Site accessed 17.7.2017.

6.1 JAK structure

The last decade has produced a wealth of structural information about JAKs. The first JH1 domain structure was published in 2005 (Boggon et al. 2005), and since then, all JAK domains have had their crystal structures solved individually or paired to their neighbouring domain (Figure 11). Currently, no complete full-length JAK structure (or tested model) exists, beyond cryo-EM structures of full-length JAK1 (Lupardus et al. 2011). Despite their low resolution, the cryo-EM JAK1 structures do show a flexible JAK molecule, composed of two mostly rigid substructures most likely corresponding to the FERM-SH2 and JH2-JH1 modules (Lupardus et al. 2011). These modules are able to adopt multiple conformations ranging from completely "open" (so-called 'beads-on-a-string' conformation) to "closed" with presumably extensive, but as-of-yet unknown, contacts between FERM-SH2 and JH2-JH1 (Lupardus et al. 2011). How, or whether, these correspond to activated or inactivated states of JAKs remains to be determined.

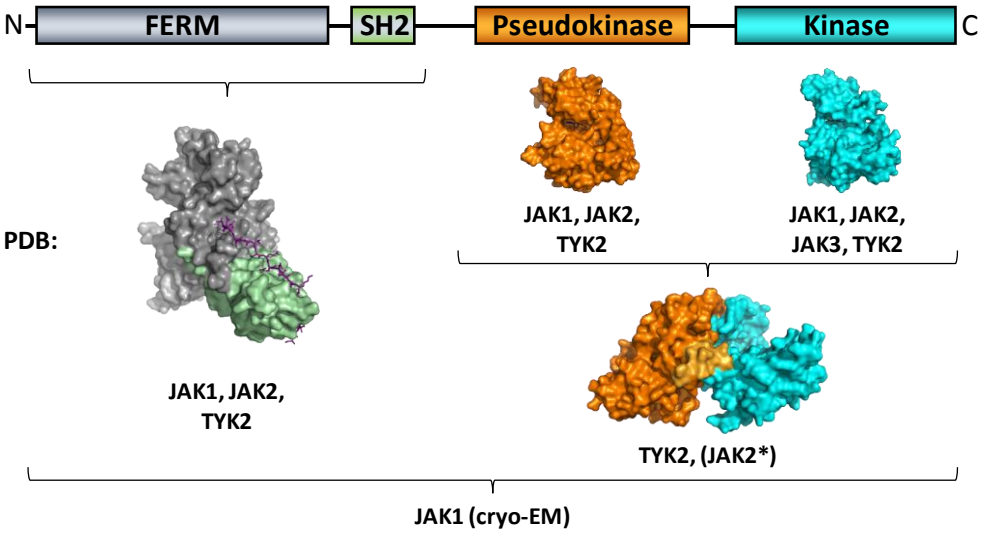

*Figure 11: Known JAK structures. The PDB codes for the first-published individual crystal structures are: FERM-SH2: 5IXI (JAK1), 4Z32 (JAK2), 4PO6 (TYK2); JH2: 4L00 (JAK1), 4FVP (JAK2), 3ZON (TYK2); JH1: 3EYG (JAK1), 2B7A (JAK2), 1YVJ (JAK3), 3LXN (TYK2); JH2-JH1: 4OLI (TYK2). *JAK2 JH2-JH1 model based on the MD simulation from Article III. Shown are 4Z32, 4FVQ, 2B7A, and the autoinhibitory JH2-JH1 model from Article III.*

6.2 Structure–function considerations of JH2

6.2.1 Protein kinase (in)activity of JH2s

Currently, three out of the four JAKs have published crystal structures of JH2 (Figure 11). While the structures (including the structure solved in Article I) are highly similar, some notable differences, especially between JAK2 and JAK1/TYK2 exist. Superficially, all JH2s have a similar, structured activation loop helix (αAL, Figure 1), which is in a conformation not suited for catalysis in the crystal structure, since the peptide substrate-binding site is occluded (Toms et al. 2013). Interestingly, comparison of the side-chain interaction network around αAL suggests, however, that this loop could be significantly more rigid in TYK2 and JAK1 than in JAK2 JH2. For both TYK2 and JAK1, the JH2 αAL is fixed to both the N and C lobes via two salt bridges (R600–E771 and R769–E824 for TYK2), while in JAK2 JH2 the first salt bridge is substituted for by hydrophobic residues (JAK2 F556–I711) and the second is missing (JAK2 K709- -L763).[9]

Accordingly, no protein kinase activity has been detected for JAK1 JH2 (Toms et al. 2013) or TYK2 JH2 (Article I), whereas JAK2 JH2 has been shown to autophosphorylate *in vitro* (Ungureanu et al. 2011). Whether this lack of activity for JAK1 and TYK2 is due to the aforementioned interactions around αAL, or a lack of suitable substrate residues, remains to be determined.

6.2.2 Nucleotide binding in JH2s

Despite the lack of detectable catalytic activity for TYK2 and JAK1 JH2s, all JAK JH2 domains bind ATP (Ungureanu et al. 2011, Murphy et al. 2014) (JAKs 1&2 and TYK2: Figure 4; JAK3: J. Raivola, H. Hammarén, O. Silvennoinen, *unpublished observations*). Although the binding mode is non-canonical (Figure 1), it is nowhere near the most exotic ATP-binding modes seen in pseudokinases (Cui et al. 2017). In fact, the one-cation architecture including a K72–D184^{PKA} bond is the most common nucleotide-binding mode seen in pseudokinases (Hammarén, Virtanen & Silvennoinen 2015).

[9] In JAK3 JH2, both interaction pairs are replaced by hydrophobics, presumably also stabilizing an inactivating αAL (based on homology modelling).

The MANT-ATP-binding affinities of JAK JH2s are in the micromolar range (Figure 4), with JAK2 JH2 being the tightest of the three with a Kd of ∼1 μM for MANT-ATP. This affinity is ∼50-fold weaker than that measured for JH1 in an identical MANT-ATP binding assay (Niranjan et al. 2013), but significantly stronger than the published affinity of PKA for MANT-ATP (Kd = 36 μM) (Ni, Shaffer & Adams 2000)—although some of these differences could be attributed to the effects of the addition of the MANT-group to ATP, as earlier discussed (see 5.1.3 above). In a thermal shift assay, JAK2 JH2, which has a relatively low melting temperature (∼35–43 °C depending on the assay conditions), is significantly stabilised by the addition of Mn-ATP or Mg-ATP (Murphy et al. 2014). Given that the ATP concentrations in living cells are in the millimolar range (Traut 1994), it is likely that JAK JH2s are constitutively nucleotide-bound, even if the significantly lower affinities suggested by DSF assays were correct. ATP thus probably functions as a structural cofactor in the domain in cells. Indeed, mutations of the JAK2 JH2 ATP-binding site do alter the function of JAK2, especially in regards to the activity of hyperactivating disease mutations (discussed in more detail in 6.3.4).

6.3 Activation and inhibition of JAKs

6.3.1 The JH2–JH1 interaction

6.3.1.1 Previous models for inhibition of JH1 by JH2

Since the discovery of JH2 inhibiting JH1, various hypotheses about the mechanism have been proposed (Constantinescu et al. 2013). First hints of a physical interaction between JH2 and JH1 came from coimmunoprecipitation (coIP) experiments with differentially tagged JAK3 JH2 and JH1 fragments (Chen et al. 2000). An early model for a direct JH2–JH1 interaction (Lindauer et al. 2001) was proposed based on homology modelling from a crystallographic dimer seen in the crystal structure of the fibroblast growth factor receptor (FGFR) tyrosine kinase domain (Mohammadi, Schlessinger & Hubbard 1996). In this model, the JH2 and JH1 domains would interact via their respective C helices, which was proposed to inhibit JH1 activity by forcing its activation loop into an inactive conformation (Lindauer et al. 2001). This model made multiple predictions for

potential sites for mutational activation of JAKs by relieving the inhibitory interactions. Despite being able to predict some mutations correctly (especially those in exon 14, including V617 mutations, Table 3), many more of the predicted mutation sites have not held true, including practically the whole JH1 side of the proposed interface, calling the model into question.

In contrast, the model proposed by our co-workers and us (Article III), is not based on previous crystallographic information, but rather on extensive long-scale molecular dynamics simulations of multiple initial JH2–JH1 interfaces. In our model, JH2 binds to the hinge-side of JH1 via its C helix in a front-to-back orientation, somewhat resembling the interaction seen in the inactive conformation of Src kinases, where SH2 and SH3 domains bind the hinge-side of the protein kinase domain (Bradshaw 2010). Crucially, the simultaneously (but independently) published TYK2 JH2-JH1 crystal structure (Lupardus et al. 2014) strongly supports our model showing a practically identical architecture (Figure 7).

6.3.2 The JH2-JH1 inhibitory interaction model

In our JH2-JH1 model, inhibition of JH1 is achieved by conformational restriction of the JH1 lobes, as well as an opening of the catalytic site. Molecular dynamics simulations (Article III) show this as a breaking of the conserved salt bridge between the β3 lysine ($K882^{JAK2\ JH1}$; $K72^{PKA}$) and the αC glutamate ($E898^{JAK2\ JH1}$; $E91^{PKA}$) (Taylor, Kornev 2011), which could facilitate a further inactivating 'DFG-out' flip, in which the catalytically crucial aspartate ($D976^{JAK2\ JH1}$; $D184^{PKA}$) is expelled from the active site.

Interestingly, data from the TYK2 JH2-JH1 crystal structure and our simulation model (Article III) also imply that activation of JAKs does not primarily hinge on expelling the activation loop from the active site, as is the case for many other tyrosine kinases (Endicott, Noble & Johnson 2012). In the TYK2 JH2-JH1 crystal structure (as in our simulation), the activation loop is in the outwards 'active' position despite being unphosphorylated and the domain being kinase dead (TYK2 D1023N) (Lupardus et al. 2014). Furthermore, no crystal structures of JH1s thus far show the domain in an inactive state with the activation loop occluding its active site (Lucet, Bamert 2013). However, kinase assays with recombinant TYK2 JH2-JH1 showed that TYK2 JH2-JH1 is only active when the JH1 activation

loop is phosphorylated (Lupardus et al. 2014). In our simulations, phosphorylation of the JH1 activation loop did cause destabilisation of the JH2–JH1 interaction, suggesting that activation loop phosphorylation is still part of the activation mechanism (i.e., in changing the dynamic balance from 'inhibited' to 'active'), even if possibly not by the traditional means of causing expulsion of the activation loop from the enzymatic site.

It is interesting to speculate, why crystallisation of TYK2 JH2-JH1 succeeded, where JAK2 JH2-JH1 failed, despite numerous attempts (D. Ungureanu, H. Hammarén, O. Silvennoinen, S. R. Hubbard, *unpublished observations*). It is possible, that the JH2–JH1 interaction is inherently less stable in JAK2, as suggested by small-angle light scattering (SAXS) experiments with active recombinant JAK2 (Varghese et al. 2014). These experiments show JAK2 JH2-JH1 in an elongated, loose structure incompatible with the compact JH2-JH1 structure seen in our simulations and the TYK2 crystal structure (Varghese et al. 2014). A likely explanation for this is that experiments involving recombinant JAK2 JH2 (including crystallisation trials) are complicated by the two JAK2-specific inhibitory phosphorylation sites, Y570 and S523. Both are part of the inhibitory interface in JH2, and obtaining homogeneously phosphorylated recombinant protein can be difficult.

6.3.2.1 Is JH1 inhibited by JH2 in *cis* or *trans*?

Recently, work on the growth hormone receptor (GHR) complex suggested that the intracellular portions of pre-dimerised receptor chains would move apart during cytokine activation (Brooks et al. 2014). This led the study authors to propose a hypothesis for JAK2 activation/inhibition, in which JH2-mediated inhibition of JH1 occurs *in trans*, i.e. JH2 of one JAK2 molecule inhibiting JH1 of the other, and *vice versa* (Waters, Brooks 2015). Although our model or experimental evidence does not rule out the possibility of a *trans* interaction, it currently seems unlikely at least for the many heterodimeric JAK configurations (Table 1), which have evolved from ancestral JAK2-receptor systems (Nicola, Hilton 1998, Zeidler, Bausek 2013). The TYK2 JH2-JH1 crystal structure shows an excellent intra-TYK2 fit (Lupardus et al. 2014), and as described in 5.4.2 above, our JAK1 JH2–JH1 charge-reversal experiments suggest that an intra-JAK1 (i.e. *cis*) JH2–JH1 interaction is likely. Neither of these findings are expected with JAK inhibition in *trans* since neither TYK2 nor JAK1 signal as homodimers (Table 1).

Furthermore, the presumption that JAK-associated receptors, such as GHR or EPOR, would primarily exist as inactive, pre-dimerised complexes *in vivo* have been lately called into question (see discussion in section 6.3.5 below), thus also challenging the assumptions and methodology that lead to the notion of *trans*-inhibition/activation of JAKs (Brooks et al. 2014).

6.3.3 JAK activation by mutation (cytokine-independent)

JAKs are hotspots for clinical mutations causing constitutive, ligand-independent activation of JAK kinase activity. There are two (not mutually exclusive) hypotheses to explain the function of these mutations: Firstly, hyperactivating mutations might act through disruption of existing inhibitory interactions, or secondly, hyperactivation could (also) be achieved through stabilisation of activating interactions/direct activation of JH1 catalytic activity. Critically, detailed understanding of either of these potential mechanisms has been lacking, which has precluded the development of targeted mutation-specific drugs.

6.3.3.1 The JH2-JH1 model provides explanations for known disease mutations

As shown in Figure 7, most known clinical and experimental activating mutations (Table 3) fall into (or close to) our JH2–JH1 interface. This suggests that these mutations act through the first mechanism (i.e. breaking of an inhibitory interface). The most striking examples here are mutations of R683 in JH2 and D873 in JH1, as the parental residues form an ionic interaction along the JH2–JH1 interface. This region around the β7-β8 and αC-β4 loops in JH2, and β2-β3 loop in JH1, harbours many other known mutations as well, including H606Q, K607N, H608Y, I682F, R867Q, and T875N, all of which probably act through disruption of the JH2–JH1 interface (Table 8).

The multitude of known exon 12 mutations (see Table 3 and Table 8) fall into the JH2-SH2 linker region (including S523), which makes extensive contacts to both JH2 and JH1 in our JAK2 model (linker shown in green in Figure 7). Residues in this linker from JAK2 residue D519 onwards have been shown to be important for the suppression of basal JH1 activity (Zhao et al. 2009). The importance of this region in stabilising the JH2–JH1 interaction also provides rationale for the

function of V617F, which does not lie directly in the JH2–JH1 interface, but rather between the C-terminus of the SH2-JH2 linker, JH2 αC, and the rest of the JH2 N lobe. In this model, V617F is expected to weaken the JH2–JH1 interaction by disturbing the JH2-SH2 linker, especially via interactions with F537 (Toms et al. 2013). This hypothesis is supported by molecular dynamics simulations showing disruption of the linker region in JAK2 V617F, which results in stabilisation of the active state of JH1 (Article III).

In the TYK2 JH2-JH1 crystal structure (Lupardus et al. 2014), the SH2-JH2 linker is only structured from residue $L579^{TYK2}$ onwards (corresponding to $M535^{JAK2}$), even though the expression construct used starts at $G566^{TYK2}$ ($\sim T522^{JAK2}$). This could suggest that the conformation of the linker region, and its involvement in strengthening the JH2–JH1 interface, N-terminal of $L579^{TYK2}$/$M535^{JAK2}$ is less rigid/strong. Indeed, also in JAK2 most of the known activating exon 12 mutations fall between $N531^{JAK2}$ and $F547^{JAK2}$ (Table 3).

Whether a weakening of the JH2–JH1 interaction alone can explain the high activating potency of V617F (or indeed other activating mutations), or whether a distinct activating intra- or intermolecular interaction is involved has still not conclusively been shown. Practically all activating mutations require the presence of cytokine receptors to unleash their transformation potential (Lu, Huang & Lodish 2008, Wernig et al. 2008, Yao et al. 2017). Although receptors might be needed to enable formation of an activating JAK dimer, they could also simply act as a scaffold to co-localise activated JAK2 with its substrate(s), as correct orientation of the receptor is not needed for activation by V617F (Dusa et al. 2010).

There are a few lines of evidence supporting an activation model including a specific activating interaction, however. For example, coIP experiments with full-length JAK2 have shown that addition of the V617F mutation leads to a JAK2–JAK2 interaction *in vitro*, which cannot be detected with wild-type JAK2 (Gorantla et al. 2010). Furthermore, the concentration of activating mutations in JH2 + SH2-JH2 linker, and the relative rarity of JH1 mutations, have been suggested to be a sign of an activating interaction, probably involving the N lobe of JH2, since mutations on the JH1 side of the interface should be equally likely, if activation relied solely on disruption of the JH2–JH1 inhibitory interaction (Silvennoinen, Hubbard 2015). This activating interaction could be an allosteric

means of activating JH1, or simply an interaction leading to correct structural positioning of JH1 to allow transphosphorylation.

*Table 8: Presumed activation mechanisms of known, activating clinical JAK2 mutations based on the JH2–JH1 inhibitory interaction model. *Multiple mutations (Lupardus et al. 2014).*

# Exon	Domain	Structure	Mutation	Mechanism of action	Additional information
3	FERM	F1-β3	E 61 K	Unclear	Could face towards JH2/JH1
4	FERM	F1-β5-β6	T 108 A	Unclear	Could face towards JH2/JH1
6	FERM	F2-α2	E 177 V	In interface with box1	Could increase affinity towards receptor
7	FERM	F3-β1-β2	G 276 A	Unclear	Could face towards JH2/JH1
8	FERM	F3-β6	R 340 Q	Unclear	Could face towards JH2/JH1
9	-		L 393 V	Unclear	
11	SH2				
12	Linker		T 514 M	Unclear	
			N 533 I/Y	Could sequester SH2-JH2 linker towards L539 (in K539L)	
			M 535 I	Probably distorts SH2-JH2 linker and thus weakens interaction with JH1.	Might (additionally) be needed for an activating interaction.
			K 539 L		
			I 540 T		
			538-547		
			D 544 G		
			L 545 S		
			F 547 L		
13	JH2	β1-β2	F 556 L	Unclear	In Gly-rich loop
		β2	R 564 Q	In JH2-linker interface	R564 interacts with backbone amides of F537 and H538 in SH2-JH2 loop
		β2	V 567 A	In JH2–JH1 interface	Could change conformation of β2-β3 loop or disrupt interaction with JH1 β1
		β3-αC	H 587 N	Unclear	Could strengthen activating interaction.
		αC	S 591 L	Unclear	Could strengthen activating interaction.
14		αC-β4	H 606 Q	In JH2–JH1 interface	Opposite of R867, D873, T875 in JH1.
			K 607 N		
			H 608 Y		
			L 611 S	Could distort αC-β4 loop	Distortion of loop expected to weaken interaction with JH1 (see above).
		β4-β5	V 617 F	Somewhat unclear. Could distort SH2-JH2 linker	Distortion of SH2-JH2 linker could weaken interaction with JH1. Could also strengthen activating interaction.
			V 617 I		
			C 618 R		
			D 620 E		
15		β5	L 624 P	Unclear	Near αC.
		αD-αE	I 645 V	Unclear	In αD-αE loop. Opposite face of JH2 to JH1
16		β7	I 682 F	In JH2–JH1 interface	
		β7-β8	R 683 *	In JH2–JH1 interface. Contacts D873.	
17		αF-αG	S 755 R	Unclear	Distal face of JH2 to JH1
19	Link		Y 813 D	In JH2–JH1 interface	In-between JH2 αE and β8
			E 846 D	In JH2–JH1 interface	In the binding site of pY570
20	JH1	β2	R 867 Q	In JH2–JH1 interface	Opposite of H606, K607, H608, and R683 in JH2.
		β2-β3	D 873 N		
			T 875 N		
21		Hinge	P 933 R	In JH2–JH1 interface	
		αD	R 938 Q	Unclear	
24		αG	R 1063 H	Unclear	
25		αH-αI	N 1108 S	Unclear	Distal face of JH1 to JH2

6.3.4 Inhibitory mutations and loss of ATP binding to JH2 suppress ligand-independent activation

Understanding of the activation mechanism of hyperactivating mutations is complemented by the existence of a multitude of experimental JAK mutations capable of inhibiting hyperactivation (Articles II, IV) (Dusa et al. 2010, Gnanasambandan, Magis & Sayeski 2010, Gorantla et al. 2010, Bandaranayake et al. 2012, Yan, Hutchison & Mohi 2012, Toms et al. 2013). Examples of these mutations have been reported in FERM, SH2, and JH2, and many of them seem to be specific in inhibiting only ligand-independent activation (as discussed in 2.5.3). Our results show that mutations blocking ATP binding to JH2 also have this characteristic: suppression of ligand-independent activation, without affecting ligand-dependent signalling (Article II).

6.3.4.1 How do inhibitory mutations inhibit JAK hyperactivation?

The activation model delineated above presents two likely options for the action of inhibitory mutations. Firstly, inhibitory mutations might "hyperstabilise" the autoinhibitory JH2–JH1 interaction, thus counteracting the weakening of the interface by activating mutations. Secondly, inhibitory mutations could act by disrupting a potential activating interaction needed for a mutation to activate.

For some inhibitory mutations, rationalisation of their mode of action is relatively clear. For example, JAK2 F595A was initially designed to inhibit V617F (Dusa et al. 2010, Gnanasambandan, Magis & Sayeski 2010), and molecular dynamics simulations show that adding F595A to V617F does restore the conformation and rigidity of the SH2-JH2 linker disturbed by V617F back to wild-type levels (Article III), thus arguing for a stabilisation of the autoinhibitory interface. How this would translate into suppression of other mutations (especially R683S/G, Figure 9 D, (Dusa et al. 2010)), however, remains unclear.

Contrary to some previous reports (Dusa et al. 2010), we found that all inhibitory mutations decreased basal activation of JAK2 evident in the presence of EPOR coexpression (Figure 9 A). This finding seems to support the notion that inhibitory mutations strengthen basal autoinhibition. Additionally we found that disrupting the link between SH2 and JH2 (with JAK2 V511R) causes lowering of basal activation, as well as inhibition of some activating mutations. Based on our

current knowledge (limited by the lack of full-length JAK structures), this can hardly be attributed to strengthening of the JH2–JH1 interaction. Rather, our result argues that positioning of JH2 between FERM-SH2 and JH1 is important for ligand-independent activation, when the autoinhibitory JH2–JH1 interface is broken (e.g. by R683S or T875N), and that V511R disrupts this positioning. Similarly, we hypothesise that our JH2 ATP-binding site mutations, which block binding of ATP to the domain (Article II), act through a similar mechanism by increasing the conformational flexibility of JH2 normally stabilised by bound ATP.

Interestingly, the different inhibition pattern of K539L compared to R683S suggests a different activation mechanism for K539L. This mutation is unlikely to simply interfere with the autoinhibitory JH2–JH1 interaction, and our inhibitory profile analysis suggests, that its activation mechanism could involve direct activation of JH1 (Leroy et al. 2016), and/or is dependent on strengthening of an activating interaction, which might involve JH1 αC (see E896A+E900A in Figure 9 C). Interestingly, mutations destabilizing the JH2 N lobe (ATP-binding site or F595A) do still partially inhibit K539L, thus indicating that the activation mechanism includes this region.

It is interesting to speculate, whether this activating interaction resulting from correct positioning of JH2 and JH1 simply leads to the conformational freedom JH1 requires for catalysis, or whether a defined intermolecular interaction (presumably with another JAK2 molecule) is required. We found that mutating residues in JH1 αC (JAK2 E896A+E900A) can partially inhibit activation of either K539L or R683S (Figure 9 C, D), which could indicate that a specific interaction involving this region of JH1 is part of the mechanism.

In conclusion, we thus hypothesise, that basal state inhibition of JAK2 is a dynamic equilibrium, in which the autoinhibitory JH2–JH1 interaction favours inhibition, but the positioning of JH1 by JH2 simultaneously enables activation, thus creating a JAK2 molecule with a strong propensity to activate (presumably in the presence of another JAK2 molecule) . Activating mutations exaggerate this propensity by reducing inhibition (e.g. R683 or D873 mutations Table 8), by strengthening the activating position mediated by JH2, or allosterically activating JH1 (as is possible for K539L and V617F). Inhibitory mutations lower this propensity probably by both strengthening the inhibitory interface (e.g., F537A

and E592R) and/or by disturbing the JH2 conformation needed for the activating interaction (ATP-binding site mutations, V511R, maybe E896A+E900A).

It should be noted, that the function of inhibitory mutations is distinct from mutations that completely destabilize JH2 structure (e.g. F739R Table 5; or deletion of JH2 αG (Saharinen, Vihinen & Silvennoinen 2003)). These alterations, while also possibly suppressing activating mutations like V617F, also remove cytokine stimulatability and increase basal JAK activation, thus mimicking JH2 deletions.

6.3.5 JAK activation by cytokine

JAK-associated receptors (Table 1) have highly variable architectures, including 'short receptors' (e.g., GHR, EPOR, γ_c family, and IFNGR) where the ligand-binding domain is proximal to the membrane, and 'tall receptors' (e.g., gp130, TCCR, and LIFRβ) with ligand-binding domains up to 10 nm removed from it (Skiniotis et al. 2005, Matadeen et al. 2007, Wang et al. 2009, Spangler et al. 2015). There are numerous crystal structures of the extracellular domains of JAK-associated receptors, both in the cytokine-bound and unbound states, showing how the conformation of the extracellular domains could change in response to cytokine stimulation (Wang et al. 2009). Yet, no published structures exist from which the conformation of the transmembrane and intracellular portions of the receptor chains in different states of activation could be accurately deduced. Thus, how binding of a cytokine to its receptor is translated into JAK activation is currently unknown.

The simplest model of cytokine receptor activation is an induced dimer/oligomer model, in which binding of a ligand induces dimerisation of receptor chains, which brings associated protein kinases into proximity resulting in activation by transphosphorylation. This mode of activation is widely used by RTKs (Hubbard, Miller 2007, Lemmon, Schlessinger 2010), with notable exceptions like insulin receptor kinase (IRK), which exists as a preformed dimer that is rearranged upon ligand binding (Menting et al. 2013). For JAKs, studies with highly artificial chimeric receptor constructs have shown, that simple dimerisation can be enough to activate associated JAKs (Saka et al. 2012), and this may actually be the activation mechanism of some JAK-receptor systems (Moraga et al. 2015,

Spangler et al. 2015). Many natural JAK-associated receptors[10], however, have been reported to pre-dimerise (Constantinescu et al. 2001, Gent et al. 2002, Brown et al. 2005, Malka et al. 2008, Lupardus et al. 2011). Many of these data may be hampered, however, by the use of artificial overexpression systems, and dimerisation-prone fusion proteins. More accurate and less invasive methodologies in (at least near-to) *in vivo* conditions are thus needed. Additionally, a lack of methodologies simultaneously measuring oligomerisation and activation state of a receptor complex means, that some of the pre-dimerised receptors observed could be active, and thus contribute to 'basal' signalling activity, as opposed to being inactive dimers as previously assumed. Still, correct orientation of dimeric EPOR and TPOR has been shown to be crucial for activation of wild-type JAK2, with some orientations not being able to signal (Seubert et al. 2003, Lu, Gross & Lodish 2006, Staerk et al. 2011), which has been used as an argument for the presence of inactive dimers. More recent studies have shown a distinct lack of pre-formed dimers for EPOR, however, and approaches using engineered protein ligands have suggested that activation of EPOR/JAK2 is mainly determined by the inter-chain distance (Moraga et al. 2015), thus arguing for a ligand-induced dimer model.

6.3.5.1 The role of JH2 in ligand-induced JAK signalling

The first JH2 deletion experiment showed that deletion of TYK2 JH2 resulted in complete unresponsiveness of cells to IFN-α, while deletion of TYK2 JH1 only lowered sensitivity (Velazquez et al. 1995). Similarly, deletion of JAK2 JH2 removed stimulatability by IFN-γ, and deletion of JAK3 JH2 stimulatability by IL-2 (Saharinen, Silvennoinen 2002). Interestingly, similar deletion and mutagenesis experiments have revealed for multiple heteromeric JAK systems, that kinase activity of both JAKs is not required for signalling (Li et al. 2013, Haan et al. 2011), but the presence of JH2s is (Eletto et al. 2016). These data clearly show, that the JH2 domains of receptor-associated JAKs have an important role in relaying the activating signal from an activated (i.e. ligand-bound) cytokine receptor to downstream targets—presumably by enabling activation of the tyrosine kinase activity of one (or more) of the JH1 domains in the JAK–receptor complex.

[10] at least EPOR, GHR, gp130, and IL-2Rβ/IL-9Rα and γ_c

Our results showing practically no STAT1 phosphorylation following IFN-γ stimulation with point mutations in JAK2 JH2 αC (F595A, E592R) and the SH2-JH2 linker (F537A) refine these findings (Article IV), by identifying a previously unknown interface on JH2, which is critically needed for JAK-mediated relaying of signals in IFN-γ stimulation. Furthermore, our finding that JAK2 E592R only partially suppresses EPO signalling (Article IV), suggests that the relative contributions of JAK2 JH2 on signalling are different in the contexts of IFN-γ and EPO, although both rely critically on JAK2 kinase activity (Witthuhn et al. 1993, Briscoe et al. 1996). Similar findings have earlier been made about mutations in JAK2 JH1 (I1065A), which actually showed strongly suppressed EPO signalling, but lesser effects on IFN-γ (Haan et al. 2009). Future research is needed to exactly elucidate the molecular nature of homo-/heteromeric JAK activation, and the role of the specific JH2 interface identified here.

6.3.6 The consequences of ATP binding to JAK2 JH2

Our results shed light on the effects of ATP binding to JH2 (Articles I, II, IV). In Article II, we hypothesised, that the inhibitory effects of ATP binding to JH2 could be due to destabilisation of JH2 αC, as predicted by MD simulations. Our results showing distinct inhibitory profiles as well as distinct effects on cytokine stimulation for inhibitory αC and ATP-binding site mutations suggest, however, that the mechanisms of action of these two classes of inhibitory mutations are distinct (Article IV). Using a thermal shift assay (Article IV), we also show that the effect of ATP binding on JH2 is not simple stabilisation of a domain destabilised by activating mutations, as might have been the case for JAK2 V617F (Article II). Rather, our data suggests that ATP binding to JH2 could be necessary for JH2 to fulfil its structural role as mediator between FERM-SH2 and JH1 and/or as allosteric activator of JH1.

6.4 Implications for JAKs as Drug Targets

JAKs are a prime target for drug development, and the need for inhibitors with novel mode-of-actions is great. Our results presented here potentially provide such a novel drug target within the JAK molecule, by identifying the importance of the JH2 ATP-binding site for ligand-independent activation.

6.4.1 The JH2 ATP-binding site as a drug target

Protein kinases have become the most important target for novel cancer drugs over the last two decades or so and currently are of increasing interest in the treatment of other disease types as well (Cohen, Alessi 2012). All currently approved protein kinase inhibitors target the catalytic ATP-binding sites of protein kinase domains, making understanding and availability of pharmacological scaffolds targeting this site plentiful.

Identification of the JAK JH2 ATP-binding site as a potential pharmacological target has thus been rapidly translated into attempts to find suitable, functional small-molecule binders (Tokarski et al. 2015, Moslin et al. 2017, Newton et al. 2017, Puleo et al. 2017). However, mutant-specific (e.g. V617F) JAK2 inhibition via pharmacological targeting to the JH2 ATP-binding site has yet to be demonstrated. The challenge lies in the pseudokinase nature of JH2: an ATP-competitive inhibitor cannot mimic the natural nucleotide to such an extent as to enable activation of, e.g., V617F, as is the case with the natural ligand ATP. Thus, as ATP binding is needed for mutational activation, replacing ATP with an inactive substrate, which preserves the conformation of ATP-bound JH2, would be expected to backfire (Claus, Cameron & Parker 2013). Furthermore, the special nature of JAK2 JH2 as a potentially active protein kinase phosphorylating two inhibitory residues (S523 and Y570) has also raised doubts about the rationale of targeting the pseudokinase domain. Our results indicate, however, that for the regulation of basal inhibition/activation, the structural role of ATP binding to JAK2 JH2 is more important than a catalytic role, as mutations blocking the ATP-binding site actually lower basal activation (Figure 9 A). Furthermore, similar results obtained for JAK1 mutations (Articles II, IV) suggest that this structural role of JH2 is similarly important in other JAKs as well.

Recently work done at Bristol-Myers Squibb identified multiple small molecule scaffolds specifically binding TYK2 JH2 and (strikingly!) able to inhibit IL-23 signalling in a cell culture model (Tokarski et al. 2015). Interestingly, the authors reported that they were able to find a large number of JH2 ATP-binding site-binding compounds for both JAK1 and TYK2, but only a subset of the TYK2 JH2-binders actually affected cytokine-mediated activation, while none of the numerous JAK1 JH2-binders showed effects on cytokine activation of JAK1 (Tokarski et al. 2015). This finding is in line with our mutagenesis studies, which

suggest that simply blocking ATP binding to JH2 should have a limited (or no) effect on the cytokine-mediated activation of wild-type JAKs (Articles II, IV). Our data, however, also shows that it should be possible to generate inhibitors of cytokine signalling (even through the ATP-binding pocket), by altering the characteristics of JH2 αC or the SH2-JH2 linker in a way mimicking the mutations F537A, F595A, or E592R. We thus hypothesise, that the scaffold identified by Tokarski and colleagues is able to affect TYK2-mediated cytokine signalling by this mechanism.

The full pharmacostructural determinants of a successful JAK JH2 ATP-binding site inhibitor are still unknown—whether for the inhibition of cytokine activation of wild-type JAK as demonstrated for TYK2 (Tokarski et al. 2015, Moslin et al. 2017), or for the mutation-specific inhibition of hyperactivated JAK, e.g., JAK2 V617F, as suggested in Articles II and IV. Our results in Article IV indicate that inhibition of mutational hyperactivation via the JH2 ATP-binding site should be possible with "traditional" purine-pocket binding compounds, as breaking of the so-called C spine is not required for inhibition. Encouragingly, successful development of conformation modulators targeting the ATP-binding site of pseudokinases has been recently demonstrated for Kinase suppressor of Ras (KSR) (Dhawan, Scopton & Dar 2016).

Beyond direct, targeted conformational effects caused by ATP-binding site occupation, functional nucleotide binding sites (as characterised for JAK1, JAK2, and TYK2 JH2 in Articles I and II) offer also the opportunity for pharmacological modulation of protein function via other modes-of-action. One such alternative approach is to tag selective nucleotide-binding site-binders with chemical groups that cause the shuttling of the tagged protein for degradation (Huang, Dixit 2016). This approach has recently been utilised, for example, in the targeting of the HER3 pseudokinase (Xie et al. 2014, Lim et al. 2015).

Recently, also other substructures of JH2 have been proposed to be potential drug target sites (Leroy, Constantinescu 2017). Specifically, identification of JH2 αC outer face residues as critical for mutational hyperactivation of JAKs (Leroy et al. 2016), has led to the proposition of targeting this region with protein-protein interaction (PPI) inhibitors (Leroy, Constantinescu 2017). Pharmacologically, PPI inhibitors have proven challenging to develop and currently remain highly experimental. With the inevitable advancements in the

field of pharmacological peptide synthesis, it will be interesting to see, how also this approach of targeting JAKs will develop—especially given the potential for JAK signalling pathway specificity that targeting this region of JAKs presents (Article IV).

7 Summary and Conclusions

Cellular signalling controls most biological processes. Much of this signalling is mediated by soluble signalling proteins called cytokines, which bind specific receptors on cell surfaces to activate series of intracellular biochemical events in a process called signal transduction. Janus kinases (JAK1–3, TYK2) are intracellular, non-receptor tyrosine kinases that mediate signalling of around 60 different cytokines critically involved in haematopoiesis, metabolism, development, and control of the immune system (O'Shea, Plenge 2012). JAKs consist of multiple domains, including a pseudokinase domain (JH2), which precedes the active tyrosine kinase domain (JH1). JH2 has critical regulatory functions, and harbours many oncogenic driver mutations underlying haematopoietic malignancies (JAK2 mutations), leukaemia (JAKs 1–3), and cancer (JAK1, JAK3) (Vainchenker, Constantinescu 2013).

The work presented here describes characterisation of the structure and functions of JAK JH2s. We found that all JAK JH2s have functional nucleotide-binding sites accessible to ATP and small molecule inhibitors. Using rational mutagenesis, we identify the JAK2 JH2 ATP-binding site as a target for potentially mutation-specific inhibitors, which would be a distinct improvement over current JAK2 inhibitors that are unable to eradicate the disease (Sonbol et al. 2013). In collaboration with researchers at NYU and DE Shaw research, we established a model for JH2-mediated inhibition of JH1, based on long-scale molecular dynamics simulations. Our model explains the mechanism of inhibition of JH1 by JH2, and provides rationale for most known clinical JAK2 mutations. We also present a systematic analysis of JAK2 mutations capable of inhibiting ligand-independent hyperactivation. The analysis enables functional grouping of activating mutations based on mechanism, and identifies a novel interface in JAK2 JH2 needed for heteromeric JAK2 activation in IFN-γ signalling.

Our results refine our understanding of JAK function at a time, when clinical JAK inhibitors are being increasingly applied not only to diseases driven by JAK mutations (e.g., myeloproliferative neoplasms), but also to immunological

disorders, in which JAKs present a tempting target as signalling hubs in numerous proinflammatory pathways (Yamaoka 2016, O'Sullivan, Harrison 2017, Banerjee et al. 2017). The ubiquitous involvement of JAKs in cytokine signalling, however, presents challenges of specificity and our limited understanding of the interplay of different JAKs on different cytokine receptors has left much of the development of JAK-targeted drugs down to trial and error. In the future, elucidation of the molecular mechanisms of JAK activation on their associated receptors, and the involvement of the different JAK domains (including their potential druggable sites) in this process, will certainly be of paramount importance for the ultimate unlocking of JAKs for targeted therapeutics.

8 Acknowledgements

The list of people that deserve thanking for enabling the completion of the work presented here is delightfully long, as I have had the magnificent opportunity and pleasure to work together with a great many helpful people over the last few years.

In practice, the work presented was carried out in the research group for Molecular Immunology and Cytokine Signalling at the Faculty of Medicine and Life Sciences at the University of Tampere, in Tampere, Finland, under the expert supervision of Professor Olli Silvennoinen (MD, PhD).

I wish to express my deep gratitude to you, Olli, as you have not only provided an excellent working environment with all the necessary facilities in Tampere, but also given me the opportunity to meet up with leading minds in the field and visit top research organizations. You have had faith in me (sometimes much more than I had myself) to help set up a lab across the ocean, introduce and develop new methods, and tackle challenging scientific questions. You have let me work independently, which has taught me much. You have also been patient with me, when patience was called for, and you have given me the necessary nudge into the right direction, when that was required. Thank you for everything!

Secondly, I wish to thank Prof. Stevan R. Hubbard (PhD) from New York University, who has practically been a second scientific supervisor to me, and mastermind in all thinks kinases. Thank you for invaluable comments, thorough discussions, and teaching me the way and value of proper scientific thinking and experimentation.

I also thank our excellent scientific collaborators from around the world. Prof. Radek Skoda (MD, PhD) and Jean Grisouard (PhD) from Basel, Switzerland, and their patient and expertly work on the MPN mouse model. Also David E. Shaw

(PhD) and Yibing Shan (PhD) from New York for their outstanding and unique contribution in molecular modelling of JAKs.

My gratitude also goes out to the members of my thesis follow-up group: Vesa Hytönen (PhD), Marko Pesu (MD, PhD), and Olli Pentikäinen (PhD), as well as my expert pre-examiners Outi Kilpivaara (PhD) and Michael Courtney (PhD). Thank you for extremely valuable criticism and discussions.

This work was financially supported in part by the Doctoral Programme of the School of Medicine at the University of Tampere.

Luckily, daily lab work does not have to be a lonely endeavour, nor does it have to ever be boring, and for this a huge Thank You belongs to all Ollilab members: Juha Saarikettu, Merja Lehtinen, Pia Isomäki, Heidi Peussa, Anniina Virtanen, Saara Lehmusvaara, Bobin George Abraham, Juuli Raivola, Maaria Palmroth, Krista Lehtinen, Guillermo Nieto, and Teemu Haikarainen. Juha, thanks for all the valuable comments, banter and good discussions over the years. Krista and Merja, thank you for keeping the lab running, providing excellent and friendly technical assistance whenever needed, as well as doing countless minipreps. Speaking of minipreps: thank you Heidi! Working with you has been a joy. Your energy, never-failing can-do attitude even when facing large tasks on a sometimes tight schedule, as well as your excellent lab "handwriting" has been amazing to watch and this work would not have been possible in its current form without you. Thank you Anniina for taking the drug screening project and running with it with admirable consistency and confidence. Thank you also Juuli for bringing your uncurbed enthusiasm and some much-needed vitality to the day-to-day lab work. I would have liked to work longer with you on JAKs. Thanks also to Maaria for providing great discussions and puzzles also outside the world of JAKs and for being a very enjoyable lab neighbour. Bobin and Teemu, thank you for showing me what professional science can be like, and how genuine technical expertise can transform projects practically overnight. I would have definitely liked to work longer with the both of you, and my only regret is, that you didn't join the lab earlier than you did.

I also thank all former lab members from Ollilab. Firstly, Daniela Ungureanu, who was effectively my JAK mentor in the beginning of my PhD work, and taught me the value and necessity of independent work and enquiry. Additionally, I wish to thank former lab members Juha Grönholm, Yashavanthi Niranjan, Tekele Fashe,

Ellin-Kristina Hillert, Paula Kosonen, Minna Hankaniemi, and Elina Koskenalho. Thank you for all the good discussions, help and being part in creating a nice, productive and humane working atmosphere. Also, a big Thank You to all summer students that I had the chance to work with – most importantly Anna U. Laitinen and Saku Pelttari.

A massive thank you goes out to friends and former co-workers from overseas: Kaury and Nathan Kucera, David Puleo, and Shai Naparstek. Kaury, thank you for being so incredibly friendly, helpful, and welcoming. Our little US adventure would definitely not have been anywhere near the great positive experience it was, had it not been for your and your family's hospitality, unquestioning and immediate friendliness and overall extremely valuable help. I fondly remember our Rhode Island road trip, our walk enjoying New England nature in fall, as well as yummy lobster evening. Thank you.

I also wish to thank friends and colleagues from local neighbouring labs, including the whole Pesu lab (especially Saara Aittomäki for help and insight into Luc-reporters), Vesa Hytönen's Protein Dynamics lab with special thanks to Rolle Rahikainen, as well as Juha Määttä for expert technical assistance on the spectrofluorometer.

A great many thanks go also to what is nearest and dearest to me: my family. Mama, Danke das Du es mir durch meine Erziehung ermöglichst hast, die nötige Neugier, Selbstsicherheit und Ruhe – aber auch den notwendigen Antrieb – zu entwickeln, um eine Aufgabe wie diese Dissertation anzugehen. Du hast mich immer, und tust es immernoch, meinen Weg selber wählen lassen. Für all das, und vieles mehr, bin ich Dir dankbar, und deswegen gehört ein großes Danke für diese Arbeit auch an Dich. Gleichfalls geht ein Teil des vohergehenden Dankeschöns auch an meine Geschwister, Michael, Johanna und Magdaleena.

Osakiitos tämän työn mahdollistamisesta kuuluu myös isoisälleni, Pappa Reino Henrik Hammarénille, joka tosin ei aivan ehtinyt nähdä tämän työn valmistumista. Kiitos Pappa, että loit aina uskoa kykyihini ja hyväksyvällä tavallasi ja hienolla esimerkilläsi rohkaisit minua valitsemaan oman elämäntieni. Kiitosta kuuluu myös isälleni, jonka kautta sain ensimmäisen kosketuksen luonnontieteiden ihmeelliseen maailmaan.

Suurkiitos myös Ira-Mummalle ja Kimmo-Ukille. Oli apu sitten lasten-, kodin-, tai terveydenhoidon saralla, olette aina olleet läsnä ja tarjoamassa aikaanne. Voin hyvällä omallatunnolla todeta, ettei perheemme olisi selvinnyt näin hyvin tämän työn valmistumista edeltävistä haastavistakin ajoista ilman teidän suurta apuanne. Kiitos siitä.

Lastly, but most certainly not leastly, there are my amazing wife and two magnificent daughters. Mea und Fia, Ihr zwei habt mir besser und gründlicher gelehrt, was wirklich wichtig ist im Leben, als es jeder Lehrer, Professor oder Mentor je gekonnt hat. Und das konntet ihr beide, ohne anfangs auch nur ein Wort benutzen zu müssen. Zusätzlich, habt Ihr mir einen besseren Grund gegeben schlaflose Nächte zu verbringen als es kein Buch der Welt (einschließlich das Vorliegende) jemals hätte können.

Finally, my wonderful wife, Milka, who actually is to thank for my little endeavour into the world of medical biosciences. Thank You for your unwavering friendship, patience, support, and love. Science is team-work, but so is life. Thank You, Milka, for being on my team.

Henrik Hammarén

Tampere 7.11.2017

9 References

Alberts, B., Bray, D., Hopkin, K., Johnson, A., Lewis, J., Raff, M., Roberts, K. & Walter, P. 2013, *Essential cell biology,* Garland Science.

Andraos, R., Qian, Z., Bonenfant, D., Rubert, J., Vangrevelinghe, E., Scheufler, C., Marque, F., Régnier, C.H., De Pover, A. & Ryckelynck, H. 2012, "Modulation of activation-loop phosphorylation by JAK inhibitors is binding mode dependent", *Cancer Discovery,* vol. 2, no. 6, pp. 512-523.

Aparicio-Siegmund, S. & Garbers, C. 2015, "The biology of interleukin-27 reveals unique pro-and anti-inflammatory functions in immunity", *Cytokine & growth factor reviews,* vol. 26, no. 5, pp. 579-586.

Araki, M. & Komatsu, N. 2017, "Novel molecular mechanism of cellular transformation by a mutant molecular chaperone in myeloproliferative neoplasms", *Cancer science,* vol. 108, no. 10, pp. 1907-1912.

Aranaz, P., Ormazábal, C., Hurtado, C., Erquiaga, I., Calasanz, M.J., García-Delgado, M., Novo, F.J. & Vizmanos, J.L. 2010, "A new potential oncogenic mutation in the FERM domain of JAK2 in BCR/ABL1-negative and V617F-negative chronic myeloproliferative neoplasms revealed by a comprehensive screening of 17 tyrosine kinase coding genes", *Cancer genetics and cytogenetics,* vol. 199, no. 1, pp. 1-8.

Argetsinger, L.S., Kouadio, J.L.K., Steen, H., Stensballe, A., Jensen, O.N. & Carter-Su, C. 2004, "Autophosphorylation of JAK2 on tyrosines 221 and 570 regulates its activity", *Molecular and cellular biology,* vol. 24, no. 11, pp. 4955-4967.

Argetsinger, L.S., Stuckey, J.A., Robertson, S.A., Koleva, R.I., Cline, J.M., Marto, J.A., Myers Jr, M.G. & Carter-Su, C. 2010, "Tyrosines 868, 966, and 972 in the Kinase Domain of JAK2 Are Autophosphorylated and Required for Maximal JAK2 Kinase Activity", *Molecular Endocrinology,* vol. 24, no. 5, pp. 1062-1076.

Babon, J.J., Kershaw, N.J., Murphy, J.M., Varghese, L.N., Laktyushin, A., Young, S.N., Lucet, I.S., Norton, R.S. & Nicola, N.A. 2012, "Suppression of Cytokine Signaling by SOCS3: Characterization of the Mode of Inhibition and the Basis of Its Specificity", *Immunity,* vol. 36, no. 2, pp. 239-250.

Babon, J.J., Lucet, I.S., Murphy, J.M., Nicola, N.A. & Varghese, L.N. 2014, "The molecular regulation of Janus kinase (JAK) activation", *Biochemical Journal,* vol. 462, no. 1, pp. 1-13.

Bahar, B., Barton, K. & Kini, A.R. 2016, "The role of the Exon 13 G571S JAK2 mutation in myeloproliferative neoplasms", *Leukemia research reports,* vol. 6, pp. 27-28.

Baker, S., Rane, S. & Reddy, E. 2007, "Hematopoietic cytokine receptor signaling", *Oncogene,* vol. 26, no. 47, pp. 6724-6737.

Bandaranayake, R.M., Ungureanu, D., Shan, Y., Shaw, D.E., Silvennoinen, O. & Hubbard, S.R. 2012, "Crystal structures of the JAK2 pseudokinase domain and the pathogenic mutant V617F", *Nature Structural & Molecular Biology,* vol. 19, pp. 754-759.

Banerjee, S., Biehl, A., Gadina, M., Hasni, S. & Schwartz, D.M. 2017, "JAK–STAT Signaling as a Target for Inflammatory and Autoimmune Diseases: Current and Future Prospects", *Drugs,* vol. 77, no. 5, pp. 521-546.

Baxter, E.J., Scott, L.M., Campbell, P.J., East, C., Fourouclas, N., Swanton, S., Vassiliou, G.S., Bench, A.J., Boyd, E.M. & Curtin, N. 2005, "Acquired mutation of the tyrosine kinase JAK2 in human myeloproliferative disorders", *The Lancet,* vol. 365, no. 9464, pp. 1054-1061.

Bayliss, R., Haq, T. & Yeoh, S. 2015, "The ys and wherefores of protein kinase autoinhibition", *Biochimica et Biophysica Acta (BBA)-Proteins and Proteomics,* vol. 1854, no. 10, pp. 1586-1594.

Becker, S., Groner, B. & Müller, C.W. 1998, "Three-dimensional structure of the Stat3β homodimer bound to DNA", *Nature,* vol. 394, no. 6689, pp. 145-151.

Bellanger, D., Jacquemin, V., Chopin, M., Pierron, G., Bernard, O., Ghysdael, J. & Stern, M. 2014, "Recurrent JAK1 and JAK3 somatic mutations in T-cell prolymphocytic leukemia", *Leukemia,* vol. 28, no. 2, pp. 417-419.

Bercovich, D., Ganmore, I., Scott, L.M., Wainreb, G., Birger, Y., Elimelech, A., Shochat, C., Cazzaniga, G., Biondi, A. & Basso, G. 2008, "Mutations of JAK2 in acute lymphoblastic leukaemias associated with Down's syndrome", *The Lancet,* vol. 372, no. 9648, pp. 1484-1492.

Boggon, T.J., Li, Y., Manley, P.W. & Eck, M.J. 2005, "Crystal structure of the Jak3 kinase domain in complex with a staurosporine analog", *Blood,* vol. 106, no. 3, pp. 996-1002.

Bonjardim, C. 1998, "JAK/STAT-deficient cell lines", *Brazilian journal of medical and biological research,* vol. 31, no. 11, pp. 1389-1395.

Boudeau, J., Miranda-Saavedra, D., Barton, G.J. & Alessi, D.R. 2006, "Emerging roles of pseudokinases", *Trends in cell biology,* vol. 16, no. 9, pp. 443-452.

Bradshaw, J.M. 2010, "The Src, Syk, and Tec family kinases: distinct types of molecular switches", *Cellular signalling,* vol. 22, no. 8, pp. 1175-1184.

Brennan, D.F., Dar, A.C., Hertz, N.T., Chao, W.C., Burlingame, A.L., Shokat, K.M. & Barford, D. 2011, "A Raf-induced allosteric transition of KSR stimulates phosphorylation of MEK", *Nature,* vol. 472, no. 7343, pp. 366-369.

Briscoe, J., Rogers, N., Witthuhn, B., Watling, D., Harpur, A., Wilks, A., Stark, G., Ihle, J. & Kerr, I. 1996, "Kinase-negative mutants of JAK1 can sustain interferon-gamma-inducible gene expression but not an antiviral state.", *The EMBO journal,* vol. 15, no. 4, pp. 799.

Brooks, A.J., Dai, W., O'Mara, M.L., Abankwa, D., Chhabra, Y., Pelekanos, R.A., Gardon, O., Tunny, K.A., Blucher, K.M., Morton, C.J., Parker, M.W., Sierecki, E., Gambin, Y., Gomez, G.A., Alexandrov, K., Wilson, I.A., Doxastakis, M., Mark, A.E. & Waters, M.J. 2014, "Mechanism of activation of protein kinase JAK2 by the growth hormone receptor", *Science (New York, N.Y.),* vol. 344, no. 6185, pp. 1249783.

Brown, R.J., Adams, J.J., Pelekanos, R.A., Wan, Y., McKinstry, W.J., Palethorpe, K., Seeber, R.M., Monks, T.A., Eidne, K.A. & Parker, M.W. 2005, "Model for growth hormone receptor activation based on subunit rotation within a receptor dimer", *Nature structural & molecular biology,* vol. 12, no. 9, pp. 814-821.

Bugge, K., Papaleo, E., Haxholm, G.W., Hopper, J.T., Robinson, C.V., Olsen, J.G., Lindorff-Larsen, K. & Kragelund, B.B. 2016, "A combined computational and structural model of the full-length human prolactin receptor", *Nature communications,* vol. 7, no. 13, pp. 11578.

Cacalano, N.A., Migone, T.S., Bazan, F., Hanson, E.P., Chen, M., Candotti, F., O'Shea, J.J. & Johnston, J.A. 1999, "Autosomal SCID caused by a point mutation in the N-terminus of Jak3: mapping of the Jak3-receptor interaction domain", *The EMBO journal,* vol. 18, no. 6, pp. 1549-1558.

Camps, C.D., Petousi, N., Bento, C., Cario, H., Copley, R.R., McMullin, M.F., vanWijk, R., Ratcliffe, P.J., Robbins, P.A. & Taylor, J.C. 2016, "Gene panel sequencing improves the diagnostic work-up of patients with idiopathic erythrocytosis and identifies new mutations", *Haematologica,* vol. 101, no. 11, pp. 1306-1318.

Carrera, A.C., Alexandrov, K. & Roberts, T.M. 1993, "The conserved lysine of the catalytic domain of protein kinases is actively involved in the phosphotransfer reaction and not required for anchoring ATP", *Proceedings of the National*

Academy of Sciences of the United States of America, vol. 90, no. 2, pp. 442-446.

Casanova, J., Holland, S.M. & Notarangelo, L.D. 2012, "Inborn errors of human JAKs and STATs", *Immunity,* vol. 36, no. 4, pp. 515-528.

Cazzola, M. & Kralovics, R. 2014, "From Janus kinase 2 to calreticulin: the clinically relevant genomic landscape of myeloproliferative neoplasms", *Blood,* vol. 123, no. 24, pp. 3714-3719.

Ceccarelli, D.F.J., Song, H.K., Poy, F., Schaller, M.D. & Eck, M.J. 2006, "Crystal structure of the FERM domain of focal adhesion kinase", *Journal of Biological Chemistry,* vol. 281, no. 1, pp. 252-259.

Chatti, K., Farrar, W.L. & Duhé, R.J. 2004, "Tyrosine phosphorylation of the Janus kinase 2 activation loop is essential for a high-activity catalytic state but dispensable for a basal catalytic state", *Biochemistry,* vol. 43, no. 14, pp. 4272-4283.

Chen, M., Cheng, A., Candotti, F., Zhou, Y.J., Hymel, A., Fasth, A., Notarangelo, L.D. & O'Shea, J.J. 2000, "Complex effects of naturally occurring mutations in the JAK3 pseudokinase domain: evidence for interactions between the kinase and pseudokinase domains", *Molecular and cellular biology,* vol. 20, no. 3, pp. 947-56.

Chen, X., Vinkemeier, U., Zhao, Y., Jeruzalmi, D., Darnell, J.E. & Kuriyan, J. 1998, "Crystal structure of a tyrosine phosphorylated STAT-1 dimer bound to DNA", *Cell,* vol. 93, no. 5, pp. 827-839.

Cheng, K. & Koland, J. 1998, "Nucleotide-binding properties of kinase-deficient epidermal-growth-factor-receptor mutants", *Biochem.J,* vol. 330, pp. 353-359.

Chishti, A.H., Kim, A.C., Marfatia, S.M., Lutchman, M., Hanspal, M., Jindal, H., Liu, S., Low, P.S., Rouleau, G.A., Mohandas, N., Chasis, J.A., Conboy, J.G., Gascard, P., Takakuwa, Y., Huang, S., Benz Jr, E.J., Bretscher, A., Fehon, R.G., Gusella, J.F., Ramesh, V., Solomon, F., Marchesi, V.T., Tsukita, S., Tsukita, S., Arpin, M., Louvard, D., Tonks, N.K., Anderson, J.M., Fanning, A.S., Bryant, P.J., Woods, D.F. & Hoover, K.B. 1998, "The FERM domain: a unique module involved in the linkage of cytoplasmic proteins to the membrane", *Trends in biochemical sciences,* vol. 23, no. 8, pp. 281-282.

Chrencik, J.E., Patny, A., Leung, I.K., Korniski, B., Emmons, T.L., Hall, T., Weinberg, R.A., Gormley, J.A., Williams, J.M. & Day, J.E. 2010, "Structural and thermodynamic characterization of the TYK2 and JAK3 kinase domains in complex with CP-690550 and CMP-6", *Journal of Molecular Biology,* vol. 400, no. 3, pp. 413-433.

Claus, J., Cameron, A.J. & Parker, P.J. 2013, "Pseudokinase drug intervention: a potentially poisoned chalice", *Biochemical Society transactions,* vol. 41, no. 4, pp. 1083-1088.

Cohen, P. 2002, "The origins of protein phosphorylation", *Nature cell biology,* vol. 4, no. 5, pp. E127-E130.

Cohen, P. & Alessi, D.R. 2012, "Kinase drug discovery–what's next in the field?", *ACS chemical biology,* vol. 8, no. 1, pp. 96-104.

Commins, S., Steinke, J.W. & Borish, L. 2008, "The extended IL-10 superfamily: IL-10, IL-19, IL-20, IL-22, IL-24, IL-26, IL-28, and IL-29", *Journal of Allergy and Clinical Immunology,* vol. 121, no. 5, pp. 1108-1111.

Constantinescu, S.N., Keren, T., Socolovsky, M., Nam, H., Henis, Y.I. & Lodish, H.F. 2001, "Ligand-independent oligomerization of cell-surface erythropoietin receptor is mediated by the transmembrane domain", *Proceedings of the National Academy of Sciences of the United States of America,* vol. 98, no. 8, pp. 4379-4384.

Constantinescu, S.N., Leroy, E., Gryshkova, V., Pecquet, C. & Dusa, A. 2013, "Activating Janus kinase pseudokinase domain mutations in myeloproliferative and other blood cancers", *Biochemical Society transactions,* vol. 41, no. 4, pp. 1048-1054.

Corwin, H.O. & Hanratty, W.P. 1976, "Characterization of a unique lethal tumorous mutation in Drosophila", *Molecular and General Genetics MGG,* vol. 144, no. 3, pp. 345-347.

Cui, J., Zhu, Q., Zhang, H., Cianfrocco, M.A., Leschziner, A.E., Dixon, J.E. & Xiao, J. 2017, "Structure of Fam20A reveals a pseudokinase featuring unique disulfide pattern and inverted ATP-binding", *eLife,* vol. 6, pp. e23990.

Damsky, W. & King, B.A. 2017, "JAK inhibitors in dermatology: The promise of a new drug class", *Journal of the American Academy of Dermatology,* vol. 76, no. 4, pp. 736-744.

Darnell Jr, J.E., Kerr, I.M. & Stark, G.R. 1994, "Jak-STAT pathways and transcriptional activation in response to IFNs and other extracellular signaling proteins", *Science-AAAS-weekly paper edition-including guide to scientific information,* vol. 264, no. 5164, pp. 1415-1420.

Darnell, J.E.,Jr 1997, "STATs and gene regulation", *Science (New York, N.Y.),* vol. 277, no. 5332, pp. 1630-1635.

Delic, S., Rose, D., Kern, W., Nadarajah, N., Haferlach, C., Haferlach, T. & Meggendorfer, M. 2016, "Application of an NGS-based 28-gene panel in myeloproliferative neoplasms reveals distinct mutation patterns in essential

thrombocythaemia, primary myelofibrosis and polycythaemia vera", *British journal of haematology,* vol. 175, no. 3, pp. 419-426.

Dey, G., Radhakrishnan, A., Syed, N., Thomas, J.K., Nadig, A., Srikumar, K., Mathur, P.P., Pandey, A., Lin, S. & Raju, R. 2013, "Signaling network of Oncostatin M pathway", *J Cell Commun Signal,* vol. 7, pp. 103-108.

Dhawan, N.S., Scopton, A.P. & Dar, A.C. 2016, "Small molecule stabilization of the KSR inactive state antagonizes oncogenic Ras signalling", *Nature,* vol. 537, no. 7618, pp. 112-116.

Dusa, A., Mouton, C., Pecquet, C., Herman, M. & Constantinescu, S.N. 2010, "JAK2 V617F Constitutive Activation Requires JH2 Residue F595: A Pseudokinase Domain Target for Specific Inhibitors", *PloS one,* vol. 5, no. 6, pp. 207-212.

Dusa, A., Staerk, J., Elliott, J., Pecquet, C., Poirel, H.A., Johnston, J.A. & Constantinescu, S.N. 2008, "Substitution of pseudokinase domain residue Val-617 by large non-polar amino acids causes activation of JAK2", *Journal of Biological Chemistry,* vol. 283, no. 19, pp. 12941.

Eletto, D., Burns, S.O., Angulo, I., Plagnol, V., Gilmour, K.C., Henriquez, F., Curtis, J., Gaspar, M., Nowak, K., Daza-Cajigal, V., Kumararatne, D., Doffinger, R., Thrasher, A.J. & Nejentsev, S. 2016, "Biallelic JAK1 mutations in immunodeficient patient with mycobacterial infection", *Nature communications,* vol. 7, pp. 13992.

Elf, S., Abdelfattah, N.S., Chen, E., Perales-Paton, J., Rosen, E.A., Ko, A., Peisker, F., Florescu, N., Giannini, S., Wolach, O., Morgan, E.A., Tothova, Z., Losman, J.A., Schneider, R.K., Al-Shahrour, F. & Mullally, A. 2016, "Mutant Calreticulin Requires Both Its Mutant C-terminus and the Thrombopoietin Receptor for Oncogenic Transformation", *Cancer discovery,* vol. 6, no. 4, pp. 368-381.

Endicott, J.A., Noble, M.E. & Johnson, L.N. 2012, "The structural basis for control of eukaryotic protein kinases", *Annual Review of Biochemistry,* vol. 81, pp. 587-613.

Etheridge, S.L., Cosgrove, M.E., Sangkhae, V., Corbo, L.M., Roh, M.E., Seeliger, M.A., Chan, E.L. & Hitchcock, I.S. 2014, "A novel activating, germline JAK2 mutation, JAK2R564Q, causes familial essential thrombocytosis", *Blood,* vol. 123, no. 7, pp. 1059-1068.

Feener, E.P., Rosario, F., Dunn, S.L., Stancheva, Z. & Myers Jr, M.G. 2004, "Tyrosine phosphorylation of Jak2 in the JH2 domain inhibits cytokine signaling", *Molecular and cellular biology,* vol. 24, no. 11, pp. 4968-4978.

Feng, J., Witthuhn, B.A., Matsuda, T., Kohlhuber, F., Kerr, I.M. & Ihle, J.N. 1997, "Activation of Jak2 catalytic activity requires phosphorylation of Y1007 in the

kinase activation loop", *Molecular and cellular biology,* vol. 17, no. 5, pp. 2497-2501.

Ferrao, R. & Lupardus, P.J. 2017, "The Janus Kinase (JAK) FERM and SH2 Domains: Bringing Specificity to JAK–Receptor Interactions", *Frontiers in Endocrinology,* vol. 8, no. 18, pp. 71.

Ferrao, R., Wallweber, H.J., Ho, H., Tam, C., Franke, Y., Quinn, J. & Lupardus, P.J. 2016, "The Structural Basis for Class II Cytokine Receptor Recognition by JAK1", *Structure,* vol. 24, no. 6, pp. 897-905.

Firmbach-Kraft, I., Byers, M., Shows, T., Dalla-Favera, R. & Krolewski, J.J. 1990, "Tyk2, Prototype of a Novel Class of Non-Receptor Tyrosine Kinase Genes", *Oncogene,* vol. 5, no. 9, pp. 1329-1336.

Fischer, E.H. & Krebs, E.G. 1955, "Conversion of phosphorylase b to phosphorylase a in muscle extracts", *The Journal of biological chemistry,* vol. 216, no. 1, pp. 121-132.

Flex, E., Petrangeli, V., Stella, L., Chiaretti, S., Hornakova, T., Knoops, L., Ariola, C., Fodale, V., Clappier, E., Paoloni, F., Martinelli, S., Fragale, A., Sanchez, M., Tavolaro, S., Messina, M., Cazzaniga, G., Camera, A., Pizzolo, G., Tornesello, A., Vignetti, M., Battistini, A., Cave, H., Gelb, B.D., Renauld, J.C., Biondi, A., Constantinescu, S.N., Foa, R. & Tartaglia, M. 2008, "Somatically acquired JAK1 mutations in adult acute lymphoblastic leukemia", *The Journal of experimental medicine,* vol. 205, no. 4, pp. 751-758.

Fukuda, K., Knight, J.D., Piszczek, G., Kothary, R. & Qin, J. 2011, "Biochemical, Proteomic, Structural, and Thermodynamic Characterizations of Integrin-linked Kinase (ILK) CROSS-VALIDATION OF THE PSEUDOKINASE", *Journal of Biological Chemistry,* vol. 286, no. 24, pp. 21886-21895.

Funakoshi-Tago, M., Pelletier, S., Matsuda, T., Parganas, E. & Ihle, J.N. 2006, "Receptor specific downregulation of cytokine signaling by autophosphorylation in the FERM domain of Jak2", *The EMBO journal,* vol. 25, no. 20, pp. 4763-4772.

Funakoshi-Tago, M., Pelletier, S., Moritake, H., Parganas, E. & Ihle, J.N. 2008a, "Jak2 FERM domain interaction with the erythropoietin receptor regulates Jak2 kinase activity", *Molecular and cellular biology,* vol. 28, no. 5, pp. 1792-1801.

Funakoshi-Tago, M., Tago, K., Kasahara, T., Parganas, E. & Ihle, J.N. 2008b, "Negative regulation of Jak2 by its auto-phosphorylation at tyrosine 913 via the Epo signaling pathway", *Cellular signalling,* vol. 20, no. 11, pp. 1995-2001.

Gadina, M., Hilton, D., Johnston, J.A., Morinobu, A., Lighvani, A., Zhou, Y., Visconti, R. & O'Shea, J.J. 2001, "Signaling by type I and II cytokine receptors: ten years after", *Current opinion in immunology,* vol. 13, no. 3, pp. 363-373.

Gao, S.P., Chang, Q., Mao, N., Daly, L.A., Vogel, R., Chan, T., Liu, S.H., Bournazou, E., Schori, E., Zhang, H., Brewer, M.R., Pao, W., Morris, L., Ladanyi, M., Arcila, M., Manova-Todorova, K., de Stanchina, E., Norton, L., Levine, R.L., Altan-Bonnet, G., Solit, D., Zinda, M., Huszar, D., Lyden, D. & Bromberg, J.F. 2016, "JAK2 inhibition sensitizes resistant EGFR-mutant lung adenocarcinoma to tyrosine kinase inhibitors", *Science signaling,* vol. 9, no. 421, pp. ra33.

Garbett, N.C. & Chaires, J.B. 2012, "Thermodynamic studies for drug design and screening", *Expert Opinion on Drug Discovery,* vol. 7, no. 4, pp. 299-314.

Gent, J., van Kerkhof, P., Roza, M., Bu, G. & Strous, G.J. 2002, "Ligand-independent growth hormone receptor dimerization occurs in the endoplasmic reticulum and is required for ubiquitin system-dependent endocytosis", *Proceedings of the National Academy of Sciences of the United States of America,* vol. 99, no. 15, pp. 9858-9863.

Gherardini, P.F., Ausiello, G., Russell, R.B. & Helmer-Citterich, M. 2010, "Modular architecture of nucleotide-binding pockets", *Nucleic acids research,* vol. 38, no. 11, pp. 3809-3816.

Gibbs, C.S. & Zoller, M.J. 1991, "Rational scanning mutagenesis of a protein kinase identifies functional regions involved in catalysis and substrate interactions", *The Journal of biological chemistry,* vol. 266, no. 14, pp. 8923-8931.

Giese, B., Au-Yeung, C., Herrmann, A., Diefenbach, S., Haan, C., Küster, A., Wortmann, S.B., Roderburg, C., Heinrich, P.C. & Behrmann, I. 2003, "Long term association of the cytokine receptor gp130 and the Janus kinase Jak1 revealed by FRAP analysis", *Journal of Biological Chemistry,* vol. 278, no. 40, pp. 39205-39213.

Gnanasambandan, K. & Sayeski, P. 2011, "A structure-function perspective of jak2 mutations and implications for alternate drug design strategies: the road not taken", *Current medicinal chemistry,* vol. 18, no. 30, pp. 4659-4673.

Gnanasambandan, K., Magis, A. & Sayeski, P.P. 2010, "The constitutive activation of Jak2-V617F is mediated by a π stacking mechanism involving phenylalanines 595 and 617", *Biochemistry,* vol. 49, no. 46, pp. 9972-9984.

Godeny, M.D., Sayyah, J., VonDerLinden, D., Johns, M., Ostrov, D.A., Caldwell-Busby, J. & Sayeski, P.P. 2007, "The N-terminal SH2 domain of the tyrosine phosphatase, SHP-2, is essential for Jak2-dependent signaling via the angiotensin II type AT< sub> 1 receptor", *Cellular signalling,* vol. 19, no. 3, pp. 600-609.

Gorantla, S.P., Dechow, T.N., Grundler, R., Illert, A.L., zum Büschenfelde, C.M., Kremer, M., Peschel, C. & Duyster, J. 2010, "Oncogenic JAK2V617F requires an intact SH2-like domain for constitutive activation and induction of a myeloproliferative disease in mice", *Blood,* vol. 116, no. 22, pp. 4600-4611.

Gordon, G., Lambert, Q., Daniel, K. & Reuther, G. 2010, "Transforming JAK1 mutations exhibit differential signalling, FERM domain requirements and growth responses to interferon-gamma", *Biochem.J,* vol. 432, pp. 255-265.

Grant, B.D., Hemmer, W., Tsigelny, I., Adams, J.A. & Taylor, S.S. 1998, "Kinetic analyses of mutations in the glycine-rich loop of cAMP-dependent protein kinase", *Biochemistry,* vol. 37, no. 21, pp. 7708-7715.

Gu, J., Wang, Y. & Gu, X. 2002, "Evolutionary analysis for functional divergence of Jak protein kinase domains and tissue-specific genes", *Journal of Molecular Evolution,* vol. 54, no. 6, pp. 725-733.

Haan, C., Rolvering, C., Raulf, F., Kapp, M., Drückes, P., Thoma, G., Behrmann, I. & Zerwes, H.G. 2011, "Jak1 Has a Dominant Role over Jak3 in Signal Transduction through [gamma] c-Containing Cytokine Receptors", *Chemistry & biology,* vol. 18, no. 3, pp. 314-323.

Haan, C., Kreis, S., Margue, C. & Behrmann, I. 2006, "Jaks and cytokine receptors—an intimate relationship", *Biochemical pharmacology,* vol. 72, no. 11, pp. 1538-1546.

Haan, C., Is'harc, H., Hermanns, H.M., Schmitz-Van De Leur, H., Kerr, I.M., Heinrich, P.C., Grotzinger, J. & Behrmann, I. 2001, "Mapping of a region within the N terminus of Jak1 involved in cytokine receptor interaction", *The Journal of biological chemistry,* vol. 276, no. 40, pp. 37451-37458.

Haan, C., Kroy, D.C., Wuller, S., Sommer, U., Nocker, T., Rolvering, C., Behrmann, I., Heinrich, P.C. & Haan, S. 2009, "An unusual insertion in Jak2 is crucial for kinase activity and differentially affects cytokine responses", *Journal of immunology (Baltimore, Md.: 1950),* vol. 182, no. 5, pp. 2969-2977.

Hama, A., Muramatsu, H., Makishima, H., Sugimoto, Y., Szpurka, H., Jasek, M., O'Keefe, C., Takahashi, Y., Sakaguchi, H. & Doisaki, S. 2012, "Molecular lesions in childhood and adult acute megakaryoblastic leukaemia", *British journal of haematology,* vol. 156, no. 3, pp. 316-325.

Hammarén, H.M., Virtanen, A.T. & Silvennoinen, O. 2015, "Nucleotide-binding mechanisms in pseudokinases", *Bioscience reports,* vol. 36, no. 1, pp. e00282.

Hanks, S.K., Quinn, A.M. & Hunter, T. 1988, "The protein kinase family: conserved features and deduced phylogeny of the catalytic domains", *Science (New York, N.Y.),* vol. 241, no. 4861, pp. 42-52.

Hanratty, W.P. & Ryerse, J.S. 1981, "A genetic melanotic neoplasm of Drosophila melanogaster", *Developmental biology,* vol. 83, no. 2, pp. 238-249.

Hayashi, T., Kobayashi, Y., Kohsaka, S. & Sano, K. 2006, "The mutation in the ATP-binding region of JAK1, identified in human uterine leiomyosarcomas, results in defective interferon-γ inducibility of TAP1 and LMP2", *Oncogene,* vol. 25, no. 29, pp. 4016-4026.

Hirahara, K., Schwartz, D., Gadina, M., Kanno, Y. & O'Shea, J.J. 2016, "Targeting cytokine signaling in autoimmunity: back to the future and beyond", *Current opinion in immunology,* vol. 43, pp. 89-97.

Hornakova, T., Springuel, L., Devreux, J., Dusa, A., Constantinescu, S.N., Knoops, L. & Renauld, J. 2011, "Oncogenic JAK1 and JAK2-activating mutations resistant to ATP-competitive inhibitors", *Haematologica,* vol. 96, no. 6, pp. 845-853.

Huang, L.J., Constantinescu, S.N. & Lodish, H.F. 2001, "The N-terminal domain of Janus kinase 2 is required for Golgi processing and cell surface expression of erythropoietin receptor", *Molecular cell,* vol. 8, no. 6, pp. 1327-1338.

Huang, X. & Dixit, V.M. 2016, "Drugging the undruggables: exploring the ubiquitin system for drug development", *Cell research,* vol. 26, no. 4, pp. 484-498.

Hubbard, S.R. & Miller, W.T. 2007, "Receptor tyrosine kinases: mechanisms of activation and signaling", *Current opinion in cell biology,* vol. 19, no. 2, pp. 117-123.

Humphrey, W., Dalke, A. & Schulten, K. 1996, "VMD: visual molecular dynamics", *Journal of Molecular Graphics,* vol. 14, no. 1, pp. 33-38.

Ihle, J.N., Witthuhn, B.A., Quelle, F.W., Yamamoto, K. & Silvennoinen, O. 1995, "Signaling through the hematopoietic cytokine receptors", *Annual Review of Immunology,* vol. 13, no. 1, pp. 369-398.

Ishida-Takahashi, R., Rosario, F., Gong, Y., Kopp, K., Stancheva, Z., Chen, X., Feener, E.P. & Myers Jr, M.G. 2006, "Phosphorylation of Jak2 on Ser523 inhibits Jak2-dependent leptin receptor signaling", *Molecular and cellular biology,* vol. 26, no. 11, pp. 4063-4073.

Iyer, G.H., Garrod, S., Woods, V.L. & Taylor, S.S. 2005, "Catalytic independent functions of a protein kinase as revealed by a kinase-dead mutant: study of the Lys72His mutant of cAMP-dependent kinase", *Journal of Molecular Biology,* vol. 351, no. 5, pp. 1110-1122.

James, C., Ugo, V., Le Couédic, J.P., Staerk, J., Delhommeau, F., Lacout, C., Garçon, L., Raslova, H., Berger, R. & Bennaceur-Griscelli, A. 2005, "A unique clonal JAK2 mutation leading to constitutive signalling causes polycythaemia vera", *Nature,* vol. 434, no. 7037, pp. 1144-1148.

Jeong, E.G., Kim, M.S., Nam, H.K., Min, C.K., Lee, S., Chung, Y.J., Yoo, N.J. & Lee, S.H. 2008, "Somatic mutations of JAK1 and JAK3 in acute leukemias and solid cancers", *Clinical cancer research : an official journal of the American Association for Cancer Research,* vol. 14, no. 12, pp. 3716-3721.

Jura, N., Shan, Y., Cao, X., Shaw, D.E. & Kuriyan, J. 2009, "Structural analysis of the catalytically inactive kinase domain of the human EGF receptor 3", *Proceedings of the National Academy of Sciences,* vol. 106, no. 51, pp. 21608-21613.

Kannan, N., Taylor, S.S., Zhai, Y., Venter, J.C. & Manning, G. 2007, "Structural and functional diversity of the microbial kinome", *PLoS biology,* vol. 5, no. 3, pp. e17.

Kapralova, K., Horvathova, M., Pecquet, C., Fialova Kucerova, J., Pospisilova, D., Leroy, E., Kralova, B., Milosevic Feenstra, J.D., Schischlik, F., Kralovics, R., Constantinescu, S.N. & Divoky, V. 2016, "Cooperation of germ line JAK2 mutations E846D and R1063H in hereditary erythrocytosis with megakaryocytic atypia", *Blood,* vol. 128, no. 10, pp. 1418-1423.

Kawamura, M., McVicar, D.W., Johnston, J.A., Blake, T.B., Chen, Y.Q., Lal, B.K., Lloyd, A.R., Kelvin, D.J., Staples, J.E. & Ortaldo, J.R. 1994, "Molecular cloning of L-JAK, a Janus family protein-tyrosine kinase expressed in natural killer cells and activated leukocytes", *Proceedings of the National Academy of Sciences of the United States of America,* vol. 91, no. 14, pp. 6374-6378.

Kershaw, N.J., Murphy, J.M., Liau, N.P., Varghese, L.N., Laktyushin, A., Whitlock, E.L., Lucet, I.S., Nicola, N.A. & Babon, J.J. 2013, "SOCS3 binds specific receptor–JAK complexes to control cytokine signaling by direct kinase inhibition", *Nature Structural & Molecular Biology,* vol. 20, no. 4, pp. 469-476.

Knight, Z.A. & Shokat, K.M. 2007, "Chemical genetics: where genetics and pharmacology meet", *Cell,* vol. 128, no. 3, pp. 425-430.

Knighton, D.R., Xuong, N.H., Taylor, S.S. & Sowadski, J.M. 1991, "Crystallization studies of cAMP-dependent protein kinase: Cocrystals of the catalytic subunit with a 20 amino acid residue peptide inhibitor and MgATP diffract to 3.0 Å resolution", *Journal of Molecular Biology,* vol. 220, no. 2, pp. 217-220.

Kohlhuber, F., Rogers, N.C., Watling, D., Feng, J., Guschin, D., Briscoe, J., Witthuhn, B.A., Kotenko, S.V., Pestka, S., Stark, G.R., Ihle, J.N. & Kerr, I.M. 1997, "A JAK1/JAK2 chimera can sustain alpha and gamma interferon responses", *Molecular and cellular biology,* vol. 17, no. 2, pp. 695-706.

Koo, G.C., Tan, S.Y., Tang, T., Poon, S.L., Allen, G.E., Tan, L., Chong, S.C., Ong, W.S., Tay, K. & Tao, M. 2012, "Janus Kinase 3–Activating Mutations Identified in Natural Killer/T-cell Lymphoma", *Cancer Discovery,* vol. 2, no. 7, pp. 591-597.

Kornev, A.P., Haste, N.M., Taylor, S.S. & Ten Eyck, L.F. 2006, "Surface comparison of active and inactive protein kinases identifies a conserved activation mechanism", *Proceedings of the National Academy of Sciences,* vol. 103, no. 47, pp. 17783-17788.

Kornev, A.P., Taylor, S.S. & Ten Eyck, L.F. 2008, "A helix scaffold for the assembly of active protein kinases", *Proceedings of the National Academy of Sciences,* vol. 105, no. 38, pp. 14377-14382.

Kotenko, S.V. 2011, "IFN-λs", *Current Opinion in Immunology,* vol. 23, no. 5, pp. 583-590.

Kovanen, P.E. & Leonard, W.J. 2004, "Cytokines and immunodeficiency diseases: critical roles of the γc-dependent cytokines interleukins 2, 4, 7, 9, 15, and 21, and their signaling pathways", *Immunological reviews,* vol. 202, no. 1, pp. 67-83.

Kralovics, R., Passamonti, F., Buser, A.S., Teo, S.S., Tiedt, R., Passweg, J.R., Tichelli, A., Cazzola, M. & Skoda, R.C. 2005, "A gain-of-function mutation of JAK2 in myeloproliferative disorders", *New England Journal of Medicine,* vol. 352, no. 17, pp. 1779-1790.

Krebs, E.G. 1994, "The growth of research on protein phosphorylation", *Trends in biochemical sciences,* vol. 19, no. 11, pp. 439.

Krebs, E.G. & Fischer, E.H. 1956, "The phosphorylase b to a converting enzyme of rabbit skeletal muscle", *Biochimica et biophysica acta,* vol. 20, pp. 150-157.

Kreins, A.Y., Ciancanelli, M.J., Okada, S., Kong, X.F., Ramirez-Alejo, N., Kilic, S.S., El Baghdadi, J., Nonoyama, S., Mahdaviani, S.A., Ailal, F., Bousfiha, A., Mansouri, D., Nievas, E., Ma, C.S., Rao, G., Bernasconi, A., Sun Kuehn, H., Niemela, J., Stoddard, J., Deveau, P., Cobat, A., El Azbaoui, S., Sabri, A., Lim, C.K., Sundin, M., Avery, D.T., Halwani, R., Grant, A.V., Boisson, B., Bogunovic, D., Itan, Y., Moncada-Velez, M., Martinez-Barricarte, R., Migaud, M., Deswarte, C., Alsina, L., Kotlarz, D., Klein, C., Muller-Fleckenstein, I., Fleckenstein, B., Cormier-Daire, V., Rose-John, S., Picard, C., Hammarstrom, L., Puel, A., Al-Muhsen, S., Abel, L., Chaussabel, D., Rosenzweig, S.D., Minegishi, Y., Tangye, S.G., Bustamante, J., Casanova, J.L. & Boisson-Dupuis, S. 2015, "Human TYK2 deficiency: Mycobacterial and viral infections without hyper-IgE syndrome", *The Journal of experimental medicine,* vol. 212, no. 10, pp. 1641-1662.

Kung, J.E. & Jura, N. 2016, "Structural basis for the non-catalytic functions of protein kinases", *Structure,* vol. 24, no. 1, pp. 7-24.

Kurzer, J.H., Argetsinger, L.S., Zhou, Y.J., Kouadio, J.L., O'Shea, J.J. & Carter-Su, C. 2004, "Tyrosine 813 is a site of JAK2 autophosphorylation critical for

activation of JAK2 by SH2-B beta", *Molecular and cellular biology,* vol. 24, no. 10, pp. 4557-4570.

Lacronique, V., Boureux, A., Valle, V.D., Poirel, H., Quang, C.T., Mauchauffe, M., Berthou, C., Lessard, M., Berger, R., Ghysdael, J. & Bernard, O.A. 1997, "A TEL-JAK2 fusion protein with constitutive kinase activity in human leukemia", *Science (New York, N.Y.),* vol. 278, no. 5341, pp. 1309-1312.

Lanikova, L., Babosova, O., Swierczek, S., Wang, L., Wheeler, D.A., Divoky, V., Korinek, V. & Prchal, J.T. 2016, "Coexistence of gain-of-function JAK2 germline mutations with JAK2V617F in polycythemia vera", *Blood,* vol. 128, no. 18, pp. 2266-2270.

Lemmon, M.A. & Schlessinger, J. 2010, "Cell signaling by receptor-tyrosine kinases", *Cell,* vol. 141, no. 7, pp. 1117.

Leroy, E. & Constantinescu, S.N. 2017, "Rethinking JAK2 inhibition: Towards novel strategies of more specific and versatile Janus kinase inhibition", *Leukemia,* vol. 31, no. 5, pp. 1023-1038.

Leroy, E., Dusa, A., Colau, D., Motamedi, A., Cahu, X., Mouton, C., Huang, L.J., Shiau, A.K. & Constantinescu, S.N. 2016, "Uncoupling JAK2 V617F activation from cytokine-induced signalling by modulation of JH2 alphaC helix", *The Biochemical journal,* vol. 473, no. 11, pp. 1579-1591.

Levine, R.L., Wadleigh, M., Cools, J., Ebert, B.L., Wernig, G., Huntly, B.J.P., Boggon, T.J., Wlodarska, I., Clark, J.J. & Moore, S. 2005, "Activating mutation in the tyrosine kinase JAK2 in polycythemia vera, essential thrombocythemia, and myeloid metaplasia with myelofibrosis", *Cancer cell,* vol. 7, no. 4, pp. 387-397.

Li, Z., Gakovic, M., Ragimbeau, J., Eloranta, M., Rönnblom, L., Michel, F. & Pellegrini, S. 2013, "Two Rare Disease-Associated Tyk2 Variants Are Catalytically Impaired but Signaling Competent", *The Journal of Immunology,* vol. 190, no. 5, pp. 2335-2344.

Lim, S.M., Xie, T., Westover, K.D., Ficarro, S.B., Tae, H.S., Gurbani, D., Sim, T., Marto, J.A., Jänne, P.A. & Crews, C.M. 2015, "Development of small molecules targeting the pseudokinase Her3", *Bioorganic & medicinal chemistry letters,* vol. 25, no. 16, pp. 3382-3389.

Lindauer, K., Loerting, T., Liedl, K.R. & Kroemer, R.T. 2001, "Prediction of the structure of human Janus kinase 2 (JAK2) comprising the two carboxy-terminal domains reveals a mechanism for autoregulation", *Protein engineering,* vol. 14, no. 1, pp. 27.

Liongue, C., O'Sullivan, L.A., Trengove, M.C. & Ward, A.C. 2012, "Evolution of JAK-STAT pathway components: mechanisms and role in immune system development", *PloS one,* vol. 7, no. 3, pp. e32777.

Liongue, C., Sertori, R. & Ward, A.C. 2016, "Evolution of Cytokine Receptor Signaling", *Journal of immunology (Baltimore, Md.: 1950),* vol. 197, no. 1, pp. 11-18.

Liongue, C. & Ward, A.C. 2007, "Evolution of Class I cytokine receptors", *BMC evolutionary biology,* vol. 7, pp. 120.

Losdyck, E., Hornakova, T., Springuel, L., Degryse, S., Gielen, O., Cools, J., Constantinescu, S.N., Flex, E., Tartaglia, M., Renauld, J.C. & Knoops, L. 2015, "Distinct Acute Lymphoblastic Leukemia (ALL)-associated Janus Kinase 3 (JAK3) Mutants Exhibit Different Cytokine-Receptor Requirements and JAK Inhibitor Specificities", *The Journal of biological chemistry,* vol. 290, no. 48, pp. 29022-29034.

Lu, X., Huang, L.J.S. & Lodish, H.F. 2008, "Dimerization by a cytokine receptor is necessary for constitutive activation of JAK2V617F", *Journal of Biological Chemistry,* vol. 283, no. 9, pp. 5258-5266.

Lu, X., Levine, R., Tong, W., Wernig, G., Pikman, Y., Zarnegar, S., Gilliland, D.G. & Lodish, H. 2005, "Expression of a homodimeric type I cytokine receptor is required for JAK2V617F-mediated transformation", *Proceedings of the National Academy of Sciences of the United States of America,* vol. 102, no. 52, pp. 18962-18967.

Lu, X., Gross, A.W. & Lodish, H.F. 2006, "Active conformation of the erythropoietin receptor: random and cysteine-scanning mutagenesis of the extracellular juxtamembrane and transmembrane domains", *The Journal of biological chemistry,* vol. 281, no. 11, pp. 7002-7011.

Lucet, I.S., Fantino, E., Styles, M., Bamert, R., Patel, O., Broughton, S.E., Walter, M., Burns, C.J., Treutlein, H. & Wilks, A.F. 2006, "The structural basis of Janus kinase 2 inhibition by a potent and specific pan-Janus kinase inhibitor", *Blood,* vol. 107, no. 1, pp. 176-183.

Lucet, I.S. & Bamert, R. 2013, "Production and Crystallization of Recombinant JAK Proteins" in *JAK-STAT Signalling* Springer, , pp. 275-300.

Lundberg, P., Takizawa, H., Kubovcakova, L., Guo, G., Hao-Shen, H., Dirnhofer, S., Orkin, S.H., Manz, M.G. & Skoda, R.C. 2014, "Myeloproliferative neoplasms can be initiated from a single hematopoietic stem cell expressing JAK2-V617F", *The Journal of experimental medicine,* vol. 211, no. 11, pp. 2213-2230.

Luo, H., Rose, P., Barber, D., Hanratty, W.P., Lee, S., Roberts, T.M., D'Andrea, A.D. & Dearolf, C.R. 1997, "Mutation in the Jak kinase JH2 domain hyperactivates Drosophila and mammalian Jak-Stat pathways.", *Molecular and cellular biology,* vol. 17, no. 3, pp. 1562-1571.

Luo, H., Hanratty, W.P. & Dearolf, C.R. 1995, "An amino acid substitution in the Drosophila hopTum-l Jak kinase causes leukemia-like hematopoietic defects", *The EMBO journal,* vol. 14, no. 7, pp. 1412-1420.

Lupardus, P.J., Skiniotis, G., Rice, A.J., Thomas, C., Fischer, S., Walz, T. & Garcia, K.C. 2011, "Structural snapshots of full-length Jak1, a transmembrane gp130/IL-6/IL-6Rα cytokine receptor complex, and the receptor-Jak1 holocomplex", *Structure,* vol. 19, no. 1, pp. 45-55.

Lupardus, P.J., Ultsch, M., Wallweber, H., Bir Kohli, P., Johnson, A.R. & Eigenbrot, C. 2014, "Structure of the pseudokinase–kinase domains from protein kinase TYK2 reveals a mechanism for Janus kinase (JAK) autoinhibition", *Proceedings of the National Academy of Sciences,* vol. 111, no. 22, pp. 8025-8030.

Ma, W., Kantarjian, H., Zhang, X., Yeh, C.H., Zhang, Z.J., Verstovsek, S. & Albitar, M. 2009, "Mutation profile of JAK2 transcripts in patients with chronic myeloproliferative neoplasias", *The Journal of molecular diagnostics: JMD,* vol. 11, no. 1, pp. 49.

Majoros, A., Platanitis, E., Kernbauer-Hölzl, E., Rosebrock, F., Müller, M. & Decker, T. 2017, "Canonical and Non-Canonical Aspects of JAK–STAT Signaling: Lessons from Interferons for Cytokine Responses", *Frontiers in Immunology,* vol. 8, no. 29.

Malka, Y., Hornakova, T., Royer, Y., Knoops, L., Renauld, J.C., Constantinescu, S.N. & Henis, Y.I. 2008, "Ligand-independent homomeric and heteromeric complexes between interleukin-2 or -9 receptor subunits and the gamma chain", *The Journal of biological chemistry,* vol. 283, no. 48, pp. 33569-33577.

Manning, G., Whyte, D.B., Martinez, R., Hunter, T. & Sudarsanam, S. 2002, "The protein kinase complement of the human genome", *Science,* vol. 298, no. 5600, pp. 1912-34.

Marty, C., Saint-Martin, C., Pecquet, C., Grosjean, S., Saliba, J., Mouton, C., Leroy, E., Harutyunyan, A.S., Abgrall, J.F., Favier, R., Toussaint, A., Solary, E., Kralovics, R., Constantinescu, S.N., Najman, A., Vainchenker, W., Plo, I. & Bellanne-Chantelot, C. 2014, "Germ-line JAK2 mutations in the kinase domain are responsible for hereditary thrombocytosis and are resistant to JAK2 and HSP90 inhibitors", *Blood,* vol. 123, no. 9, pp. 1372-1383.

Matadeen, R., Hon, W., Heath, J.K., Jones, E.Y. & Fuller, S. 2007, "The dynamics of signal triggering in a gp130-receptor complex", *Structure,* vol. 15, no. 4, pp. 441-448.

Matsuda, T., Feng, J., Witthuhn, B.A., Sekine, Y. & Ihle, J.N. 2004, "Determination of the transphosphorylation sites of Jak2 kinase", *Biochemical and biophysical research communications,* vol. 325, no. 2, pp. 586-594.

Matulis, D., Kranz, J.K., Salemme, F.R. & Todd, M.J. 2005, "Thermodynamic stability of carbonic anhydrase: measurements of binding affinity and stoichiometry using ThermoFluor", *Biochemistry,* vol. 44, no. 13, pp. 5258-5266.

Mazurkiewicz-Munoz, A.M., Argetsinger, L.S., Kouadio, J.K., Stensballe, A., Jensen, O.N., Cline, J.M. & Carter-Su, C. 2006, "Phosphorylation of JAK2 at serine 523: a negative regulator of JAK2 that is stimulated by growth hormone and epidermal growth factor", *Molecular and cellular biology,* vol. 26, no. 11, pp. 4052-4062.

McNally, R., Toms, A.V. & Eck, M.J. 2016, "Crystal Structure of the FERM-SH2 Module of Human Jak2", *PloS one,* vol. 11, no. 5, pp. e0156218.

Menting, J.G., Whittaker, J., Margetts, M.B., Whittaker, L.J., Kong, G.K.W., Smith, B.J., Watson, C.J., Žáková, L., Kletvíková, E. & Jiráček, J. 2013, "How insulin engages its primary binding site on the insulin receptor", *Nature,* vol. 493, no. 7431, pp. 241-245.

Mercher, T., Wernig, G., Moore, S.A., Levine, R.L., Gu, T.L., Frohling, S., Cullen, D., Polakiewicz, R.D., Bernard, O.A., Boggon, T.J., Lee, B.H. & Gilliland, D.G. 2006, "JAK2T875N is a novel activating mutation that results in myeloproliferative disease with features of megakaryoblastic leukemia in a murine bone marrow transplantation model", *Blood,* vol. 108, no. 8, pp. 2770-2779.

Milosevic Feenstra, J.D., Nivarthi, H., Gisslinger, H., Leroy, E., Rumi, E., Chachoua, I., Bagienski, K., Kubesova, B., Pietra, D., Gisslinger, B., Milanesi, C., Jager, R., Chen, D., Berg, T., Schalling, M., Schuster, M., Bock, C., Constantinescu, S.N., Cazzola, M. & Kralovics, R. 2016, "Whole-exome sequencing identifies novel MPL and JAK2 mutations in triple-negative myeloproliferative neoplasms", *Blood,* vol. 127, no. 3, pp. 325-332.

Min, X., Lee, B., Cobb, M.H. & Goldsmith, E.J. 2004, "Crystal structure of the kinase domain of WNK1, a kinase that causes a hereditary form of hypertension", *Structure,* vol. 12, no. 7, pp. 1303-1311.

Minegishi, Y., Saito, M., Morio, T., Watanabe, K., Agematsu, K., Tsuchiya, S., Takada, H., Hara, T., Kawamura, N. & Ariga, T. 2006, "Human tyrosine kinase 2 deficiency reveals its requisite roles in multiple cytokine signals involved in innate and acquired immunity", *Immunity,* vol. 25, no. 5, pp. 745-755.

Möbitz, H. 2015, "The ABC of protein kinase conformations", *Biochimica et Biophysica Acta (BBA)-Proteins and Proteomics,* vol. 1854, no. 10 Pt B, pp. 1555-1566.

Mohammadi, M., Schlessinger, J. & Hubbard, S.R. 1996, "Structure of the FGF receptor tyrosine kinase domain reveals a novel autoinhibitory mechanism", *Cell,* vol. 86, no. 4, pp. 577-587.

Moraga, I., Wernig, G., Wilmes, S., Gryshkova, V., Richter, C.P., Hong, W., Sinha, R., Guo, F., Fabionar, H. & Wehrman, T.S. 2015, "Tuning cytokine receptor signaling by re-orienting dimer geometry with surrogate ligands", *Cell,* vol. 160, no. 6, pp. 1196-1208.

Moslin, R., Gardner, D., Santella, J., Zhang, Y., Duncia, J., Liu, C., Lin, J., Tokarski, J., Strnad, J. & Pedicord, D. 2017, "Identification of imidazo [1, 2-b] pyridazine TYK2 pseudokinase ligands as potent and selective allosteric inhibitors of TYK2 signalling", *MedChemComm,* vol. 8, no. 4, pp. 700-712.

Mukherjee, K., Sharma, M., Urlaub, H., Bourenkov, G.P., Jahn, R., Südhof, T.C. & Wahl, M.C. 2008, "CASK Functions as a Mg2+-Independent Neurexin Kinase", *Cell,* vol. 133, no. 2, pp. 328-339.

Müller, M., Briscoe, J., Laxton, C., Guschin, D., Ziemiecki, A., Silvennoinen, O., Harpur, A.G., Barbieri, G., Witthuhn, B.A. & Schindler, C. 1993, "The protein tyrosine kinase JAK1 complements defects in interferon-α/β and-γ signal transduction", vol. 366, no. 6451, pp. 129-135.

Mullighan, C.G., Zhang, J., Harvey, R.C., Collins-Underwood, J.R., Schulman, B.A., Phillips, L.A., Tasian, S.K., Loh, M.L., Su, X., Liu, W., Devidas, M., Atlas, S.R., Chen, I.M., Clifford, R.J., Gerhard, D.S., Carroll, W.L., Reaman, G.H., Smith, M., Downing, J.R., Hunger, S.P. & Willman, C.L. 2009, "JAK mutations in high-risk childhood acute lymphoblastic leukemia", *Proceedings of the National Academy of Sciences of the United States of America,* vol. 106, no. 23, pp. 9414-9418.

Murakami, M., Narazaki, M., Hibi, M., Yawata, H., Yasukawa, K., Hamaguchi, M., Taga, T. & Kishimoto, T. 1991, "Critical cytoplasmic region of the interleukin 6 signal transducer gp130 is conserved in the cytokine receptor family", *Proceedings of the National Academy of Sciences of the United States of America,* vol. 88, no. 24, pp. 11349-11353.

Murphy, J.M., Zhang, Q., Young, S.N., Reese, M.L., Bailey, F.P., Eyers, P.A., Ungureanu, D., Hammaren, H., Silvennoinen, O., Varghese, L.N., Chen, K., Tripaydonis, A., Jura, N., Fukuda, K., Qin, J., Nimchuk, Z., Mudgett, M.B., Elowe, S., Gee, C.L., Liu, L., Daly, R.J., Manning, G., Babon, J.J. & Lucet, I.S.

2014, "A robust methodology to subclassify pseudokinases based on their nucleotide-binding properties", *Biochemical Journal,* vol. 457, pp. 323-334.

Neubauer, H., Cumano, A., Müller, M., Wu, H., Huffstadt, U. & Pfeffer, K. 1998, "Jak2 deficiency defines an EssentialDevelopmental checkpoint in DefinitiveHematopoiesis", *Cell,* vol. 93, no. 3, pp. 397-409.

Newton, A.S., Deiana, L., Puleo, D., Cisneros, J.A., Cutrona, K.J., Schlessinger, J. & Jorgensen, W.L. 2017, "JAK2 JH2 Fluorescence Polarization Assay and Crystal Structures for Complexes with Three Small Molecules", *ACS Medicinal Chemistry Letters,* vol. 8, no. 6, pp. 614-617.

Ni, D.Q., Shaffer, J. & Adams, J.A. 2000, "Insights into nucleotide binding in protein kinase A using fluorescent adenosine derivatives", *Protein Science,* vol. 9, no. 9, pp. 1818-1827.

Nicola, N.A. & Hilton, D.J. 1998, "General classes and functions of four-helix bundle cytokines", *Advances in Protein Chemistry,* vol. 52, pp. 1-65.

Niranjan, Y., Ungureanu, D., Hammarén, H., Sanz-Sanz, A., Westphal, A.H., Borst, J.W., Silvennoinen, O. & Hilhorst, R. 2013, "Analysis of steady-state FRET data by avoiding pitfalls: Interaction of JAK2 tyrosine kinase with MANT-nucleotides", *Analytical Biochemistry,* vol. 442, no. 2, pp. 213-222.

Norman, P. 2014, "Selective JAK inhibitors in development for rheumatoid arthritis", *Expert opinion on investigational drugs,* vol. 23, no. 8, pp. 1067-1077.

O'Shea, J.J., Husa, M., Li, D., Hofmann, S.R., Watford, W., Roberts, J.L., Buckley, R.H., Changelian, P. & Candotti, F. 2004, "Jak3 and the pathogenesis of severe combined immunodeficiency", *Molecular immunology,* vol. 41, no. 6, pp. 727-737.

Oh, S.T. & Gotlib, J. 2010, "JAK2 V617F and beyond: role of genetics and aberrant signaling in the pathogenesis of myeloproliferative neoplasms", *Expert review of hematology,* vol. 3, no. 3, pp. 323-337.

Oppenheim, J.J. 2001, "Cytokines: past, present, and future", *International journal of hematology,* vol. 74, no. 1, pp. 3-8.

O'Shea, J.J. & Plenge, R. 2012, "JAK and STAT Signaling Molecules in Immunoregulation and Immune-Mediated Disease", *Immunity,* vol. 36, no. 4, pp. 542-550.

O'Sullivan, J.M. & Harrison, C.N. 2017, "JAK-STAT signaling in the therapeutic landscape of myeloproliferative neoplasms", *Molecular and cellular endocrinology,* vol. 451, pp. 71-79.

Pencik, J., Pham, H.T.T., Schmoellerl, J., Javaheri, T., Schlederer, M., Culig, Z., Merkel, O., Moriggl, R., Grebien, F. & Kenner, L. 2016, "JAK-STAT signaling in cancer: From cytokines to non-coding genome", *Cytokine,* vol. 87, pp. 26-36.

Pradhan, A., Lambert, Q.T., Griner, L.N. & Reuther, G.W. 2010, "Activation of JAK2-V617F by components of heterodimeric cytokine receptors", *The Journal of biological chemistry,* vol. 285, no. 22, pp. 16651-16663.

Puleo, D., Kucera, K., Hammaren, H., Ungureanu, D., Newton, A., Silvennoinen, O., Jorgensen, W.L. & Schlessinger, J. 2017, "Identification and Characterization of JAK2 Pseudokinase Domain Small Molecule Binders", *ACS Medicinal Chemistry Letters,* vol. 8, no. 6, pp. 618-621.

Qiu, H., Garcia-Barrio, M.T. & Hinnebusch, A.G. 1998, "Dimerization by translation initiation factor 2 kinase GCN2 is mediated by interactions in the C-terminal ribosome-binding region and the protein kinase domain", *Molecular and cellular biology,* vol. 18, no. 5, pp. 2697-2711.

Quintás-Cardama, A., Kantarjian, H., Cortes, J. & Verstovsek, S. 2011, "Janus kinase inhibitors for the treatment of myeloproliferative neoplasias and beyond", *Nature reviews Drug discovery,* vol. 10, no. 2, pp. 127-140.

Rabellino, A., Andreani, C. & Scaglioni, P.P. 2017, "The Role of PIAS SUMO E3-Ligases in Cancer", *Cancer research,* vol. 77, no. 7, pp. 1542-1547.

Radtke, S., Haan, S., Jörissen, A., Hermanns, H.M., Diefenbach, S., Smyczek, T., Schmitz-VandeLeur, H., Heinrich, P.C., Behrmann, I. & Haan, C. 2005, "The Jak1 SH2 domain does not fulfill a classical SH2 function in Jak/STAT signaling but plays a structural role for receptor interaction and up-regulation of receptor surface expression", *Journal of Biological Chemistry,* vol. 280, no. 27, pp. 25760-25768.

Reiterer, V., Eyers, P.A. & Farhan, H. 2014, "Day of the dead: pseudokinases and pseudophosphatases in physiology and disease", *Trends in cell biology,* vol. 24, no. 9, pp. 489-505.

Renauld, J. 2003, "Class II cytokine receptors and their ligands: key antiviral and inflammatory modulators", *Nature Reviews Immunology,* vol. 3, no. 8, pp. 667-676.

Rikova, K., Guo, A., Zeng, Q., Possemato, A., Yu, J., Haack, H., Nardone, J., Lee, K., Reeves, C. & Li, Y. 2007, "Global survey of phosphotyrosine signaling identifies oncogenic kinases in lung cancer", *Cell,* vol. 131, no. 6, pp. 1190-1203.

Robertson, S.A., Koleva, R.I., Argetsinger, L.S., Carter-Su, C., Marto, J.A., Feener, E.P. & Myers Jr, M.G. 2009, "Regulation of Jak2 function by phosphorylation

of Tyr317 and Tyr637 during cytokine signaling", *Molecular and cellular biology,* vol. 29, no. 12, pp. 3367-3378.

Robinson, M.J., Harkins, P.C., Zhang, J., Baer, R., Haycock, J.W., Cobb, M.H. & Goldsmith, E.J. 1996, "Mutation of position 52 in ERK2 creates a nonproductive binding mode for adenosine 5'-triphosphate", *Biochemistry,* vol. 35, no. 18, pp. 5641-5646.

Rodig, S.J., Meraz, M.A., White, J.M., Lampe, P.A., Riley, J.K., Arthur, C.D., King, K.L., Sheehan, K.C., Yin, L. & Pennica, D. 1998, "Disruption of the Jak1 gene demonstrates obligatory and nonredundant roles of the Jaks in cytokine-induced biologic responses", *Cell,* vol. 93, no. 3, pp. 373-383.

Rutz, S., Wang, X. & Ouyang, W. 2014, "The IL-20 subfamily of cytokines [mdash] from host defence to tissue homeostasis", *Nature reviews Immunology,* vol. 14, no. 12, pp. 783-795.

Saharinen, P. & Silvennoinen, O. 2002, "The pseudokinase domain is required for suppression of basal activity of Jak2 and Jak3 tyrosine kinases and for cytokine-inducible activation of signal transduction", *Journal of Biological Chemistry,* vol. 277, no. 49, pp. 47954-63.

Saharinen, P., Takaluoma, K. & Silvennoinen, O. 2000, "Regulation of the Jak2 tyrosine kinase by its pseudokinase domain", *Molecular and cellular biology,* vol. 20, no. 10, pp. 3387-95.

Saharinen, P., Vihinen, M. & Silvennoinen, O. 2003, "Autoinhibition of Jak2 tyrosine kinase is dependent on specific regions in its pseudokinase domain", *Molecular biology of the cell,* vol. 14, no. 4, pp. 1448-1459.

Saka, K., Kawahara, M., Ueda, H. & Nagamune, T. 2012, "Activation of target signal transducers utilizing chimeric receptors with signaling-molecule binding motifs", *Biotechnology and bioengineering,* vol. 109, no. 6, pp. 1528-1537.

Sanz, A., Ungureanu, D., Pekkala, T., Ruijtenbeek, R., Touw, I.P., Hilhorst, R. & Silvennoinen, O. 2011, "Analysis of Jak2 catalytic function by peptide microarrays: The role of the JH2 domain and V617F mutation", *PLoS One,* vol. 6, no. 4, pp. e18522.

Sayyah, J., Gnanasambandan, K., Kamarajugadda, S., Tsuda, S., Caldwell-Busby, J. & Sayeski, P.P. 2011, "Phosphorylation of Y372 is critical for Jak2 tyrosine kinase activation", *Cellular signalling,* vol. 23, no. 11, pp. 1806-1815.

Scheeff, E.D. & Bourne, P.E. 2005, "Structural evolution of the protein kinase–like superfamily", *PLoS computational biology,* vol. 1, no. 5, pp. e49.

Schindler, C. & Plumlee, C. 2008, "Inteferons pen the JAK–STAT pathway", *Seminars in Cell and Developmental Biology,* vol. 19, no. 4, pp. 311-318.

Schnittger, S., Bacher, U., Kern, W., Schröder, M., Haferlach, T. & Schoch, C. 2006, "Report on two novel nucleotide exchanges in the JAK2 pseudokinase domain: D620E and E627E", *Leukemia,* vol. 20, no. 12, pp. 2195-2197.

Schwartz, D.M., Bonelli, M., Gadina, M. & O'Shea, J.J. 2016, "Type I/II cytokines, JAKs, and new strategies for treating autoimmune diseases", *Nature Reviews Rheumatology,* vol. 12, no. 1, pp. 25-36.

Scott, L.M., Tong, W., Levine, R.L., Scott, M.A., Beer, P.A., Stratton, M.R., Futreal, P.A., Erber, W.N., McMullin, M.F. & Harrison, C.N. 2007, "JAK2 exon 12 mutations in polycythemia vera and idiopathic erythrocytosis", *New England Journal of Medicine,* vol. 356, no. 5, pp. 459-468.

Seubert, N., Royer, Y., Staerk, J., Kubatzky, K.F., Moucadel, V., Krishnakumar, S., Smith, S.O. & Constantinescu, S.N. 2003, "Active and inactive orientations of the transmembrane and cytosolic domains of the erythropoietin receptor dimer", *Molecular cell,* vol. 12, no. 5, pp. 1239-1250.

Shan, Y., Gnanasambandan, K., Ungureanu, D., Kim, E.T., Hammaren, H., Yamashita, K., Silvennoinen, O., Shaw, D.E. & Hubbard, S.R. 2014, "Molecular basis for pseudokinase-dependent autoinhibition of JAK2 tyrosine kinase", *Nature Structural & Molecular Biology,* vol. 21, pp. 579-584.

Shaw, D.E., Deneroff, M.M., Dror, R.O., Kuskin, J.S., Larson, R.H., Salmon, J.K., Young, C., Batson, B., Bowers, K.J. & Chao, J.C. 2008, "Anton, a special-purpose machine for molecular dynamics simulation", *Communications of the ACM,* vol. 51, no. 7, pp. 91-97.

Shi, F., Telesco, S.E., Liu, Y., Radhakrishnan, R. & Lemmon, M.A. 2010, "ErbB3/HER3 intracellular domain is competent to bind ATP and catalyze autophosphorylation", *Proceedings of the National Academy of Sciences,* vol. 107, no. 17, pp. 7692-7.

Shuai, K., Schindler, C., Prezioso, V.R. & Darnell, J.E.,Jr 1992, "Activation of transcription by IFN-gamma: tyrosine phosphorylation of a 91-kD DNA binding protein", *Science (New York, N.Y.),* vol. 258, no. 5089, pp. 1808-1812.

Silvennoinen, O. & Hubbard, S.R. 2015, "Molecular insights into regulation of JAK2 in myeloproliferative neoplasms", *Blood,* vol. 125, no. 22, pp. 3388-3392.

Silvennoinen, O., Witthuhn, B.A., Quelle, F.W., Cleveland, J.L., Yi, T. & Ihle, J.N. 1993, "Structure of the murine Jak2 protein-tyrosine kinase and its role in interleukin 3 signal transduction", *Proceedings of the National Academy of Sciences of the United States of America,* vol. 90, no. 18, pp. 8429-8433.

Sims, N.A. 2015, "Cardiotrophin-like cytokine factor 1 (CLCF1) and neuropoietin (NP) signalling and their roles in development, adulthood, cancer and

degenerative disorders", *Cytokine & growth factor reviews,* vol. 26, no. 5, pp. 517-522.

Skiniotis, G., Boulanger, M.J., Garcia, K.C. & Walz, T. 2005, "Signaling conformations of the tall cytokine receptor gp130 when in complex with IL-6 and IL-6 receptor", *Nature structural & molecular biology,* vol. 12, no. 6, pp. 545-551.

Skoda, R.C., Duek, A. & Grisouard, J. 2015, "Pathogenesis of myeloproliferative neoplasms", *Experimental hematology,* vol. 43, no. 8, pp. 599-608.

Sliva, D., Wood, T.J., Schindler, C., Lobie, P.E. & Norstedt, G. 1994, "Growth hormone specifically regulates serine protease inhibitor gene transcription via gamma-activated sequence-like DNA elements", *The Journal of biological chemistry,* vol. 269, no. 42, pp. 26208-26214.

Sonbol, M.B., Firwana, B., Zarzour, A., Morad, M., Rana, V. & Tiu, R.V. 2013, "Comprehensive review of JAK inhibitors in myeloproliferative neoplasms", *Therapeutic advances in hematology,* vol. 4, no. 1, pp. 15-35.

Spangler, J.B., Moraga, I., Mendoza, J.L. & Garcia, K.C. 2015, "Insights into cytokine–receptor interactions from cytokine engineering", *Annual Review of Immunology,* vol. 33, pp. 139-167.

Springuel, L., Hornakova, T., Losdyck, E., Lambert, F., Leroy, E., Constantinescu, S.N., Flex, E., Tartaglia, M., Knoops, L. & Renauld, J.C. 2014, "Cooperating JAK1 and JAK3 mutants increase resistance to JAK inhibitors", *Blood,* vol. 124, no. 26, pp. 3924-3931.

Staerk, J., Defour, J., Pecquet, C., Leroy, E., Antoine-Poirel, H., Brett, I., Itaya, M., Smith, S.O., Vainchenker, W. & Constantinescu, S.N. 2011, "Orientation-specific signalling by thrombopoietin receptor dimers", *The EMBO journal,* vol. 30, no. 21, pp. 4398-4413.

Staerk, J., Kallin, A., Demoulin, J., Vainchenker, W. & Constantinescu, S.N. 2005, "JAK1 and Tyk2 Activation by the Homologous Polycythemia Vera JAK2 V617F Mutation Cross-talk with IGF1 receptor", *Journal of Biological Chemistry,* vol. 280, no. 51, pp. 41893-41899.

Stark, G.R. & Darnell, J.E. 2012, "The JAK-STAT Pathway at Twenty", *Immunity,* vol. 36, no. 4, pp. 503-514.

Stark, G.R., Cheon, H. & Wang, Y. 2017, "Responses to Cytokines and Interferons that Depend upon JAKs and STATs", *Cold Spring Harbor Perspectives in Biology,* , pp. a028555.

Suryani, S., Bracken, L.S., Harvey, R.C., Sia, K.C., Carol, H., Chen, I., Evans, K., Dietrich, P.A., Roberts, K.G. & Kurmasheva, R.T. 2014, "Evaluation of the in

vitro and in vivo efficacy of the JAK inhibitor AZD1480 against JAK-mutated acute lymphoblastic leukemia", *Molecular cancer therapeutics,* vol. 14, no. 2, pp. 364-374.

Takahashi, T. & Shirasawa, T. 1994, "Molecular cloning of rat JAK3, a novel member of the JAK family of protein tyrosine kinases", *FEBS letters,* vol. 342, no. 2, pp. 124-128.

Taylor, S., Yang, J., Wu, J., Haste, N., Radzio-Andzelm, E. & Anand, G. 2004, "PKA: a portrait of protein kinase dynamics", *Biochimica et Biophysica Acta (BBA)-Proteins and Proteomics,* vol. 1697, no. 1, pp. 259-269.

Taylor, S.S. & Kornev, A.P. 2011, "Protein kinases: evolution of dynamic regulatory proteins", *Trends in biochemical sciences,* vol. 36, no. 2, pp. 65-77.

Tiedt, R., Hao-Shen, H., Sobas, M.A., Looser, R., Dirnhofer, S., Schwaller, J. & Skoda, R.C. 2008, "Ratio of mutant JAK2-V617F to wild-type Jak2 determines the MPD phenotypes in transgenic mice", *Blood,* vol. 111, no. 8, pp. 3931-3940.

Tokarski, J.S., Zupa-Fernandez, A., Tredup, J.A., Pike, K., Chang, C., Xie, D., Cheng, L., Pedicord, D., Muckelbauer, J., Johnson, S.R., Wu, S., Edavettal, S.C., Hong, Y., Witmer, M.R., Elkin, L.L., Blat, Y., Pitts, W.J., Weinstein, D.S. & Burke, J.R. 2015, "Tyrosine Kinase 2-Mediated Signal Transduction in T Lymphocytes Is Blocked by Pharmacological Stabilization of its Pseudokinase Domain", *The Journal of biological chemistry,* vol. 290, no. 17, pp. 11061-74.

Toms, A.V., Deshpande, A., McNally, R., Jeong, Y., Rogers, J.M., Kim, C.U., Gruner, S.M., Ficarro, S.B., Marto, J.A. & Sattler, M. 2013, "Structure of a pseudokinase-domain switch that controls oncogenic activation of Jak kinases", *Nature Structural & Molecular Biology,* vol. 20, no. 10, pp. 1221-1223.

Traut, T.W. 1994, "Physiological concentrations of purines and pyrimidines", *Molecular and cellular biochemistry,* vol. 140, no. 1, pp. 1-22.

Trivedi, P.M., Graham, K.L., Scott, N.A., Jenkins, M.R., Majaw, S., Sutherland, R.M., Fynch, S., Lew, A.M., Burns, C.J., Krishnamurthy, B., Brodnicki, T.C., Mannering, S.I., Kay, T.W. & Thomas, H.E. 2017, "Repurposed JAK1/JAK2 Inhibitor Reverses Established Autoimmune Insulitis in Non-Obese Diabetic Mice", *Diabetes,* vol. 66, no. 6, pp. 1650-1660.

Ungureanu, D., Wu, J., Pekkala, T., Niranjan, Y., Young, C., Jensen, O.N., Xu, C.F., Neubert, T.A., Skoda, R.C., Hubbard, S.R. & Silvennoinen, O. 2011, "The pseudokinase domain of JAK2 is a dual-specificity protein kinase that negatively regulates cytokine signaling", *Nature Structural & Molecular Biology,* vol. 18, no. 9, pp. 971-976.

Vainchenker, W. & Constantinescu, S. 2013, "JAK/STAT signaling in hematological malignancies", *Oncogene,* vol. 32, pp. 2601-2613.

Valiev, M., Kawai, R., Adams, J.A. & Weare, J.H. 2003, "The role of the putative catalytic base in the phosphoryl transfer reaction in a protein kinase: first-principles calculations", *Journal of the American Chemical Society,* vol. 125, no. 33, pp. 9926-9927.

Varghese, L.N., Ungureanu, D., Liau, N.P.D., Young, S.N., Laktyushin, A., Hammaren, H., Lucet, I.S., Nicola, N.A., Silvennoinen, O., Babon, J.J. & Murphy, J.M. 2014, "Mechanistic insights into activation and SOCS3-mediated inhibition of myeloproliferative neoplasm-associated JAK2 mutants from biochemical and structural analyses", *Biochemical Journal,* vol. 458, no. 2, pp. 395-405.

Vedadi, M., Niesen, F.H., Allali-Hassani, A., Fedorov, O.Y., Finerty, P.J.,Jr, Wasney, G.A., Yeung, R., Arrowsmith, C., Ball, L.J., Berglund, H., Hui, R., Marsden, B.D., Nordlund, P., Sundstrom, M., Weigelt, J. & Edwards, A.M. 2006, "Chemical screening methods to identify ligands that promote protein stability, protein crystallization, and structure determination", *Proceedings of the National Academy of Sciences of the United States of America,* vol. 103, no. 43, pp. 15835-15840.

Velazquez, L., Mogensen, K.E., Barbieri, G., Fellous, M., Uzé, G. & Pellegrini, S. 1995, "Distinct domains of the protein tyrosine kinase tyk2 required for binding of interferon-/and for signal transduction", *Journal of Biological Chemistry,* vol. 270, no. 7, pp. 3327-3334.

Velazquez, L., Fellous, M., Stark, G.R. & Pellegrini, S. 1992, "A protein tyrosine kinase in the interferon αβ signaling pathway", *Cell,* vol. 70, no. 2, pp. 313-322.

Vertommen, D., Bertrand, L., Sontag, B., Di Pietro, A., Louckx, M.P., Vidal, H., Hue, L. & Rider, M.H. 1996, "The ATP-binding site in the 2-kinase domain of liver 6-phosphofructo-2-kinase/fructose-2,6-bisphosphatase. Study of the role of Lys-54 and Thr-55 by site-directed mutagenesis", *The Journal of biological chemistry,* vol. 271, no. 30, pp. 17875-17880.

Vignali, D.A. & Kuchroo, V.K. 2012, "IL-12 family cytokines: immunological playmakers", *Nature immunology,* vol. 13, no. 8, pp. 722-728.

Villarino, A.V., Kanno, Y. & O'Shea, J.J. 2017, "Mechanisms and consequences of Jak-STAT signaling in the immune system", *Nature immunology,* vol. 18, no. 4, pp. 374-384.

Wakao, H., Gouilleux, F. & Groner, B. 1994, "Mammary gland factor (MGF) is a novel member of the cytokine regulated transcription factor gene family and

confers the prolactin response", *The EMBO journal,* vol. 13, no. 9, pp. 2182-2191.

Waksman, G., Kominos, D., Robertson, S.C., Pant, N., Baltimore, D., Birge, R.B., Cowburn, D., Hanafusa, H., Mayer, B.J., Overduin, M., Resh, M.D., Rios, C.B., Silverman, L. & Kuriyan, J. 1992, "Crystal structure of the phosphotyrosine recognition domain SH2 of v-src complexed with tyrosine-phosphorylated peptides", *Nature,* vol. 358, no. 6388, pp. 646-653.

Wallweber, H.J., Tam, C., Franke, Y., Starovasnik, M.A. & Lupardus, P.J. 2014, "Structural basis of recognition of interferon-α receptor by tyrosine kinase 2", *Nature Structural & Molecular Biology,* vol. 21, no. 5, pp. 443-448.

Wan, X., Ma, Y., McClendon, C.L., Huang, L.J. & Huang, N. 2013, "Ab Initio Modeling and Experimental Assessment of Janus Kinase 2 (JAK2) Kinase-Pseudokinase Complex Structure", *PLoS computational biology,* vol. 9, no. 4, pp. e1003022.

Wang, X., Lupardus, P., LaPorte, S.L. & Garcia, K.C. 2009, "Structural biology of shared cytokine receptors", *Annual Review of Immunology,* vol. 27, pp. 29-60.

Waters, M.J. & Brooks, A.J. 2015, "JAK2 activation by growth hormone and other cytokines", *The Biochemical journal,* vol. 466, no. 1, pp. 1-11.

Watling, D., Guschin, D., Müller, M., Silvennoinen, O., Witthuhn, B.A., Quelle, F.W., Rogers, N.C., Schindler, C., Stark, G.R. & Ihle, J.N. 1993, "Complementation by the protein tyrosine kinase JAK2 of a mutant cell line defective in the interferon-& gamma; signal transduction pathway", vol. 366, no. 6451, pp. 166-170.

Wernig, G., Gonneville, J.R., Crowley, B.J., Rodrigues, M.S., Reddy, M.M., Hudon, H.E., Walz, C., Reiter, A., Podar, K. & Royer, Y. 2008, "The Jak2V617F oncogene associated with myeloproliferative diseases requires a functional FERM domain for transformation and for expression of the Myc and Pim proto-oncogenes", *Blood,* vol. 111, no. 7, pp. 3751-3759.

Wilks, A.F., Kurban, R.R., Hovens, C.M. & Ralph, S.J. 1989, "The application of the polymerase chain reaction to cloning members of the protein tyrosine kinase family", *Gene,* vol. 85, no. 1, pp. 67-74.

Wilks, A.F. 2008, "The JAK kinases: not just another kinase drug discovery target", *Seminars in Cell and Developmental Biology,* vol. 19, no. 4, pp. 319-328.

Wilks, A.F., Harpur, A.G., Kurban, R.R., Ralph, S.J., Zurcher, G. & Ziemiecki, A. 1991, "Two novel protein-tyrosine kinases, each with a second phosphotransferase-related catalytic domain, define a new class of protein kinase", *Molecular and cellular biology,* vol. 11, no. 4, pp. 2057-2065.

Williams, N.K., Bamert, R.S., Patel, O., Wang, C., Walden, P.M., Wilks, A.F., Fantino, E., Rossjohn, J. & Lucet, I.S. 2009, "Dissecting specificity in the Janus kinases: the structures of JAK-specific inhibitors complexed to the JAK1 and JAK2 protein tyrosine kinase domains", *Journal of Molecular Biology,* vol. 387, no. 1, pp. 219-232.

Winthrop, K.L. 2017, "The emerging safety profile of JAK inhibitors in rheumatic disease", *Nature Reviews Rheumatology,* vol. 13, no. 4, pp. 234-243.

Witthuhn, B.A., Quelle, F.W., Silvennoinen, O., Yi, T., Tang, B., Miura, O. & Ihle, J.N. 1993, "JAK2 associates with the erythropoietin receptor and is tyrosine phosphorylated and activated following stimulation with erythropoietin", *Cell,* vol. 74, no. 2, pp. 227-236.

Witthuhn, B.A., Silvennoinen, O., Miura, O., Lai, K.S., Cwik, C., Liu, E.T. & Ihle, J.N. 1994, "Involvement of the Jak-3 Janus kinase in signalling by interleukins 2 and 4 in lymphoid and myeloid cells", *Nature,* vol. 370, no. 6485, pp. 153-157.

Wu, Q.Y., Li, F., Guo, H.Y., Cao, J., Chen, C., Chen, W., Zhao, K., Zeng, L.Y., Han, Z.X. & Li, Z.Y. 2012, "Amino acid residue E543 in JAK2 C618R is a potential therapeutic target for myeloproliferative disorders caused by JAK2 C618R mutation", *Archives of Biochemistry and Biophysics,* vol. 528, no. 1, pp. 57-66.

Xie, T., Lim, S.M., Westover, K.D., Dodge, M.E., Ercan, D., Ficarro, S.B., Udayakumar, D., Gurbani, D., Tae, H.S., Riddle, S.M., Sim, T., Marto, J.A., Janne, P.A., AUID, C.C. & AUID, G.N. 2014, "Pharmacological targeting of the pseudokinase Her3", *Nature chemical biology,* vol. 10, no. 12, pp. 1006-12.

Xu, B., English, J.M., Wilsbacher, J.L., Stippec, S., Goldsmith, E.J. & Cobb, M.H. 2000, "WNK1, a novel mammalian serine/threonine protein kinase lacking the catalytic lysine in subdomain II", *The Journal of biological chemistry,* vol. 275, no. 22, pp. 16795-16801.

Yamaoka, K., Saharinen, P., Pesu, M., Holt 3rd, V., Silvennoinen, O. & O'Shea, J.J. 2004, "The Janus kinases (Jaks)", *Genome Biol,* vol. 5, no. 12, pp. 253.

Yamaoka, K. 2016, "Janus kinase inhibitors for rheumatoid arthritis", *Current opinion in chemical biology,* vol. 32, pp. 29-33.

Yan, D., Hutchison, R.E. & Mohi, G. 2012, "Tyrosine 201 is required for constitutive activation of JAK2V617F and efficient induction of myeloproliferative disease in mice", *Blood,* vol. 120, no. 9, pp. 1888-1898.

Yao, H., Ma, Y., Hong, Z., Zhao, L., Monaghan, S.A., Hu, M.C. & Huang, L.S. 2017, "Activating JAK2 mutants reveal cytokine receptor coupling differences that impact outcomes in myeloproliferative neoplasm", *Leukemia,* vol. 31, no. 10, pp. 2122-2131.

Yeh, T.C., Dondi, E., Uzé, G. & Pellegrini, S. 2000, "A dual role for the kinase-like domain of the tyrosine kinase Tyk2 in interferon-α signaling", *Proceedings of the National Academy of Sciences,* vol. 97, no. 16, pp. 8991-6.

Zeidler, M.P. & Bausek, N. 2013, *The Drosophila JAK-STAT pathway,* vol. 2, no. 3, pp. e25353.

Zeqiraj, E. & van Aalten, D.M. 2010, "Pseudokinases-remnants of evolution or key allosteric regulators?", *Current opinion in structural biology,* vol. 20, no. 6, pp. 772-781.

Zhang, D., Wlodawer, A. & Lubkowski, J. 2016, "Crystal Structure of a Complex of the Intracellular Domain of Interferon λ Receptor 1 (IFNLR1) and the FERM/SH2 Domains of Human JAK1", *Journal of Molecular Biology,* vol. 428, no. 23, pp. 4651-4668.

Zhang, J., Ding, L., Holmfeldt, L., Wu, G., Heatley, S.L., Payne-Turner, D., Easton, J., Chen, X., Wang, J. & Rusch, M. 2012, "The genetic basis of early T-cell precursor acute lymphoblastic leukaemia", *Nature,* vol. 481, no. 7380, pp. 157-163.

Zhang, Q., Putheti, P., Zhou, Q., Liu, Q. & Gao, W. 2008, "Structures and biological functions of IL-31 and IL-31 receptors", *Cytokine & growth factor reviews,* vol. 19, no. 5, pp. 347-356.

Zhang, X., Gureasko, J., Shen, K., Cole, P.A. & Kuriyan, J. 2006, "An allosteric mechanism for activation of the kinase domain of epidermal growth factor receptor", *Cell,* vol. 125, no. 6, pp. 1137-1149.

Zhang, B.Y., Riska, S.M., Mahoney, D.W., Costello, B.A., Kohli, R., Quevedo, J.F., Cerhan, J.R. & Kohli, M. 2016, "Germline genetic variation in JAK2 as a prognostic marker in castration-resistant prostate cancer", *BJU international,* vol. 119, no. 3, pp. 489-495.

Zhao, L., Dong, H., Zhang, C.C., Kinch, L., Osawa, M., Iacovino, M., Grishin, N.V., Kyba, M. & Huang, L.J. 2009, "A JAK2 interdomain linker relays Epo receptor engagement signals to kinase activation", *Journal of Biological Chemistry,* vol. 284, no. 39, pp. 26988.

Zhao, L., Ma, Y., Seemann, J. & Huang, L. 2010, "A regulating role of the JAK2 FERM domain in hyperactivation of JAK2 (V617F)", *Biochem.J,* vol. 426, pp. 91-98.

Zheng, Z., Goncearenco, A. & Berezovsky, I.N. 2015, "Nucleotide binding database NBDB–a collection of sequence motifs with specific protein-ligand interactions", *Nucleic acids research,* vol. 44, no. D1, pp. D301-D307.

Zhong, J., Sharma, J., Raju, R., Palapetta, S.M., Prasad, T., Huang, T., Yoda, A., Tyner, J.W., van Bodegom, D. & Weinstock, D.M. 2014, "TSLP signaling

pathway map: a platform for analysis of TSLP-mediated signaling", *Database,* vol. 2014, pp. bau007.

Zhou, Y.J., Chen, M., Cusack, N.A., Kimmel, L.H., Magnuson, K.S., Boyd, J.G., Lin, W., Roberts, J.L., Lengi, A. & Buckley, R.H. 2001, "Unexpected effects of FERM domain mutations on catalytic activity of Jak3: structural implication for Janus kinases", *Molecular cell,* vol. 8, no. 5, pp. 959-969.

Zou, H., Yan, D. & Mohi, G. 2011, "Differential biological activity of disease-associated JAK2 mutants", *FEBS letters,* vol. 585, no. 7, pp. 1007-1013.

Zouein, F.A., Duhé, R.J. & Booz, G.W. 2011, "JAKs go nuclear: emerging role of nuclear JAK1 and JAK2 in gene expression and cell growth", *Growth factors,* vol. 29, no. 6, pp. 245-252.

10 Original Communications

THE JOURNAL OF BIOLOGICAL CHEMISTRY VOL. 290, NO. 45, pp. 27261–27270, November 6, 2015

Structural and Functional Characterization of the JH2 Pseudokinase Domain of JAK Family Tyrosine Kinase 2 (TYK2)*

Received for publication, June 24, 2015, and in revised form, September 2, 2015 Published, JBC Papers in Press, September 10, 2015, DOI 10.1074/jbc.M115.672048

Xiaoshan Min[‡], Daniela Ungureanu[§], Sarah Maxwell[¶], Henrik Hammarén[‖], Steve Thibault[‡], Ellin-Kristina Hillert[§], Merrill Ayres[‡], Brad Greenfield[¶], John Eksterowicz[‡], Chris Gabel[¶], Nigel Walker[‡], Olli Silvennoinen[‖1], and Zhulun Wang[‡2]**

*From the Departments of [‡]Therapeutic Discovery and [¶]Inflammation, Amgen Inc., South San Francisco, California 94080, the [§]Institute of Biomedical Technology, University of Tampere, 33014 Tampere, Finland, the [‖]School of Medicine, University of Tampere, 33014 Tampere, Finland, and the **Department of Clinical Hematology, Tampere University Hospital, 33520 Tampere, Finland*

Background: JAK JH2s (pseudokinase domains) mediate important regulatory functions; it is unclear whether TYK2 JH2 binds ATP and possesses enzymatic activity.
Results: TYK2 JH2 binds ATP, but is catalytically inactive; ATP stabilizes JH2 and modulates TYK2 activity.
Conclusion: ATP binding to JH2 is functionally important; the rigid activation loop probably hinders substrate phosphorylation.
Significance: The TYK2 JH2 domain can be targeted with ATP-competitive compounds for therapeutics.

JAK (Janus family of cytoplasmic tyrosine kinases) family tyrosine kinase 2 (TYK2) participates in signaling through cytokine receptors involved in immune responses and inflammation. JAKs are characterized by dual kinase domain: a tyrosine kinase domain (JH1) that is preceded by a pseudokinase domain (JH2). The majority of disease-associated mutations in JAKs map to JH2, demonstrating its central regulatory function. JH2s were considered catalytically inactive, but JAK2 JH2 was found to have low autoregulatory catalytic activity. Whether the other JAK JH2s share ATP binding and enzymatic activity has been unclear. Here we report the crystal structure of TYK2 JH2 in complex with adenosine 5′-*O*-(thiotriphosphate) (ATP-γS) and characterize its nucleotide binding by biochemical and biophysical methods. TYK2 JH2 did not show phosphotransfer activity, but it binds ATP and the nucleotide binding stabilizes the protein without inducing major conformational changes. Mutation of the JH2 ATP-binding pocket increased basal TYK2 phosphorylation and downstream signaling. The overall structural characteristics of TYK2 JH2 resemble JAK2 JH2, but distinct stabilizing molecular interactions around helix αAL in the activation loop provide a structural basis for differences in substrate access and catalytic activities among JAK family JH2s. The structural and biochemical data suggest that ATP binding is functionally important for both TYK2 and JAK2 JH2s, whereas the regulatory phosphorylation appears to be a unique property of JAK2. Finally, the co-crystal structure of TYK2 JH2 complexed with a small molecule inhibitor demonstrates that JH2 is accessible to ATP-competitive compounds, which offers novel approaches for targeting cytokine signaling as well as potential therapeutic applications.

TYK2 belongs to the Janus family of cytoplasmic tyrosine kinases (JAK1–3, TYK2) and functions as a critical mediator in signaling for several immunomodulatory cytokines that regulate diverse cellular responses such as viral defense (type I and type III interferons), immunity and inflammation (IL-6, IL-12, IL-22, IL-23, and IL-26), and anti-inflammatory responses (IL-10) (1–3). TYK2 associates with the cytoplasmic domains of cytokine receptors, and ligand-induced receptor rearrangement facilitates TYK2 *trans*-interaction with either JAK1 or JAK2 and phosphorylation of activation loop tyrosine residues 1054/1055 in JH1 (tyrosine kinase domain), leading to its activation and progression of signal transduction (4–6). TYK2 deficiencies are associated with susceptibility to viral and bacterial infections, and several TYK2 polymorphisms show strong linkage to autoimmune diseases such as multiple sclerosis, systemic lupus erythematosus, Crohn disease, primary biliary cirrhosis, and type I diabetes (7). TYK2 polymorphism has also been linked to acute myeloid leukemia, and T cell acute lymphoblastic leukemias have been shown to be TYK2-dependent for survival (8, 9). TYK2 thus shows characteristics of a suitable drug target, but thus far development of TYK2 specific inhibitors has not been successful.

The tandem kinase domains are the hallmark of JAKs (10). JH1 is a canonical protein tyrosine kinase domain, whereas JH2 is classified as a pseudokinase domain. The human genome encodes more than 500 protein kinases, and almost 10% of them are predicted to be enzymatically inactive and classified as pseudokinases due to alterations in one or several of the motifs considered to be essential for nucleotide binding or catalysis (11, 12). The recent availability of pseudokinase crystal struc-

* The authors declare that they have no conflicts of interest with the contents of this article.
The atomic coordinates and structure factors (codes 5C03 and 5C01) have been deposited in the Protein Data Bank (http://wwpdb.org/).
[1] To whom correspondence may be addressed. Tel.: 358-50-359-5740; E-mail: olli.silvennoinen@uta.fi.
[2] To whom correspondence may be addressed: Tel.: 650-244-2446; E-mail: zwang@amgen.com.

tures has significantly advanced our understanding of the functions and structure-function relationship of these proteins (13–16). Interestingly, almost half of pseudokinases have been found to bind nucleotides, although only a few display catalytic activity, leaving the functional role of nucleotide binding and its determinants largely elusive. The JH2s of JAKs lack aspartic acid in the HRD (His-Arg-Asp) motif of the catalytic loop and have an incomplete Gly-rich loop. Recently, JAK2 JH2 and HER3, which also has a non-canonical substitution at the aspartic acid position in the HRD motif, were shown to bind ATP and retain low catalytic activity, indicating that the lack of Asp can be at least partly compensated for (17, 18).

JH2 has an important regulatory role in JAK kinases, and mutations in JH2 of JAKs have been shown to cause, or be linked to, hematological and immunological diseases. Biochemical data supported by clinical evidence suggest that JH2 possesses both negative as well as positive regulatory function (19, 20). Deletion of JH2 causes increased basal activity in JAK2 and JAK3 while abrogating cytokine-induced signaling (21). Clinical JAK2 mutations are presently the best studied example of the negative regulatory function of JH2. The most frequent somatic mutation, V617F, results in constitutively active JAK2 and is responsible for >95% of polycythemia vera cases and ~50% of essential thrombocythemia and primary myelofibrosis cases (22–24). The homologous mutations V678F in TYK2 and V658F in JAK1 JH2 also result in a gain-of-function phenotype, suggesting that JH2 plays a similar regulatory function in these JAK kinases (25). The JAK3 JH2 mutations resulting in defective γc receptor signaling and causing severe combined immunodeficiency serve as a clinical example of the potential positive regulatory function of JH2 (26). Random mutagenesis approaches identified mutations in TYK2 JH2 that abrogate the intrinsic catalytic activity and formation of the high-affinity IFN type I receptor (27). A similar phenotype is also observed in the autoimmune disease-linked I684S variant of TYK2 (28).

Recent biochemical and structural data suggests that the pseudokinase domain of JAK2 has low levels of catalytic activity and negatively regulates the activity of the kinase domain (13, 16). Crystal structures of inhibitor-bound TYK2 JH2 have recently been solved, but its biochemical and nucleotide binding characteristics are still elusive. Several members of the pseudokinase family, including TYK2, are linked to human diseases, which has raised interest toward their therapeutic targeting. Elucidation of the determinants of nucleotide binding and catalytic activity in pseudokinases is of significant relevance in this context as ATP competitive compounds are one of the most rapidly growing class of drugs. Here we have investigated the structure and function of the pseudokinase domain of TYK2, with a focus on the role of nucleotide binding and determinants of catalytic activity.

Experimental Procedures

Protein Purification and Crystallization—TYK2 JH2 (556–871) was subcloned into a pFastBac HT vector (Invitrogen) with a His_6 tag at the N terminus and a tobacco etch virus protease cleavage site between the His_6 tag and TYK2. TYK2 protein was expressed in baculovirus High Five cells (Invitrogen) grown at 27 °C for 72 h in ESF921 insect cell media (Expression Systems). Cells were processed with a Microfluidizer, and the supernatant was loaded on an affinity column containing Talon IMAC beads (Clontech) and eluted with a gradient of 5–500 mM imidazole. The protein was cleaved with recombinant tobacco etch virus at 4 °C overnight. The digested protein was desalted into MonoQ buffer (50 mM Tris, pH 7.9, 50 mM NaCl, 1 mM EDTA, 1 mM DTT, and 10% glycerol). The protein was further purified using anion-exchange (MonoQ) and size exclusion (Superdex 200) chromatography. The purified protein was highly homogeneous and was concentrated to 7 mg/ml in the crystallization buffer (25 mM Hepes, pH 7.9, 50 mM NaCl, 2 mM DTT, 1 mM tris(2-carboxyethyl)phosphine, 10% glycerol) before crystallization. TYK2 JH2 was incubated with 2 mM ATP-γS[3] and 5 mM $MgCl_2$, or with 0.1 mM compound, for 1 h on ice before setting up the crystallization tray. The protein was crystallized by mixing with 18–22% PEG 4000, 0.1 M Tris, pH 8.5, and 200 mM $CaCl_2$ in a 1:1 ratio. Large single crystals were obtained through microseeding. For data collection, a single crystal was transferred to a cryoprotection solution containing 22% PEG4000, 0.1 M Tris, pH 8.5, 200 mM $CaCl_2$, and 25% ethylene glycol, and then frozen in liquid nitrogen.

Data Collection and Structure Solution—X-ray diffraction data sets were collected at synchrotron beamline 5.0.2 at the Advanced Light Source (ALS) (Berkeley, CA), processed using MOSFLM (29), and scaled using SCALA in CCP4 package. The structure was solved by molecular replacement method using the program PHASER (30). The resulting density map is of high quality, and the model tracing was carried out in COOT (31) with the aid of ARP/wARP auto tracing. Structure refinement was done with REFMAC5 (32) in the CCP4 package (33).

Biacore Analysis—Binding affinities were calculated by SPR on a Biacore T-1000 (GE Healthcare). Biotinylated TYK2 JH2 was coupled to immobilized streptavidin on a CM7 sensor chip (GE Healthcare). For kinetic experiments, a flow rate of 50 μl/min was used. The running buffer contains 75 mM NaCl, 4 mM $MgCl_2$, 2 mM $CaCl_2$, 0.05% Tween 20, 2 mM DTT, and 1 mM tris(2-carboxyethyl)phosphine. The concentration of ATP was changed from 300 μM to 400 nM. Data were analyzed with the Biacore T-1000 evaluation software, version 2.0 (GE Healthcare).

Differential Scanning Fluorometry Analysis—20 μl of 0.5 mg/ml TYK2 JH2 domain (556–871) was incubated with 1 mM ATP and 5 mM $MgCl_2$. 5 μl of 100× SYPRO Orange dye was added to the mixture. The fluorescence was measured on a Bio-Rad CFX-96 real time PCR machine, and the temperature was increased from 25 to 95 °C with a ramping speed of 1 °C/min.

SAXS Analysis—Small-angle x-ray scattering (SAXS) data were collected at synchrotron beamline 12.3.1 at the Advanced Light Source (ALS) (Berkeley, CA). The wavelength $\lambda = 1.0$ Å and sample-to-detector distance were set to 1.5 m, resulting in scattering vectors, q, ranging from 0.01 to 0.33 $Å^{-1}$. The scattering vector is defined as $q = 4\pi \sin\theta/\lambda$, where 2θ is the scat-

[3] The abbreviations used are: ATP-γS, adenosine 5′-*O*-(thiotriphosphate); Mant-ATP, 2′-(3′)-*O*-(*N*-methylanthraniloyl)-adenosine-5′-triphosphate; SAXS, small-angle x-ray scattering.

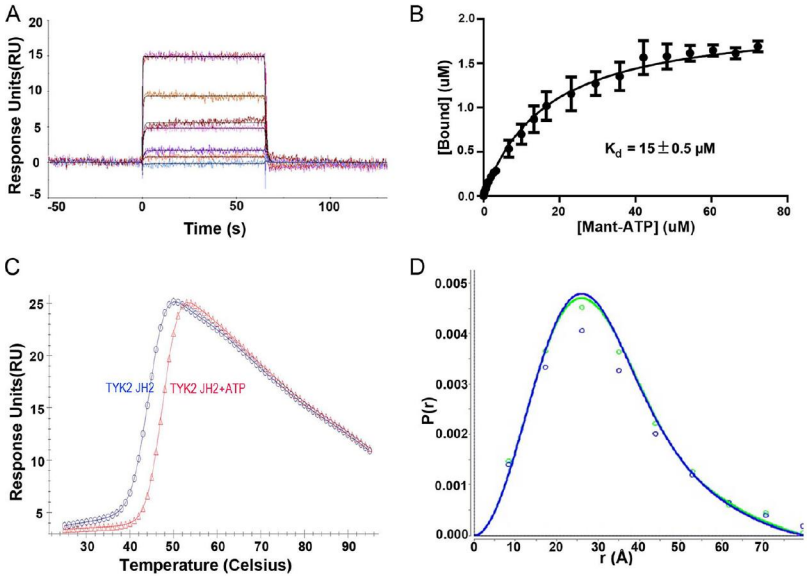

FIGURE 1. **ATP binding to TYK2 JH2.** *A*, surface plasmon resonance sensorgram of ATP binding to TYK2 JH2. *B*, Mant-ATP titration curve. Points represent the average from four individual measurements. *Error bars* are standard deviation. *C*, thermal melting curve of JH2 in the absence (*blue*) and presence (*red*) of ATP. *D*, the pair-distance distribution function from SAXS of JH2 in the absence (*blue*) and presence (*green*) of ATP.

tering angle. All experiments were performed at 20 °C, and data were processed as described (34). The experimental SAXS data for different protein concentrations were investigated for aggregation using Guinier plots (35). The radius of gyration R_g was derived by the Guinier approximation $I(q) = I(0)\exp(-q^2R_g^2/3)$ with the limits $qR_g < 1.3$. The program SCATTER was used to compute the pair-distance distribution functions, P(r) (36).

ADP Production Assay—ADP production following ATP hydrolysis was measured using the ADP-Glo kinase assay (Promega, Madison, WI). Activity measurements were done following the manufacturer's instructions. Briefly, ADP production was measured in 25-μl reaction volumes in 40 mM Tris-Cl (pH 7.5), 20 mM $MnCl_2$, and 100 μM ATP. Reactions were started by adding 500 or 400 ng of recombinant TYK2 JH2 or JAK2 JH2, respectively, and stopped after 0, 20, 40, or 60 min by adding the ADP-Glo reagent. After the addition of the kinase detection reagent, produced luminescence was compared with results from an ADP/ATP standard curve. Measurements were done in triplicate.

Mant-ATP Binding Assay—Mant-ATP (Jena Biosciences) binding to TYK2 JH2 was measured using a QuantaMaster spectrofluorometer (Photon Technology International) by analyzing FRET between the protein and Mant. Excitation wavelength was 280 nm, while emitted fluorescence was scanned from 300 to 500 nm. For K_d determination, increasing concentrations of concentrated Mant-ATP stocks were added to a buffer solution of 20 mM Tris-HCl (pH 8.0), 200 mM NaCl, 10% glycerol, 2 mM DTT, and 2 μM recombinant JH2 protein in the presence of 10 mM $MgCl_2$. Binding was observed as emitted fluorescence at 440–450 nm, and the measured fluorescence values were corrected for the primary inner filter effect. The K_d value was calculated from quadruplicate measurements using GraphPad Prism 5.02 essentially as described in Ref. 37.

Plasmids, Transfections, and Western Blots—Human TYK2 cDNA (TYK2 WT) was cloned into the pCINeo vector (Promega) with a C-terminal HA tag. TYK2 K642A and K930R mutations were introduced using QuikChange site-directed mutagenesis (Stratagene) and verified by sequencing. TYK2-deficient 11,1 cells and Sββ cells (kindly provided by S. Pellegrini) have been described previously (38, 39), and they were transfected as reported earlier. After 8 h, cells were starved overnight and stimulated with 1000 units/ml IFN-α (PeproTech) or 100 units/ml IL-12 (PeproTech) followed by lysis in 50 mM Tris-HCl, pH 8.0, 150 mM NaCl, 100 mM NaF, 10% glycerol, 1% Nonidet P-40, and protease inhibitor cocktail (Roche Applied Science). TYK2 was immunoprecipitated using anti-TYK2 antibody (Millipore, catalogue number 06-638), and phosphorylation was analyzed by Western blotting with anti-phospho-Tyr (4G10, Millipore, catalogue number 05-321). STAT1 phosphorylation was analyzed using anti-pSTAT1 antibody (Cell Signaling, catalogue number 9171L).

Results

ATP Binding to TYK2 JH2 Domain—The binding of ATP to TYK2 JH2 was assessed using multiple analytic methods. We measured the binding kinetics of ATP to TYK2 JH2 using surface plasmon resonance (Biacore). The experiments used recombinant human TYK2 JH2 (556–871). As shown in Fig. 1*A*, ATP binds to TYK2 JH2 with a fast-on and fast-off rate and a measured K_d of 24 μM. We also used a fluorescent methylanthraniloyl ATP analog (Mant-ATP) in a spectrofluorometric assay (37) to confirm the binding of ATP to TYK2 JH2. The results showed a K_d of 15 μM for Mant-ATP (Fig. 1*B*), which is

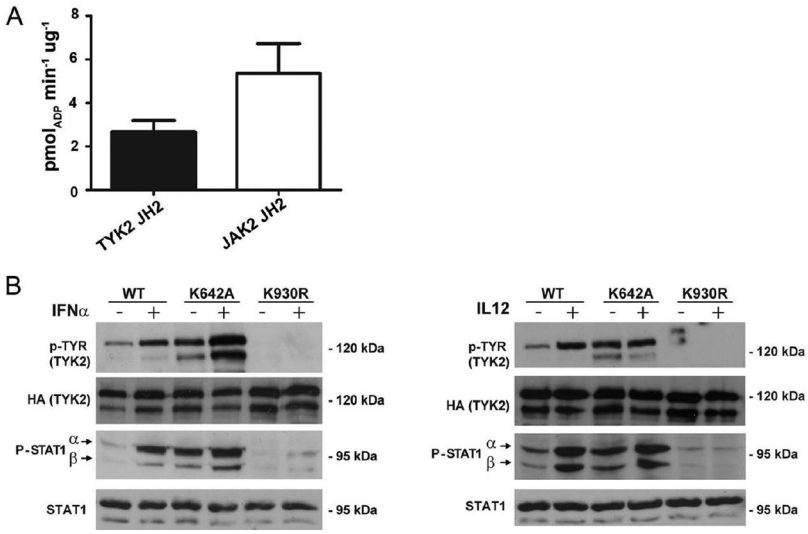

FIGURE 2. **Functional characterization of TYK2 JH2.** *A*, ATP hydrolysis as measured by ADP-Glo assay. *Error bars* are S.D. from triplicate experiments. *B*, analysis of TYK2 signaling in mammalian cells. TYK2-deficient 11,1 cells (*left*) or S$\beta\beta$ cells (*right*) were transfected with TYK2 wild type and mutants thereof and stimulated with IFN-α or IL-12 as indicated. Phosphorylation of TYK2 was analyzed by anti-TYK2 immunoprecipitation followed by anti-phosphotyrosine (*p-TYR*) blot. STAT1 phosphorylation was analyzed directly by anti-phospho-STAT1 (*p-STAT1*) blot. Anti-HA blot shows TYK2 protein levels.

weaker than the Mant-ATP binding affinity for JAK2 JH2 (K_d ~1 μM) (18).

Next we examined the effect of ATP binding to TYK2 JH2. We used a differential scanning fluorescence assay to study the thermal melting of TYK2 JH2 in the presence and absence of ATP. In this assay, the fluorescent dye SYPRO Orange binds to the hydrophobic regions that are exposed when proteins undergo thermal unfolding, leading to an increase in fluorescence intensity. As shown in Fig. 1*C*, the apo TYK2 JH2 showed a T_m of 44 °C. Upon ATP binding, the melting temperature of JH2 increased by 4 °C, suggesting that ATP binding stabilizes JH2. To find out whether ATP binding results in conformational changes, we performed SAXS experiments on both apo and ATP-bound JH2s. The scattering profiles of JH2 are virtually identical in the presence and absence of Mg-ATP (Fig. 1*D*) with a calculated radius of gyration (R_g) of 24.2 nm for apo and 24.0 nm in the presence of Mg-ATP. Taken together, these data suggest that ATP binding does not induce major overall conformational change in JH2, but rather stabilizes the domain.

Enzymatic Activity of TYK2 JH2—To address the question whether TYK2 JH2 possesses enzymatic kinase activity, we employed an ADP-Glo kinase assay to compare hydrolysis activity of TYK2 JH2 with JAK2 JH2, which was recently found to be an active, albeit weak kinase (18). The results show that TYK2 JH2 was able to catalyze ADP production from ATP at rates of ~50% of that of JAK2 JH2 (Fig. 2*A*), demonstrating that, despite deviations in its sequence from canonical protein kinases, TYK2 JH2 possesses some residual activity. To further assess the possible kinase activity, we performed *in vitro* kinase reactions to test for autophosphorylation activity and subjected the purified proteins to mass spectrometry analysis. However, we could not identify any consistent phosphorylation in JH2 (data not shown). Thus, although TYK2 JH2 retains very low ability to hydrolyze ATP, it does not show autophosphorylation and can be considered a catalytically incompetent pseudokinase. In accordance, the regulatory autophosphorylation sites in JAK2 JH2 are not conserved in TYK2 JH2.

Analysis of TYK2 JH2 in IFNα and IL-12 Signaling—We were interested to investigate whether the ATP binding capability of TYK2 JH2 is involved in the JH2-mediated regulation of TYK2 activity, as has been earlier reported for JAK2 JH2 (40). To this end, the catalytic lysine in the β3 strand of JH2 was mutated to alanine and the full-length TYK2 harboring the corresponding JH2 K642A mutation was analyzed in IFNα and IL-12 signaling. TYK2-deficient 11,1 or S$\beta\beta$ cells were transfected with HA-tagged TYK2 constructs and analyzed for TYK2 JH1 activation loop phosphorylation by Western blotting. Fig. 2*B* shows that wild type TYK2 displays a low level of basal phosphorylation of the activation loop tyrosine residues that is readily induced by IFNα or IL-12 stimulation. The JH2 K642A mutation increases TYK2 phosphorylation in both unstimulated and IFNα-stimulated conditions, whereas the JH1 kinase-inactive K930R mutant remains unphosphorylated. The JH2 K642A mutation also results in an increased level of basal STAT1 phosphorylation, suggesting that the ATP-binding pocket of JH2 is regulating not only autophosphorylation of the TYK2 activation loop but also downstream signaling.

Crystal Structure of TYK2 JH2 Bound with a Nucleotide—In parallel, we determined the crystal structure of TYK2 JH2 in complex with an ATP analogue, ATP-γS, at 1.9 Å resolution (Table 1). The overall structure is practically identical to those of recently reported inhibitor co-crystal structures of TYK2 JH2 (Protein Data Bank (PDB) codes: 3ZON, 4OLI, and 4WOV) (15, 16). TYK2 JH2 adopts a canonical bilobal protein kinase fold (Fig. 3*A*). The N-terminal lobe (N-lobe) is made up of five β-strands and one helix (αC), and the larger C-terminal lobe

TABLE 1
Statistics of crystallographic data and refinement
Values in parentheses are for the highest resolution shell.

	ATP	Pyrazine compound
Data collection		
Space group	P 21	P 21
Unit cell dimensions	56.12 47.69 112.75 90 93.72 90	56.34 48.17 114.21 90 93.28 90
Wavelength (Å)	1.000	1.000
Resolution (Å)	48.88–1.9 (2–1.9)	49.34–2.15 (2.27–2.15)
No. of total reflections	161,958	119,960
No. of unique reflections	47,007	33,546
Wilson B factor (Å^2)	22.14	25.14
Average multiplicity	3.4 (3.5)	3.6 (3.2)
Completeness (%)	99.27 (99.30)	99.57 (98.29)
Mean intensity I/σ	9.88 (2.73)	8.87 (2.57)
R_{sym} [a]	0.082 (0.503)	0.099 (0.411)
Refinement		
Resolution (Å)	30–1.9 (1.98–1.9)	30–2.15 (2.24–2.15)
R_{work}/R_{free} [b]	0.181/0.218	0.196 /0.243
No. of reflections	44,577	31,803
No. of atoms	4568	4435
Protein	4152	4112
Water	298	245
Ligand	118	78
Ramachandran statistics		
Residue in favored regions	94.1	93.2
Residues in allowed regions	5.9	6.8
Residues in disallowed regions	0	0
Average B-factors (Å^2)	26.4	29.4
Protein	25.9	29.3
Ligand	17.9	26.4
Water	32.7	32.3
r.m.s.d in bond length (Å)[c]	0.008	0.009
r.m.s.d in bond angles (°)	1.28	1.34

[a] $R_{sym} = \Sigma|I_{avg} - I_j|/\Sigma I_j$, where I_j is the observed intensity for the jth measurement and I_{avg} is the average intensity of all measurements.
[b] $R_{factor} = \Sigma|F_o - F_c|/\Sigma F_o$, where F_o and F_c are observed and calculated structure factors, respectively, R_{free} was calculated from a randomly chosen 5% of reflections excluded from the refinement, and R_{factor} was calculated from the remaining 95% of reflections.
[c] r.m.s.d. is the root-mean-square deviation from ideal geometry.

(C-lobe) comprises mainly α-helices. While maintaining the overall structural fold of canonical protein kinases, the structure reveals a few notable non-canonical characteristics at the active site. The most evident difference is in the activation loop, which normally starts from DFG (Asp-Phe-Gly) and ends with APE (Ala-Pro-Glu). TYK2 JH2 presents a shorter activation loop of 17 residues as compared with 25 residues in TYK2 JH1 and 27 residues in phosphorylase kinase (PHK) (PDB code: 2PHK). The activation loop is unphosphorylated, but well ordered, and forms an unusual two-turn α-helix (αAL: residues 769–775) toward the C terminus. The residues in αAL of TYK2 JH2 correspond to the so-called P+1 loop in canonical kinases. This loop forms the substrate-binding groove and allows positioning of the exogenous substrate's Ser/Thr/Tyr residue next to the γ-phosphate of ATP (Fig. 3*B*). The next notable difference in TYK2 JH2 is a longer β7-β8 loop of 9 residues as compared with 4 and 5 residues in TYK2 JH1 and PHK, respectively. The function of this extended loop is unclear.

Similar to canonical protein kinases, ATP-γS in JH2 binds in the cleft between the N- and C-lobes with the adenine ring forming hydrogen bond interactions to the hinge linker. There are, however, a few distinct differences. The phosphate groups are sandwiched between the glycine-rich loop (G-loop) and the catalytic loop with a signature motif of HGN instead of HRD. A single metal ion coordinates the oxygen atoms from all three phosphate groups of ATP (Fig. 3*C*), instead of two metal ions in canonical kinases that coordinate α- and γ- and β- and γ-phosphate groups, respectively. The catalytic lysine Lys^{642} (β3) engages the β-phosphate of ATP-γS and forms a salt bridge with Asp^{759} of the DPG motif. The conformation of the HGN catalytic loop in TYK2 JH2 shows hardly any changes compared with the typical HRD loop, with Asn^{734} positioning close to the γ-phosphate group. Thus, despite some critical residue differences, the ATP-binding site of TYK2 JH2 supports all key interactions to accommodate ATP binding, but via a non-canonical binding mode, which is highly similar to that of JAK2 JH2 (13).

JH2 of TYK2 adopts a closed conformation, with the two lobes closed in on each other and the αC helix rotated inward. Such a conformation is regarded as the "active conformation" in canonical protein kinases and is usually maintained by a salt bridge between the catalytic lysine and an invariant acidic residue (Asp/Glu) from αC. In TYK2 JH2, however, this interaction is abolished because the acidic residue is replaced by a threonine (Thr^{658}). Instead, TYK2 JH2 exploits two unique interactions to hold the closed domain conformation via αC, *i.e.* Thr^{658} (αC) donating a hydrogen bond to the carbonyl of Gly^{761} of the DPG and Tyr^{656} (αC) making a hydrogen bond with Asn^{683} (β5) (Fig. 3*D*).

In addition, the structure shows that the extra αAL in the activation loop plays an important role for the closed conformation in TYK2 JH2. Residues from the αAL bridge to both the G-loop in the N-lobe and helix αG in the C-lobe through a network of salt bridges and hydrogen bond interactions (Fig. 3*E*). The G-loop and αAL are pulled together by a salt bridge between Arg^{600} (G-loop) and Glu^{771} (αAL). On the other side, both ends of the helix αAL are anchored to the nearby helix αG through electrostatic interactions. The N-terminal end of αAL is bridged to αG through a salt bridge between Glu^{824} (αG) and Arg^{769} (αAL), and the C-terminal end of αAL engages in hydrogen bond interactions with Lys^{823} (αG) through the carbonyls of Glu^{774} and Ile^{776} in αAL.

Comparison of JH2 Structures—Comparison with the recently published crystal structures of the JAK1 and JAK2 JH2s (13, 14) shows that TYK2 JH2 adopts a nearly identical fold and many similar structural features. These include the non-canonical ATP binding mode with one metal ion in JAK2 (13), and in both JAK1 and JAK2 a short activation loop with a helix αAL substituting the typical P+1 loop, as well as a closed conformation that is not maintained by the conventional Lys (β3)-Glu (αC) salt bridge. Unexpectedly, sequence alignment of all four JAK JH2s (Fig. 4*A*) and comparison of the three JH2 structures reveal that some of the structural similarities between JAK2 and TYK2 JH2s actually originate from distinct molecular interactions. In the JAK2 JH2 structure (13), Arg^{715} (αAL) makes a hydrogen-bonding interaction with Thr^{555} (G-loop), which keeps JAK2 JH2 in a closed conformation and ready for catalytic activity. Such an interaction is lacking in TYK2 JH2 as the corresponding Arg^{775} and Thr^{599} are 3.7 Å apart. Instead, αAL and the G-loop in TYK2 JH2 are brought together by the Glu^{771} (αAL)-Arg^{600} (G-loop) salt bridge, which in JAK2 is substituted with a hydrophobic interaction with the corresponding residues being Ile^{771} (αAL) and Phe^{566} (G-loop) (Fig. 4*B*). Furthermore, the interactions that link αAL and αG in TYK2 JH2 are significantly impaired in JAK2 JH2. Although Lys^{823} (and thus the interaction with Ile^{776} and Glu^{774} backbones) of TYK2 JH2

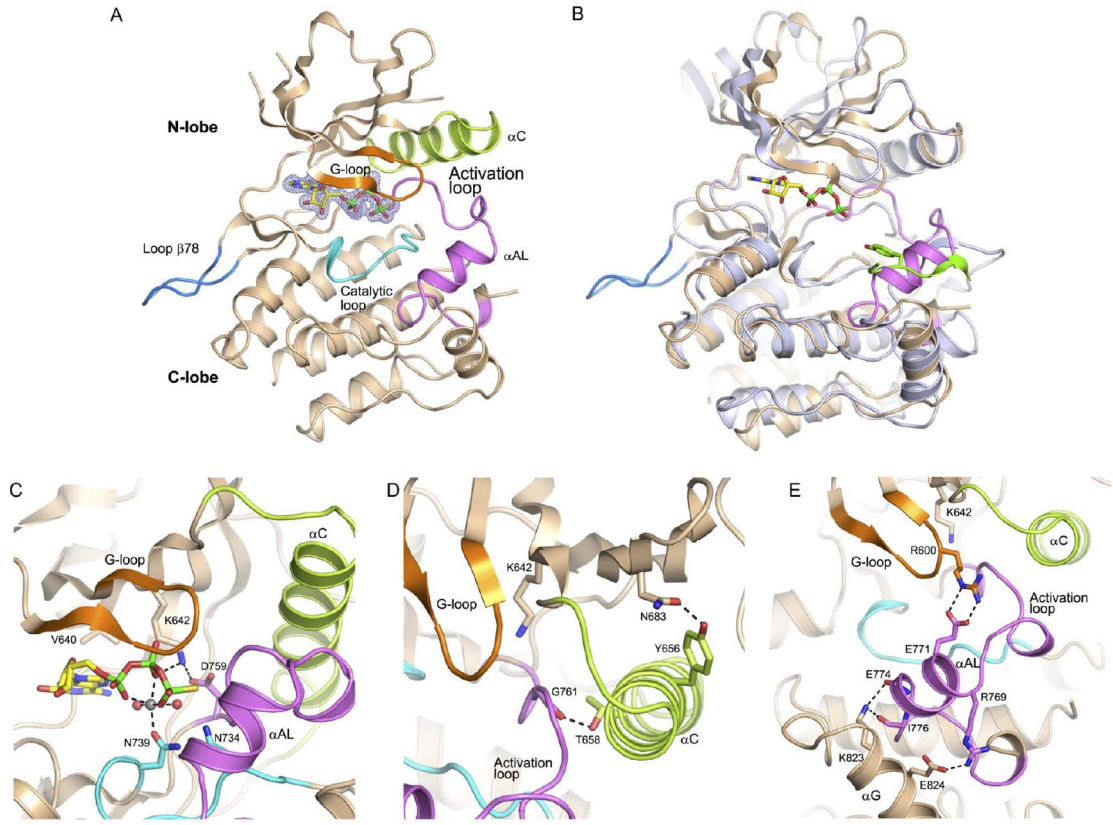

FIGURE 3. **Crystal structure of TYK2 JH2 in complex with ATP-γS.** *A*, overall structure of the TYK2 pseudokinase domain. The protein is shown in graphic representation with the activation loop highlighted in *violet*, αC helix in *green*, G-loop in *orange*, catalytic loop in *cyan*, and loop β8-β9 in *blue*. ATP-γS is shown in sticks in atomic color scheme with *yellow* for carbon, *red* for oxygen, *blue* for nitrogen, *light yellow* for sulfur, and *green* for phosphor, and the metal ion is shown as a *gray sphere*. The electron density map ($F_o - F_c$, contoured at 3σ calculated with ATP-γS omitted in the model) is shown in mesh. *B*, superposition of the structure of insulin receptor tyrosine kinase structure (*light blue*) in complex with ATP and a substrate peptide (*green*) onto TYK2 JH2. *C*, close-up view of the phosphate-binding site. *D*, close-up view of the helix αC area. *E*, close-up view of the helix αAL site in the activation loop.

is conserved in all JAK JH2s, neither Glu^{824} (αG) nor Arg^{769} (αAL) in the salt bridge between αAL and αG is conserved in JAK2 JH2. The corresponding residues in JAK2 are Leu^{763} (αG) and Lys^{709} (αAL). Thus, as a result of the interactions described above (especially the two salt bridges), αAL of TYK2 JH2 is not only in the closed conformation but also in a highly stable state that is unlikely to tolerate any conformational changes. The closed αC conformation in TYK2 JH2 is further strengthened by two hydrogen bond interactions, neither of which, *i.e.* Thr^{658} (αC) to Gly^{761} (DPG) and Tyr^{656} (αC) to Asn^{683} (β5), is present in the JAK2 JH2 structure.

The two salt bridges between αAL-G-loop (Glu^{571}–Arg^{594}) and αAL-αG (Arg^{749}–Glu^{803}) observed in TYK2 JH2 are also present in the JAK1 JH2 structure (14), indicating that αAL is also probably very stable in JAK1 JH2 (Fig. 4*B*). However, the two hydrogen bond interactions between αC to DPG and β5 in TYK2 JH2 (Fig. 3*D*) are absent in JAK1 JH2 because the corresponding residues to Tyr^{656} and Thr^{658} in αC of TYK2 JH2 are Phe^{636} and Ala^{638}, respectively.

Inhibitor Binding to the ATP Pocket—Because the ATP-binding site in TYK2 JH2 maintains all critical nucleotide binding interactions despite sequence differences compared with canonical kinases, we tested whether the ATP pocket in TYK2 JH2 is accessible to an ATP-competitive inhibitor. Using the crystal structure of TYK2 JH2, we performed an *in silico* screen against an Amgen internal kinase inhibitor library. A panel of compounds was identified as possible TYK2 JH2 binders. One such pyrazine compound showed binding to TYK2 JH2 with a K_d of 0.25 μM (Fig. 5*A*). We co-crystallized this pyrazine compound with TYK2 JH2 and solved the structure to 2.15 Å. The pyrazine compound adopts a U-shape pose in the ATP-binding pocket (Fig. 5*B*) with the pyrazine nitrogen atom forming a hydrogen bond interaction with the hinge residue Val^{690}, reminiscent of the adenosine hinge interaction. The piperidine reaches deep into the ATP-binding pocket, and its nitrogen atom forms a water-mediated hydrogen bond interaction with the gatekeeper residue Thr^{687}. The indole group sits underneath the β2 strand and is stabilized by an edge-to-face interaction with Pro^{694}. The inhibitor-bound co-crystal structure suggests that despite a non-canonical ATP binding mode, the ATP-binding site of TYK2 JH2 maintains the scaffold needed to bind ATP competitive inhibitors.

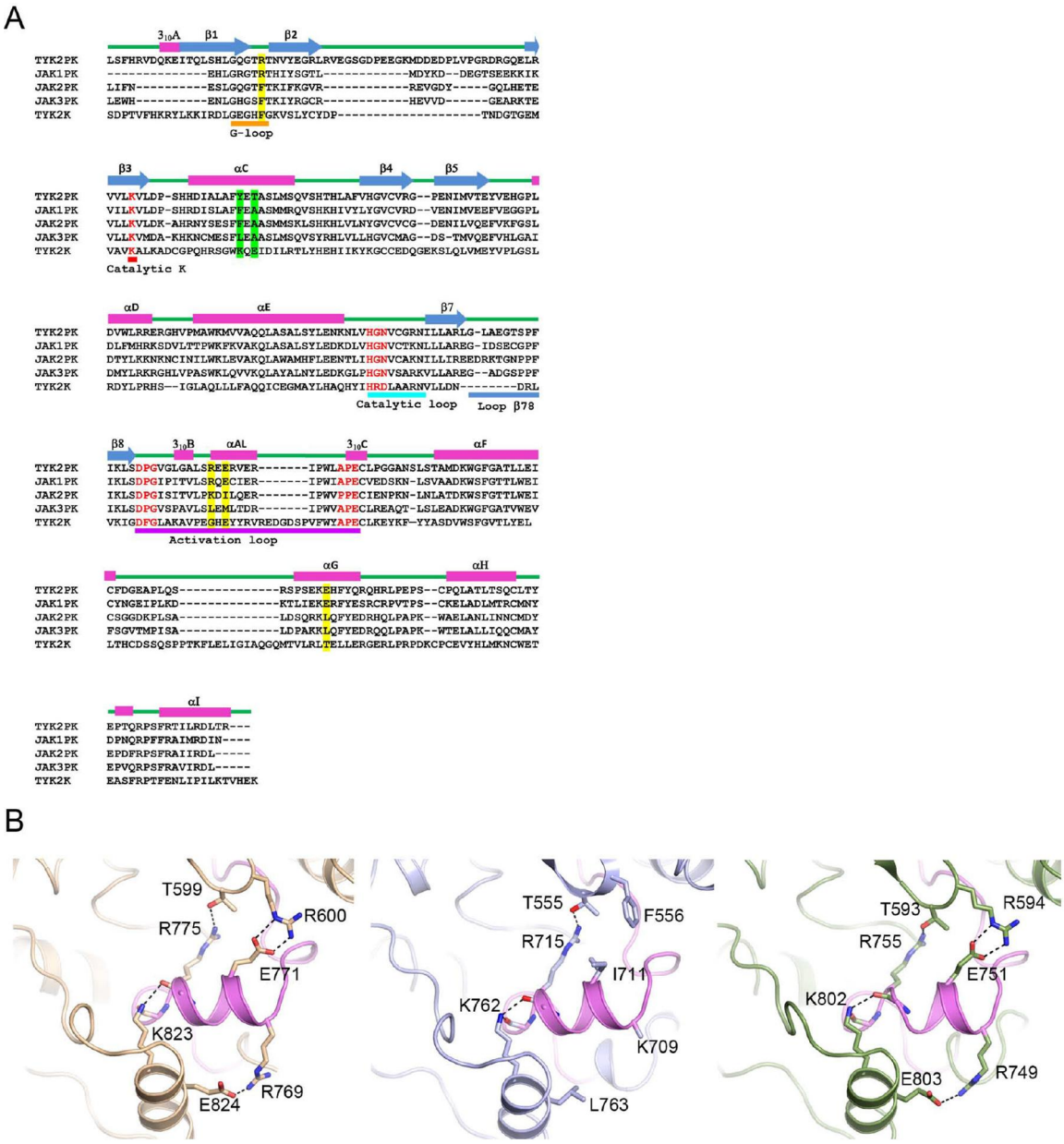

FIGURE 4. **Comparison of TYK2 JH2 with other JAK pseudokinase domains.** *A*, sequence alignment of JAK JH2s. *B*, comparison of key interactions around helix αAL in JH2s of TYK2 (*left panel*), JAK2 (*middle panel*, PDB code: 4FVP), and JAK1 (*right panel*, PDB code: 4L00).

Discussion

The structure of TYK2 JH2 shows that its overall structural characteristics closely resemble those of JAK1 and JAK2 JH2. Both structural and biochemical data showed that TYK2 JH2 is able to bind ATP, but we did not detect phosphotransfer activity. The structure and sequence comparison of TYK2 JH2 with JAK2 JH2, a pseudokinase reported to possess catalytic activity, and the recently reported JAK1 JH2, also devoid of phosphotransfer activity, allowed us to inspect the determinants for kinase/pseudokinase catalytic activity.

In canonical kinases, the closed position of helix αC presents one of the hallmarks for the active state of a kinase where an invariant Glu residue forms a salt bridge with the catalytic Lys, which also binds to the phosphate groups of ATP. In the three JAK pseudokinases compared here, the invariant Glu is substituted by other residues. Instead, the catalytic Lys finds the Asp

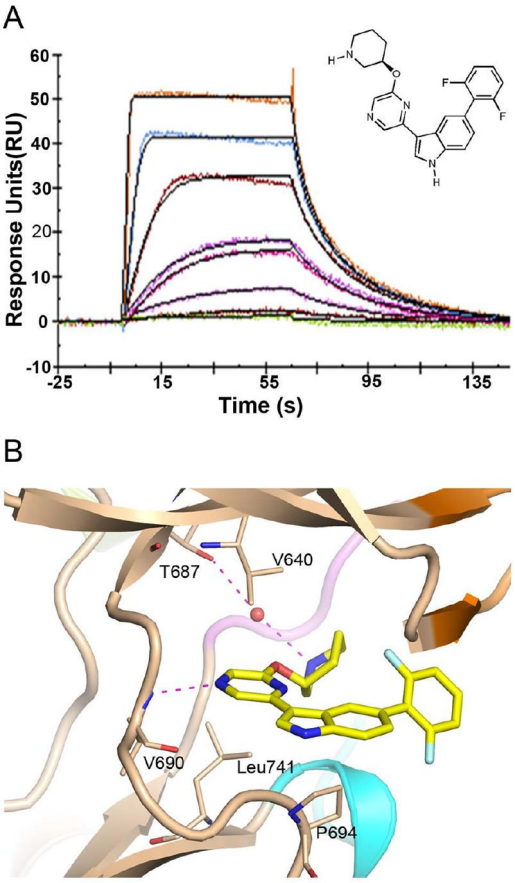

FIGURE 5. **A small molecule inhibitor binding to TYK2 JH2.** *A*, chemical structure of the pyrazine inhibitor and surface plasmon resonance sensorgram of the pyrazine inhibitor binding to TYK2 JH2. *B*, molecular interactions of the pyrazine inhibitor in the ATP-binding pocket in TYK2 JH2.

in the DPG or DFG motif of the activation loop as an alternative salt bridge partner, as well as binding to a phosphate group of ATP. Thus, the position of αC is likely to be less critical for potential catalytic reactions. This is further supported by the structure of ErbB3 pseudokinase in which the αC is pushed outward, yet the protein can still catalyze phosphoryl transfer (17). Another critical residue in the phosphorylation reaction is the catalytic base Asp, which facilitates the phosphoryl transfer in canonical kinases. However, all JAK and ErbB3 pseudokinases have an Asp-to-Asn substitution here, and an alternative phosphoryl transfer pathway has been proposed for ErbB3 that would not require the catalytic base for catalytic activity (17). Thus, the incompetent catalytic residue features *per se* do not appear to account for the different catalytic activity of JAK2 and ErbB3 *versus* TYK2 and JAK1 pseudokinases.

Besides the actual phosphoryl transfer reaction, orientation of the substrate is the first pivotal step in a kinase reaction. The P+1 loop of the activation loop together with helix αG provide a platform for the substrate to bind and position the hydroxyl moiety of Ser, Thr, or Tyr close to the γ-phosphate of ATP. All three JAK JH2s substitute the P+1 loop by a helix αAL, which blocks proper positioning of the substrate for catalysis, especially the N-terminal part of the helix αAL. To allow the substrate to access the catalytic site, αAL is required to make a movement or conformational change. Remarkably, the αAL of TYK2 JH2 as well as JAK1 JH2 has two additional salt bridges, which anchor to the nearby αG and G-loop, offering αAL in TYK2 and JAK1 JH2s superb stability. Both of these salt bridges are lacking in JAK2 JH2. These results suggest that the αAL might act as a "substrate gate" in JAK JH2s. Although this substrate gate in TYK2 JH2 as well JAK1 JH2 is tightly closed due to the two salt bridges anchoring the αAL at the N-terminal end, the gate is more susceptible to opening in JAK2 JH2, allowing the substrate entrance and thus enabling the catalytic activity of JAK2 JH2. The characteristic of αAL in ErbB3 further supports this model where the C-terminal end of αAL interacts with αG and hydrogen-bonds to the loop αF-αG. Thus, the substrate gate in ErbB3 is largely, if not completely open, and no major conformational changes are required for the substrate to enter.

The structure of TYK2 JH2, as well as its comparison with JAK1 and JAK2 JH2, provides insights into the function of this domain in the regulation of JAK activity and cytokine signaling. The three JH2s share the ATP binding property, and in TYK2 as well as in JAK2 (40), it appears to be required for structural stabilization and supports a conformation that provides regulation for controlled cytokine signaling. The recently reported crystal structure of TYK2 and molecular model of JAK2 pseudokinase-kinase domains suggested an autoinhibitory mechanism for the pseudokinase domain in JAK kinases (16, 41). The structural stability of JH2 appears to be of critical importance for its allosteric or scaffolding function in maintaining the tyrosine kinase domain in an inactive conformation. In line with these data, ATP binding to TYK2 JH2 increased the thermal stability but did not result in major structural alterations. The increase of T_m by 4 °C is consistent with the micromolar affinity of ATP. In a previous study of analyzing nucleotide binding properties of pseudokinases, ATP binding was not found to significantly affect the thermal stability of TYK2 JH2 (42). Such variations could be due to the differences in protein construct design, protein purification procedure, and ATP concentration used in the assay. Our purification procedure was very rigorous to generate pure and homogenous protein for crystallization. We also observed that the T_m of TYK2 JH2 increased at ATP concentrations up to 1 mM, whereas in the previous study, a concentration of 200 μM ATP was used.

The structure of TYK2 JH2 allows analysis of previously identified clinical and functional mutations. Screening of a TYK2 cDNA library containing randomly mutated JH2 sequences identified four loss-of-function JH2 mutations (V584D, G596V, H669P, and R856G) with different effects on TYK2 (27). V584D and G596V mutants were able to convey sensitivity to high doses of IFNα to TYK2-null cells with slightly elevated basal phosphorylation for V584D and virtually no change in G596V phosphorylation. H669P and R856G, on the other hand, showed no TYK2-mediated signaling but were heavily phosphorylated even in the basal state. Val^{584} is located before sheet β1 and is an integral part of the hydrophobic core

of the β-sheet region of the N-lobe, a region that was recently also found to harbor a disease-associated TYK2 variant I684S (β5-strand). This variant is also competent for IFNα signaling, although TYK2 JH1 kinase activity seems impaired (28). Gly^{596} is the first invariant glycine in the G-loop. Given that TYK2 JH2 is able to bind nucleotides, and the importance of the G-loop for nucleotide binding, the reported deleterious effects of the G596V mutation are likely mediated by changes in ATP binding to JH2.

Interestingly, the αC helix and its surrounding residues (especially Phe^{655} and Tyr^{656}) in TYK2 JH2 are perfectly poised to support structural changes as seen in the V617F mutation in JAK2 JH2. Moreover, the homologous mutation has been shown to lead to constitutive activation in both TYK2 (V678F) and JAK1 (V658F), suggesting a common mechanism of activation for JAK1, JAK2, and TYK2 mutants (25, 43). These data, together with mutation information from *in vivo* models, validates systematic analysis of JAK JH2 mutations in human diseases.

In summary, the structure of TYK2 JH2, as well as its comparison with JAK1 and JAK2 JH2, provides novel insights into the function of this domain in the regulation of JAK activity and cytokine signaling. All three JH2s bind ATP, which appears to be required for structural stabilization and controlled cytokine signaling at least in TYK2 and JAK2. Structural comparison with the catalytically active JAK2 and ErbB3 pseudokinases identified the helix αAL in the activation loop as a substrate gate that is likely to control substrate binding and thus the catalytic activity in JAK JH2s. Based on this comparative analysis, we could separate the JAK JH2s into catalytically active JAK2 and catalytically incompetent TYK2 and JAK1. The catalytic activity of JAK2 JH2 is low and functions to phosphorylate two regulatory residues involved in JAK2 regulation. These regulatory sites are not conserved in other JAK kinases, and the regulation likely relates to the unique property of JAK2 to mediate signaling as a homodimer (for example, in EpoR, TpoR, and GHR) as compared with the other JAK1 and TYK2 that rely on interaction with another JAK member for signaling. Thus, the determinants for the catalytic activity, and in the case of TYK2 JH2 for catalytic incompetence, appear to rely on three characteristics: low inherent ATP hydrolysis activity, closed rigid substrate gate, and lack of suitable substrate residues.

Key findings of our study are the stabilizing function of ATP for TYK2 JH2 and the druggability of the ATP-binding pocket. The previously reported structures of TYK2 JH2 bound to inhibitor (PDB codes: 3ZON, 4OLI, and 4WOV) are overall very similar to our ATP- and inhibitor-bound structures. Tokarski *et al.* (44) described a compound that binds the JH2 ATP pocket and specifically inhibits cytokine receptor-induced TYK2 signaling. However, the authors did not detect ATP binding and concluded that the pocket could not accommodate ATP (15). Our biochemical, calorimetric, and structural results show that TYK2 JH2 binds ATP, which furthermore has an important stabilizing function for the domain and the regulation of TYK2 activity. Thus, ATP competitive compounds may provide means to specifically target TYK2 JH2 in autoimmune and inflammatory diseases.

Author Contributions—X. M., C. G., N. W., O. S., and Z. W. coordinated the study and wrote the paper. X. M., D. U., S. M., H. H., S. T., E.-K. H., M. A., B. G., J. E., O. S., and Z. W. designed, performed, analyzed the experiments. All authors reviewed the results and approved the final version of the manuscript.

Acknowledgments—We thank Tuija Pekkala, Juha Saarikettu, Yashavanthi Niranjan, Clifford Young, and Ole N. Jensen for experimental contribution and Paula Kosonen, Merja Lehtinen, and Elina Koskenalho for technical assistance. We also thank Michal Hammel and Gregory Hura at the SIBYLS beamline at ALS for data collection and analysis of the SAXS experiments. The ALS is supported by the U. S. Department of Energy under Contract DE-AC03-76SF00098 at the Lawrence Berkeley National Laboratory.

References

1. Karaghiosoff, M., Neubauer, H., Lassnig, C., Kovarik, P., Schindler, H., Pircher, H., McCoy, B., Bogdan, C., Decker, T., Brem, G., Pfeffer, K., and Müller, M. (2000) Partial impairment of cytokine responses in Tyk2-deficient mice. *Immunity* **13,** 549–560
2. Shimoda, K., Kato, K., Aoki, K., Matsuda, T., Miyamoto, A., Shibamori, M., Yamashita, M., Numata, A., Takase, K., Kobayashi, S., Shibata, S., Asano, Y., Gondo, H., Sekiguchi, K., Nakayama, K., Nakayama, T., Okamura, T., Okamura, S., Niho, Y., and Nakayama, K. (2000) Tyk2 plays a restricted role in IFN α signaling, although it is required for IL-12-mediated T cell function. *Immunity* **13,** 561–571
3. Velazquez, L., Fellous, M., Stark, G. R., and Pellegrini, S. (1992) A protein tyrosine kinase in the interferon α/β signaling pathway. *Cell* **70,** 313–322
4. Gauzzi, M. C., Velazquez, L., McKendry, R., Mogensen, K. E., Fellous, M., and Pellegrini, S. (1996) Interferon-α-dependent activation of Tyk2 requires phosphorylation of positive regulatory tyrosines by another kinase. *J. Biol. Chem.* **271,** 20494–20500
5. Richter, M. F., Duménil, G., Uzé, G., Fellous, M., and Pellegrini, S. (1998) Specific contribution of Tyk2 JH regions to the binding and the expression of the interferon α/β receptor component IFNAR1. *J. Biol. Chem.* **273,** 24723–24729
6. Velazquez, L., Mogensen, K. E., Barbieri, G., Fellous, M., Uzé, G., and Pellegrini, S. (1995) Distinct domains of the protein tyrosine kinase tyk2 required for binding of interferon-α/β and for signal transduction. *J. Biol. Chem.* **270,** 3327–3334
7. Strobl, B., Stoiber, D., Sexl, V., and Mueller, M. (2011) Tyrosine kinase 2 (TYK2) in cytokine signalling and host immunity. *Front. Biosci.* **16,** 3214–3232
8. Sanda, T., Tyner, J. W., Gutierrez, A., Ngo, V. N., Glover, J., Chang, B. H., Yost, A., Ma, W., Fleischman, A. G., Zhou, W., Yang, Y., Kleppe, M., Ahn, Y., Tatarek, J., Kelliher, M. A., Neuberg, D. S., Levine, R. L., Moriggl, R., Müller, M., Gray, N. S., Jamieson, C. H., Weng, A. P., Staudt, L. M., Druker, B. J., and Look, A. T. (2013) TYK2-STAT1-BCL2 pathway dependence in T-cell acute lymphoblastic leukemia. *Cancer Discov.* **3,** 564–577
9. Tomasson, M. H., Xiang, Z., Walgren, R., Zhao, Y., Kasai, Y., Miner, T., Ries, R. E., Lubman, O., Fremont, D. H., McLellan, M. D., Payton, J. E., Westervelt, P., DiPersio, J. F., Link, D. C., Walter, M. J., Graubert, T. A., Watson, M., Baty, J., Heath, S., Shannon, W. D., Nagarajan, R., Bloomfield, C. D., Mardis, E. R., Wilson, R. K., and Ley, T. J. (2008) Somatic mutations and germline sequence variants in the expressed tyrosine kinase genes of patients with *de novo* acute myeloid leukemia. *Blood* **111,** 4797–4808
10. Yamaoka, K., Saharinen, P., Pesu, M., Holt, V. E., 3rd, Silvennoinen, O., and O'Shea, J. J. (2004) The Janus kinases (Jaks). *Genome Biol.* **5,** 253
11. Boudeau, J., Miranda-Saavedra, D., Barton, G. J., and Alessi, D. R. (2006) Emerging roles of pseudokinases. *Trends Cell Biol.* **16,** 443–452
12. Zeqiraj, E., and van Aalten, D. M. (2010) Pseudokinases: remnants of evolution or key allosteric regulators? *Curr. Opin. Struct. Biol.* **20,** 772–781
13. Bandaranayake, R. M., Ungureanu, D., Shan, Y., Shaw, D. E., Silvennoinen, O., and Hubbard, S. R. (2012) Crystal structures of the JAK2 pseudokinase domain and the pathogenic mutant V617F. *Nat. Struct. Mol. Biol.* **19,**

754–759
14. Lai, S. Y., Xu, W., Gaffen, S. L., Liu, K. D., Longmore, G. D., Greene, W. C., and Goldsmith, M. A. (1996) The molecular role of the common γc subunit in signal transduction reveals functional asymmetry within multimeric cytokine receptor complexes. *Proc. Natl. Acad. Sci. U.S.A.* **93,** 231–235
15. Bream, J. H., Hodge, D. L., Gonsky, R., Spolski, R., Leonard, W. J., Krebs, S., Targan, S., Morinobu, A., O'Shea, J. J., and Young, H. A. (2004) A distal region in the interferon-γ gene is a site of epigenetic remodeling and transcriptional regulation by interleukin-2. *J. Biol. Chem.* **279,** 41249–41257
16. Goldsmith, M. A., Mikami, A., You, Y., Liu, K. D., Thomas, L., Pharr, P., and Longmore, G. D. (1998) Absence of cytokine receptor-dependent specificity in red blood cell differentiation *in vivo*. *Proc. Natl. Acad. Sci. U.S.A.* **95,** 7006–7011
17. Shi, F., Telesco, S. E., Liu, Y., Radhakrishnan, R., and Lemmon, M. A. (2010) ErbB3/HER3 intracellular domain is competent to bind ATP and catalyze autophosphorylation. *Proc. Natl. Acad. Sci. U.S.A.* **107,** 7692–7697
18. Ungureanu, D., Wu, J., Pekkala, T., Niranjan, Y., Young, C., Jensen, O. N., Xu, C. F., Neubert, T. A., Skoda, R. C., Hubbard, S. R., and Silvennoinen, O. (2011) The pseudokinase domain of JAK2 is a dual-specificity protein kinase that negatively regulates cytokine signaling. *Nat. Struct. Mol. Biol.* **18,** 971–976
19. Saharinen, P., Takaluoma, K., and Silvennoinen, O. (2000) Regulation of the Jak2 tyrosine kinase by its pseudokinase domain. *Mol. Cell. Biol.* **20,** 3387–3395
20. Saharinen, P., Vihinen, M., and Silvennoinen, O. (2003) Autoinhibition of Jak2 tyrosine kinase is dependent on specific regions in its pseudokinase domain. *Mol. Biol. Cell* **14,** 1448–1459
21. Saharinen, P., and Silvennoinen, O. (2002) The pseudokinase domain is required for suppression of basal activity of Jak2 and Jak3 tyrosine kinases and for cytokine-inducible activation of signal transduction. *J. Biol. Chem.* **277,** 47954–47963
22. Baxter, E. J., Scott, L. M., Campbell, P. J., East, C., Fourouclas, N., Swanton, S., Vassiliou, G. S., Bench, A. J., Boyd, E. M., Curtin, N., Scott, M. A., Erber, W. N., Green, A. R., and Cancer Genome Project (2005) Acquired mutation of the tyrosine kinase JAK2 in human myeloproliferative disorders. *Lancet* **365,** 1054–1061
23. Kralovics, R., Passamonti, F., Buser, A. S., Teo, S. S., Tiedt, R., Passweg, J. R., Tichelli, A., Cazzola, M., and Skoda, R. C. (2005) A gain-of-function mutation of JAK2 in myeloproliferative disorders. *N. Engl. J. Med.* **352,** 1779–1790
24. Levine, R. L., Loriaux, M., Huntly, B. J., Loh, M. L., Beran, M., Stoffregen, E., Berger, R., Clark, J. J., Willis, S. G., Nguyen, K. T., Flores, N. J., Estey, E., Gattermann, N., Armstrong, S., Look, A. T., Griffin, J. D., Bernard, O. A., Heinrich, M. C., Gilliland, D. G., Druker, B., and Deininger, M. W. (2005) The JAK2V617F activating mutation occurs in chronic myelomonocytic leukemia and acute myeloid leukemia, but not in acute lymphoblastic leukemia or chronic lymphocytic leukemia. *Blood* **106,** 3377–3379
25. Staerk, J., Kallin, A., Demoulin, J. B., Vainchenker, W., and Constantinescu, S. N. (2005) JAK1 and Tyk2 activation by the homologous polycythemia vera JAK2 V617F mutation: cross-talk with IGF1 receptor. *J. Biol. Chem.* **280,** 41893–41899
26. Macchi, P., Villa, A., Giliani, S., Sacco, M. G., Frattini, A., Porta, F., Ugazio, A. G., Johnston, J. A., Candotti, F., O'Shea, J. J., *et al.* (1995) Mutations of Jak-3 gene in patients with autosomal severe combined immune deficiency (SCID). *Nature* **377,** 65–68
27. Yeh, T. C., Dondi, E., Uze, G., and Pellegrini, S. (2000) A dual role for the kinase-like domain of the tyrosine kinase Tyk2 in interferon-α signaling. *Proc. Natl. Acad. Sci. U.S.A.* **97,** 8991–8996
28. Li, Z., Gakovic, M., Ragimbeau, J., Eloranta, M. L., Rönnblom, L., Michel, F., and Pellegrini, S. (2013) Two rare disease-associated Tyk2 variants are catalytically impaired but signaling competent. *J. Immunol.* **190,** 2335–2344
29. Leslie, A. G. W., and Powell, H. R. (2007) Processing diffraction data with mosflm. in *Evolving methods for macromolecular crystallography* (Read, R. J., and Sussman, J. L., eds.), Vol. 245, pp. 41–51, Springer, Dordrecht, The Netherlands
30. McCoy, A. J., Grosse-Kunstleve, R. W., Adams, P. D., Winn, M. D., Storoni, L. C., and Read, R. J. (2007) Phaser crystallographic software. *J. Appl. Crystallogr.* **40,** 658–674
31. Emsley, P., and Cowtan, K. (2004) Coot: model-building tools for molecular graphics. *Acta Crystallogr. D Biol. Crystallogr.* **60,** 2126–2132
32. Murshudov, G. N., Vagin, A. A., and Dodson, E. J. (1997) Refinement of macromolecular structures by the maximum-likelihood method. *Acta Crystallogr. D Biol. Crystallogr.* **53,** 240–255
33. Collaborative Computational Project, Number 4 (1994) The CCP4 suite: programs for protein crystallography. *Acta Crystallogr. D Biol. Crystallogr.* **50,** 760–763
34. Ten Eyck, L. F., Taylor, S. S., and Kornev, A. P. (2008) Conserved spatial patterns across the protein kinase family. *Biochim. Biophys. Acta* **1784,** 238–243
35. Guinier, A., and Fournet, G. (1955) Small-angle scattering of x-rays. Wiley, New York
36. Förster, S., Apostol, L., and Bras, W. (2010) Scatter: software for the analysis of nano- and mesoscale small-angle scattering. *J. Appl. Crystallogr.* **43,** 639–646
37. Zeqiraj, E., Filippi, B. M., Goldie, S., Navratilova, I., Boudeau, J., Deak, M., Alessi, D. R., and van Aalten, D. M. (2009) ATP and MO25α regulate the conformational state of the STRADα pseudokinase and activation of the LKB1 tumour suppressor. *PLoS Biol.* **7,** e1000126
38. Pellegrini, S., John, J., Shearer, M., Kerr, I. M., and Stark, G. R. (1989) Use of a selectable marker regulated by α interferon to obtain mutations in the signaling pathway. *Mol. Cell. Biol.* **9,** 4605–4612
39. Ragimbeau, J., Dondi, E., Vasserot, A., Romero, P., Uzé, G., and Pellegrini, S. (2001) The receptor interaction region of Tyk2 contains a motif required for its nuclear localization. *J. Biol. Chem.* **276,** 30812–30818
40. Liu, K. D., Gaffen, S. L., Goldsmith, M. A., and Greene, W. C. (1997) Janus kinases in interleukin-2-mediated signaling: JAK1 and JAK3 are differentially regulated by tyrosine phosphorylation. *Curr. Biol.* **7,** 817–826
41. Shan, Y., Gnanasambandan, K., Ungureanu, D., Kim, E. T., Hammarén, H., Yamashita, K., Silvennoinen, O., Shaw, D. E., and Hubbard, S. R. (2014) Molecular basis for pseudokinase-dependent autoinhibition of JAK2 tyrosine kinase. *Nat. Struct. Mol. Biol.* **21,** 579–584
42. Murphy, J. M., Zhang, Q., Young, S. N., Reese, M. L., Bailey, F. P., Eyers, P. A., Ungureanu, D., Hammaren, H., Silvennoinen, O., Varghese, L. N., Chen, K., Tripaydonis, A., Jura, N., Fukuda, K., Qin, J., Nimchuk, Z., Mudgett, M. B., Elowe, S., Gee, C. L., Liu, L., Daly, R. J., Manning, G., Babon, J. J., and Lucet, I. S. (2014) A robust methodology to subclassify pseudokinases based on their nucleotide-binding properties. *Biochem. J.* **457,** 323–334
43. Gakovic, M., Ragimbeau, J., Francois, V., Constantinescu, S. N., and Pellegrini, S. (2008) The Stat3-activating Tyk2 V678F mutant does not upregulate signaling through the type I interferon receptor but confers ligand hypersensitivity to a homodimeric receptor. *J. Biol. Chem.* **283,** 18522–18529
44. Tokarski, J. S., Zupa-Fernandez, A., Tredup, J. A., Pike, K., Chang, C., Xie, D., Cheng, L., Pedicord, D., Muckelbauer, J., Johnson, S. R., Wu, S., Edavettal, S. C., Hong, Y., Witmer, M. R., Elkin, L. L., Blat, Y., Pitts, W. J., Weinstein, D. S., and Burke, J. R. (2015) Tyrosine kinase 2-mediated signal transduction in T lymphocytes is blocked by pharmacological stabilization of its pseudokinase domain. *J. Biol. Chem.* **290,** 11061–11074

ATP binding to the pseudokinase domain of JAK2 is critical for pathogenic activation

Henrik M. Hammarén[a], Daniela Ungureanu[a], Jean Grisouard[b], Radek C. Skoda[b], Stevan R. Hubbard[c,d], and Olli Silvennoinen[a,e,1]

[a]School of Medicine, University of Tampere, FI-33014 Tampere, Finland; [b]Department of Biomedicine, Experimental Hematology, University Hospital Basel, CH-4031 Basel, Switzerland; [c]Kimmel Center for Biology and Medicine at the Skirball Institute and [d]Department of Biochemistry and Molecular Pharmacology, New York University School of Medicine, New York, NY 10016; and [e]Clinical Hematology, Department of Internal Medicine, Tampere University Hospital, FI-33520 Tampere, Finland

Edited by Joseph Schlessinger, Yale University School of Medicine, New Haven, CT, and approved March 12, 2015 (received for review December 4, 2014)

Pseudokinases lack conserved motifs typically required for kinase activity. Nearly half of pseudokinases bind ATP, but only few retain phosphotransfer activity, leaving the functional role of nucleotide binding in most cases unknown. Janus kinases (JAKs) are nonreceptor tyrosine kinases with a tandem pseudokinase–kinase domain configuration, where the pseudokinase domain (JAK homology 2, JH2) has important regulatory functions and harbors mutations underlying hematological and immunological diseases. JH2 of JAK1, JAK2, and TYK2 all bind ATP, but the significance of this is unclear. We characterize the role of nucleotide binding in normal and pathogenic JAK signaling using comprehensive structure-based mutagenesis. Disruption of JH2 ATP binding in wild-type JAK2 has only minor effects, and in the presence of type I cytokine receptors, the mutations do not affect JAK2 activation. However, JH2 mutants devoid of ATP binding ameliorate the hyperactivation of JAK2 V617F. Disrupting ATP binding in JH2 also inhibits the hyperactivity of other pathogenic JAK2 mutants, as well as of JAK1 V658F, and prevents induction of erythrocytosis in a JAK2 V617F myeloproliferative neoplasm mouse model. Molecular dynamic simulations and thermal-shift analysis indicate that ATP binding stabilizes JH2, with a pronounced effect on the C helix region, which plays a critical role in pathogenic activation of JAK2. Taken together, our results suggest that ATP binding to JH2 serves a structural role in JAKs, which is required for aberrant activity of pathogenic JAK mutants. The inhibitory effect of abrogating JH2 ATP binding in pathogenic JAK mutants may warrant novel therapeutic approaches.

JAK | pseudokinase domain | nucleotide binding | cytokine | myeloid neoplasia

The Janus kinases (JAK1–3, TYK2) are a family of nonreceptor tyrosine kinases with essential functions in the regulation of hematopoiesis, the immune system, and cellular metabolism. JAKs interact specifically with various cytokine receptors and couple cytokine binding to cytoplasmic signaling cascades, including the signal transducers and activators of transcription (STAT) pathway. JAKs consist of an N-terminal FERM domain, an SH2-like (Src homology 2) domain, a pseudokinase domain (JAK homology 2, JH2), and the C-terminal tyrosine kinase domain (JH1). JH2 mediates critical regulatory functions in JAKs and primarily serves to inhibit basal JH1 activity. Experimental deletion of JH2 increases JH1 activity in full-length JAK in the absence of stimulation (1–3), and in recombinant systems addition of JH2 suppresses JH1 activity (4–6). JH2 is, however, also required for ligand-induced activation of full-length JAKs in cell (1–3, 6, 7). The regulatory functions of JH2 are corroborated by the multitude of human disease mutations identified in the domain. The most common *JAK2* mutation, V617F, leads to cytokine-independent signaling through the exclusively JAK2-dependent homotypic receptors for erythropoietin (EPO), granulocyte colony stimulating factor (G-CSF), and thrombopoietin (8). The V617F mutation is found in ∼95% of patients with polycythemia vera (PV) (9–12) as well as in ∼60% of patients with essential thrombocythemia (ET) and primary myelofibrosis (PMF). After identification of the V617F mutation, a multitude of other mutations in JAK2, JAK1, and JAK3 have been found that are linked to myeloid and lymphoid malignancies and to immunological diseases as well as to some solid cancers (13, 14). The mutations cluster mainly in exon 12 in the SH2–JH2 linker (numbering for human *JAK2*), exon 14 near Val617, and exon 16 (13). Although most JAK JH2 mutations are gain-of-function, some JH2 mutations in JAK3 suppress JH1 activity, leading to severe combined immunodeficiency (2, 15).

The mechanism by which JH2 regulates JAK activity has long been enigmatic, but recent studies have provided previously unidentified insights. The crystal structure of JAK2 JH2 (16) revealed a prototypical kinase-domain fold that binds ATP (17), but with a noncanonical binding mode. Additionally, JAK2 JH2 was found to possess weak kinase activity in vitro and autophosphorylate two regulatory sites: Ser523 in the SH2–JH2 linker and Tyr570 in JH2 itself (17). The structure of JAK2 JH2 V617F is highly similar to wild-type JH2 but shows a rigidified C helix (αC) in the kinase N lobe and a slightly altered ATP binding cleft (16). These structural differences, however, do not provide an obvious explanation for the mechanism of pathogenic activation. A recent simulation-based model of the JAK2 tandem kinase domains (JH2–JH1) (18) and a crystal structure of TYK2 JH2–JH1 (5) show an extensive interaction interface between JH2 and the backside of JH1, providing a rationale for the autoinhibitory interaction mediated by JH2. Importantly, practically all known

Significance

Mutations in the JAK pseudokinase domain are bona fide oncogenic drivers that underlie many myeloproliferative and autoimmune diseases in humans. The *JAK2* V617F mutation is responsible for ∼95% of polycythemia vera and ∼60% of primary myelofibrosis and essential thrombocytosis cases. Currently, developed JAK2 tyrosine kinase inhibitors have not been able to eradicate disease caused by mutated JAK2. The data presented here show that alteration of the ATP binding site of the pseudokinase domain has the potential to suppress JAK hyperactivation caused by pathogenic mutations, with minimal effects on wild-type JAK, thus establishing the ATP binding site of the pseudokinase domain as a potential pharmacological target.

Author contributions: H.M.H., R.C.S., S.R.H., and O.S. designed research; H.M.H. and J.G. performed research; D.U. contributed new reagents/analytic tools; H.M.H. and J.G. analyzed data; and H.M.H., S.R.H., and O.S. wrote the paper.

The authors declare no conflict of interest.

This article is a PNAS Direct Submission.

Freely available online through the PNAS open access option.

[1]To whom correspondence should be addressed. Email: olli.silvennoinen@uta.fi.

This article contains supporting information online at www.pnas.org/lookup/suppl/doi:10.1073/pnas.1423201112/-/DCSupplemental.

disease-causing JH1 and JH2 mutations localize in or near the JH2–JH1 interface and are expected to destabilize the interaction (13, 18). The structures of JAK1 and TYK2 JH2 are highly similar to JAK2 JH2 (5, 19), and all three JH2s bind ATP (20). The regulatory residues Ser523 and Tyr570 in JAK2 are not conserved in other JAK family members, and the catalytic function of JH2 appears to be a unique characteristic of JAK2, which is also the only JAK to function as homodimers on type I cytokine receptors. The conserved function of nucleotide binding in all JAK JH2s, however, is currently unknown.

Research on JH2 also ties into the field of pseudokinases in general. Pseudokinases are kinase-like proteins that lack one or more conserved catalytic residues and constitute almost 10% of the human kinome (21). Many pseudokinases have retained the ability to bind nucleotides, yet the physiological function of this binding has remained unknown in most cases. Deciphering the function of these nucleotide binding sites is of practical importance, as the ATP binding pocket is a well-validated pharmacological target (22). Intrigued by these questions, we set out to investigate the functional role of ATP binding in JAK JH2, focusing on its role in the regulation of JAK2 signaling in wild-type and pathogenic contexts.

Results

Establishing JAK2 JH2 ATP Binding Site Mutations. JAK2 JH2 has an ATP binding pocket with unusual characteristics (Fig. 1*A*) (16).

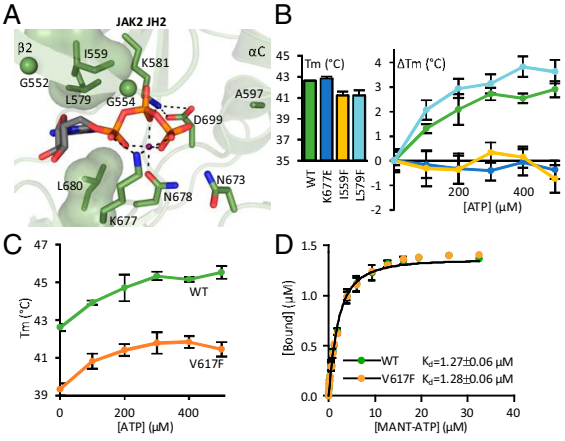

Fig. 1. Characterizing the ATP binding pocket of JAK2 JH2. (*A*) The ATP binding pocket of JAK2 JH2 (16) [Protein Data Bank (PDB) ID code 4FVQ] highlighting the noncanonical mode of nucleotide binding. JAK2 JH2 contains a bulky leucine (Leu579) on the *N*-lobe side of the purine pocket substituting for the canonical alanine in the VAIK motif. The glycine-rich loop consists of two glycines (shown as spheres) rather than three. The phosphates of bound ATP (shown as sticks) are coordinated by only one divalent cation (shown in magenta) instead of two in typical kinases. Furthermore, Asp699 of the DPG motif (consensus DFG) forms a salt bridge to the β3 lysine (Lys581), and Lys677 from the catalytic loop binds directly to the α and γ phosphates of ATP. Dotted lines highlight hydrogen bonds and salt bridges participating in the binding of ATP. The hydrophobic amino acids lining the purine base and sugar moiety binding site are shown as volume-filling models. (*B*) Fluorometric TSA of recombinant JAK2 JH2. Tms of JAK2 JH2 ATP binding site mutants are shown in the bar graph. TSA shows no thermal stabilization for JAK2 JH2 I559F or JAK2 JH2 K677E upon addition of ATP (ΔTm, line graph). (*C*) Thermal stability of recombinant JAK2 JH2 wild type and V617F upon addition of ATP to wild-type and V617F JH2 shows similar ATP responses yet overall reduced thermal stability in V617F. The data for wild type are the same as shown in *B*. (*D*) MANT-ATP binding assay on recombinant JAK2 JH2 reveals identical MANT-ATP binding affinities for wild type and V617F. All experiments were done in the presence of Mg^{2+}. All error bars are standard deviations (SD) from triplicate experiments.

To study the role of nucleotide binding, we used a systematic, structure-based mutagenesis approach designed to distinguish the effect of nucleotide binding from possible structural effects caused by the mutation, as has been observed with, for example, β-strand 3 (β3) lysine mutations (23, 24). We thus mutated not only the β3 lysine (K581A) and its interaction partner (D699A) but also the glycine-rich loop (G552A G554A) residues on the catalytic loop interacting directly with ATP (K677E) or the divalent cation (N678A), as well as residues lining the purine binding pocket (I559F, L579F). To compare the ATP binding site mutations with a structurally destabilizing mutation, we mutated Phe739 to arginine in the hydrophobic core of the C lobe (16) (Table 1).

To verify the effects of the mutations on ATP binding, we produced recombinant JAK2 JH2. Fluorometric thermal-shift analysis (TSA) showed that the mutations K677E, I559F, and L579F have only a marginal effect on the melting temperature (Tm) of apo JH2 (Fig. 1*B*, bar graph). ATP binding-induced stabilization, however, was completely abrogated in K677E and I559F but not in L579F (Fig. 1*B*, line graph). These results indicate that I559F and K677E do not affect the proper folding of the domain but that they effectively block ATP binding. L579F evidently did not prevent ATP binding. The effect of the other mutations described above could not be explicitly analyzed due to lack of recombinant expression (Table 1).

ATP Binding in JAK2 JH2 V617F. The crystal structure of JAK2 JH2 V617F is highly similar to the wild-type structure (16), with small changes in αC and the β3–αC linker and a slight change in the topography of the ATP binding pocket due to alignment of Phe617, Phe595, and Phe594 (the latter two in αC) in V617F (Fig. S1). To gauge whether these differences have any effect on the stability of JH2 and its affinity for ATP, we used TSA and a FRET-based 2′/3′-(*N*-methyl-anthraniloyl)–ATP (MANT-ATP) binding assay on recombinant JAK2 JH2. TSA showed that the V617F mutation lowers the overall thermal stability of the domain (Tm = 39.3 ± 0.3 °C compared with 42.6 ± 0.2 °C for wild type). Addition of Mg-ATP caused similar stabilization for both domains, with Tm shifts of up to 3 °C, which was, however, still not enough to bring the Tm of V617F to the level of wild type (Fig. 1*C*). Quantification of Mg–MANT-ATP binding affinity showed no difference between JAK2 JH2 wild type and V617F, with dissociation constants of 1.3 ± 0.1 μM for both (Fig. 1*D*). Thus, V617F lowers the thermal stability of JH2 but does not substantially affect ATP binding.

Analysis of JAK2 JH2 ATP Binding Site Mutations in the Absence of JAK2-Associated Type I Receptors. The ATP-coordinating residues were mutated in the context of full-length JAK2, and activation was analyzed in transfected JAK2-deficient γ2A cells by measuring JH1 activation-loop phosphorylation (pY1007–pY1008) (Fig. 2). γ2A is a fibroblast cell line and thus lacks expression of JAK2-associated homotypic type I myeloid cytokine receptors (EPOR, MPL, and G-CSF-R). In the context of wild-type JAK2, the JH2 mutations resulted generally in small increases in basal JAK2 activity. Specifically, the verified ATP binding-deficient mutants K677E and I559F showed 1.6- and 1.9-fold increases over wild-type JAK2, whereas the less conservative change K581A caused a larger ∼fivefold increase in pY1007–pY1008 levels, as did the structurally disruptive F739R mutation (Fig. 2).

Next, the different ATP binding site mutations were introduced into full-length JAK2 V617F, and the role of JH2 nucleotide binding on cytokine-independent activation was analyzed. Expression of V617F resulted in >20-fold hyperphosphorylation compared with wild type. Strikingly, almost all ATP binding site mutations reverted the high basal activity of V617F to near wild-type levels (Fig. 2). The inhibition was most prominent in the glycine-rich loop mutant (G552A G554A) and both catalytic loop mutants (N678A, K677E), with pY1007–pY1008 levels nearly wild type (1.4–1.8-fold of wild type). L579F, which did not abrogate ATP binding (Fig. 1*B*), gave the smallest reduction in hyperphosphorylation (Fig. 2). Furthermore, mutation of JH2 autophosphorylation sites (Ser523 and Tyr570) (17) did not lower

BIOCHEMISTRY

Table 1. Summary of JAK2 and JAK1 point mutations used to study the function of the ATP binding site of JH2

Mutation	Rationale/effect	Producible JH2
JAK2		
S523A	Removes Ser523 phosphorylation	—
K539L	Hyperactivating MPN mutation in JH2–JH1 interface (5, 18)	—
G552A G554A	Removes flexible glycines usually needed for ATP binding	No
I559F	β2; designed to sterically inhibit ATP binding; verifiably inhibits ATP binding (Fig. 1*B*)	Yes
I559E	β2; designed to electrostatically inhibit ATP binding	No
Y570F	Removes Tyr570 phosphorylation	—
K581A	Removes β3 lysine needed for ATP binding	No
L579F	β3; designed to sterically inhibit ATP binding; does not inhibit ATP binding (Fig. 1*B*)	Yes
V617F	Hyperactivating MPN mutation	Yes
K677E	Exchanges catalytic loop lysine interacting with α and γ phosphates of ATP with oppositely charged residue; verifiably inhibits ATP binding (Fig. 1*B*)	Yes
N678A	Removes catalytic loop asparagine coordinating binding of cation needed for ATP binding	No
R683S	Hyperactivating MPN mutation directly in JH2–JH1 interface (5, 18)	—
D699A	DFG (DPG in JAK2) motif; disrupts Lys581-Asp699 salt bridge	No
F739R	Designed to disrupt JH2 by introducing charged residue into hydrophobic core of C lobe (16)	No
JAK1		
G590A G592A	Analogous to JAK2(G552A G554A)	—
K622A	Analogous to JAK2(K581A)	—
V658F	Analogous to JAK2(V617F)	—

Constructs not tested for recombinant production are marked with a "—."

V617F hyperactivity (Fig. S2), demonstrating that the suppression of aberrant activation by the JH2 ATP binding mutations is not due to loss of JH2 catalytic activity.

Removal of ATP Binding Is Distinct From Structural Disruption of JH2 and Does Not Affect Type I or Type II Cytokine Receptor Signaling. To assess the effect of JH2 ATP binding site mutations on the cytokine inducibility of JAK2, we coexpressed type I cytokine receptor EPOR, STAT5A, and the JAK2 mutants in γ2A cells. A kinase-inactivating mutation in JH1 (K882A) was included as a control. In the presence of EPOR, the ATP binding site mutations did not increase basal JAK2 activation compared with wild-type JAK2, whereas the destabilizing mutation F739R still caused a marked increase (Fig. 3*A*). This result was also evident in downstream signaling, with anti-pSTAT5A blotting showing low basal STAT5A phosphorylation for the ATP binding site mutants yet increased phosphorylation for F739R (Fig. 3*B*). EPO-induced JAK2 activation and signaling remained essentially unchanged in all ATP site mutants. In contrast, the destabilizing JH2 mutation (F739R) was refractory to EPO stimulation (Fig. 3 *A* and *B*), resembling the effect of JH2 deletion (1, 6, 7).

In addition to homodimeric type I cytokine receptors, JAK2 functions on type II cytokine receptors where signaling relies on *trans*-activation of two different JAKs. We thus analyzed activation of STAT1 through the interferon γ (IFNγ) receptor in γ2A cells. Congruent with the effect observed on pJAK2, basal pSTAT1 was increased in K581A, whereas the less invasive G552A G554A, K677E, and I559F did not affect basal STAT1 phosphorylation (Fig. 3*C*). Upon IFNγ stimulation, all four tested JH2 mutants showed induction of STAT1 phosphorylation (Fig. 3*C*).

Taken together, these results indicate that an intact ATP binding site in JAK2 JH2 is required for full JH2-mediated autoinhibition of JH1 activity in the absence of type I cytokine receptors. However, the ATP binding ability of JAK2 JH2 is not essential for ligand-induced signaling via type I or type II cytokine receptors. Furthermore, these results clearly indicate that loss of JH2 ATP binding is distinct from structural disruption of JH2.

Loss of ATP Binding in JAK2 JH2 Suppresses the V617F Phenotype. Cytokine-independent signaling of JAK2 V617F has previously been shown to be reliant on expression of type I cytokine receptors, when JAK2 is expressed at physiological levels (25, 26). Even when coexpressed with EPOR, the JH2 ATP binding site mutants were found to suppress V617F-induced hyperactivity (Fig. 4*A*). In accordance with the results in the absence of type I receptor expression, activity of V617F L579F also remained high in the presence of EPOR (Fig. 4*A*). Inhibition of JH2 ATP binding also suppressed cytokine inducibility of JAK2 V617F (Fig. 4*A* and Fig. S3).

To assess the effects of JH2 ATP binding-deficient mutations in vivo, the K581A mutation was introduced into human JAK2, wild type and V617F, in a pMSCV–IRES GFP vector, and its effect on development of myeloid lineage cells was analyzed in a mouse bone marrow transplantation model (27). Hematological analysis showed that mice expressing JAK2 V617F developed erythrocytosis within 3 mo, typical for V617F-induced cytokine-independent JAK2 signaling, with increased hemoglobin (Fig. 4*B*), mean corpuscular volume (MCV), hematocrit, and reticulocyte numbers (Fig. S4) (27). Mature red blood cell, platelet, and neutrophil counts did not differ between control and any of the JAK2 constructs (Fig. S4). Mice expressing JAK2 K581A V617F did not develop erythrocytosis and showed blood counts indistinguishable from wild-type JAK2-transplanted mice

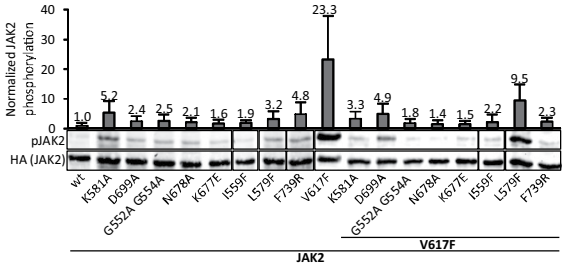

Fig. 2. Mutation of the JAK2 JH2 ATP binding site removes V617F-mediated hyperactivation. Shown is the whole-cell lysate immunoblot from γ2A cells transfected with full-length human JAK2-HA without exogenous receptors. JAK2 expression levels are shown using anti-HA staining from the same blots. Bar graph shows pJAK2(Y1007–Y1008) quantification normalized to HA levels from immunoblots like the one shown, as averages from three independent experiments. Error bars are SDs. See Table 1 for explanation of the mutants.

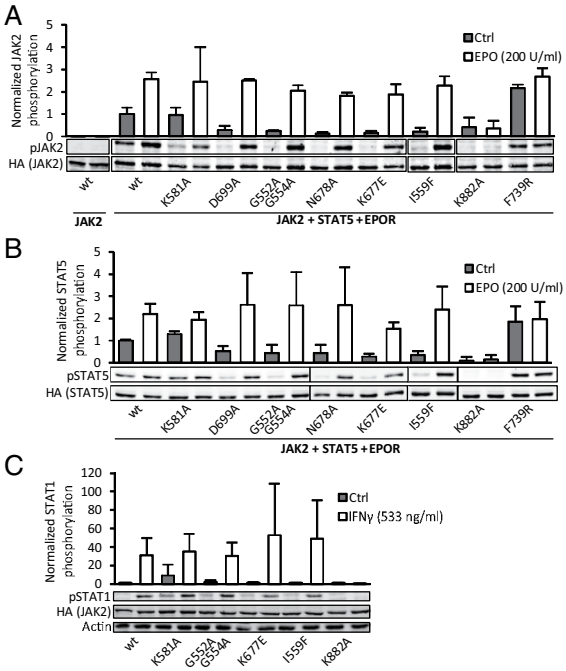

Fig. 3. Disruption of the JAK2 JH2 ATP binding site is distinct from structural disruption. (*A*) JAK2(Y1007–Y1008) phosphorylation of JAK2 mutants in the presence of type I cytokine receptor (EPOR) in γ2A cells. Basal JAK2 phosphorylation in the absence of EPOR expression is shown on the left. (*B*) STAT5A(Y694) phosphorylation from the same samples as pJAK2 in *A*. Phosphorylation was measured from whole-cell lysates of transfected γ2A cells using immunoblotting and normalized to JAK2-HA and STAT5-HA expression levels, respectively. Expression levels of EPOR were analyzed by immunoblotting with anti-HA and found to be equal. (*C*) STAT1(Y701) phosphorylation of endogenous STAT1 in γ2A cells. Bar graph shows quantification of pSTAT1 from immunoblots normalized to basal pSTAT1 levels in cells transfected with wild-type JAK2 (leftmost sample). Actin is shown as a loading control. All error bars are SDs from three independent experiments.

(Fig. 4*B* and Fig. S4). In line with the cell culture data with coexpressed EPOR, K581A in otherwise wild-type JAK2 did not affect the myeloid phenotype (Fig. 4*B* and Fig. S4).

An Intact ATP Binding Pocket of JH2 Is Required for Hyperactivity of JAK2 Exon 12 and 16 Mutations and JAK1 V658F. To analyze whether other hyperactivating JAK2 mutations are also dependent on ATP binding to JH2, K581A and G552A G554A were inserted to exon 12 (K539L, mutated in PV) and exon 16 JAK2 mutants (R683S, mutated in acute B lymphoblastic leukemia) (13). K581A and G552A G554A significantly lowered hyperphosphorylation of both mutants (Fig. 5*A*).

To test the generality and functional conservation of ATP binding in JH2 within the JAK family, studies were performed with JAK1. Binding of MANT-ATP to JAK1 JH2 revealed tight binding in the presence of both Mg^{2+} and Mn^{2+}, with a K_d of 3.1 ± 0.2 μM (Fig. S5), which is comparable to that of JAK2 JH2 (1.3 μM). Analysis of JAK1 V658F (analogous to JAK2 V617F) showed that mutating the ATP binding site of JAK1 JH2 with K622A or G590A G592A (corresponding to K581A and G552A G554A in JAK2, respectively) resulted in abrogation of V658F-induced JAK1 hyperphosphorylation (Fig. 5*B*). In contrast to the results for JAK2, basal phosphorylation levels of JAK1 were reduced to nearly undetectable levels in K622A and G590A G592A in the context of both wild type and V658F.

Molecular Dynamic Simulations Imply a Stabilizing Effect for ATP Binding on the Structure of JH2. Molecular dynamic simulations were performed to explore the structural consequences of JH2 ATP binding. JAK2 JH2 wild type and V617F were simulated for 3.5 μs in the presence of ATP, and the results were compared with simulations of the domains without ATP (16). An overall reduction in flexibility of JH2 was observed upon ATP binding, with reductions in root-mean-square fluctuation and deviation (Fig. S6 *A*–*C*). The largest stabilization was seen in loop regions in both the N and C lobes that participate in the autoinhibitory JH2–JH1 interaction (5, 18), such as the β2–β3 loop (containing Tyr570) and the β6–β7 loop (containing Arg683), the latter of which showed large reduction in mobility only in wild-type JH2 (Fig. S6*A*). Interestingly, the dynamics of ATP-bound wild-type and V617F JH2 were highly similar, with the exception of the region encompassing αC, which was more stable in V617F (Fig. 6). Secondary structure analysis of αC showed that the time αC residues (587–602) were in an α-helical conformation increased upon ATP binding from 41% to 65% in wild type and from 73% to 84% in V617F (Fig. S6*D*) (16). Taken together, these data imply a stabilizing effect for ATP binding on JH2 and a difference in the αC region of ATP-bound JAK2 JH2 V617F compared with wild type.

Discussion

A recent study evaluating nucleotide binding in 30 pseudokinase domains indicated that almost half of pseudokinases retain nucleotide binding, which in most cases is not associated with phosphotransfer activity (20). These and similar observations (23, 28–31) have brought up the question about the functional role of ATP binding in pseudokinases. Here we have addressed this question in the JAK2 pseudokinase domain, focusing on its pathogenic mutants. The most striking finding of our study is that JH2 nucleotide binding plays a critical role in pathogenic activation of JAKs. Specifically, our in vitro and in vivo results show that ATP binding-deficient JH2 mutants suppress the hyperactivation of pathogenic JAK2, whereas the same alterations do not significantly affect the activation characteristics of wild-type JAK2.

Our results are consistent with an earlier study, in which mutation of the JH2 β3 lysine (K581R) was found to decrease

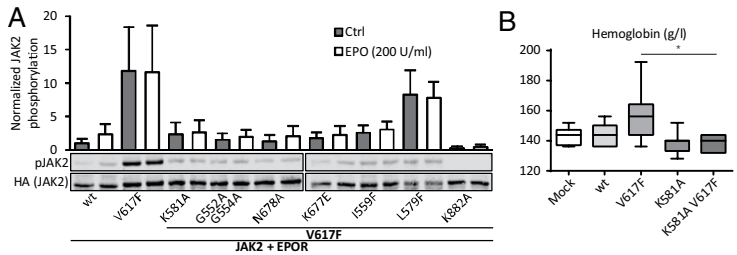

Fig. 4. Loss of ATP binding in JH2 suppresses the V617F phenotype. (*A*) JAK2(Y1007–Y1008) phosphorylation in γ2A cells normalized as explained for Fig. 2. Error bars are SDs from three independent experiments. (*B*) Hemoglobin levels from mice transplanted with retrovirally transduced bone marrow. Mice were analyzed 12 wk posttransplantation. Results show mean ± SEM. $n = 8$ for each group. *$P < 0.05$.

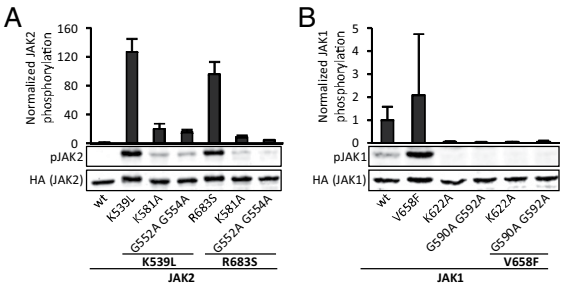

Fig. 5. Analysis of ATP binding site mutants in other JAK2 disease mutations and JAK1 JH2. (*A*) JAK2(Y1007–Y1008) phosphorylation in γ2A cells transfected with JAK2 mutants. K539L and R683S are disease mutations located in JAK2 JH2. (*B*) JAK1(Y1022–Y1023) phosphorylation from COS7 cells transfected with full-length JAK1-HA. JAK1 V658F is analogous to JAK2 V617F. Bar graph shows quantification of phosphorylation from immunoblots, as described for Fig. 2. Error bars are SDs from three independent experiments.

JAK2 V617F hyperphosphorylation (32). Our characterization of the nucleotide binding and thermal stability of JH2 ATP binding site mutants (Fig. 1*B*) distinguishes the effect of ATP binding from potential structural destabilization caused by the mutations. This leads us to conclude that the inhibition of V617F hyperactivity is due to changes in JH2 caused by loss of nucleotide binding (Figs. 2 and 4*A*). The loss of pathogenic activation was observed with three pathogenic mutations (V617F, R683S, and K539L) (Figs. 2 and 5), all of which disrupt the autoinhibitory JH2–JH1 interdomain interaction (18). The mutations are located in different regions of JH2, indicating that the underlying mechanism for reduction of hyperactivity is not mutation specific but rather is a common effect on aberrantly activated JAK2.

The effects of JH2 ATP binding site mutations on otherwise wild-type JAK2 were small: normal cytokine stimulation but a slightly increased basal activity in the absence of type I cytokine receptors (Fig. 2), which was abolished by expression of EPOR (Fig. 3*A*). This is distinctly different from structurally disrupted JH2, as demonstrated by F739R, which effectively removes both aspects of JH2 function—namely, inhibition of basal activity and response to stimulation (Fig. 3 *A* and *B*)—thus mimicking JAK JH2 deletion (1, 6, 7). Interestingly, mutating the ATP binding site of JAK1 JH2 showed reduced basal activity (Fig. 5*B*), which we speculate is due to different modes of regulation of basal JAK activity in homo- (JAK2) and heterodimeric (all JAKs) receptor configurations.

The JH2 domain likely arose early in evolution through duplication of JH1, and the two domains have since taken a different evolutionary path with distinct regions conserved in each of them (33), indicative of their respective separate functional roles. As JH1 maintained the substrate phosphorylation function, the catalytic function in JH2 became redundant and has consequently been lost, with the exception of regulatory autophosphorylation in JAK2. Interestingly, JH2 ATP binding ability is conserved in JAK1 and TYK2 (JAK3 unknown), even though a precise function in wild-type JAK1/TYK2 cannot be ascertained from current data. Nevertheless, the relatively high binding affinity (Fig. 1*D*, Fig. S5, and ref. 17), combined with low or absent hydrolysis and high cellular ATP concentrations, likely results in constitutively bound ATP in JH2, thus making ATP essentially a structural component of the JAK pseudokinase domain.

The effects of nucleotide binding to the structure of JH2 are subtle: mainly rigidification of αC in the ATP-bound form (16). Why is it then that the loss of nucleotide binding has a pronounced effect in V617F but not in wild type? TSA shows that the V617F mutation significantly reduces the Tm of JAK2 JH2 compared with wild type (Fig. 1*C*), yet ATP binding to both wild type and V617F causes equal thermal stabilization. These data suggest that the V617F mutation destabilizes JAK2 JH2 and renders it thus more sensitive to the loss of the stabilizing effect of ATP, as even ATP-bound JH2 V617F does not reach the Tm of wild type (Fig. 1*C*). Whether this sensitivity is due to overall destabilization of JH2 V617F or a specific structural alteration cannot be definitively determined from current data, but molecular dynamic simulations hint at a critical role for the αC region.

The main structural effects due to ATP binding in JH2 are observed in αC, and mutations in αC (e.g., F594A, F595A) have been shown to reverse hyperactivation of several mutations scattered throughout the JAK2 JH2–JH1 interface (18, 34, 35). Although in the case of V617F, which is proximal to αC, F595A might reconstitute a disrupted autoinhibitory JH2–JH1 interface, a more likely explanation for the suppressive effects of ATP binding mutations (and of F594A, F595A) is that pathogenic hyperactivation is dependent on a yet-to-be-characterized positive regulatory interaction mediated by JH2, which probably involves αC and is therefore sensitive to its conformation.

The modulatory nature of nucleotide binding pocket occupation has previously been documented in the kinase and pseudokinase literature. Protein kinase C, for example, has been shown to be regulated by noncatalytic nucleotide binding (30). Also, in the pseudokinases STRADα (28, 36) and integrin-linked kinase (ILK) (23, 31), ATP binding is required to enable critical protein–protein interactions. Interestingly, ATP binding is necessary for ILK function, even though no major ATP binding-induced structural changes could be detected using multiple biophysical methods (23). Also, the allosteric regulatory function of the HER3 pseudokinase has been shown to be sensitive to modulation by an ATP mimetic inhibitor (29). Furthermore, some pseudokinases that are incapable of binding ATP, like Vaccinia-related kinase 3, effectively mimic the ATP-bound conformation through bulky and acidic amino acid substitutions in the active site (37). Because almost half of pseudokinases studied so far possess some form of nucleotide binding activity (20), it seems likely that future studies will find even more evidence for a functional role of ATP binding in this group of proteins.

The results presented here reveal that the ATP binding site of JAK JH2 has characteristics to serve as a potential target site for modulators and/or mutant-selective inhibitors of JAK activity. Loss of JH2 ATP binding abrogates hyperactivation of mutant JAK2 in cells and in vivo while leaving wild-type JAK2 largely unaffected. Current pharmacological interventions at JAKs target JH1, and although these inhibitors have brought important advances in the treatment of PMF and PV patients, they are unable to eradicate the disease and they also affect wild-type JAKs (38). Targeting JH2 with conformation-specific ATP binding site inhibitors may give rise to novel pharmacological compounds able to allosterically inhibit pathogenic JAK activity.

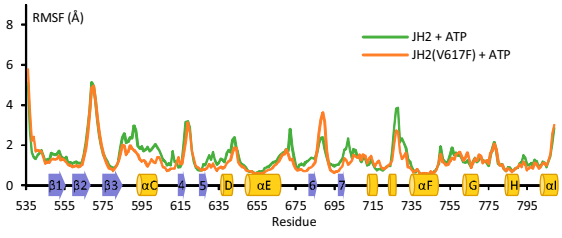

Fig. 6. Comparison of ATP-bound JAK2 JH2 wild type and V617F in molecular dynamic simulations. Root-mean-square fluctuation of each residue in JAK2 JH2 wild type and V617F with ATP bound over the course of the simulation (3.5 μs). The secondary structure of JAK2 JH2 is shown schematically on the *x* axis.

Materials and Methods

Cell Culture, Transfection, and Immunoblotting. JAK2-deficient γ2A fibrosarcoma cells and COS7 cells were cultured using standard cell culture methods and transfected with full-length human JAK2-HA, human STAT5A-HA, and human EPOR-HA using FuGENE6 (Promega) or Xtreme-GENE9 (Roche) according to the manufacturers' instructions. After 10 h cells were starved in serum-free medium overnight and stimulated for 30 min with human EPO or human IFNγ. After stimulation, cells were lysed into Triton-X cell lysis buffer and centrifuged, and the supernatant was used directly for SDS/PAGE and immunoblotting. Blots were double-stained with phosphospecific antibodies and anti-HA and detected with a mix of IRDye-labeled secondaries. Blots were read and quantified using a LI-COR Odyssey CLx. A minimum of three independent experiments were performed for each condition.

Retroviral Transduction and Bone Marrow Transplantation. For details on retroviral transduction and bone marrow transplantation, see *SI Materials and Methods*. All experiments were performed in strict adherence to Swiss laws for animal welfare and approved by the Swiss Cantonal Veterinary Office of Basel-Stadt.

Molecular Dynamic Simulations. Simulations were carried out as described previously (16). Trajectories were analyzed using VMD (visual molecular dynamics) (39).

In Vitro Biochemical Assays on Recombinant Proteins. Recombinant proteins were expressed in Sf9 cells as detailed earlier (17). After cell collection and Ni-NTA purification, protein was either used as such [JAK2(536–812-6xHis) for TSA] or subjected to anion exchange purification as described earlier (17) [JAK2(513–827-6xHis) and JAK1(553–856-6xHis) for MANT-ATP binding assays]. TSA experiments were carried out essentially as described in ref. 20. The MANT-ATP binding assay is described in ref. 40.

ACKNOWLEDGMENTS. We thank Yibing Shan for kindly providing the JAK2 JH2 molecular dynamic simulation data, Heidi Peussa, Anna U. Laitinen, and Ellin-Kristina Hillert for excellent technical assistance, and Kaury Kucera for valuable comments on the manuscript. This work was supported in part by the Medical Research Council of the Academy of Finland, Sigrid Juselius Foundation, Medical Research Fund of Tampere University Hospital, Finnish Cancer Foundation, Novo Nordisk Foundation, and Tampere Tuberculosis Foundation (to O.S.); National Institutes of Health Grant R21 AI095808 (to S.R.H.); and Swiss National Science Foundation Grants 310000-120724/1 and 32003BB_135712/1 and Swiss Cancer League Grant KLS-2950-02-2012 (to R.C.S.).

1. Saharinen P, Silvennoinen O (2002) The pseudokinase domain is required for suppression of basal activity of Jak2 and Jak3 tyrosine kinases and for cytokine-inducible activation of signal transduction. *J Biol Chem* 277(49):47954–47963.
2. Chen M, et al. (2000) Complex effects of naturally occurring mutations in the JAK3 pseudokinase domain: Evidence for interactions between the kinase and pseudokinase domains. *Mol Cell Biol* 20(3):947–956.
3. Yeh TC, Dondi E, Uzé G, Pellegrini S (2000) A dual role for the kinase-like domain of the tyrosine kinase Tyk2 in interferon-α signaling. *Proc Natl Acad Sci USA* 97(16):8991–8996.
4. Sanz Sanz A, et al. (2014) The JH2 domain and SH2-JH2 linker regulate JAK2 activity: A detailed kinetic analysis of wild type and V617F mutant kinase domains. *Biochim Biophys Acta* 1844(10):1835–1841.
5. Lupardus PJ, et al. (2014) Structure of the pseudokinase-kinase domains from protein kinase TYK2 reveals a mechanism for Janus kinase (JAK) autoinhibition. *Proc Natl Acad Sci USA* 111(22):8025–8030.
6. Saharinen P, Vihinen M, Silvennoinen O (2003) Autoinhibition of Jak2 tyrosine kinase is dependent on specific regions in its pseudokinase domain. *Mol Biol Cell* 14(4):1448–1459.
7. Saharinen P, Takaluoma K, Silvennoinen O (2000) Regulation of the Jak2 tyrosine kinase by its pseudokinase domain. *Mol Cell Biol* 20(10):3387–3395.
8. Vainchenker W, Constantinescu SN (2013) JAK/STAT signaling in hematological malignancies. *Oncogene* 32(21):2601–2613.
9. Baxter EJ, et al.; Cancer Genome Project (2005) Acquired mutation of the tyrosine kinase JAK2 in human myeloproliferative disorders. *Lancet* 365(9464):1054–1061.
10. James C, et al. (2005) A unique clonal JAK2 mutation leading to constitutive signalling causes polycythaemia vera. *Nature* 434(7037):1144–1148.
11. Kralovics R, et al. (2005) A gain-of-function mutation of JAK2 in myeloproliferative disorders. *N Engl J Med* 352(17):1779–1790.
12. Levine RL, et al. (2005) Activating mutation in the tyrosine kinase JAK2 in polycythemia vera, essential thrombocythemia, and myeloid metaplasia with myelofibrosis. *Cancer Cell* 7(4):387–397.
13. Haan C, Behrmann I, Haan S (2010) Perspectives for the use of structural information and chemical genetics to develop inhibitors of Janus kinases. *J Cell Mol Med* 14(3):504–527.
14. Lipson D, et al. (2012) Identification of new ALK and RET gene fusions from colorectal and lung cancer biopsies. *Nat Med* 18(3):382–384.
15. Candotti F, et al. (1997) Structural and functional basis for JAK3-deficient severe combined immunodeficiency. *Blood* 90(10):3996–4003.
16. Bandaranayake RM, et al. (2012) Crystal structures of the JAK2 pseudokinase domain and the pathogenic mutant V617F. *Nat Struct Mol Biol* 19(8):754–759.
17. Ungureanu D, et al. (2011) The pseudokinase domain of JAK2 is a dual-specificity protein kinase that negatively regulates cytokine signaling. *Nat Struct Mol Biol* 18(9):971–976.
18. Shan Y, et al. (2014) Molecular basis for pseudokinase-dependent autoinhibition of JAK2 tyrosine kinase. *Nat Struct Mol Biol* 21(7):579–584.
19. Toms AV, et al. (2013) Structure of a pseudokinase-domain switch that controls oncogenic activation of Jak kinases. *Nat Struct Mol Biol* 20(10):1221–1223.
20. Murphy JM, et al. (2014) A robust methodology to subclassify pseudokinases based on their nucleotide-binding properties. *Biochem J* 457(2):323–334.
21. Manning G, Whyte DB, Martinez R, Hunter T, Sudarsanam S (2002) The protein kinase complement of the human genome. *Science* 298(5600):1912–1934.
22. Knapp S, Sundström M (2014) Recently targeted kinases and their inhibitors—The path to clinical trials. *Curr Opin Pharmacol* 17:58–63.
23. Fukuda K, Knight JD, Piszczek G, Kothary R, Qin J (2011) Biochemical, proteomic, structural, and thermodynamic characterizations of integrin-linked kinase (ILK): Cross-validation of the pseudokinase. *J Biol Chem* 286(24):21886–21895.
24. Iyer GH, Garrod S, Woods VL, Jr, Taylor SS (2005) Catalytic independent functions of a protein kinase as revealed by a kinase-dead mutant: Study of the Lys72His mutant of cAMP-dependent kinase. *J Mol Biol* 351(5):1110–1122.
25. Lu X, et al. (2005) Expression of a homodimeric type I cytokine receptor is required for JAK2V617F-mediated transformation. *Proc Natl Acad Sci USA* 102(52):18962–18967.
26. Lu X, Huang LJS, Lodish HF (2008) Dimerization by a cytokine receptor is necessary for constitutive activation of JAK2V617F. *J Biol Chem* 283(9):5258–5266.
27. Tiedt R, et al. (2008) Ratio of mutant JAK2-V617F to wild-type Jak2 determines the MPD phenotypes in transgenic mice. *Blood* 111(8):3931–3940.
28. Zeqiraj E, et al. (2009) ATP and MO25α regulate the conformational state of the STRADalpha pseudokinase and activation of the LKB1 tumour suppressor. *PLoS Biol* 7(6):e1000126.
29. Littlefield P, Moasser MM, Jura N (2014) An ATP-competitive inhibitor modulates the allosteric function of the HER3 pseudokinase. *Chem Biol* 21(4):453–458.
30. Cameron AJ, Escribano C, Saurin AT, Kostelecky B, Parker PJ (2009) PKC maturation is promoted by nucleotide pocket occupation independently of intrinsic kinase activity. *Nat Struct Mol Biol* 16(6):624–630.
31. Lange A, et al. (2009) Integrin-linked kinase is an adaptor with essential functions during mouse development. *Nature* 461(7266):1002–1006.
32. Andraos R, et al. (2012) Modulation of activation-loop phosphorylation by JAK inhibitors is binding mode dependent. *Cancer Discov* 2(6):512–523.
33. Gu J, Wang Y, Gu X (2002) Evolutionary analysis for functional divergence of Jak protein kinase domains and tissue-specific genes. *J Mol Evol* 54(6):725–733.
34. Dusa A, Mouton C, Pecquet C, Herman M, Constantinescu SN (2010) JAK2 V617F constitutive activation requires JH2 residue F595: A pseudokinase domain target for specific inhibitors. *PLoS ONE* 5(6):e11157.
35. Gnanasambandan K, Magis A, Sayeski PP (2010) The constitutive activation of Jak2-V617F is mediated by a π stacking mechanism involving phenylalanines 595 and 617. *Biochemistry* 49(46):9972–9984.
36. Zeqiraj E, Filippi BM, Deak M, Alessi DR, van Aalten DM (2009) Structure of the LKB1-STRAD-MO25 complex reveals an allosteric mechanism of kinase activation. *Science* 326(5960):1707–1711.
37. Scheeff ED, Eswaran J, Bunkoczi G, Knapp S, Manning G (2009) Structure of the pseudokinase VRK3 reveals a degraded catalytic site, a highly conserved kinase fold, and a putative regulatory binding site. *Structure* 17(1):128–138.
38. Sonbol MB, et al. (2013) Comprehensive review of JAK inhibitors in myeloproliferative neoplasms. *Ther Adv Hematol* 4(1):15–35.
39. Humphrey W, Dalke A, Schulten K (1996) VMD: Visual molecular dynamics. *J Mol Graph* 14(1):33–38, 27–28.
40. Niranjan Y, et al. (2013) Analysis of steady-state Förster resonance energy transfer data by avoiding pitfalls: Interaction of JAK2 tyrosine kinase with N-methylanthraniloyl nucleotides. *Anal Biochem* 442(2):213–222.

Molecular basis for pseudokinase-dependent autoinhibition of JAK2 tyrosine kinase

Yibing Shan[1§], Kavitha Gnanasambandan[2§], Daniela Ungureanu[3], Eric T. Kim[1], Henrik Hammarén[3], Kazuo Yamashita[4], Olli Silvennoinen[3], David E. Shaw[1,5], and Stevan R. Hubbard[2]

[1]D. E. Shaw Research, New York, NY, USA
[2]Kimmel Center for Biology and Medicine of the Skirball Institute, Department of Biochemistry and Molecular Pharmacology, New York University School of Medicine, New York, NY, USA
[3]School of Medicine, University of Tampere and Tampere University Hospital, Tampere, Finland
[4]Systems Immunology Laboratory, Immunology Frontier Research Center, Osaka University, Suita, Osaka, Japan
[5]Department of Biochemistry and Molecular Biophysics, Columbia University, New York, NY, USA

[§]These authors contributed equally

[*]Correspondence should be addressed to:
Dr. Stevan R. Hubbard
Stevan.Hubbard@med.nyu.edu

Dr. Yibing Shan
Yibing.Shan@DEShawResearch.com

Dr. David E. Shaw
David.Shaw@DEShawResearch.com

Janus kinase-2 (JAK2) mediates signaling by various cytokines, including erythropoietin and growth hormone. JAK2 possesses tandem pseudokinase and tyrosine kinase domains. Mutations in the pseudokinase domain are causally linked to myeloproliferative neoplasms (MPNs) in humans. The structure of the JAK2 tandem kinase domains is unknown, and therefore the molecular bases for pseudokinase-mediated autoinhibition and pathogenic activation remain obscure. Using unbiased molecular dynamics simulations of protein-protein docking, we produced a structural model for the autoinhibitory interaction between the JAK2 pseudokinase and kinase domains. A striking feature of our model, which is supported by mutagenesis experiments, is that nearly all of the disease mutations map to the domain interface. The simulations indicate that the kinase domain is stabilized in an inactive state by the pseudokinase domain, and they offer a molecular rationale for the hyperactivity of V617F, the predominant JAK2 MPN mutation.

Janus kinases (JAK1–3, TYK2) are protein tyrosine kinases that mediate cytokine signaling[1]. JAKs possess an N-terminal FERM (band 4.1, ezrin, radixin, moesin) domain and a Src homology-2 (SH2)-like domain, which are responsible for cytokine-receptor association[2], and tandem protein kinase domains: a pseudokinase domain and a tyrosine kinase domain. JAKs are activated through cytokine-induced *trans*-phosphorylation, either as heterodimeric receptor-JAK complexes (all JAKs) or as homodimeric receptor-JAK2 complexes. Signaling through JAK-STAT (signal transducer and activator of transcription) pathways are essential for cell growth, differentiation, proliferation and survival, particularly in hematopoiesis, as well as for the initial events in innate and adaptive immunity[1].

Mutations in *JAK*s are causally linked to human myeloproliferative neoplasms (MPNs), which are clonal proliferative disorders affecting different myeloid lineages[3]. The more common MPNs—polycythemia vera, essential thrombocythemia, and primary myelofibrosis—are caused in most cases by mutations in the pseudokinase domain of *JAK2* (refs. 3,4). Mutations in the pseudokinase domain of *JAK*s have also been linked to acute lymphoblastic leukemia (ALL) and

acute myeloid leukemia (AML)[4]. All of these pseudokinase domain mutations result in constitutive activity of the tyrosine kinase domain. V617F in the JAK2 pseudokinase domain is the most commonly identified mutation in MPNs[5-7], responsible for ~95% of cases of polycythemia vera, and this mutation also been implicated in non-small-cell lung cancer[8]. These clinical data, as well as biochemical data[9,10], implicate the pseudokinase domain as a negative regulatory domain necessary to maintain low basal JAK2 activity, yet the molecular basis for pseudokinase-mediated autoinhibition remains elusive.

We demonstrated previously that the pseudokinase domain of JAK2 in fact possesses low catalytic activity, phosphorylating two negative regulatory sites in JAK2 (ref. 11), and we subsequently determined its crystal structure[12]. Numerous crystal structures of the tyrosine kinase domain of JAK2 have been determined, but attempts to crystallize the tandem kinase domains of JAK2 have been unsuccessful to date. Here, we used long time-scale molecular dynamics (MD) simulations, guided by biochemical knowledge of the system, to generate a structural model for the autoinhibitory interaction between the pseudokinase and kinase domains of human JAK2. Our model, which is supported by extensive mutagenesis data, can rationalize nearly all of the gain-of-function disease mutations in JAK2.

RESULTS

Generation of the JAK2 JH2–JH1 model

To generate a structural model for the autoinhibitory interaction between the JAK2 pseudokinase domain (JAK homology-2, JH2) and tyrosine kinase domain (JH1), which could then be tested experimentally, we simulated the JH2–JH1 interaction without any presumption of the binding pose, in a manner similar to small molecule-protein binding[13]. We placed atomic structures of JH2 and JH1 in an arbitrary, untethered, and non-contacting pose within a box of explicit solvent molecules (**Fig. 1**, state 1). From this starting pose, we ran 14 independent MD simulations of 3 μs each, which, in each case, resulted in a JH2–JH1 configuration in which the two domains were in contact (**Fig. 1**, state 2). We did not include the 29-residue JH2–JH1 linker at this early

stage of the simulations, because initial simulations with the linker resulted in entanglement of JH1 or JH2 with the linker, which could not be easily resolved in the relatively short (3 μs) simulation time. We knew from mutagenesis data in the literature, and the lack of sequence conservation, that the JH2–JH1 linker was not a critical component of autoinhibition. Therefore, for computational efficiency, we chose to omit the linker initially and focus on direct JH2 and JH1 interactions.

Visual inspection revealed that there was a large variation of JH2–JH1 poses from these 14 simulations (**Fig. 1**, state 2). One of the 14 poses (pose 2) possessed two key features: the JH2–JH1 interface included α-helix C (αC) in JH2, which we and others had identified previously as a structural element in the regulation of JH1 by JH2 (refs. 12,14), and the C-terminus of JH2 and the N-terminus of JH1 could readily be connected by the JH2–JH1 linker. For these reasons, we chose to pursue pose 2. We also subjected these 14 simulations to two empirical protein-docking scoring functions (EMPIRE[15] and OSCAR[16]), and pose 2 scored better than the others (**Supplementary Fig. 1a**). However, because our final model differs substantially from this initial pose (**Supplementary Fig. 1b** and as described below), and the interaction energy of the linker is likely to be non-negligible, the docking scores were not of fundamental consequence.

In the next phase of modeling, we added the JH2–JH1 linker to JH2–JH1 pose 2 (**Fig. 1**, state 3) and performed four simulations of the resulting system (residues 536–1131). In these simulations, the addition of the linker caused major movements of JH1 relative to JH2. One simulation of 1.7 μs (**Fig. 1**, states 3 and 4) resulted in a root-mean-square deviation (RMSD) of ~9 Å for JH2 and JH1 (Cα atoms) relative to the starting position. The resultant JH2–JH1 pose from this simulation was appealing because additional interdomain contacts were established, which were between the "backside" (β7–β8 loop) of JH2 and the N lobe of JH1 (β2–β3 loop) (described in detail below). In addition, a negative regulatory phosphorylation site, Tyr570 (refs. 11,17,18), in the β2–β3 loop of JH2, which was phosphorylated from the outset of the simulations, settled into a positively charged pocket in the N lobe of JH1 (described in detail below).

Because of the negative regulatory role of the SH2–JH2 linker[19]—in particular Ser523 (refs. 20,21), a JH2 phosphorylation site[11]—we then added residues 520–535 to the model with Ser523 phosphorylated (**Fig. 1**, state 5). We simulated JAK2 residues 520–1131, encompassing the SH2–JH2 linker (C-terminal half), JH2, and JH1, for 40 μs. After several microseconds, a defined interaction between JH2, JH1, and the SH2–JH2 linker was established, which we term the JH2–JH1 autoinhibitory pose (**Fig. 1**, state 6). (A potential mechanism by which JH2 autoinhibits JH1 in this pose is presented below.) This configuration was highly stable: in the 40 μs simulation, the RMS fluctuation of Cα atoms (in JH2 and JH1) was only 2.6 Å with respect to the average structure. (Structural coordinates for the JAK2 JH2–JH1 model (a representative snapshot from the simulation) and an animation of model generation (**Supplementary Video 1**) are included in Supplementary Information.)

Description of the model

The most striking feature of our model for the autoinhibitory interaction between JH2 and JH1 of JAK2 is the positioning of nearly all of the mapped disease mutations[4], and other gain-of-function mutations[19], in or proximal to the interdomain interface (**Fig. 2a** and **Supplementary Fig. 1c**). The JH2–JH1 interface can be subdivided into four regions: region 1, the β2–β3 loop of JH2 and the β sheet in the N lobe of JH1 (**Fig. 2b**); region 2, β7–β8 of JH2 and the β2–β3 loop of JH1 (**Fig. 2c**); region 3, the end of αC in JH2 and the kinase hinge region of JH1 (**Fig. 2d**); and region 4, the SH2–JH2 linker, α-helix C (αC) of JH2 and αD of JH1 (**Fig. 2e**). Although residues in the JH2–JH1 linker also interacted with JH2 and JH1 during the simulations, these interactions were generally less stable and will not be enumerated.

In region 1 (**Fig. 2b**), pTyr570 in the β2–β3 loop of JH2 is inserted into the pocket formed by the curved β sheet in the N lobe of JH1, salt-bridged to Lys883 (β3), Lys926 (β5), and Arg922 (β4–β5 loop). In region 2 (**Fig. 2c**), the simulations showed a stable salt bridge between two residues, Arg683 (β7) in JH2 and Asp873 (β2–β3 loop) in JH1; mutation of each residue (R683S, D873N) has been linked to acute lymphoblastic leukemia (ALL)[4]. Thr875, also in the

β2–β3 loop, is the site of another disease mutation (T875N; acute megakaryoblastic leukemia[4]). In addition to Arg683, Lys607 (K607N; acute myeloid leukemia[4]) (αC–β4 loop) was also observed to salt bridge with Asp873 during the simulation. In region 3 (**Fig. 2e**), Pro933 in the JH1 hinge region, which links the N and C lobes, formed a small hydrophobic cluster with Met600 and Leu604 (αC and just after) in JH2. Val878 (β3) and Tyr931 (hinge) in JH1 also contribute to this hydrophobic cluster. P933R was mapped as an activating mutation in ALL[22]. Finally, in region 4 (**Fig. 2e**), the SH2–JH2 linker made contacts with αC of JH2 and αD of JH1. In addition to SH2–JH2 linker-mediated contacts between the domains, stable salt bridges were formed between Glu592 (αC, JH2) and Arg947 (αD–αE loop, JH1) and between Arg588 (αC, JH2) and pSer523 (SH2–JH2 linker). Arg947 also interacted with pSer523 during the simulation. Notably, the mutation R588A was shown previously to be partially activating[23].

Experimental validation of the model

To provide experimental validation for the autoinhibitory model of JAK2 JH2–JH1 derived from the MD simulations, we explored charge-reversal mutations in each of the four regions of the JH2–JH1 interface. In region 1 (**Fig. 2b**), we generated the individual point mutations Y570R (charge reversal of pTyr570; JH2) and K883E (JH1) and the double mutation Y570R K883E in full-length JAK2 and transfected them into COS7 cells. We measured JH1 activation-loop phosphorylation (pTyr1007–1008)—the standard read-out of JAK2 activation—and downstream STAT1 phosphorylation and STAT3-mediated gene transcription. The expectation was that the single point mutants would be partially activated, because of destabilization of the JH2–JH1 interaction, but that the activation state of the double mutant would be suppressed, due to formation of the "reverse" salt bridge and restoration of the autoinhibited state. Indeed, both Y570R and K883E were activated by a factor of ~4 relative to wild-type JAK2, and, strikingly, the activation state of the double mutant was similar to wild type, i.e., suppressed (**Fig. 3a** and **Supplementary Fig. 2a**), consistent with reverse salt-bridge formation.

In region 2 (**Fig. 2c**), we probed the interaction between Arg683 (JH2) and Asp873 (JH1) (both ALL mutations). We first generated the charge-reversal mutants R683E, D873R, and R683E D873R. Although R683E was activated by a factor of ~20 (**Fig. 3b** and **Supplementary Fig. 2a**), D873R was not activated, and testing of D873R in the context of JH1 alone revealed that this mutation (and also D873K) compromised JH1 activation-loop phosphorylation (**Supplementary Fig. 2b**), even though Asp873 is at a considerable distance from the JH1 active site (**Fig. 2a**). We then tested the actual disease mutant, D873N, and the double mutant R683E D873N. D873N was activated by a factor of ~17, whereas activation of the double mutant was substantially reduced compared to the two single mutants (**Fig. 3b** and **Supplementary Fig. 2a**). These data argue for a direct interaction between these two residues. It is conceivable that Asn873 interacts more favorably with Glu683 (in R683E D873N) than with Arg683 (in D873N), given that asparagine–glutamate interactions were found empirically to be energetically more favorable than asparagine–arginine interactions[24]. Consistent with this interpretation, in simulations, the single mutations (R683E, D873N) partially destabilized the JH2–JH1 interaction, while the double mutation (R683E D873N) restored wild-type stability (**Supplementary Fig. 3a**). Further support of a direct interaction of Arg683 with JH1 (Asp873) comes from a crystal structure of JAK2 JH2 R683S (data not shown), which shows that this disease mutation does not affect the structure (global or local) of JH2. Thus, it is unlikely that substitution of Arg683 destabilizes the JH2–JH1 interaction indirectly through structural perturbation of JH2.

In region 3 (**Fig. 2d**), we took advantage of a disease (ALL) mutation, P933R, which substitutes a positively charged residue in the hinge region between the JH1 kinase lobes. Residue 603 (Lys603 in human, Gln603 in mouse) in JH2 is opposite Pro933 in our JH2–JH1 model, and we tested whether substitution of a negatively charged residue at 603 could suppress the hyperactivation of P933R, by creating a favorable charge interaction across the interface. For this purpose, we generated mutants (in mouse JAK2) Q603E, P933R, and Q603E P933R. Q603E had activity comparable to wild-type JAK2, which was expected given that this residue is not

conserved in mammalian species, P933R was activated by a factor of ~13, and, as predicted from the model, Q603E suppressed the activation of P933R (Q603E P933R) (**Fig. 3c** and **Supplementary Fig. 2a**). Because in this case only one of the two single mutants in the putative JH2–JH1 interface was activated, we confirmed that Q603E (JH2) does not cause impairment of JAK2 (e.g., loss of receptor engagement) by verifying that Q603E and Q603E P933R could be activated by erythropoietin (Epo) in γ2A cells co-transfected with Epo receptor (**Supplementary Fig. 2c**).

Finally, in region 4 (**Fig. 2e**), we created charge-reversal mutants E592R (JH2), R947E (JH1), and E592R R947E. R947E was activated by a factor of ~4 (**Fig. 3d** and **Supplementary Fig. 2a**). E592R, however, was not activated, which was unexpected because mutation to alanine (E592A) was shown previously to be partially activating[23]. MD simulations of E592R could rationalize the experimental result: Arg592 can form a salt bridge with pSer523, along with Arg947 (**Supplementary Fig. 3b**), to stabilize the autoinhibitory state. Importantly, the double mutant (E592R R947E) was not activated (**Fig. 3d** and **Supplementary Fig. 2a**), i.e., E592R suppressed the hyperactivation of R947E, consistent with formation of the reverse salt bridge (Arg592–Glu947), which indeed formed and was stable in the simulation of E592R R947E (**Supplementary Fig. 3b**). As for Q603E above, because E592R (JH2) was not activated on its own (yet suppressed R947E), we confirmed that this mutation does not impair JAK2 by co-expressing E592R and E592R R947E with Epo receptor and stimulating with Epo (**Supplementary Fig. 2c**).

Thus, based on the JH2–JH1 model, we predicted and confirmed experimentally three novel activating mutations in JAK2—two in JH1 (K883E and R947E) and one in JH2 (Y570R)—each of which could be suppressed with a mutation across the JH2–JH1 interface. We also predicted and confirmed that a mutation in JH2 (Q603E) could suppress a disease mutation in JH1 (P933R).

Autoinhibitory mechanism

In our model for the interaction between JAK2 JH2 and JH1, the activation loop of JH1 is unencumbered, and the active site is accessible to substrates (**Fig. 2a**). However, our simulations suggest that the interaction with JH2 leads to a more extended configuration of the JH1 lobes (**Supplementary Fig. 4a**), which is reminiscent of the effect of the SH2 and SH3 domains on the kinase domain of Abl in the autoinhibited state[25]. Because substantial lobe movements occur in protein kinases during the phosphoryl-transfer process[26], and the JH2 interaction with JH1 in the model involves both lobes of JH1, this interaction should suppress JH1 catalytic activity. In addition, the simulations indicate that binding of JH2 to JH1 destabilizes the catalytically important β3–αC (Lys882–Glu898) salt bridge in JH1 (**Fig. 4a**) and might facilitate the so-called "DFG flip" in the activation loop[25,27]. Indeed, the DFG-out, catalytically inactive state was reached in the simulation of JH2–JH1, starting from the DFG-in (active) state (**Fig. 4b**). Taken together, the simulations suggest that the interaction of JH2 with JH1 stabilizes an inactive state of JH1 (**Fig. 5**).

While phosphorylation of Ser523 and Tyr570 are posited to fortify the JH2–JH1 autoinhibitory interaction (**Fig. 2b,e**), phosphorylation of the JH1 activation loop (Tyr1007–1008), which stabilizes the active state, conversely might destabilize the JH2–JH1 interaction. This concept is supported by MD simulations of JH2–JH1, in which phosphorylation of the JH1 activation loop leads to a higher JH1 RMSD than when the activation loop is unphosphorylated (**Supplementary Fig. 4b**). Presumably, a high degree of conformational freedom for JH1 is necessary for phosphorylation of other sites in JAKs (e.g., Tyr813 in JAK2), the cytokine receptor, and recruited STAT proteins.

Mechanism of V617F activation

Val617, the site of the predominant MPN-causing mutation, V617F[5-7], is not situated directly in the JH2–JH1 interface, but rather is proximal to the SH2–JH2 linker (**Fig. 2e**), which was shown previously to be important for maintenance of the JAK2 basal state[19]. To gain insights as to how

this mutation results in constitutive activation of JAK2, we simulated V617F JH2–JH1. Analysis of the simulation trajectories suggest that the bulky phenylalanine at residue 617 destabilizes the position of the SH2–JH2 linker between JH2 and JH1 (**Supplementary Fig. 4c**), which results in increased conformational heterogeneity of JH1 relative to JH2 (**Supplementary Fig. 4d**). Accordingly, the catalytically active conformation of αC in JH1 (β3–αC salt bridge; see **Fig. 4b**) is more stable in V617F than in wild-type JAK2 (**Supplementary Fig. 4e**). A mutation in αC of JH2, F595A, was shown previously to suppress V617F[14,28], and in a simulation of the double mutant V617F F595A, the SH2–JH2 linker position is again stable between JH2 and JH1 (**Supplementary Fig. 4c**).

Applicability to other JAKs

The proposed autoinhibitory interaction between JH2 and JH1 of JAK2 should be applicable to the other JAKs as well, in particular JAK1, which shares several disease mutations with JAK2, including V658F (V617F in JAK2) and R724S (R683S in JAK2). Indeed, a 12-μs simulation of JH2 and JH1 of JAK1 (whose interdomain linker is 14 residues shorter than in JAK2) showed that the key interface interactions are conserved, with most of the known activating mutations in JAK1 clustered in the interface (**Supplementary Fig. 5a**). During the simulation, salt bridges were established between Arg724 in JH2 (Arg683 in JAK2) and Asp899 and Glu897 (Asp873 and Leu871 in JAK2) in the β2–β3 loop of JH1, despite Arg724 being located >9 Å from these acidic residues at the start of the simulation. Although the β2–β3 loop in JAK1 JH2 does not contain a known phosphorylation site, Glu609 in the loop is observed in the simulation to interact with Lys888 (β2) and Lys911 (β3–αC loop) in the N lobe of JH1 (**Supplementary Fig. 5a**), similar to the interaction in JAK2 between pTyr570 and Lys883 (β3) and Lys926 (β5) (**Fig. 2b**). (Structural coordinates for the JAK1 JH2–JH1 model (a representative snapshot from the simulation) are included in Supplementary Information.)

DISCUSSION

In this study, we used long time-scale MD simulations to generate a molecular model for the autoinhibitory interaction between the pseudokinase domain (JH2) and tyrosine kinase domain (JH1) of JAK2. Our goal in performing the MD simulations was to see whether we could generate a plausible model for the JH2–JH1 interaction, which we could then test experimentally. While the particular MD simulation approach we took, which entailed decisions based on biochemical and structural knowledge of JAK2, is far from a "turnkey" method for *ab initio* modeling of protein-protein interactions, the current work highlights the potential of MD simulations as a powerful tool for structural elucidation of such interactions.

In our model, nearly all of the activating disease mutations are present in the JH2–JH1 interface, thus providing a molecular rationale for oncogenic activation through mutation: destabilization of the JH2–JH1 interaction results in more facile JH1 *trans*-phosphorylation (**Fig. 5**). Although the MD simulations of JH2–JH1 can provide insights into specific oncogenic mutations, such as D873N or V617F (**Supplementary Figs. 3a** and **4c**–**e**), they are not able to predict, for example, the relative degree to which a mutation in JAK2 will be activating in cells. Moreover, whether destabilization of the SH2–JH2 linker is the sole mechanism by which V617F is activated will require additional structural and mechanistic studies.

Our JAK2 JH2–JH1 model is fundamentally different from models proposed previously[23,29,30], in which only V617F among the many MPN mutations is present in the respective JH2–JH1 interfaces (**Supplementary Fig. 5b**). In the prevailing model in the field[29], JH2 sterically prevents the JH1 activation loop from adopting an active conformation, and the SH2–JH2 linker plays no role in the JH2–JH1 interaction. In our model, JH2 binds to the "backside" of JH1, stabilizing an inactive conformation of JH1, and the SH2–JH2 linker serves as a bridging element between JH2 and JH1. The conformation of the SH2–JH2 linker in our model differs from that in the crystal structure of JAK1 JH2 (ref. 31), but this may be due to the absence of JH1 in the crystallized protein.

After our study was completed, a crystal structure of TYK2 JH2–JH1 was reported[32]. Our simulations-based models for JAK2 and JAK1 JH2–JH1 are in striking accord with the TYK2 structure. All of the key JH2–JH1 interactions in the JAK2 and JAK1 models are present in the TYK2 structure, in particular, those between the β7–β8 loop in JH2 and the β2–β3 loop in JH1 (**Fig. 2c**) and between the end of αC in JH2 and the hinge region in JH1 (**Fig. 2d**). On average (over the simulation), the JAK2 model is 3.7 Å (RMSD for Cα atoms in JH2–JH1) away from the TYK2 crystal structure (PDB code 4OLI), and the JAK1 model is 3.3 Å away.

The JH2-mediated autoinhibitory mechanism described above would serve to limit *trans*-phosphorylation of JAK molecules associated either with heterodimeric receptors juxtaposed through ligand binding or with preformed homodimeric receptors (e.g., Epo receptor) reconfigured by ligand binding. For JAK2, which is the only JAK to associate with preformed homodimeric receptors, phosphorylation of Ser523 (refs. 11,20,21) and Tyr570 (refs. 11,17,18), which is unique to JAK2, provides an additional mechanism of JH2–JH1 stabilization (**Figs. 2b,e** and **5**).

Finally, there is considerable interest in developing V617F-specific inhibitors of JAK2 for treatment of MPNs, which would minimize the toxicities associated with concomitant inhibition of wild-type JAK2 (ref. 33). By providing an understanding of how JH2 and JH1 interact in the basal state, our model should be valuable for the screening and design of small molecules that could fortify this interaction, which could potentially serve as novel therapeutic inhibitors of V617F or other oncogenic JAK2 mutants.

ACKNOWLEDGMENTS

This work was supported in part by the US National Institutes of Health grant R21 AI095808 (S.R.H.), Medical Research Council of Academy of Finland, Sigrid Juselius Foundation, Medical Research Fund of Tampere University Hospital, Finnish Cancer Foundation, and Tampere Tuberculosis Foundation (O.S.). The APRE-Rluc and pRG-TK plasmids were gifts from D. Levy and J. Belasco, respectively. We thank R. Bandaranayake for crystallographic support, A.

Philippsen for animation support, and W.T. Miller, M. Mohammadi, and M.P. Eastwood for critical reading of the manuscript.

AUTHOR CONTRIBUTIONS

Y.S., Conceiver of project, supervisor of MD simulations, and manuscript author; K.G., biochemical experiments and manuscript author; D.U. and H.H., biochemical experiments and protein production; E.T.K., MD simulations; K.Y., protein docking analysis; O.S., supervisor of biochemical studies and manuscript author; D.E.S., supervisor of MD simulations and manuscript author; S.R.H., Conceiver of project, supervisor of biochemical experiments, and manuscript author.

REFERENCES

1. O'Shea, J.J., Holland, S.M. & Staudt, L.M. JAKs and STATs in immunity, immunodeficiency, and cancer. *N. Engl. J. Med.* **368**, 161-170 (2013).
2. Wallweber, H.J., Tam, C., Franke, Y., Starovasnik, M.A. & Lupardus, P.J. Structural basis of recognition of interferon-alpha receptor by tyrosine kinase 2. *Nat. Struct. Mol. Biol.* **21**, 443-448 (2014).
3. Vainchenker, W., Delhommeau, F., Constantinescu, S.N. & Bernard, O.A. New mutations and pathogenesis of myeloproliferative neoplasms. *Blood* **118**, 1723-1735 (2011).
4. Haan, C., Behrmann, I. & Haan, S. Perspectives for the use of structural information and chemical genetics to develop inhibitors of Janus kinases. *J. Cell. Mol. Med.* **14**, 504-527 (2010).
5. Kralovics, R.*, et al.* A gain-of-function mutation of JAK2 in myeloproliferative disorders. *N. Engl. J. Med.* **352**, 1779-1790 (2005).
6. Baxter, E.J.*, et al.* Acquired mutation of the tyrosine kinase JAK2 in human myeloproliferative disorders. *Lancet* **365**, 1054-1061 (2005).
7. Levine, R.L.*, et al.* Activating mutation in the tyrosine kinase JAK2 in polycythemia vera, essential thrombocythemia, and myeloid metaplasia with myelofibrosis. *Cancer Cell* **7**, 387-397 (2005).
8. Lipson, D.*, et al.* Identification of new ALK and RET gene fusions from colorectal and lung cancer biopsies. *Nat. Med.* **18**, 382-384 (2012).
9. Saharinen, P. & Silvennoinen, O. The pseudokinase domain is required for suppression of basal activity of Jak2 and Jak3 tyrosine kinases and for cytokine-inducible activation of signal transduction. *J. Biol. Chem.* **277**, 47954-47963 (2002).
10. Saharinen, P., Takaluoma, K. & Silvennoinen, O. Regulation of the Jak2 tyrosine kinase by its pseudokinase domain. *Mol. Cell. Biol.* **20**, 3387-3395 (2000).
11. Ungureanu, D.*, et al.* The pseudokinase domain of JAK2 is a dual-specificity protein kinase that negatively regulates cytokine signaling. *Nat. Struct. Mol. Biol.* **18**, 971-976 (2011).
12. Bandaranayake, R.M.*, et al.* Crystal structures of the JAK2 pseudokinase domain and the pathogenic mutant V617F. *Nat. Struct. Mol. Biol.* **19**, 754-759 (2012).
13. Shan, Y.*, et al.* How does a drug molecule find its target binding site? *J. Am. Chem. Soc.* **133**, 9181-9183 (2011).
14. Dusa, A., Mouton, C., Pecquet, C., Herman, M. & Constantinescu, S.N. JAK2 V617F constitutive activation requires JH2 residue F595: a pseudokinase domain target for specific inhibitors. *PloS One* **5**, e11157 (2010).
15. Liang, S., Liu, S., Zhang, C. & Zhou, Y. A simple reference state makes a significant improvement in near-native selections from structurally refined docking decoys. *Proteins* **69**, 244-253 (2007).
16. Liang, S., Zhang, C., Sarmiento, J. & Standley, D.M. Protein loop modeling with optimized backbone potential functions. *J. Chem. Theor. Comp.* **8**, 1820-1827 (2012).
17. Argetsinger, L.S.*, et al.* Autophosphorylation of JAK2 on tyrosines 221 and 570 regulates its activity. *Mol. Cell. Biol.* **24**, 4955-4967 (2004).
18. Feener, E.P., Rosario, F., Dunn, S.L., Stancheva, Z. & Myers, M.G. Tyrosine phosphorylation of Jak2 in the JH2 domain inhibits cytokine signaling. *Mol. Cell. Biol.* **24**, 4968-4978 (2004).
19. Zhao, L.*, et al.* A JAK2 interdomain linker relays Epo receptor engagement signals to kinase activation. *J. Biol. Chem.* **284**, 26988-26998 (2009).

20. Ishida-Takahashi, R.*, et al.* Phosphorylation of Jak2 on Ser(523) inhibits Jak2-dependent leptin receptor signaling. *Mol. Cell. Biol.* **26**, 4063-4073 (2006).
21. Mazurkiewicz-Munoz, A.M.*, et al.* Phosphorylation of JAK2 at serine 523: a negative regulator of JAK2 that is stimulated by growth hormone and epidermal growth factor. *Mol. Cell. Biol.* **26**, 4052-4062 (2006).
22. Mullighan, C.G.*, et al.* JAK mutations in high-risk childhood acute lymphoblastic leukemia. *Proc. Natl. Acad. Sci. U.S.A.* **106**, 9414-9418 (2009).
23. Wan, X., Ma, Y., McClendon, C.L., Huang, L.J. & Huang, N. Ab Initio Modeling and Experimental Assessment of Janus Kinase 2 (JAK2) Kinase-Pseudokinase Complex Structure. *PLoS Comput. Biol.* **9**, e1003022 (2013).
24. Miyazawa, S. & Jernigan, R.L. Residue-residue potentials with a favorable contact pair term and an unfavorable high packing density term, for simulation and threading. *J. Mol. Biol.* **256**, 623-644 (1996).
25. Nagar, B.*, et al.* Structural basis for the autoinhibition of c-Abl tyrosine kinase. *Cell* **112**, 859-871 (2003).
26. Huse, M. & Kuriyan, J. The conformational plasticity of protein kinases. *Cell* **109**, 275-282 (2002).
27. Shan, Y.*, et al.* A conserved protonation-dependent switch controls drug binding in the Abl kinase. *Proc. Natl. Acad. Sci. U.S.A.* **106**, 139-144 (2009).
28. Gnanasambandan, K., Magis, A. & Sayeski, P.P. The constitutive activation of Jak2-V617F is mediated by a pi stacking mechanism involving phenylalanines 595 and 617. *Biochemistry* **49**, 9972-9984 (2010).
29. Lindauer, K., Loerting, T., Liedl, K.R. & Kroemer, R.T. Prediction of the structure of human Janus kinase 2 (JAK2) comprising the two carboxy-terminal domains reveals a mechanism for autoregulation. *Protein Eng.* **14**, 27-37 (2001).
30. Wan, S. & Coveney, P.V. Regulation of JAK2 activation by Janus homology 2: evidence from molecular dynamics simulations. *J. Chem. Inf. Model.* **52**, 2992-3000 (2012).
31. Toms, A.V.*, et al.* Structure of a pseudokinase-domain switch that controls oncogenic activation of Jak kinases. *Nat. Struct. Mol. Biol.* **20**, 1221-1223 (2013).
32. Lupardus, P.J.*, et al.* Structure of the pseudokinase-kinase domains from protein kinase TYK2 reveals a mechanism for Janus kinase (JAK) autoinhibition. *Proc. Natl. Acad. Sci. U.S.A.* (2014).
33. LaFave, L.M. & Levine, R.L. JAK2 the future: therapeutic strategies for JAK-dependent malignancies. *Trends Pharmacol. Sci.* **33**, 574-582 (2012).
34. Baffert, F.*, et al.* Potent and selective inhibition of polycythemia by the quinoxaline JAK2 inhibitor NVP-BSK805. *Mol. Cancer Ther.* **9**, 1945-1955 (2010).

FIGURE LEGENDS

Figure 1 Steps of JAK2 JH2–JH1 model generation. (1) Starting positions of JAK2 JH2 (PDB code 4FVQ[12]), residues 536–810, and JAK2 JH1 (PDB code 3KRR[34]), residues 840–1131. The center-of-mass distance is 67 Å, with a minimum separation of 26 Å. JH2 is colored orange and JAK2 JH1 is colored cyan, with the activation loop (residues 994–1016) colored red. Structural elements that will converge in the final model of JH2–JH1 (αC (JH2) with αD (JH1) and β7-β8 (JH2) with β2-β3 (JH1)) are labeled at key steps. (2) JH2–JH1 interaction poses after 14 3-μs MD simulations (different initial random velocities for each simulation), superimposed on JH2. Pose 2, shown in solid coloring, was used in the subsequent modeling steps. (3) After adding the JH2–JH1 linker in an extended conformation. (4) After simulating JH2–JH1, residues 536–1131, for 1.7 μs. (5) After adding the SH2–JH2 linker in an extended conformation. (6) After simulating JH2–JH1, residues 520–1131, for 40 μs. RMSD values of JH1 and JH2 (Cα atoms) relative to the final model (state 6) are given in parenthesis for states 3 and 4.

Figure 2 Model of JAK2 JH2–JH1 derived from MD simulations. (**a**) Autoinhibitory pose of JAK2 JH2–JH1. The coloring scheme is the same as in **Fig. 1**. Residues that cause JAK2 activation upon mutation (to the indicated residues) are shown in sphere representation (side chains) and colored pink (carbon atoms). Phosphorylated Ser523 and Tyr570 are shown in stick representation and colored according to their location. Oxygen atoms are colored red, nitrogen atoms blue, sulfur atoms yellow, and phosphorus atoms black. A red superscript in a residue label indicates the figure part showing a zoom-in of that region. The N-terminus (residue 520) is labeled 'N', and the C-terminus (residue 1131) is labeled 'C'. The JH2–JH1 interface (the SH2–JH2 and JH2–JH1 linkers excluded) buries 1670 $Å^2$ of total surface area. **(b–e)** Regions of the JH2–JH1 interface near pTyr570 (**b**), near Arg683–Asp873 (**c**), near the hinge region of JH1 (**d**), and near the SH2–JH2 linker (**e**). Select residues are shown in stick representation, some with van der Waals surfaces. Black dashed lines represent salt bridges.

Figure 3 Experimental validation of the JAK2 JH2–JH1 model. (**a**–**d**) Left: representative western blots of immunoprecipitated JAK2 from COS7 cells, wild type (WT) or the indicated JAK2 mutant, probed with anti-pTyr1007–1008 (pJAK2) (top) or anti-HA antibodies (bottom). The position of the 150-kDa molecular-weight marker is indicated. Middle: quantification of the pJAK2 signals normalized by JAK2 protein levels and plotted as fold-change relative to wild-type JAK2 (set to 1.0). Average values and standard deviations were derived from three independent experiments (N=3). Right: representative western blots of COS7 whole-cell lysates probed with anti-pTyr701 STAT1 antibodies (pSTAT1) (top) or anti-STAT1 antibodies (STAT1) (bottom) to detect endogenous STAT1 levels. The position of the 100-kDa molecular-weight marker is indicated. Original images of blots used in this study can be found in **Supplementary Figure 6**.

Figure 4 JH2-mediated autoinhibition of JH1 in JAK2. (**a**) Distance in JH1 between Lys882 (β3) and Glu898 (αC). The distance is plotted as a function of simulation time for simulations of JAK2 JH2–JH1 or JH1 alone (JH1 activation loop was unphosphorylated for both). To simplify the salt-bridge presentation (to account for both Oε1 and Oε2 of Glu898), the actual distance displayed is between Nζ of Lys882 and Cδ of Glu898, and the gray rectangle indicates the salt-bridging distance range. (**b**) DFG-in and -out states of the JH1 activation loop. Left: in the active state of JH1 (PDB code 3KRR[34]), the Lys882–Glu898 salt bridge is formed, and Asp994 and Phe995 of the DFG motif in the activation loop adopt the DFG-in (active) conformation. Right: during the simulation of JH2–JH1, the Lys882–Glu898 salt bridge is disrupted and the DFG motif more readily adopts a DFG-out (inactive) conformation (shown is a snapshot taken after 12 μs of the simulation). Coloring is the same as in **Fig. 1**.

Figure 5 Model for JAK2 JH2-mediated autoinhibition of JH1. (Not shown are the FERM and SH2 domains of JAK2 and cytokine receptor.) A conformational equilibrium exists between JH1 in the JH2–JH1 autoinhibitory interaction (state I), in which JH1 is held in an inactive state (JH1,

red), and configurations in which JH1 is disassociated from JH2 (orange) and is transiently active (state II; JH1, mixed red and green). The N and C lobes of JH2 and JH1 are labeled. Phosphorylated Ser523 and Tyr570 (magenta and mixed white and magenta spheres, respectively) stabilize the autoinhibited state by binding to positively charged residues in JH1 and JH2 (blue patches; see **Fig. 2b,e**). Ser523 is constitutively phosphorylated[20], whereas Tyr570 is sub-stoichiometrically phosphorylated in the basal state, and its phosphorylation level increases upon JAK2 activation[18], which probably serves as a negative feedback mechanism (to stabilize the autoinhibited state). In the basal state (no cytokine), the two JAK2 molecules (only one JH2–JH1 shown) associated with a cytokine-receptor dimer are maintained in positions that limit *trans*-phosphorylation of the JH1 activation loop (Tyr1007–1008). Cytokine binding and receptor rearrangement juxtapose the two JAK2 molecules to facilitate JH1 *trans*-phosphorylation of the activation loop, which activates JAK2 (state III; JH1, green). Activating mutations such as D873N, R683S, or V617F destabilize the autoinhibited state, permitting *trans*-phosphorylation of the JH1 activation loop in the basal state.

ONLINE METHODS

Molecular dynamics simulations. Simulation systems were set up by placing JH2–JH1 in a cubic simulation box (with periodic boundary conditions) of at least 100 Å per side and approximately 100,000 atoms in total. The system for the simulation of the unbiased association of JH2 and JH1 was 120 Å per side and approximately 165,000 atoms in total. Explicitly represented water molecules were added to fill the system, and Na^+ and Cl^- ions were added to maintain physiological salinity (150 mM) and to obtain a neutral total charge for the system. The systems were parameterized using the CHARMM36 force field with TIP3P water[35-37] and then equilibrated in the NPT ensemble at 1 bar and 310 K for 10 ns. Equilibrium MD simulations were performed on the special-purpose molecular dynamics machine Anton[38] in the NVT ensemble at 310 K using the Nose-Hoover thermostat[39] with a relaxation time of 1.0 ps and a time step of 2.5 fs. All bond lengths to hydrogen atoms were constrained using a recently developed implementation[40] of M-SHAKE[41]. The Lennard-Jones and the Coulomb interactions in the simulations were calculated using a force-shifted cutoff of 12 Å (ref. 42). The DFG flip in the JH1 activation loop (**Fig. 4b**) was completed in two separate JH2–JH1 simulations. In the first one, JH1 started in the catalytically active conformation, characterized by an intact Lys882–Glu898 salt bridge, and Asp994 was deprotonated. In the course of this simulation, the Lys882–Glu898 salt bridge was disrupted due to the interaction of JH1 with JH2 (**Fig. 4a**). From this conformation (disrupted salt bridge), a second simulation was launched with Asp994 protonated, and the DFG flip was completed in this simulation after approximately 12 μs. As shown previously[43], disruption of the salt bridge and protonation of this aspartic acid promote the DFG flip in a protein kinase.

Transfection and western blot analysis. Mouse JAK2 cDNA was engineered to include a C-terminal HA tag and was inserted into plasmid pcDNA6. Mutations were introduced using the QuikChange site-directed mutagenesis kit (Agilent). The mutants were verified by DNA sequencing. COS7 cells were transiently transfected with 10 μg of the respective JAK2 cDNA using X-tremeGENE 9 (Roche) according to the manufacturer's instructions. 48 h after

transfection, cells were lysed using RIPA buffer in the presence of protease inhibitors. JAK2 was immunoprecipitated from the cleared lysate using 2 µg of anti-JAK2 antibodies (HR-758, cat. no. sc-278, Santa Cruz) and Protein A/G beads (Santa Cruz) and western-blotted with anti-JAK2 pTyr1007–1008 antibodies (cat. no. 44-426G, Invitrogen) at 1:500 dilution or anti-HA antibodies (HA-7, cat. no. H9658, Sigma) at 1:3,000 dilution. Whole-cell lysates from transfected COS7 cells (~2% input) were western-blotted with anti-pTyr701 STAT1 antibodies (D4A7, cat. no. 7649P, Cell Signaling) at 1:1,000 dilution or anti-STAT1 antibodies (cat. no. 610185, BD Biosciences) at 1:1,000 dilution. Validation for the various antibodies used are available on the respective manufacturer's website. The western-blot signals were detected using the fluorescence-based Odyssey imaging system (LI-COR Biosciences). Original images of blots used in this study can be found in **Supplementary Figure 6**.

JAK2-deficient γ2A cells (fibrosarcoma cells) were transfected with the respective JAK2 plasmids, Epo receptor, and STAT5, using Fugene 6 (Promega) according to the manufacturer's instructions. After 12 h, cells were starved in serum-free media followed by stimulation with Epo (200 U/ml, NeoRecormon, Roche) for 30 min. Cells were lysed in buffer (50 mM Tris-HCl (pH 8.0), 150 mM NaCl, 100 mM NaF, 10% (v/v) glycerol, 1% (v/v) Triton-X, and protease inhibitor cocktail), and cleared whole-cell lysates were western-blotted using anti-JAK2 pTyr1007–1008 antibodies (cat. no. 3771, Cell Signaling) at 1:1000 dilution, anti-pSTAT5 antibodies (C11C5, cat. no. 9359, Cell Signaling) at 1:2000, or anti-HA antibodies (cat. no. MMS-101P, Covance) at 1:3000 dilution.

Mouse JAK2 JH1 (residues 825–1132) was cloned in pcDNA3.1 (+) with a C-terminal HA tag. HEK 293T cells were transfected with the respective JAK2 JH1 plasmids using X-tremeGENE 9 (Roche) according to the manufacturer's instructions. 48 h after transfection, cells were lysed using RIPA buffer in the presence of protease inhibitors. JAK2 JH1 was immunoprecipitated from the cleared lysate using 20 µl of EZview™ Red Anti-HA affinity gel (Sigma) and western-blotted with anti-JAK2 pTyr1007–1008 (Invitrogen) at 1:500 dilution or anti-HA antibodies (Sigma) at 1:3000 dilution.

Luciferase assay. COS7 cells were plated at 2×10^4 cells/well in a 96-well plate 36 h before transfection. Each well was transfected with 50 ng of JAK2 cDNA (wild type or mutant) or empty vector, 50 ng of APRE-luc (Acute phase response element-firefly luciferase reporter for STAT3), and 50 ng of pRG-TK (Renilla luciferase reporter) using X-tremeGENE 9 (Roche), according to the manufacturer's instructions. 48 h after transfection, the cells were assayed for luciferase activity using the Dual-Glo Luciferase assay kit (Promega), and the luminescence was measured using a Tecan SpectraFluor Plus instrument.

35. Best, R.B.*, et al.* Optimization of the additive CHARMM all-atom protein force field targeting improved sampling of the backbone phi, psi and side-chain chi(1) and chi(2) dihedral angles. *J. Chem. Theory Comput.* **8**, 3257-3273 (2012).
36. Mackerell, A.D., Jr.*, et al.* All-Atom Empirical Potential for Molecular Modeling and Dynamics Studies of Proteins. *J. Phys. Chem. B* **102**, 3586-3616 (1998).
37. Jorgensen, W.L., Chandrasekhar, J., Madura, J.D., Impey, R.W. & Klein, M.L. Comparison of simple potential functions for simulating liquid water. *J. Chem. Phys.* **79**, 926-935 (1983).
38. Shaw, D.E.*, et al.* Millisecond-scale molecular dynamics simulations on Anton. In ACM/IEEE Conference on Supercomputing. *In ACAM/IEEE Conference on Supercomputing (New York, NY, ACM Press)* (2009).
39. Hoover, W.G. Canonical dynamics: Equilibrium phase-space distributions. *Phys. Rev. A* **31**, 1695-1697 (1985).
40. Lippert, R.A.*, et al.* A common, avoidable source of error in molecular dynamics integrators. *J. Chem. Phys.* **126**, 046101 (2007).
41. Krautler, V., Van Gunsteren, W.F. & Hunenberger, P.H. A fast SHAKE algorithm to solve distance constraint equations for small molecules in molecular dynamics simulations. *J. Comput. Chem.* **22**, 501-508 (2001).
42. Fennell, C.J. & Gezelter, J.D. Is the Ewald summation still necessary? Pairwise alternatives to the accepted standard for long-range electrostatics. *J. Chem. Phys.* **124**, 234104 (2006).
43. Shan, Y.*, et al.* A conserved protonation-dependent switch controls drug binding in the Abl kinase. *Proc. Natl. Acad. Sci. U.S.A.* **106**, 139-144 (2009).

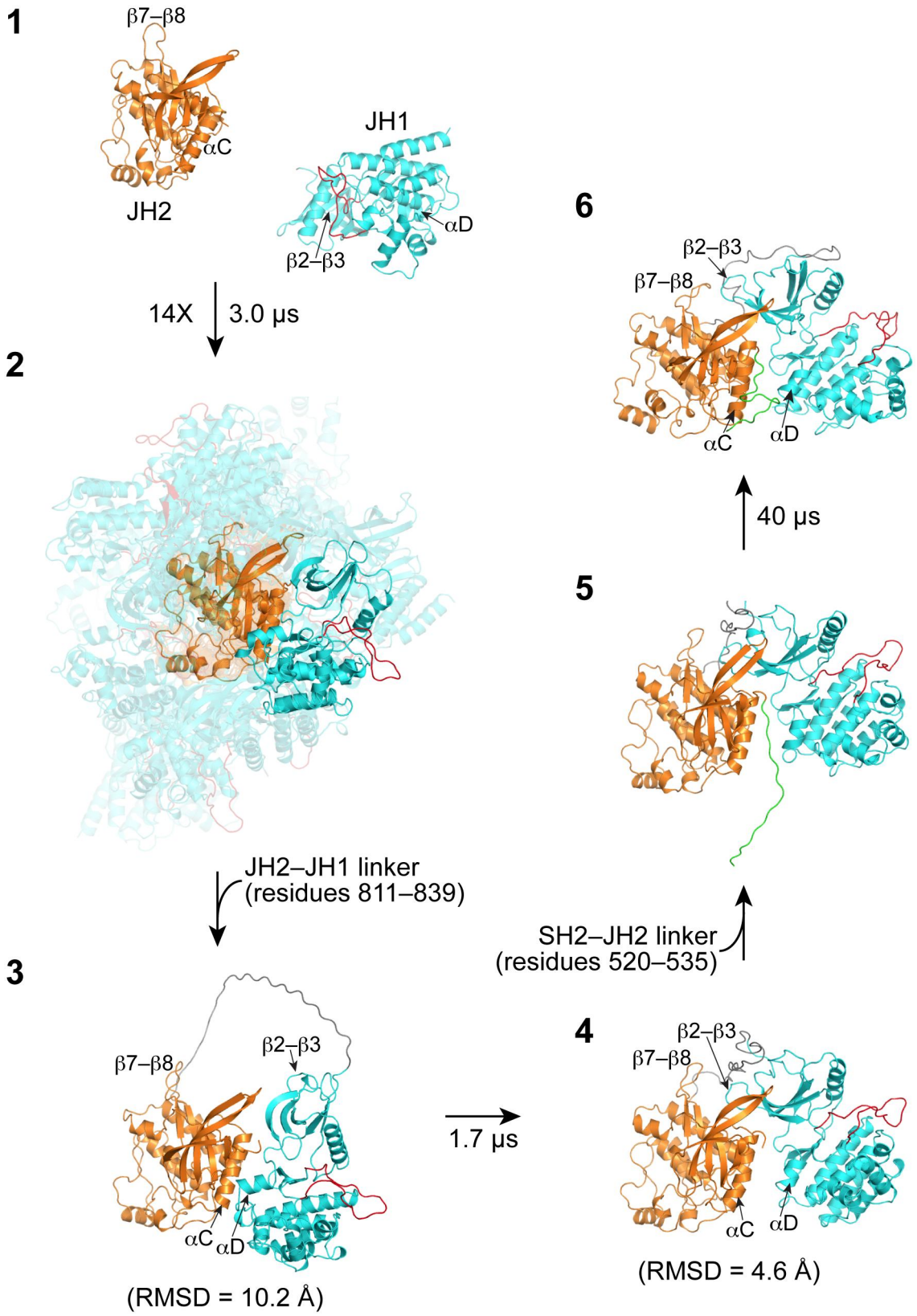
1
β7–β8
αC
JH2
JH1
αD
β2–β3
14X
3.0 μs
2
JH2–JH1 linker
(residues 811–839)
3
β7–β8
β2–β3
αC
αD
(RMSD = 10.2 Å)
1.7 μs
4
β2–β3
β7–β8
αC
αD
(RMSD = 4.6 Å)
SH2–JH2 linker
(residues 520–535)
5
40 μs
6
β2–β3
β7–β8
αC
αD

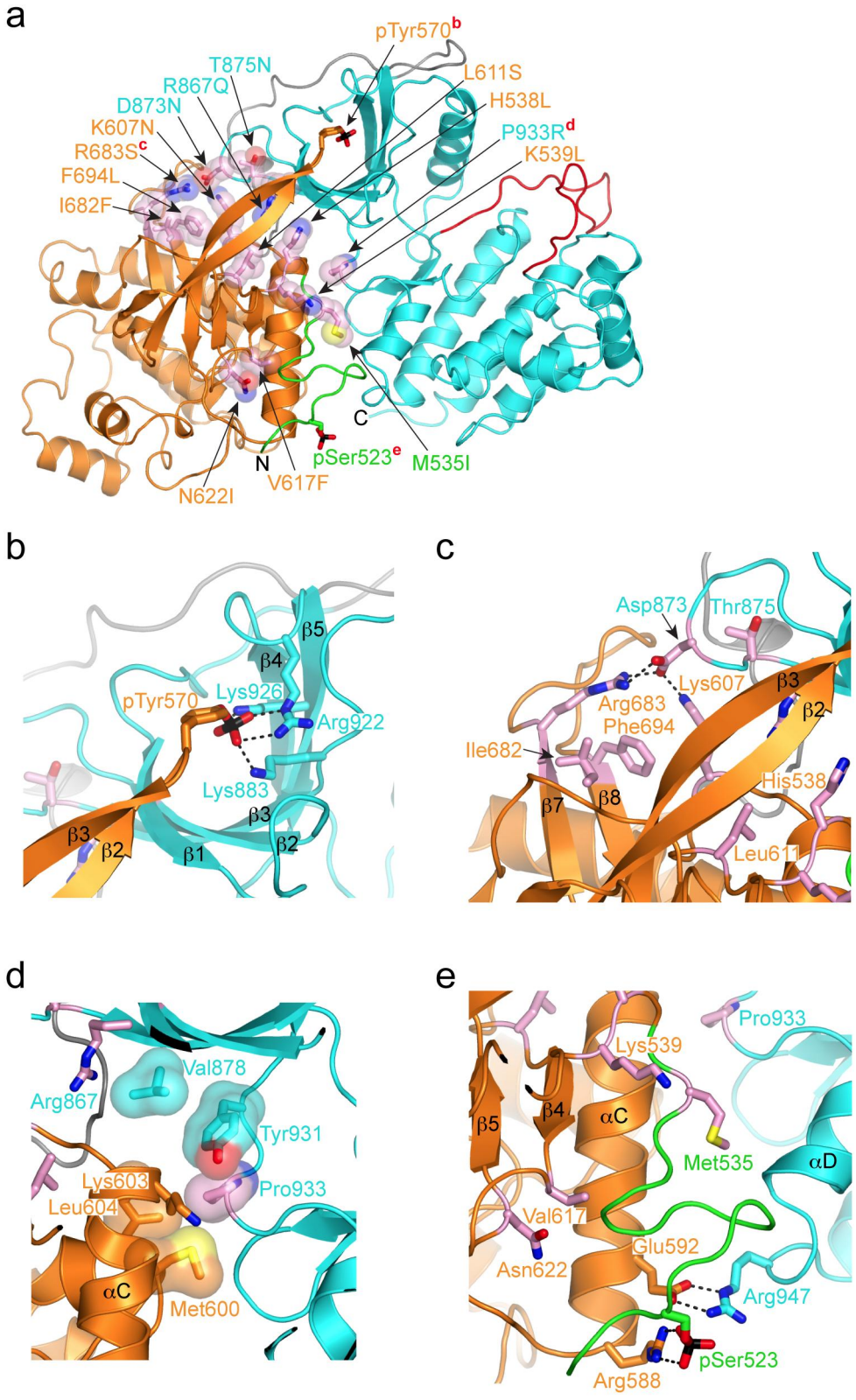
a
pTyr570[b]
T875N
R867Q
D873N
K607N
R683S[c]
F694L
I682F
L611S
H538L
P933R[d]
K539L
C
N
pSer523[e]
M535I
N622I
V617F
b
β5
β4
pTyr570
Lys926
Arg922
Lys883
β3
β3
β2
β1
β2
c
Asp873
Thr875
Lys607
β3
β2
Arg683
Phe694
Ile682
His538
β7
β8
Leu611
d
Val878
Arg867
Tyr931
Lys603
Leu604
Pro933
αC
Met600
e
Pro933
Lys539
β5
β4
αC
Met535
αD
Val617
Glu592
Asn622
Arg947
pSer523
Arg588

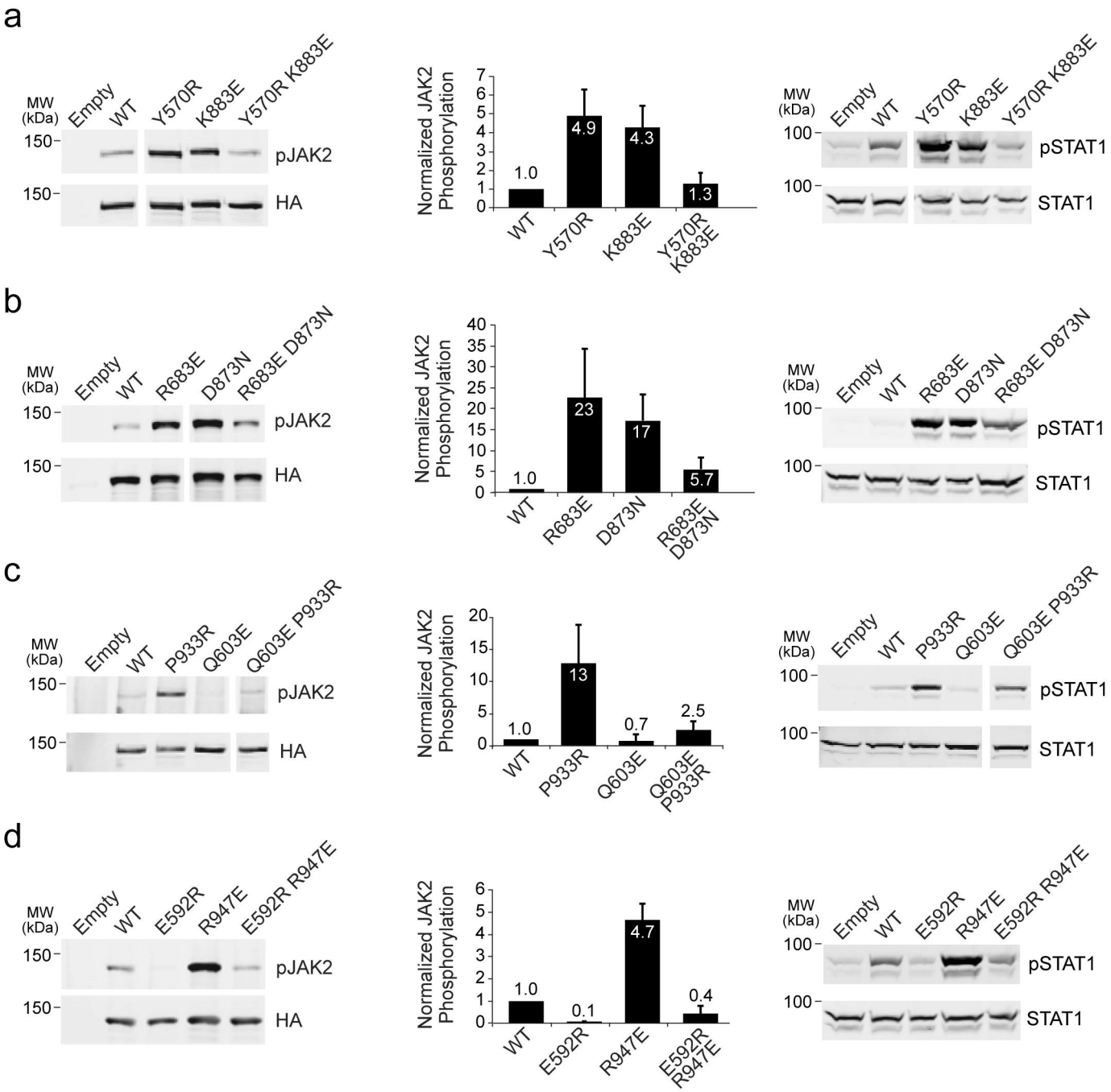
a
MW (kDa)
Empty
WT
Y570R
K883E
Y570R K883E
150
pJAK2
150
HA
Normalized JAK2 Phosphorylation
1.0
4.9
4.3
1.3
WT
Y570R
K883E
Y570R K883E
MW (kDa)
100
pSTAT1
100
STAT1
b
MW (kDa)
Empty
WT
R683E
D873N
R683E D873N
150
pJAK2
150
HA
Normalized JAK2 Phosphorylation
1.0
23
17
5.7
WT
R683E
D873N
R683E D873N
MW (kDa)
100
pSTAT1
100
STAT1
c
MW (kDa)
Empty
WT
P933R
Q603E
Q603E P933R
150
pJAK2
150
HA
Normalized JAK2 Phosphorylation
1.0
13
0.7
2.5
WT
P933R
Q603E
Q603E P933R
MW (kDa)
100
pSTAT1
100
STAT1
d
MW (kDa)
Empty
WT
E592R
R947E
E592R R947E
150
pJAK2
150
HA
Normalized JAK2 Phosphorylation
1.0
0.1
4.7
0.4
WT
E592R
R947E
E592R R947E
MW (kDa)
100
pSTAT1
100
STAT1

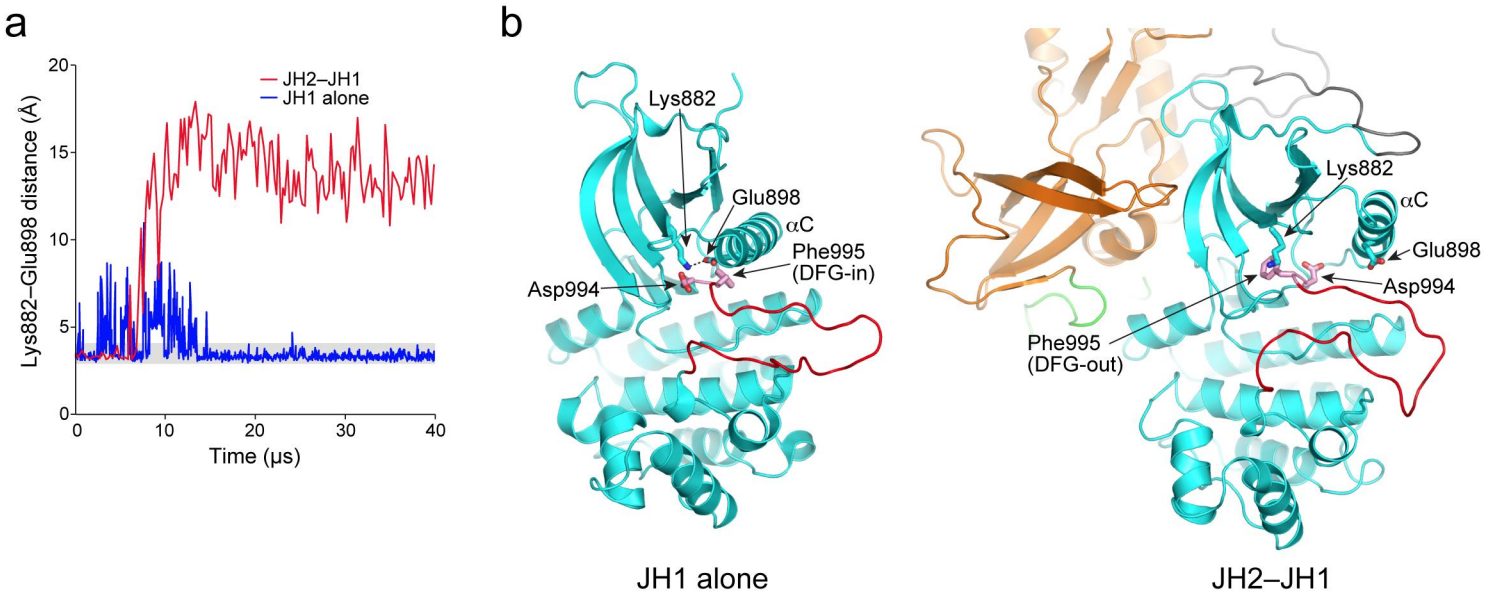
a
b
JH2–JH1
JH1 alone
Lys882–Glu898 distance (Å)
Time (μs)
Lys882
Glu898
αC
Phe995
(DFG-in)
Asp994
Phe995
(DFG-out)
JH1 alone
JH2–JH1

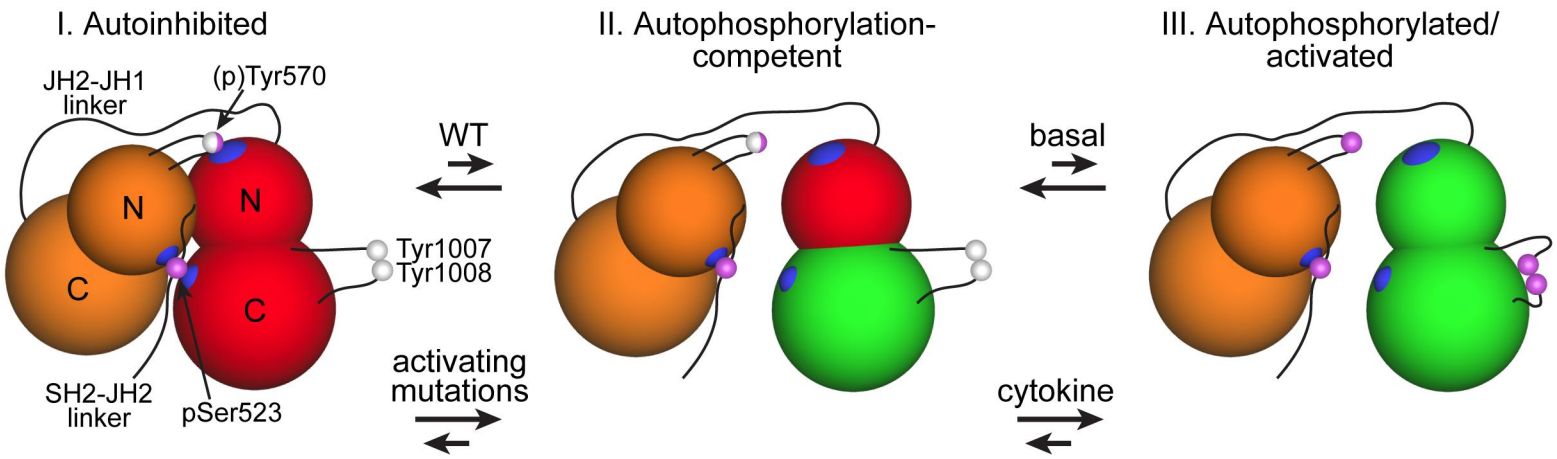
I. Autoinhibited
II. Autophosphorylation-competent
III. Autophosphorylated/ activated
JH2-JH1 linker
(p)Tyr570
N
N
C
C
Tyr1007
Tyr1008
SH2-JH2 linker
pSer523
WT
activating mutations
basal
cytokine

Molecular basis for pseudokinase-dependent autoinhibition of JAK2 tyrosine kinase

Yibing Shan, Kavitha Gnanasambandan, Daniela Ungureanu, Eric T. Kim, Henrik Hammarén, Kazuo Yamashita, Olli Silvennoinen, David E. Shaw, and Stevan R. Hubbard

This PDF includes Supplementary Figures 1–6.

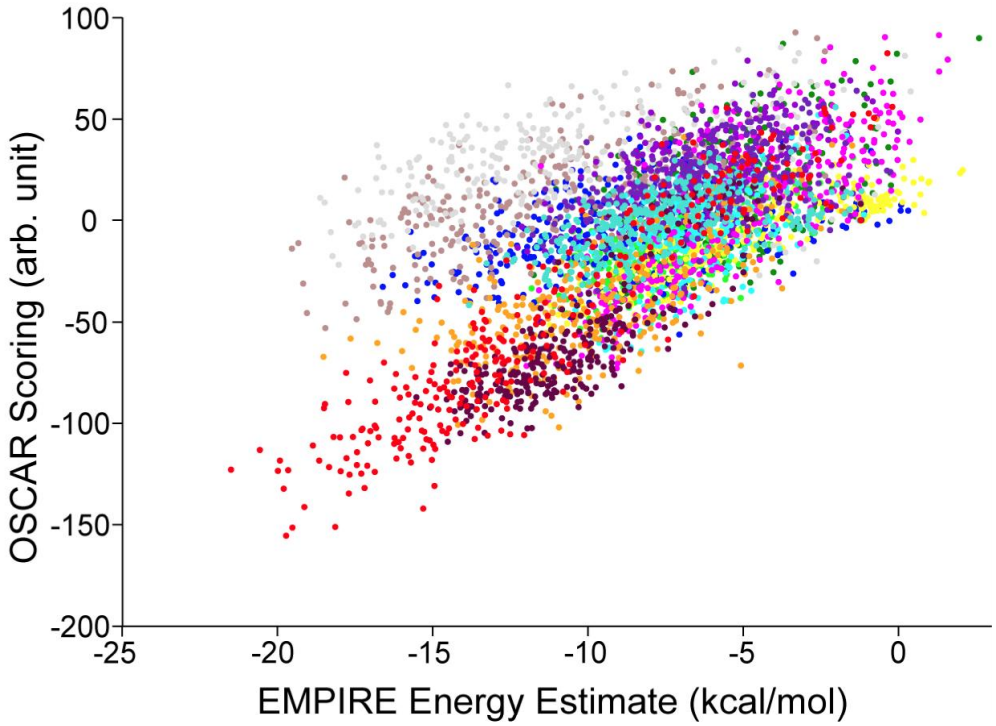

Supplementary Figure 1 Energy analysis of 14 JAK2 JH2–JH1 poses. From each of the 14 3.0-μs simulations, starting from an arbitrary JH2–JH1 non-contacting pose, 300 snapshots (10-ns interval) were evaluated using both EMPIRE and OSCAR scoring functions[1,2]. The score of each snapshot from each simulation was plotted in the two-dimensional energy space with a unique color. The dots corresponding to the simulation that generated pose 2, the JH2–JH1 interaction that was pursued further (see Fig. 1), are colored red.

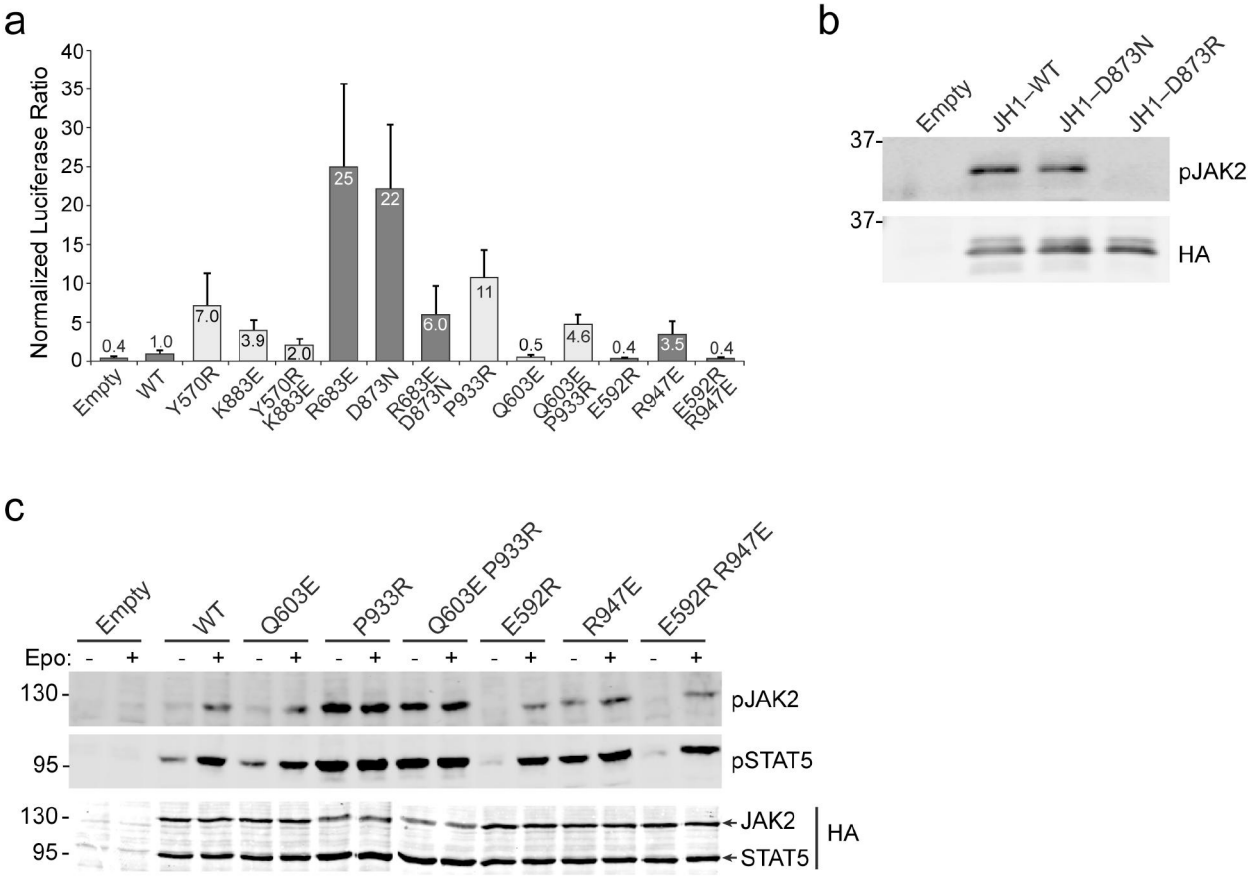

Supplementary Figure 2 Functional studies of JAK2 mutants. (**a**) Luciferase activities of wild-type and mutant JAK2 measured using an APRE-luc reporter to assess endogenous STAT3-dependent transcription in COS7 cells. The firefly luciferase activity of each sample was normalized to that of renilla luciferase (luciferase ratio) and plotted as fold-change relative to the wild-type JAK2 (WT) luciferase ratio (set to 1.0). Average values and standard deviations were derived from triplicate samples (N=3). (**b**) Analysis of JAK2 mutants D873R and D873N in JH1 alone. Representative western blot of JAK2 JH1 (HA-tagged) immunoprecipitated from transfected HEK 293T cells and probed for JAK2 Tyr1007–1008 phosphorylation (pJAK2) (top) or protein levels (HA) (bottom). A reference molecular-weight marker (in kDa) is indicated on the left. (**c**) Epo-dependent activation of JAK2 mutants. JAK2-deficient γ2A cells transfected with the indicated JAK2 and STAT5 (HA-tagged) plasmids were either left untreated (–) or stimulated with Epo (+), and the whole cell lysates were probed for JAK2 Tyr1007–1008 phosphorylation (pJAK2, top), STAT5 phosphorylation (pSTAT5, middle), or protein levels (HA, bottom). Reference molecular-weight markers (in kDa) are indicated on the left.

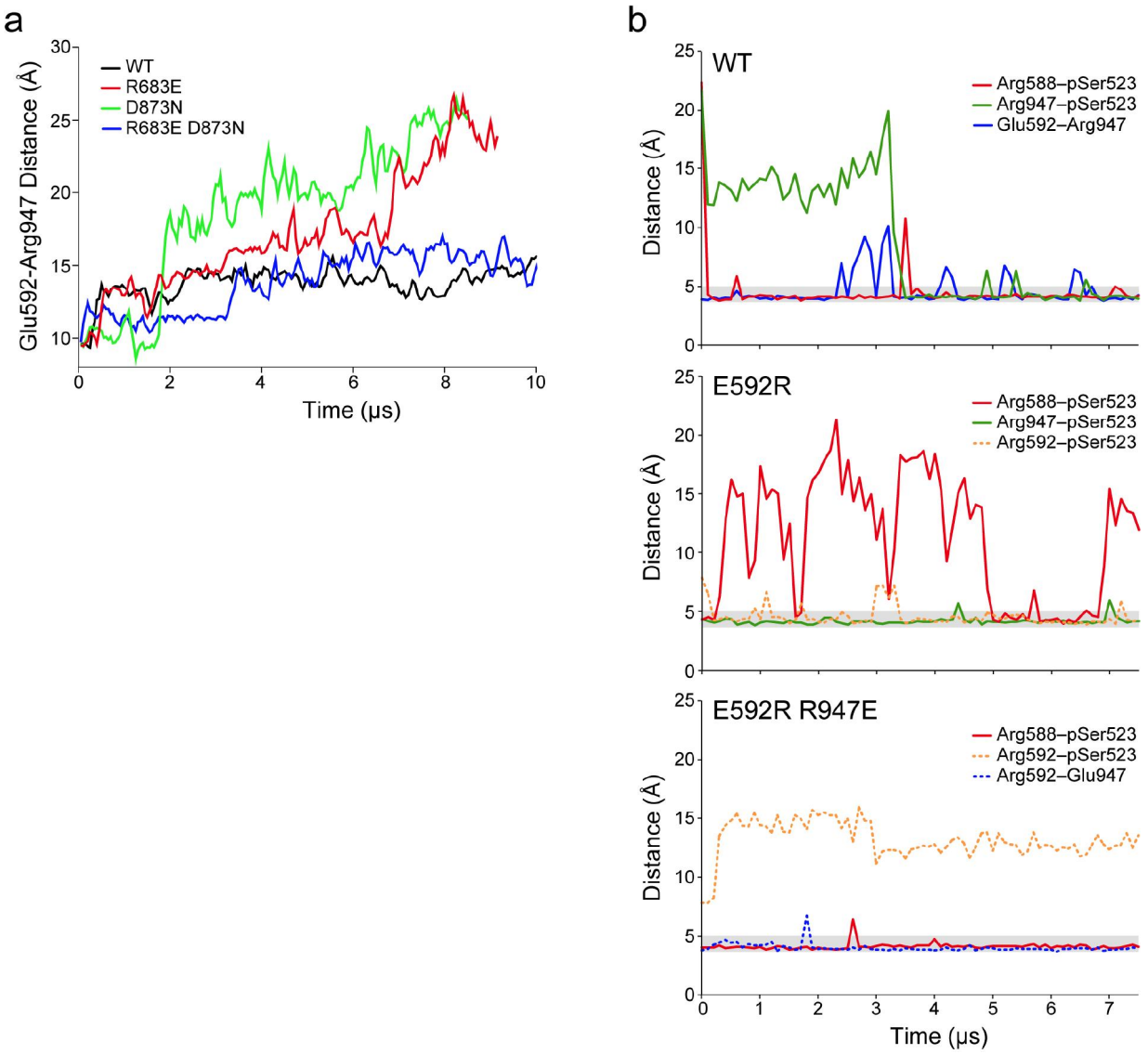

Supplementary Figure 3 Simulations of JAK2 JH2–JH1 mutants. **(a)** Analysis of R683E, D873N and R683E D873N. The distance between the Cα atoms of Glu592 (JH2) and Arg947 (JH1), interacting residues in the JH2–JH1 model (see Fig. 2e), is plotted as a function of simulation time. In the activating mutations R683E and D873N, the two residues (Glu592, Arg947) separated, whereas for wild type (WT) and the double mutation, the distance remained relatively stable. (**b**) Salt-bridge analysis for JAK2 Glu592–Arg947. WT, E592R, and E592R R947E, were simulated for 7.5 μs each. Plotted are the distances between select residues as a function of simulation time. Shown in solid lines are the distance trajectories between native residues, and shown in dashed lines are distance trajectories in which at least one of the residues involved has been introduced by mutation. To simplify the salt-bridge presentation, the actual distances displayed are between Cζ of Arg588, Arg592, or Arg947 (to account for Nε, Nη1, and Nη2 of arginine) and either Cδ of Glu592 or Glu947 (to account for Oε1 and Oε2 of glutamic acid) or P of pSer523 (to account for O1P, O2P, and O3P of phosphoserine). Thus, the representative distance for a salt bridge is ~3.8 Å rather than ~2.7 Å (typical nitrogen–oxygen distance). Gray rectangles indicate the approximate distance range for salt bridges.

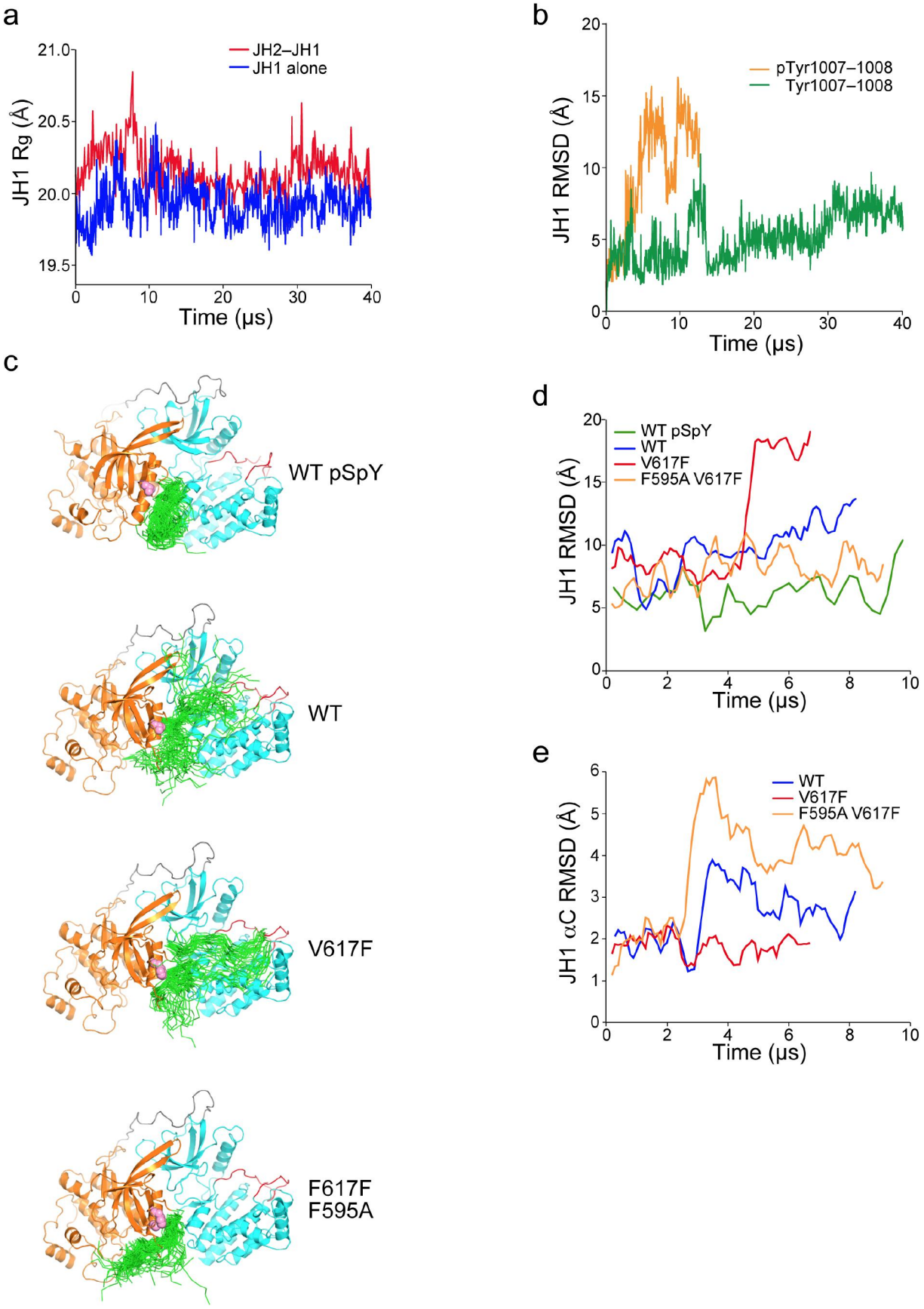
a
JH2–JH1
JH1 alone
JH1 Rg (Å)
Time (μs)
b
pTyr1007–1008
Tyr1007–1008
JH1 RMSD (Å)
Time (μs)
c
WT pSpY
WT
V617F
F617F
F595A
d
WT pSpY
WT
V617F
F595A V617F
JH1 RMSD (Å)
Time (μs)
e
WT
V617F
F595A V617F
JH1 αC RMSD (Å)
Time (μs)

Supplementary Figure 4 Conformational changes in JH1 and analysis of V617F. (**a**) Radius of gyration (R_g, an overall measure of the size) of JH1 as a function of simulation time (same simulations as in Fig. 4a). (**b**) RMSD for Cα atoms in JH1 as a function of simulation time, after aligning Cα atoms in JH2 for each time frame with the Cα atoms in their initial positions. Both simulations were initiated from an identical JH2–JH1 pose with Ser523 and Tyr570 phosphorylated. In one simulation (orange), the JH1 activation loop was phosphorylated at Tyr1007 and Tyr1008, and in the other simulation (green), the activation loop was unphosphorylated. A high RMSD is indicative of a high degree of structural deviation from the JH2–JH1 configuration (the autoinhibitory pose) shown in Fig. 2a. (**c**–**e**) Analyses of JAK2 MPN mutation V617F. In previous studies, we showed that Ser523 and Tyr570 are poorly phosphorylated in activated JAK2 mutants such as V617F[3]. Thus, to simulate V617F JH2–JH1 properly, we left Ser523 (and Tyr570) unphosphorylated and, for comparison purposes, we also simulated unphosphorylated wild type ('WT'). F595A, in αC of JH2 and proximal to Val617, was shown to suppress V617F[4,5], and therefore we also simulated F595A V617F (unphosphorylated). (**c**) The SH2–JH2 linker conformations visited during the simulations. JH2–JH1 in the first time frame (t=0) of each trajectory is shown in ribbon representation and colored as in Fig. 1. The Cα trace of the SH2–JH2 linker (residues 522–536) for each time frame is shown in green, after aligning JH2 in each frame with JH2 at t=0. As shown, the linker in V617F is least stable in the binding groove between JH2 and JH1. (**d**) RMSD for Cα atoms in JH1 as a function of simulation time, after aligning Cα atoms in JH2 for each time frame with the Cα atoms in their initial positions. Removal of pSer523 and pTyr570 ('WT' versus 'WT pSpY') led to an increase in the overall conformational heterogeneity of JH1 and thus destabilization of the JH2–JH1 complex. V617F caused a further increase in JH1 heterogeneity, and addition of F595A to V617F restored JH1 heterogeneity back to the level of phosphorylated JH2–JH1 ('WT pSpY'). (**e**) RMSD for Cα atoms in αC of JH1 (residues 889–904) relative to the active conformation, after aligning all the Cα atoms in JH1. As shown, the active conformation of αC is most stable in V617F.

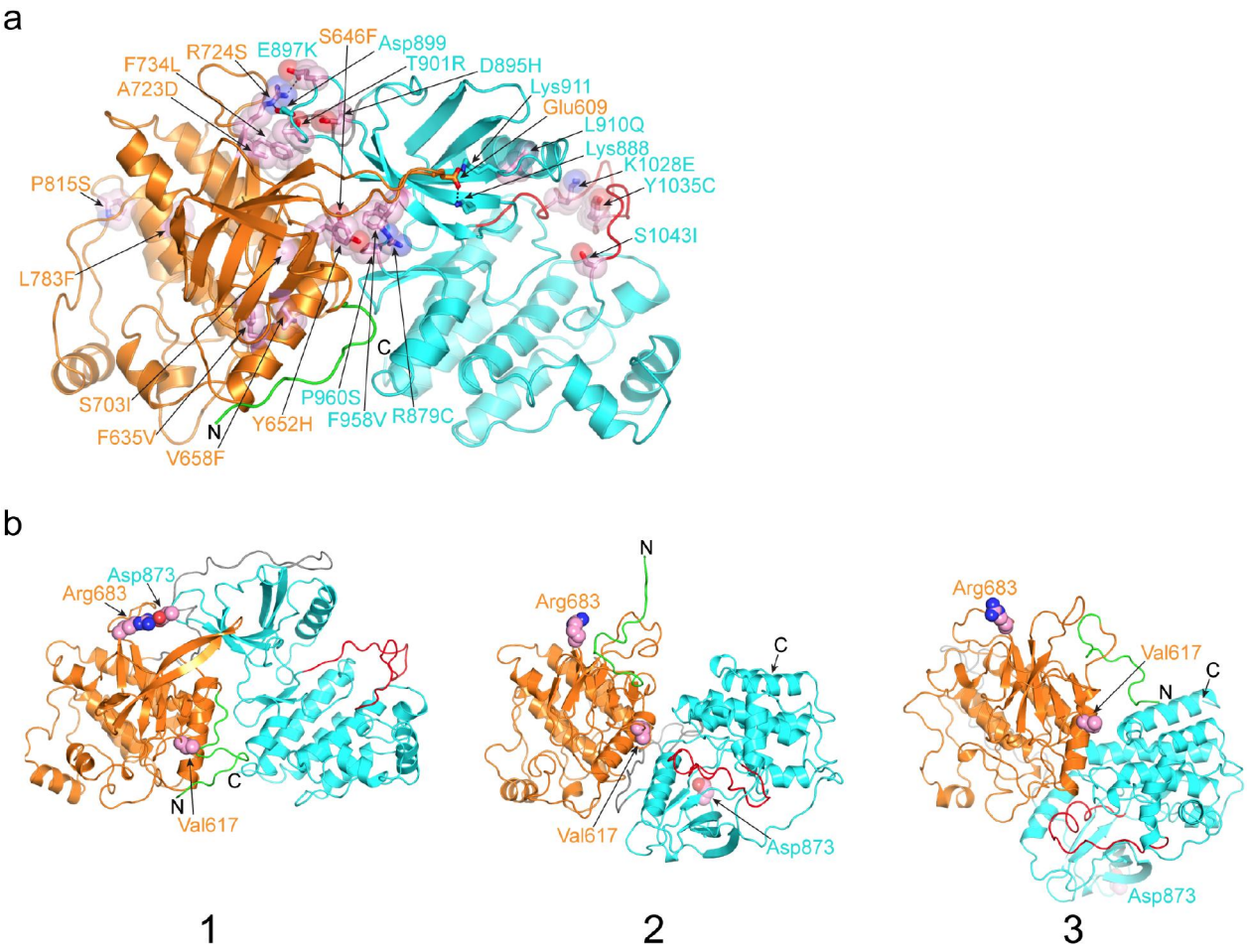

Supplementary Figure 5 JAK1 JH2–JH1 model and comparison of JAK JH2–JH1 models. (**a**) Atomic models of JAK1 JH2 (PDB code 4L00 (ref. 6)) and JH1 (PDB code 4E5W (ref. 7)) were placed by superposition into the positions of JH2 and JH1 of JAK2 (Fig. 2a). The SH2–JH2 and JH2–JH1 linkers were added, and an MD simulation was run for 12 μs. Shown is a representative pose near the end of the simulation. JH2 (residues 575–850) is colored orange, JH1 (residues 866–1154) is colored cyan, with the activation loop (residues 1021–1043) colored red, the SH2–JH2 linker (residues 563–574) is colored green, and the JH2–JH1 linker (residues 851–865) is colored gray. Mapped activating mutations[43] are shown in stick representation, colored pink, and labeled. Other residues of interest are shown in stick representation and labeled. The N-terminus (residue 563) is labeled 'N', and the C-terminus (residue 1154) is labeled 'C'. (**b**) Ribbon diagram of the JAK2 JH2–JH1 model from the current study (1), from Lindauer et al.[8] (2), and from Wan et al.[9] (3). Coloring is the same as in Fig. 1. The side chains of Val617, Arg683, and Asp873 are shown in sphere representation and colored pink (carbon atoms). The models are aligned with one another based on a superposition of JH2. The N- and C-termini for each model are labeled 'N' and 'C'.

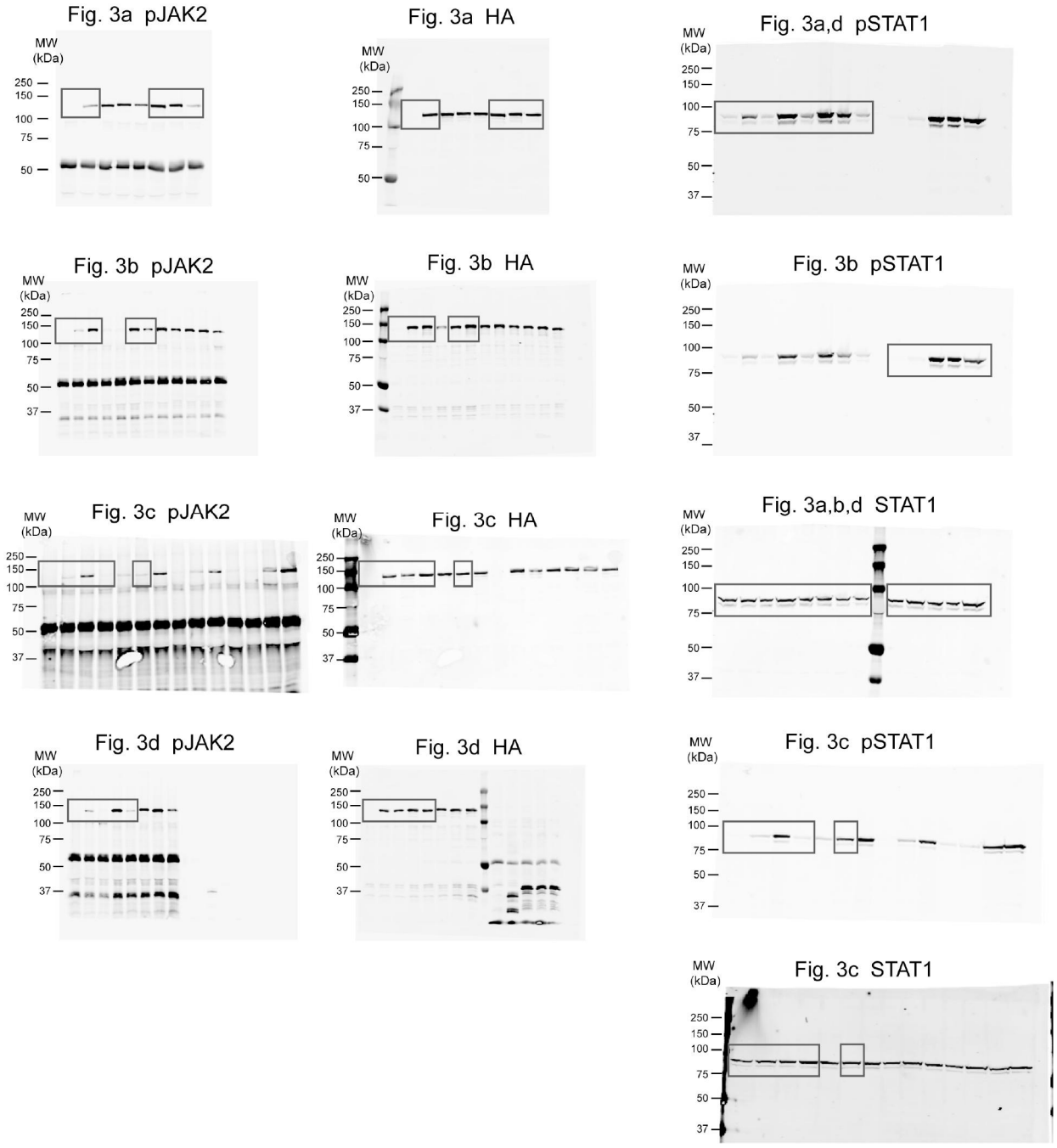

Supplementary Figure 6 Uncropped images for western blots shown in Fig. 3. For each blot (labeled accordingly), boxes mark the borders of the cropped images shown in Fig. 3.

REFERENCES

1. Liang, S., Liu, S., Zhang, C. & Zhou, Y. A simple reference state makes a significant improvement in near-native selections from structurally refined docking decoys. *Proteins* **69**, 244-253 (2007).
2. Liang, S., Zhang, C., Sarmiento, J. & Standley, D.M. Protein loop modeling with optimized backbone potential functions. *J. Chem. Theor. Comp.* **8**, 1820-1827 (2012).
3. Ungureanu, D.*, et al.* The pseudokinase domain of JAK2 is a dual-specificity protein kinase that negatively regulates cytokine signaling. *Nat. Struct. Mol. Biol.* **18**, 971-976 (2011).
4. Dusa, A., Mouton, C., Pecquet, C., Herman, M. & Constantinescu, S.N. JAK2 V617F constitutive activation requires JH2 residue F595: a pseudokinase domain target for specific inhibitors. *PloS One* **5**, e11157 (2010).
5. Gnanasambandan, K., Magis, A. & Sayeski, P.P. The constitutive activation of Jak2-V617F is mediated by a pi stacking mechanism involving phenylalanines 595 and 617. *Biochemistry* **49**, 9972-9984 (2010).
6. Toms, A.V.*, et al.* Structure of a pseudokinase-domain switch that controls oncogenic activation of Jak kinases. *Nat. Struct. Mol. Biol.* **20**, 1221-1223 (2013).
7. Kulagowski, J.J.*, et al.* Identification of imidazo-pyrrolopyridines as novel and potent JAK1 inhibitors. *J. Med. Chem.* **55**, 5901-5921 (2012).
8. Lindauer, K., Loerting, T., Liedl, K.R. & Kroemer, R.T. Prediction of the structure of human Janus kinase 2 (JAK2) comprising the two carboxy-terminal domains reveals a mechanism for autoregulation. *Protein Eng.* **14**, 27-37 (2001).
9. Wan, X., Ma, Y., McClendon, C.L., Huang, L.J. & Huang, N. Ab Initio Modeling and Experimental Assessment of Janus Kinase 2 (JAK2) Kinase-Pseudokinase Complex Structure. *PLoS Comput. Biol.* **9**, e1003022 (2013).